1997). Gingele (1996), suggests that higher precipitation, owing to an intensification of the north African monsoonal system during the 12 ka - 11 ka precessional minimum in the southern hemisphere, resulted in increased sedimentation off the Niger river. The observations do indicate, however, that the tropical climatic response only reaches a maximum thousands of years after the solstice-perihelion alignment (Short and Mengel, 1986).

Until about 1.0 Ma the dominant cycle during the Quaternary was the 41 ka period. Since then the 100 ka periodicity has become dominant and resulting glaciation periods have been characterised by greater intensity than before, and in rapid deglaciation, with a few abrupt returns to cooler conditions; in contrast, glacial cooling is slow and uneven (Williams *et al.*, 1993). If two of the orbital forcing mechanisms are in phase, as was the case at 22 ka, when obliquity and eccentricity were both low, glacial maxima are especially intense (Emiliani, 1993).

The situation is, however, more complex than the above summary may suggest. Firstly, orbital forcing only triggers the onset of an ice-age; further development depends on the internal dynamics of the ocean-ice-atmosphere system (Emiliani, 1993). It has been suggested that contributions of the various components of this system were: land ice 0.9°C, sea ice 0.7°C, decreased water vapour 1.5°C, altered cloud cover 0.7°C, reduced CO_2 0.6°C and reduced vegetation 0.3°C (Rind, 1987). CO_2 and CH_4 changes observed in the Vostok core suggest that relatively weak orbital forcing is amplified by changes in these gases, and that they may constitute the link between the hemispheres (Lorius *et al.*, 1990). Further, up to 50% of the glacial-interglacial change at a global scale may be attributed to these two gases (Genthon *et al.*, 1987; Lorius *et al.*, 1992). Secondly, deglaciation of the southern hemisphere is nearly in phase with the northern hemisphere, both with respect to initiation and rate, although it has been argued that orbital forcing would have a lesser effect in the south because of the oceanic nature of the southern hemisphere's higher latitudes. Processes such as minor destabilisation of grounded ice-sheets or the long-range effects of ocean currents have been suggested to account for southern hemisphere deglaciation (Williams, 1993). In contrast, summer insolation at 60°S and 78°S could play an important role in sea ice extent around Antarctica: variations in the Vostok isotope record display similarities to variations in annual insolation receipts at 78°S (Genthon *et al.*, 1987).

Atmospheric compositions and mass can be regarded as constant except for the Greenhouse gases CO_2, CH_4, H_2O, O_3, volcanic aerosols and dust. CO_2 fluxes affect sea surface temperatures with positive feedbacks, in that warmer oceans release CO_2 as their capacity to hold dissolved CO_2 is reduced. CO_2 is directly linked to atmospheric warming as it absorbs longwave radiation. Changes in water vapour affect cloudiness and involve both positive and negative feedbacks with respect to warming, but moisture availability is affected primarily by ocean temperature. Moisture reduction also affects ice-sheet stability, in that continental ice-sheets are starved during times of lower moisture availability (Williams, 1993). SO_2 emitted from volcanoes easily converts to sulphate particles, which reflect solar radiation and act as cloud condensation nuclei (Chahine, 1992; Kerr, 1993e).

Ice-cap size fluxes effect the equator-pole temperature gradient, resulting in changes in wind strength and ocean current intensity (Williams, 1993). Albedo is also affected, with

The last maximum angle of obliquity was at 9 ka, while the last minimum was at 29 ka (Liu, 1992). The effect of the shift in perihelion does not alter the redistribution of annual insolation, but increases seasonality at lower latitudes (Phillipps and Held, 1994; Mangerud *et al.*, 1996). Each major glacial advance has been closely correlated with a minimum in the precession index; this is clearly demonstrated in the fluctuations of the Scandinavian ice sheet (Mangerud *et al.*, 1996).

Although the effect of eccentricity on incoming radiation is weak, this cycle dominates the record over the last million years. It has been argued that variations in the frequency of the obliquity cycle can result in a strong 100 ka forcing of climate (Liu, 1992), and it has been demonstrated that changes in eccentricity modulate the precessional amplitude (Liu, 1995). Recent work on the 100 ka cycle suggests that this cycle is not caused by eccentricity variations, but by changes in the inclination of the orbital plane. Variations in the inclination do not cause changes in insolation, but could, through the extraterrestrial accretion of meteorites and dust, bring about changes in the amount of solar radiation reaching the Earth (Figure 2.2) (Muller and MacDonald, 1995).

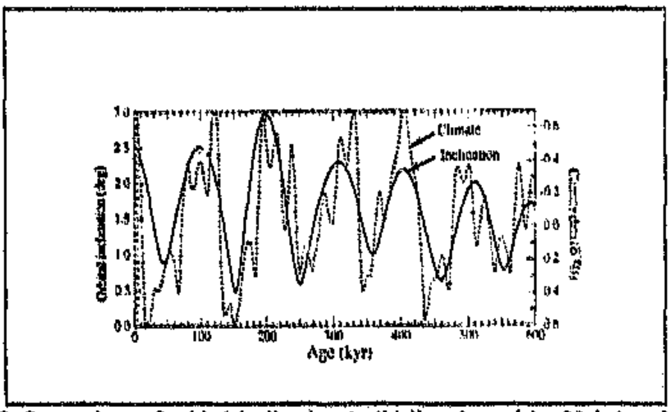

Fig. 2.2 Comparison of orbital inclination (solid line, lagged by 33 ka) and $\delta^{18}O$ climate data (dotted line) (Muller and MacDonald, 1995).

Milankovitch theory has, since the 1970s, received much support, especially since the paper by Hays *et al.*, (1976), and the Nato advanced research workshop on Milankovitch and climate (Berger *et al.*, 1984). Milankovitch orbital variations were compared with a number of indices from ocean cores including planktonic $\delta^{18}O$, SSTs, and the percentage of *Cyclodophora davisiana*, and it was concluded that frequencies observed in the geological sedimentological record matched orbital frequencies to within 5% (Hays *et al.*, 1976). Recently, the Milankovitch theory has been unsuccessfully challenged (Imbrie *et al.*, 1993; Emiliani, 1993). Results of model experiments linking the atmosphere, ocean, sea ice and other factors showed that 70% of northern hemisphere ice volume is related to astronomical forcing and related changes in albedo, while only 30% is related to CO_2 changes. Each time a decrease in insolation occurs, positive feedbacks amplify the response of the climate system, often with time lags of up to thousands of years (Berger *et al.*, 1993). Monsoonal systems, as modelled in GCMs, have been linked to precessional variations: thermally forced monsoon circulations are enhanced by the strengthened seasonal cycle of solar heating that results when the summer solstice occurs near the perihelion (Phillipps and Held, 1994; Partridge *et al.*,

CHAPTER TWO

Milankovitch, Boundary Conditions and Phase Lags

Climatic change at any scale must be considered in the light of certain boundary conditions or external forcing factors, such as solar input, atmospheric composition, ice-sheet distribution, local relationships between land and sea, ocean currents and sea-surface temperatures (Rind, 1987; Prell and Kutzbach, 1987; Harrison *et al.*, 1991; Williams *et al.*, 1993).

Boundary conditions are external variables which influence climate on a particular timescale. When considering climatic changes over the last 20 thousand years (ka),[1] position and size of continents can be regarded as constant, as can solar output. Although solar output may be regarded as constant at source, the amount of insolation received by the Earth may change over time, primarily because of orbital variations which govern the relationship between Earth and sun. The orbital variations have three major components: the obliquity of the earth with respect to the ecliptic plane, which varies by some 1.5° around a mean of 23.1° and has a period of about 41 ka, the eccentricity of the Earth's orbit with a period of about 100 ka, and the precession of the equinoxes, which affects the longitude of the perihelion and has a period of about 19 ka to 23 ka (Figure 2.1).

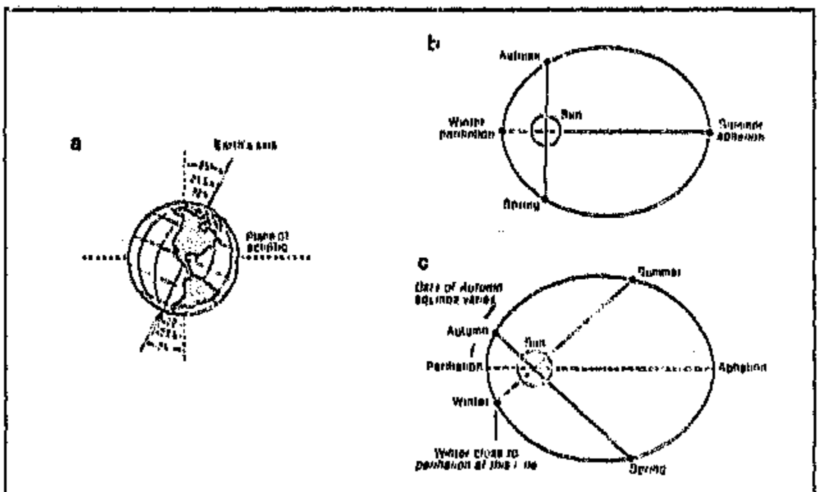

Fig. 2.1 The major components of the Milankovitch cycles: (a) variations in the obliquity of the ecliptic, (b) the eccentricity of the Earth's orbit and (c) the precession of the equinoxes, (Lindesay, 1990).

These changes in the Earth's eccentricity, axial tilt and longitude of the perihelion have given rise to glacial cycles with similar periods (Berger *et al.*, 1984; Prell and Kutzbach, 1987; COHMAP Members, 1988; Lindesay, 1990; Liu, 1992). A larger angle of obliquity results in greater seasonal changes, and is associated with rapid deglaciations (Berger *et al.*, 1984), and its effect is greatest at higher latitudes (Phillipps and Held, 1994).

[1] All dates cited in this review are ^{14}C years, where necessary, calculations follow the formula used in Jouzel *et al.*, (1995) i.e. Cal yrs = 1.24(age ^{14}C -0.84); or conversions used in Blanchon and Shaw, 1995).

200 000 years. Objectives of the PASH project are to collate and store existing high-quality data sets pertaining to the last glacial cycle using a hemispheric Geographic Information System, to extend and augment these sets where ever possible, and to analyse the records with a view to elucidating patterns and mechanisms of global change. A further objective is to provide data for use in the PAGES programme of the IGBP and its Pole - Equator - Pole (PEP) transects. Africa and its surrounding oceans can thus make a significant contribution to the understanding of global palaeoclimatic dynamics.

AIMS OF THE RESEARCH

The aim of the study is to determine the mechanisms underlying repetitive glacial-interglacial cycles during the Quaternary, with specific reference to the warming phase following the Last Glacial Maximum (LGM). The relationship between changing sea surface temperatures (SSTs) and changing rainfall and temperature patterns over southern Africa will be given prominence in order to determine whether present correlations accord with those which prevailed in the past, and to explore further the factors controlling local patterns of atmospheric circulation over land and sea.

This dissertation is based on a review of palaeoclimatic literature covering global climatic trends, and a review of literature pertaining directly to palaeoclimatic trends over Southern Africa. An analysis of palaeoclimatic maps of Southern Africa based on the data collected in the PASH project as well as data gleaned from the published literature is undertaken to determine the different moisture and temperature trends that characterized the past.

LITERATURE REVIEW

The literature review that follows covers a number of issues that are important in understanding the patterns of rainfall and temperature changes over southern Africa. Topics that are reviewed include Milankovitch orbital variations, boundary conditions and phase lags that control and modulate recurrent glacials and interglacials; recent work on the Greenland ice cores pertaining to the dynamics of climate changes; research on the thermohaline circulation and the formation of North Atlantic Deep Water (NADW) and Antarctic Bottom Water (AABW), the role of carbon dioxide in relation to climate changes and melt water pulses.

SECTION ONE

CHAPTER ONE

INTRODUCTION

Climatic change, both in the long and short term, is the focus of much current interest and research. A great deal of the latter is directed towards determining forcing mechanisms behind glacial and interglacial cycles as well as the accurate documentation of these events. Research enabling us to propose future climatic scenarios is of critical importance and relies not only on modelling, but on a clear understanding of how the climate operated in the past.

The climate of southern Africa over the last 20 000 years has been investigated using proxy indicators, and changes in temperature and moisture have been documented at a substantial number of sites (Vogel, 1984; Partridge and Williams, 1993). Notwithstanding this progress, a cursory examination of the literature suggests that considerably less information is available for southern Africa than for most areas of the northern hemisphere (Figure 1.1) (COHMAP, 1988).

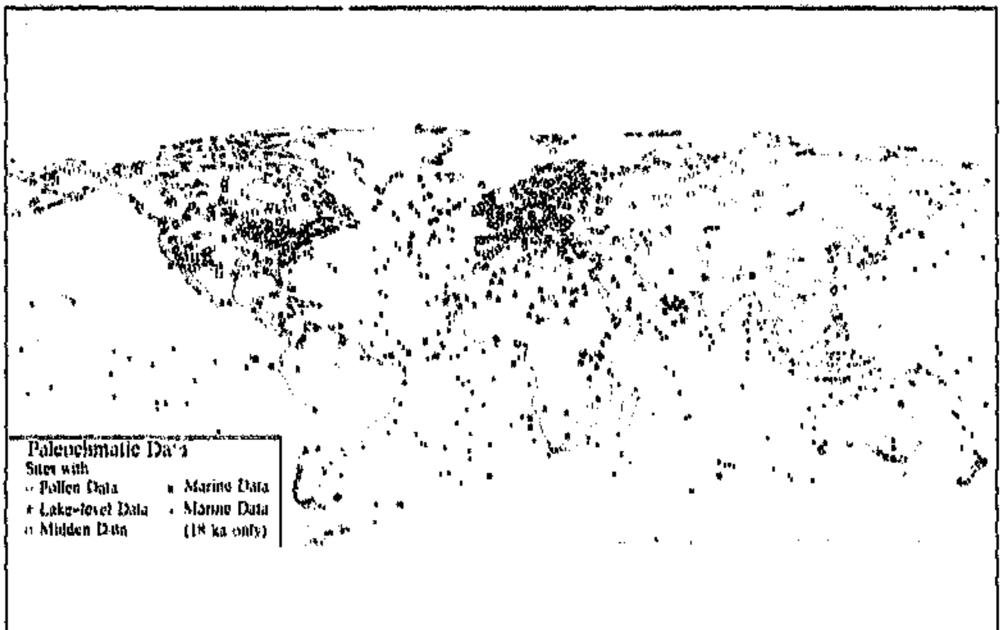

Fig. 1.1 Location of sites in the COHMAP global palaeoclimate database (COHMAP Members, 1988).

Climate is a global phenomenon and an understanding of southern hemisphere dynamics with respect to ocean-atmosphere interactions is as important as an appreciation of northern hemisphere processes for proper comprehension of the whole. It is in this light that the INQUA Project on Palaeoclimates of the Southern Hemisphere (PASH) was initiated, under the leadership of Professor T.C. Partridge of the Climatology Research Group, in order to better document southern hemispheric palaeoclimates during the last

CONTENTS

Introduction 2
Aims of the Research 3
Literature Review 3
Milankovitch, Boundary Conditions and Phase Lags 4
CO_2 and Temperature Cycles 8
Recent Evidence from Ice-cores 11
Dansgaard-Oeschger Events and Heinrich Events 18
NADW Formation and the Thermohaline Conveyor Belt 30
Models of the Thermohaline Circulation 41
Deglaciations and Melt Water Pulses 47
Data and Methodology 51
Results 52
Southern African Palaeoclimate since 40 000 B.P. 52
Present Day Southern Hemisphere Climates 80
AABW Formation and the Role of Antarctic Sea Ice 89
Southern Hemisphere – Northern Hemisphere Synchroneity 98
The Younger Dryas Cold Epoch and its Southern Hemisphere Counterpart 105
Conclusion 114
Appendix 1 116
Appendix 2 138
Appendix 3 143
References for PASH Data Only 143
References 147

To my wife, Suzanne, and my parents Carlo and Maureen Barbafiera

Climatology Research Group of the University of the Witwatersrand are thanked for helpful comments and discussion. The financial assitance of the FRD is acknowledged in making the study possible. My parents are thanked for their patience and support, and my wife Suzanne is thanked for all her typing and support in order to complete this study.

PREFACE

Palaeoclimates of southern Africa have attracted a considerable amount of attention in order to understand many of the documented changes in fauna and flora evident on the subcontinent. A large amount of literature has emerged in this respect but conflicting conclusions have compromised a clear understanding of this region's past climate. As studies concerned with future climates are based on an understanding of the past, it has become necessary to resolve these ambiguities and to provide an accurate as possible understanding of southern Africa's palaeoclimate. Regional climates are a product of global climate interactions between the ocean and the atmosphere and it is vital to understand global climate forcing mechanisms especially in terms of variations in atmospheric composition and oceanographic dynamics over time.

Chapter 1 introduces the topic under investigation, the aims of the research and the literature review that follows. *Chapter 2* discusses the boundary conditions, phase lags and underlying orbital dynamics (Milankovitch theory) that effect climate changes. The role of carbon dioxide is investigated especially in relation to ocean atmosphere interactions. *Chapter 3* examines recent discoveries concerning global climate change as revealed in Greenland, and the theories derived to explain these changes such as Dansgaard-Oeschger and Heinrich events.

Chapter 4 reviews current understanding of global ocean dynamics in terms of the thermohaline conveyor belt and the formation of deep water. A review of current modelling studies on ocean dynamics is included in this section. The relationship between deglaciations and melt water pulses concludes the chapter.

Chapter 5 introduces the focus on the southern African palaeoclimates, and describes the data and methodology used in the production of the maps that follow. *Chapter 6* reviews the palaeoclimate of southern Africa since 40 ka. This is based on the maps and a review of the available current literature. *Chapter 7* summarises current southern African climates and compares the trends derived from the maps to contemporary modelling studies. The chapter then examines the role of Antarctic deep water formation and the role of sea ice in regulating southern Africa's climate, before examining the synchroneity between the northern and southern hemispheres in terms of climate change. *Chapter 8* discusses the Younger Dryas cold epoch and its southern hemisphere counterpart before concluding the dissertation.

This study has been initiated as part of the Palaeoclimates of the Southern Hemisphere (PASH) project, as detailed in Chapter 1. Except where specified, the convention adopted for time reference is as follows: dates are given in ka BP (10^3 years Before Present) with present defined as AD 1950, and ^{14}C dates are uncalibrated.

The supervision and help of Professor T.C. Partridge, and the assistance of James Hamilton in the preparation of the maps is gratefully acknowledged. Members of the

ABSTRACT

The palaeoclimate of southern Africa for the last twenty thousand years is investigated through the production of palaeoclimate maps based on an analysis of literature and data from the ongoing PASH project. The trends from the maps are compared with published reviews and modelling studies of the region's palaeoclimates, and are contextualised in terms of global palaeoceanographic and palaeoclimatic dynamics. The changes evident in the past climate of southern Africa tend to mirror global climate changes, however, evidence exists that the timing of climate changes between the two hemispheres are not quite synchronous, and may not fit present theories of global palaeoclimate dynamics.

I declare that this dissertation is my own, unaided work. It has not been submitted before for any other degree or examination at any other University.

MARIO BARBAFIERA

University of the Witwatersrand, 1997

AN EXAMINATION OF PALAEO-SEA SURFACE TEMPERATURES AND THEIR INFLUENCE ON SOUTHERN AFRICAN PALAEOCLIMATES OVER THE LAST 20 000 YEARS

Mario Barbafiera

A Dissertation Submitted to the Faculty of Science, University of the Witwatersrand, Johannesburg, for the Degree of Master of Science

Johannesburg, 1997

Dansgaard-Oeschger Events and Heinrich Events

Heinrich events are a record of massive discharges of icebergs across the North Atlantic ocean which left layers of ice rafted debris (IRD) as they melted. In 1988, Heinrich published the results of an analysis of 13 piston cores collected from the Dreizack and surrounding deep plain (Figure 3.7). The cores were analysed in terms of the composition of the coarse fraction and dated using oxygen-isotope stratigraphy. The analysis was restricted to the last 140 000 years due to discordances below the stage 6/5 boundary in the cores. Above this boundary, the cores were all uniform, showing six distinct peaks of ice rafted debris ranging in size from 180 μm to 3000 μm (Figure 3.8). Sedimentation rates varied between 2 cm/1000 a and 3 cm/1000 a.

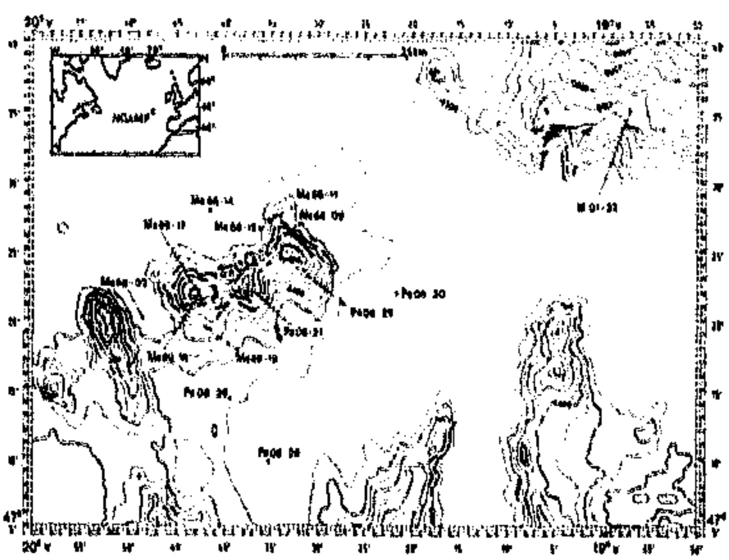

Fig. 3.7 Bathymetric map (Sea Beam) of the area around the Dreizack seamount (19°40'W, 47°23'N) showing core locations. Contour interval = 50 m (Heinrich, 1988).

An analysis of the planktic foraminifera in the cores was also undertaken in order to determine palaeo-SSTs. The absolute abundance of foraminifera is low during these events, and it is now accepted that a minimum in foraminifera per gram is acceptable as evidence of a Heinrich event (Keigwin and Lehman, 1994). Concentrations of *Neogloboquadrina pachyderma* (sinistral), a cold water (polar) species, however, correlate nearly perfectly with the ice rafted debris peaks. Not all increases in polar foraminifera are, however, associated with IRD, although all IRD layers are associated with increases in the polar foraminifera. Thus iceberg surges correlate with cold oceans, but cold seas alone are insufficient to produce IRD (McManus *et al.*, 1994).

have been absent, it appears that the global thermohaline circulation is more stable because of the absence of meltwater-induced mode switches (Broecker, 1994b).

The questions that the Summit cores pose are why the Holocene climate has not oscillated in a similar fashion to the Eemian, and how a mode switch can be sustained for between 70 years and 5 ka after it has initially been triggered by a higher frequency oscillation in the atmospheric system of 1 - 2 decades duration (GRIP Members, 1993). The search is now on for possible causes of large temperature oscillations that occur within short time periods (Charles *et al.*, 1994); boundary conditions such as insolation, ocean salt budgets, atmospheric CO_2 concentrations and ice-sheet size are considered unlikely to change rapidly enough to afford an explanation (Alley *et al.*, 1993; Grootes *et al.*, 1993). However, fresh water input from surging ice-sheets could affect the thermohaline circulation of the North Atlantic (Johnsen *et al.*, 1995). Other forcing agents which can change rapidly, i.e. on decadal time scales, are water vapor, clouds, sea ice and snow cover (Lorius *et al.*, 1990); these are possibly forced by changes in the North Atlantic Ocean mixed layer and resulting changes in SSTs (Charles *et al.*, 1994).

What ice cores do tell us, is that CO_2 and other greenhouse gases and changing climate are strongly correlated (Lorius *et al.*, 1990), and that dustiness and temperature are also linked, with increased dustiness associated with lower temperatures (Lehman, 1993b; Taylor *et al.*, 1993a). These markers indicate that interglacials begin abruptly - within a few decades - but terminate gradually in a stepwise fashion (Johnsen *et al.*, 1992; Peel, 1992). The transitions are not smooth, but alternate between preferred states. It is probable that a re-ordering of atmospheric circulation - taking into account factors such as wind speeds, surface moisture and air mass routing - could account for these repeated mode changes (Taylor *et al.*, 1993a; Johnsen, 1993). Trigger mechanisms possibly lie in the North Atlantic climate system or in a gradual slow down, (but abrupt resumption), of NADW formation (Alley *et al.*, 1993).

nonetheless be accurate since the section spanning the Eemian is 200 m above the bedrock contact, and may thus not have been affected by ice movements, despite the fact that the positioning of the divide may have changed slightly since the Eemian. Visual examination of the core reveals no disturbance of the ice layering until after Eemian times (GRIP Members, 1993). In contrast, Souchez *et al.* (1995), argued on the basis of an analysis of CO_2 and CH_4 records, that ice near the bottom of the GRIP core has been subjected to flow-induced mixing. Johnsen *et al.* (1995), analyzed the stratigraphic continuity of the Eemian layers and concluded, after deconvolution, frequency analysis and cloudy band observations of the lower sections of the core, that the inferred climatic oscillations were, in fact, real. Large scale folding in the Summit area does not occur as the bedrock is gently sloping ($\lesssim$ 40 m/km) (Dansgaard *et al.*, 1993); nor has it been possible to find two layers of identical isotopic and chemical composition, i.e. $\delta^{18}O$, acidity, and concentrations of dust and nitrate, that would suggest duplication by folding (Johnsen *et al.*, 1995). Independent reports from Central Europe suggest that the postulated Eemian instabilities may be real, in that pollen records from that area reveal similarities both in structure and timing to the changes observed in the GRIP core (Zahn, 1994).

Keigwin *et al.* (1994), record SST changes in the North Atlantic that correlate closely with the Greenland ice core record for the period 70 ka to 130 ka. No changes in NADW formation during substage 5e were identified, suggesting either that the Eemian fluctuations are an artifact of ice flow, or that the presence of large ice sheets may be a prerequisite for abrupt variations in NADW. Eemian climate instability may, however, have a different origin from that associated with later climatic events. Weaver and Hughes (1994), suggest that increased variability in the hydrological cycle associated with a warmer Eemian climate could account for the rapid climatic oscillations observed in the cores, although the variability is linked to changes in the thermohaline circulation forced by freshwater fluxes which are not necessarily connected to ice-sheets.

Johnsen *et al.* (1995), suggest that Greenland may have experienced periods of cold while the rest of Europe remained relatively warmer. This could occur if the location of deepwater formation changed. If deepwater formation moved closer to Europe, the westerlies in middle and high latitudes would gain a stronger northward component, increasing the intensity of the Gulf Stream and cold East Greenland current. This scenario is supported by an analysis of Norwegian Sea sediments and the evidence of more southerly extent of sea ice off the Greenland coast. Eemian coolings could thus be the result of longitudinal movements in flow patterns, as opposed to latitudinal changes associated with glacial periods (Johnsen *et al.*, 1995).

Assuming that the GRIP record is accurate, Eemian temperatures oscillated between much cooler and significantly warmer states with decadal rates of temperature change (White, 1993). Climatologists are concerned that this could, by analogy, be taken as a norm for the Holocene and that rapid, dramatic temperature oscillations could occur, especially now that man is performing the "greenhouse experiment" (Broecker, 1987; White, 1993). Evidence from Southern Africa suggests that the postglacial warming occurred at a rate of about 1°C per millenium; present day rates of warming calculated for the period 1950 - 1985 were as high as 0.2°C - 0.7°C per decade (Thackeray, 1990). It is now believed that the last 8 ka have been "strangely stable" (GRIP Members, 1993). On the other hand, since the beginning of the Holocene, during which large ice-sheets

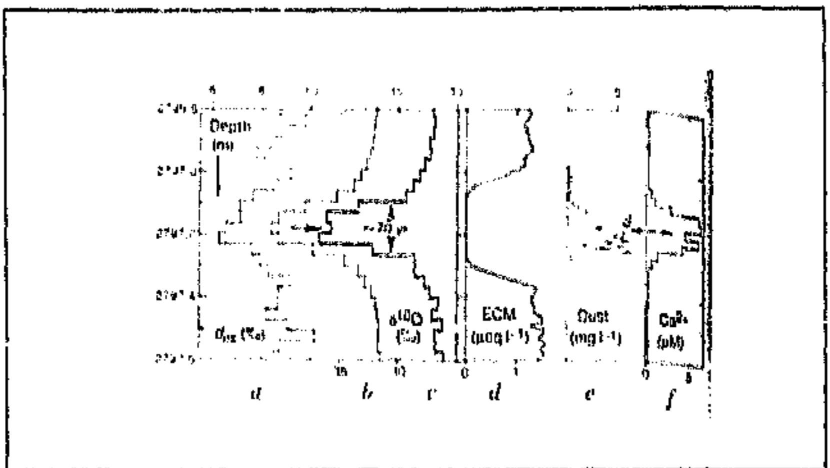

Fig. 3.5 Profiles of five parameters through 'event 1', a rapid climatic oscillation (±70 a duration) at the culmination of the Eemian interglacial at 115 ka. (a) Deuterium excess; (b) oxygen isotope ratio; (c) same as (b), but deconvoluted to account for diffusion; (d) acidity measured by ECM in microequivalents per litre; (e) dust concentration measured from scattered laser light and calibrated by Coulter Counter by integrating size distribution. (f) calcium ion concentration (GRIP Members, 1993).

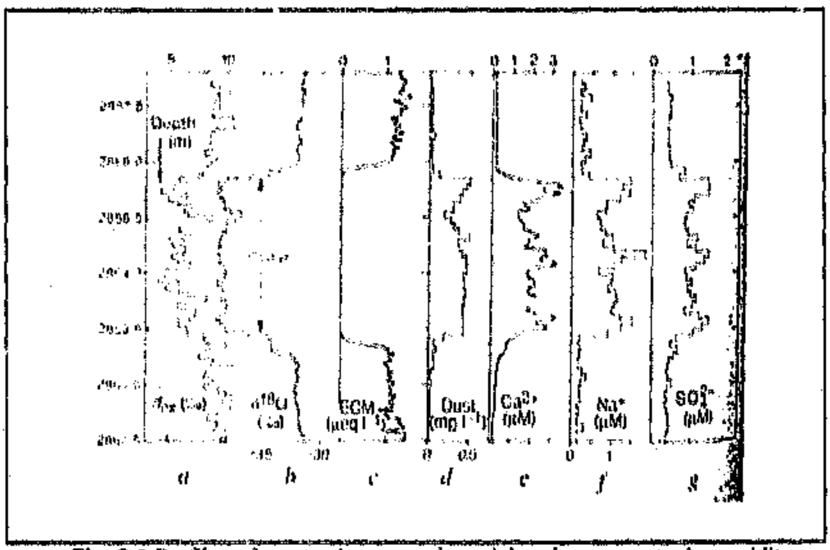

Fig. 3.6 Profiles of oxygen isotope ratio, calcium ion concentration, acidity by ECM, dust, deuterium excess, sodium and sulphate through 'event 2', a climate oscillation sustained for ±750 a in the initial stages of the Eemian interglacial at 131 ka (GRIP Members, 1993).

The validity of these conclusions is dependent on corroboration from the GISP2 core. At this depth, the cores do not correlate well, possibly because within the GISP2 core (28 km further west of GRIP at the ice divide) the lowermost layers (about 10% of the core) may have been distorted by ice movement (Appenzeller, 1993; Boulton, 1993; GRIP Members, 1993; Grootes *et al.*, 1993). The picture provided by the GRIP core may

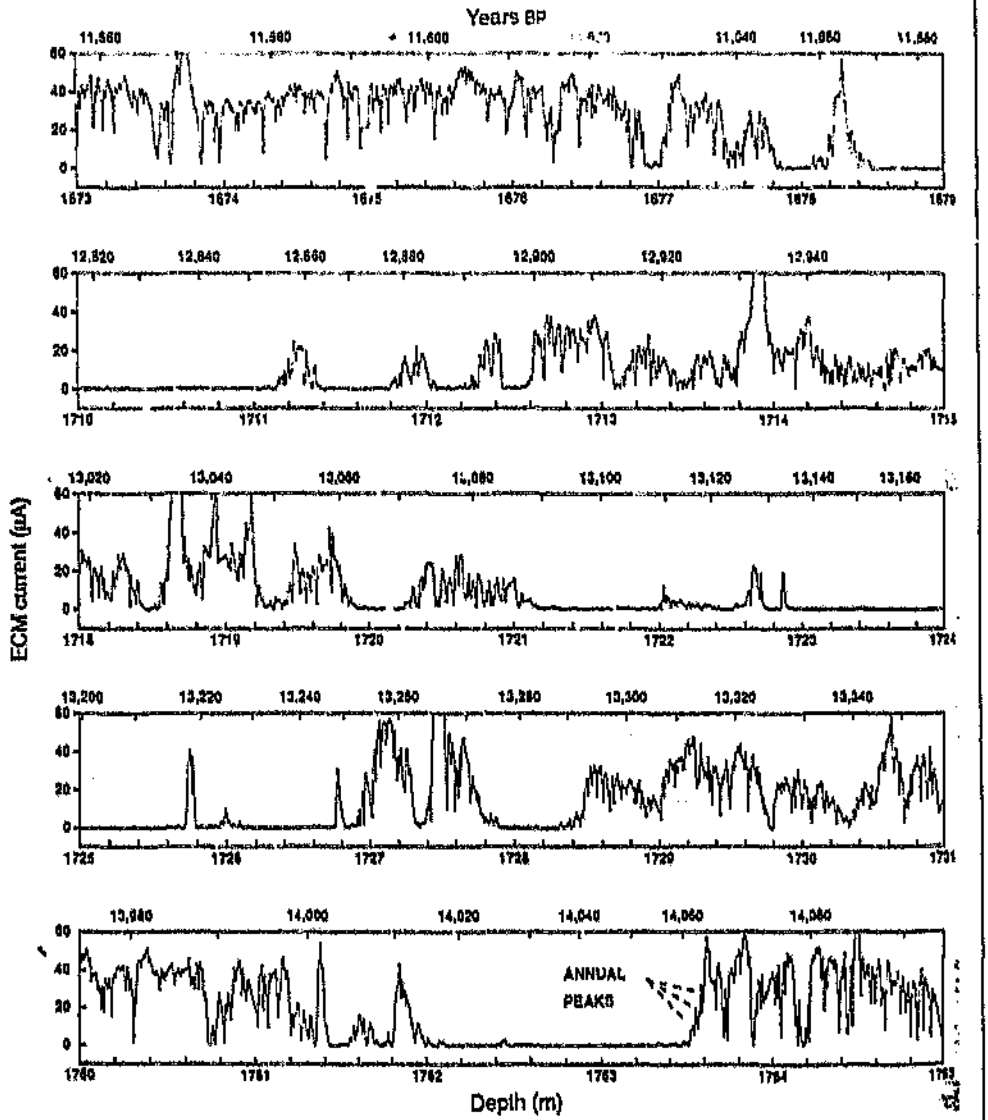

Fig. 3.4 (a - e). Expanded ECM records of recent climate transitions plotted against depth (bottom axis) with one sample per millimetre of depth. (a) Start of Holocene, end of Younger Dryas. (b) Start of Younger Dryas. (c) End of inter-Allerød cold period. (d) Start of inter-Allerød cold period. (e) Transition. The top axes are age, in years BP. At this scale the annual signal in the ECM can occasionally be resolved as small local peaks that occur once per year. During the transition at 14,060 (e) three annual peaks can be resolved. The annual layer thickness is ± 6 cm per year during warmer, less dusty conditions and 3 cm per year during colder, dusty conditions. Occasionally the number of ECM annual peaks and annual layers in a given segment differ slightly because particulate and visual stratigraphy records were also considered when annual layers were identified (Taylor *et al.*, 1993b).

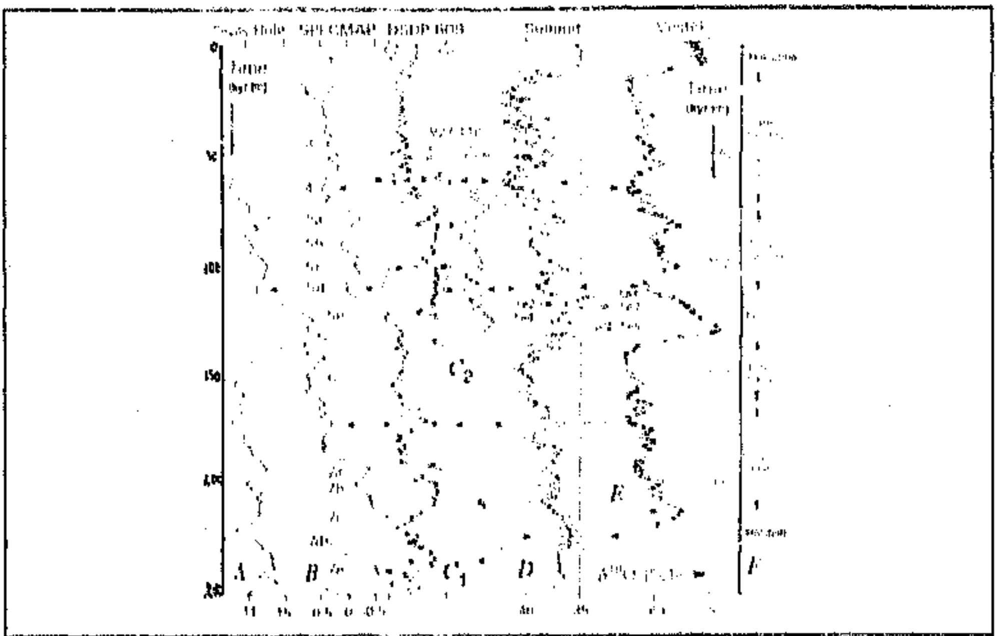

Fig. 3.2 The continuous GRIP Summit $\delta^{18}O$ record plotted in two sections on a linear depth scale: A, from surface to 1,500 m; B, from 1,500 to 3,000 m depth. Each point represents 2.2 m of core increment. Glacial interstadials are numbered to the right of the B curve. The timescale in the middle is obtained by counting annual layers back to 14.5 ka, and beyond that by ice flow modeling. The glacial interstadials of longest duration are reconciled with European pollen horizons (Dansgaard *et al.*, 1993)

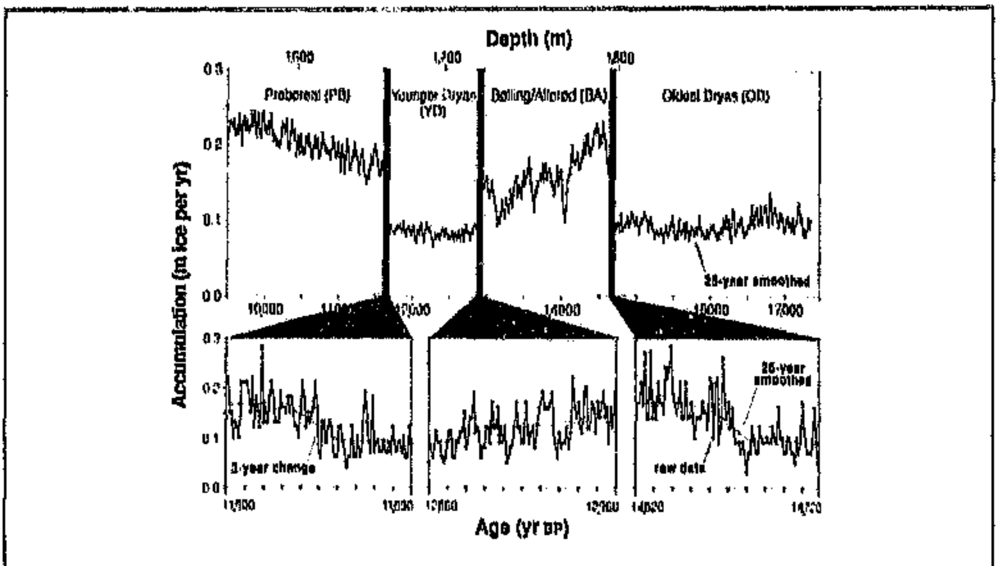

Fig. 3.3 Late-glacial accumulation-rate history at GISP 2, estimated from data and modeling. Ages are in years before 1950. The 25 year running mean is shown in all panels. Yearly data are shown for the rapid changes at the onsets of the Preboreal (b), and the Bolling/Allerod (d), and the slower change at the onset of the Younger Dryas (c). The arrow in b indicates the possible one- to three-year termination of the Younger Dryas. The resolution in b, c and d is controlled by the 5-mm precision used in recording the layer-thickness data (Alley *et al.*, 1993).

However, the gradual decreases in accumulation rates during cold periods and rapid increases from cold to warm periods may be ascribed to NADW fluxes (Alley *et al.*, 1993).

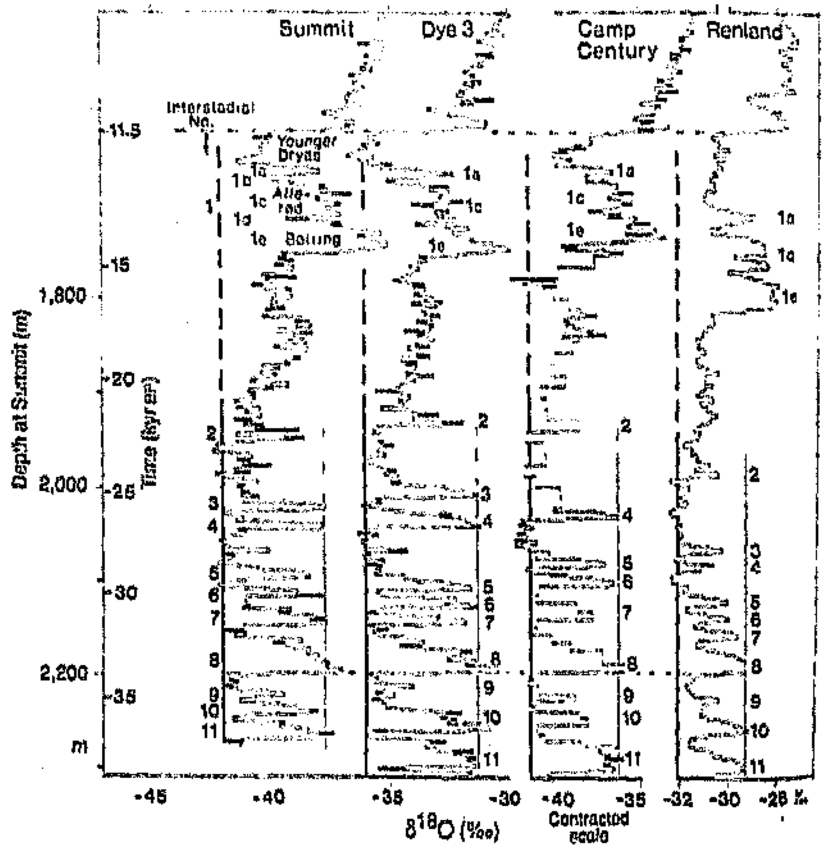

Fig. 3.1 Continuous $\delta^{18}O$ profiles along sections of four Greenland ice cores from Summit (Central), Dye 3 (Southeast), Camp Century (Northwest) and Renland (East Greenland), spanning nearly the same time interval. The four records are all plotted on linear depth scales, of which only the Summit depth scale is shown to the left along with a Summit time scale. The heavy and thin vertical lines indicate estimated δ levels characteristic of late-glacial cold and mild stages respectively. The figures close to these lines define a suggested numbering of significant mid- and late-glacial interstadials (Johnsen *et al.*, 1992).

Detailed analysis of the Eemian Interglacial (135 ka - 115 ka) as revealed in the GRIP core, using electrical conductivity and dust (Ca) content, revealed that climate and circulation patterns were similar to the present. However, three warm substages of marine isotope stage (MIS) 5e, where temperatures were 2°C warmer than present, are discernible in the ice record, and are characterised by a very different overall pattern. High-amplitude, high-frequency oscillations in the constituents of the core suggest the occurrence of two large (10°C - 14°C) decreases in temperature that lasted for 70 and 750 years respectively, followed by a rapid return to previous conditions (Figure 3.5 and 3.6) (GRIP Members, 1993).

CHAPTER THREE

Recent Evidence from Ice-cores

Reconstructions of past climates from ice-cores have many advantages in that numerous indices of temperature and available moisture are trapped in the ice (Lorius *et al.*, 1985). ^{18}O data, the chemical composition of atmospheric air bubbles and dust content can be interpreted along the core (White, 1993); high temporal resolutions have been obtained recently. A number of cores have been extracted from Greenland, the most important are two taken from the ice divide, at the so-called Summit sites (Johnsen *et al.*, 1992). These two cores, denoted as Greenland Ice Core Project (GRIP) and the Greenland Ice Sheet Project 2 (GISP2), are located at a point where horizontal ice movement is minimal (Johnsen *et al.*, 1992; Kerr, 1993a) except at the bedrock boundary (Boulton, 1993). Further, temperatures seldom rise above freezing point, which prevents distortions in the record due to post-depositional changes (Johnsen *et al.*, 1992). Thus an undisturbed climatic history of at least 95 ka can be obtained from the total of 150 ka - 200 ka spanned by the cores (Boulton, 1993; Peel, 1993; Taylor *et al.*, 1993a).

A comparison of the $^{18}O/^{16}O$ ratio (denoted by $\delta^{18}O$) of the various cores from Greenland (Figure 3.1) was undertaken. The cores are closely correlated, ruling out disturbed stratigraphy as a cause of the $\delta^{18}O$ shifts. An accurate record of climatic changes has been preserved where high $\delta^{18}O$ levels indicate mild interstadials and low $\delta^{18}O$ levels indicate stadials (Johnsen *et al.*, 1992). Most importantly, a temporal resolution of decades can be achieved, which provides to climatologists an unprecedented level of palaeoclimatic detail (Peel, 1993). Further, the cores correlate well with other records from various sources (Figure 3.2) (Dansgaard, *et al.*, 1993).Using current conversions of $\delta^{18}O\,^0/_{00}$ to temperature, the cores reveal that cold stadials were some 7°C colder than mild stadials, and between 12°C and 13°C colder than the present. Recent analysis of the borehole temperature and ice-core isotopic composition has revealed that the warming from average glacial conditions to the Holocene was up to 15°C, and that the coldest periods were possibly 21°C colder than present over the Greenland ice sheet (Cuffey *et al.*, 1995). The cores also reveal that interstadials last from 500 to 2 000 years, beginning abruptly (within decades) and terminating gradually in a stepwise fashion (Johnsen *et al.*, 1992).

The ability to resolve climatic change to decades has unleashed some surprises. For example, the Younger Dryas event ended very abruptly, within about 50 years according to Johnsen *et al.* (1992) and 20 years according to Mayewski *et al.* (1993). Massive, frequent and short-term changes in atmospheric composition are documented in the cores; these are probably the result of changes in the size of the polar atmospheric cell. An analysis of the annual layers in the cores showed that snow accumulation doubled over a period of 1 - 3 years at the Younger Dryas/Preboreal boundary (Alley *et al.*, 1993) and that the change in accumulation-rate from the Older Dryas to the Bølling Allerød was large and abrupt (Figure 3.3). Climate may, in fact, have switched from glacial to interglacial conditions within a period of 3 to 5 years (Fairbanks, 1993). Taylor *et al.* (1993b), using electrical conductivity measurements from the GISP2 core, documented fluctuations in the order of 5 - 20 years (Figure 3.4) which reflect changes in the dust content of the atmosphere. Only very rapid reorganization of the oceanic and/or atmospheric circulation can account for such rapid oscillations in dust content.

The above hypothesis is supported by a detectable increase in organic carbon production, as deduced from $\delta^{13}C$, increased sedimentary C concentrations and burial rates, (Archer and Maier-Reimer, 1994) and a change in foraminiferal assemblages as observed by the movement of the front between silica and calcite formation, which was displaced to lower latitudes during the last glacial, resulting in a shift from calcite towards siliceous production. Estimations of oceanic pH as 0.3 units higher during the last glaciation (Sanyal *et al.*, 1995) tends to support the C_{ORG} /$CaCO_3$ ratio change hypothesis.

Contrary to the above suggestions are indications that the Antarctic Ocean was characterised by lower productivity during the last glaciation, which would not favour lowering of the pCO_2 of the ocean (Mortlock *et al.*, 1991). The C_{ORG} /$CaCO_3$ ratio theory is also in contrast to the "coral reef hypothesis", which suggests an increase in $CaCO_3$ burial rates during glacials when coral reef growth is suppressed as ocean temperature and levels drop (Archer and Maier-Reimer, 1994).

It has been suggested that Southern Ocean deep water chemistry is controlled by variations in North Atlantic Deep Water (NADW) formation. Low NADW production initiates a decline in $CaCO_3$ with the attendant CO_2 reduction. NADW and $CaCO_3$ minima are correlated (Howard and Prell, 1994), but $CaCO_3$ minima precede NADW reductions in many instances, and generally $CaCO_3$ chemistry changes lead NADW fluxes.

the LGM (Barnola *et al.*, 1987), or cooler SSTs, will result in CO_2 absorption (Keller and Goldstein, 1995), with the reverse occurring with warmer SSTs (Corfield, 1994).

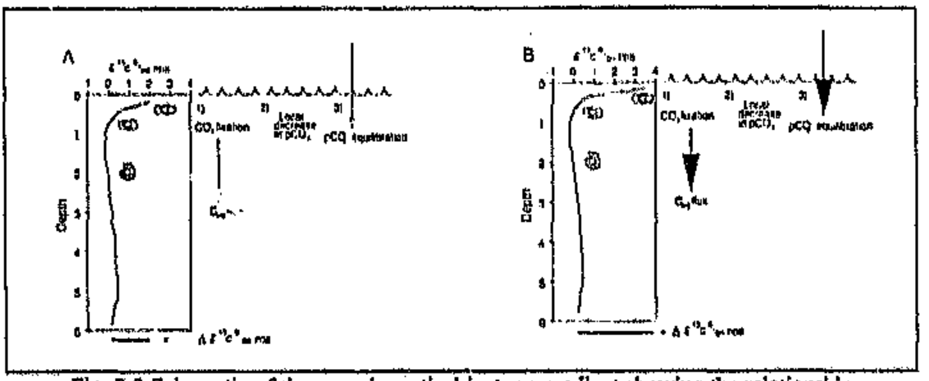

Fig. 2.3 Schematic of the oceanic vertical isotope gradient showing the relationship between increasing productivity, intensity of the sub-surface oxygen minimum and marine and atmospheric CO_2. A = low productivity ocean, B = high productivity ocean (Corfield, 1994).

CO_2 reacts with water to form H_2CO_3, HCO_3^- and CO_3^{-2}. The biological pump transports carbon in the form of biogenic debris to lower depths, and as this debris decomposes, CO_2 is released into the water (Takahashi, 1989; Corfield, 1994). Studies of $CaCO_3$ preservation in deep sea sediments (Archer and Maier-Reimer, 1994) and ocean pH (Sanyal *et al.*, 1995), suggest that a control of glacial pCO_2 is the changing ratio between organic carbon (C_{ORG}) and calcite ($CaCO_3$) in the oceans. Degradation of C_{ORG} in sediments promotes the dissolution of $CaCO_3$ which absorbs CO_2 and subsequently lowers the oceanic pCO_2 with respect to the atmosphere. CO_3^{-2} released when $CaCO_3$ dissolves, reacts with H_2O and CO_2 to form HCO_3^-; the pH of the ocean is subsequently increased through the reaction $CO_2 + CO_3^{-2} + H_2O = 2HCO_3^-$ (Figure 2.4) (Hasselmann, 1991).

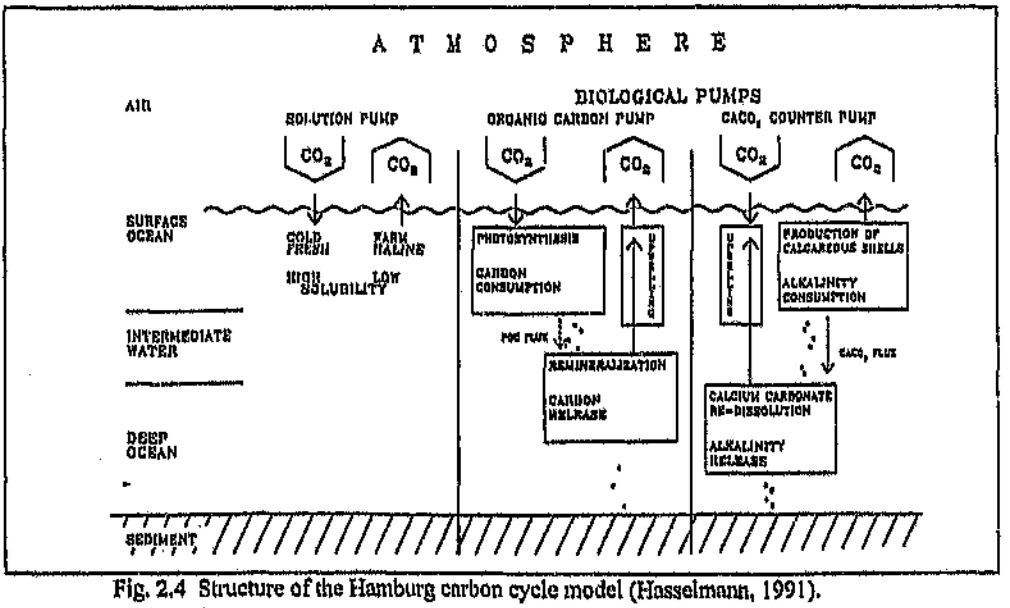

Fig. 2.4 Structure of the Hamburg carbon cycle model (Hasselmann, 1991).

CO_2 and Temperature Cycles

CO_2 fluxes have been unambiguously correlated with temperature changes (Barnola *et al.*, 1991), with atmospheric CO_2 lowered from about 280 ppmv to 200 ppmv during glacials. Only the ocean's carbon system can account for changes of this magnitude, through circulation changes, chemistry and biological activity (Lorius *et al.*, 1985; Boyle, 1990; Lorius *et al.*, 1990; Street-Perrott, 1994).

Lorius *et al.* (1985) hypothesised that CO_2 changes are not a consequence of climatic change, but a mechanism linked to the orbital variations which induce these changes; thus CO_2 would lag orbital forcing, but lead ice volume. Research suggests that climatic changes are triggered by insolational changes which are amplified by CO_2 forcing (Genthon *et al.*, 1987; Lorius *et al.*, 1993). It has been noted that high latitude winter insolation changes associated with latitudinal shifts in bottom water formation increase phytoplanktonic growth and result in CO_2 decreases (Lindstrom, 1990). Analysis of the CO_2 curve at Vostok shows a clear 21 ka peak but no clear unambiguous 41 ka obliquity cycle (Barnola *et al.*, 1987). The precise phase relationship between CO_2 levels and glacial-interglacial transitions is not fully resolved, with the suggestion that CO_2 increases are in phase with, or lag slightly (1 ka), the onset of glaciations, but post-date by up to 4 ka the onset of deglaciations (Barnola *et al.*, 1991). This would imply that CO_2 changes are a result of cooling or warming, rather than the cause thereof. The 30% decrease in partial pressure of CO_2 (pCO_2) at the LGM was probably caused by an increase in productivity or a change in ocean circulation patterns (Veum *et al.*, 1992); a redistribution of nutrients from intermediate water to deep water may provide a drawdown mechanism for atmospheric CO_2.

The oceans are the largest reservoirs of CO_2, containing 50 times more than the atmosphere and 20 times more than the biosphere (Takahashi, 1989). Atmospheric CO_2 fluxes are primarily due to ocean carbon cycle changes, with vegetation changes playing a secondary role (Ryabchenko, 1989). The interaction of the ocean and atmosphere with respect to oceanic absorption or outgassing of CO_2 depends on a number of factors, including temperature and biological activity (Corfield, 1994). The ability of the ocean to hold CO_2 is governed by the chemical properties of CO_2 in sea water, the downward biological pump, and ocean circulation rates and patterns. Mechanisms responsible for lower atmospheric CO_2 include lower polar ocean temperatures, increased salinity due to lower ocean volume, more $\Sigma\ CO_2$ in the deep ocean due to erosion of shelf organic material, increased alkalinity in deep ocean layers and an increase in primary production of phytoplankton because of increased upwelling (Takahashi, 1989).

Increased organic carbon production in surface waters absorbs oceanic CO_2 by fixing C in organic material. This lowers the pCO_2 of the ocean surface which draws down CO_2 from the atmosphere (Figure 2.3) (Corfield, 1994; Howard and Prell, 1994). The increase of biological activity results from enhanced nutrient availability which is temperature dependant. Analysis of $^{15}N/^{14}N$ records from ocean cores suggest that denitrification (degradation of nitrate by bacteria) was diminished during glacial periods, which would enhance biological activity, resulting in lower CO_2 concentrations (Ganeshram *et al.*, 1995). Thus enhanced upwelling of cold water, as argued for during large ice-caps resulting in positive cooling feedback. Fluxes in ice-cap size also alter sea level, with consequent albedo and vegetation cover changes (Williams, 1993).

Oceans are major heat sinks, as well as transfer agents. They are an almost unlimited source of moisture, although their surface temperature can control the rate at which this moisture is made available. Oceans also represent massive reservoirs of carbon in various phases. Their dynamics influence biological activity on a vast scale, which results in CO_2 being absorbed or released (Chahine, 1992). It is thus not possible to isolate one particular factor as being responsible for glacial cycles, as there is such a strong interdependence between all these variables (Williams, 1993).

When examining various boundary conditions, it must be remembered that each influences in different ways the lags between radiative forcing and climatic response. Global ice volume lags insolation changes on scales of thousands of years (Harrison *et al.*, 1992), while greenhouse gas concentrations and ocean circulation changes respond on scales of decades to centuries (Hoffert and Covey, 1992). Fast feedbacks with phase lags of decades or less occur with respect to water vapour, clouds, sea ice and snow cover (Lorius *et al.*, 1990). Phase lags occur because changes are in response to variations in receipts of solar radiation, rather than to climate forcing. Thus a relatively weak orbital trigger in northern latitudes can, through slow feedbacks associated with greenhouse gases, result in synchronous changes in temperature in both hemispheres (Lorius *et al.*, 1990).

Ice growth and ocean cooling are similarly diachronistic: it is argued that ice growth at 115 ka preceded ocean cooling by about 4 - 4.5 ka (Ruddiman *et al.*, 1980; Williams *et al.*, 1993) as terrestrial ice-sheet growth was not, initially, paralleled by declining ocean temperatures. Oceanic thermal inertia dampens the response of the climate to external forcing (Jones *et al.*, 1985; Berger and Labeyrie, 1987), in the case of increased CO_2 by between 10 and 50 years.

CHAPTER FOUR

NADW Formation and the Thermohaline Conveyor Belt

It is generally agreed that Quaternary glacial cycles were dominated by rapid reorganisations of the ocean-atmosphere system that were driven by orbitally induced changes in fresh water transport, which affected the salt structure of the sea (Broecker and Denton, 1989). Greenland climate changes are driven by oscillations in the salinity of the Atlantic Ocean which modulate the strength of the Atlantic's conveyor circulation (Broecker *et al.*, 1990), and as Greenland is situated close to the region of most intense modern NADW formation, it is well situated to record climatic events associated with changes in this process (Sakai and Peltier, 1995). Oscillations of up to 7°C within a 50 year period occurred too frequently and abruptly to be directly forced by changes in insolation (Lehman and Keigwin, 1992a); thus sudden changes in the rate of thermohaline overturn in the North Atlantic could account for the documented changes in temperature. Sporadic shutdown of NADW is recognised in sediments around the world, which also show the diminished importance of NADW during glacial periods (Berger and Vincent, 1986). Suggestions have been made that the conveyor would affect southern hemisphere climates by modulating Antarctic sea ice volumes (Kerr, 1993b; Lehman, 1993a).

The North Atlantic is characterised by an excess of evaporation over precipitation, resulting in salt enrichment (Broecker *et al.*, 1985). Denser, salt enriched water sinks to depths of about 1 000 m (Clarke, 1992) and drives the conveyor belt (Lehman, 1993a), although an alternative view suggests that thermal forcing due to intense heat loss dominates the haline forcing (Weaver, 1993). The cold, dense, deep water flows around Africa and upwells in the Indian and Pacific Oceans (Lehman, 1993a) (Figure 4.1). Further, it is believed that water evaporated off the Atlantic is precipitated over the Pacific (Broecker *et al.*, 1985), partly because north of 30°N the Pacific is cooler than the Atlantic.

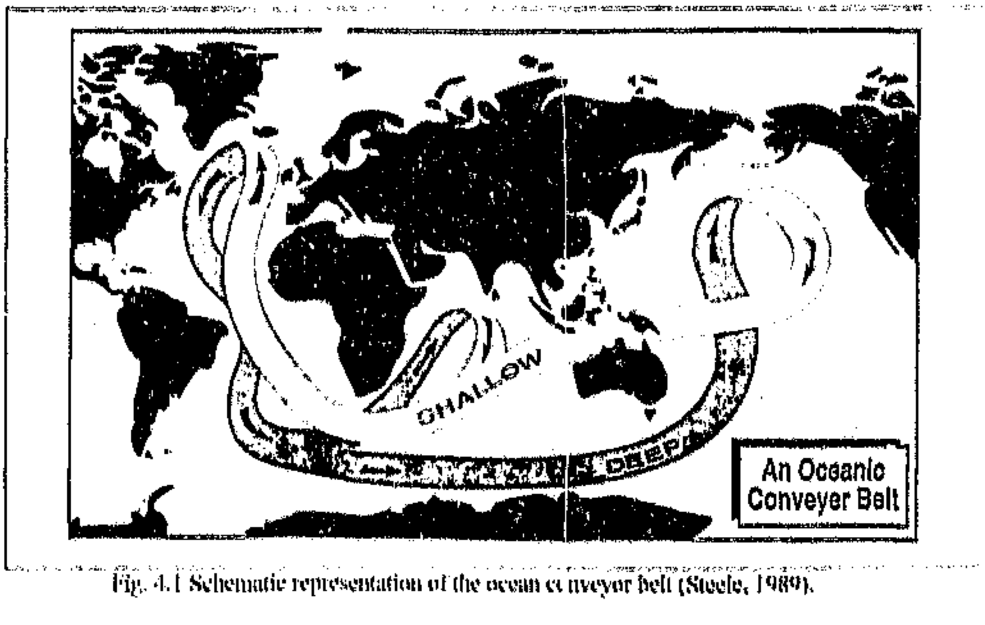

Fig. 4.1 Schematic representation of the ocean conveyor belt (Steele, 1989).

Acropora palmata reefs, which document catastrophic sea-level rise events (Blanchon and Shaw, 1995).

Work by Fronval *et al.* (1995) supports the ideas of Bond and Lotti (1995). Studies of the Vöring plateau revealed that fluctuations in the Norwegian Sea are in phase with changes in temperature over Greenland, with reduced temperatures over Greenland corresponding with glacial debris increases in the Norwegian Sea. This analysis suggests a close relationship between oceanic heat flux and Scandinavian ice-sheet variability. Evidence of iceberg discharges from the Fennoscandian ice-sheet was found, implying that this ice-sheet and its Laurentide counterpart fluctuated coherently on shorter time scales than Milankovitch cycles.

Problems that confront current research are whether ice-sheet dynamics or climate forcing, affecting the thermohaline circulation or the polar circulation index, are responsible for the iceberg discharges (Mayewski *et al.*, 1994). Although Heinrich events partially explain the intensified cooling at the culmination of the bundled Dansgaard-Oeschger cycles, the mechanism behind the intervening Dansgaard-Oeschger oscillations in air temperatures has still to be identified. The salt-induced ocean circulation oscillations as a result of ocean-Scandinavian ice-sheet interaction has been hypothesised as a possible solution (Bond *et al.*, 1993). Recent research suggests that the North Atlantic oscillations can explain only 30% of the magnitude of temperature change over Greenland, and further climatic processes need to be invoked to account for the balance (Charles *et al.*, 1994). Collapse of the North American ice-sheet, upwind of the Atlantic, cannot easily be explained by this process (Fairbanks, 1993). Finally, although Heinrich events do not correlate well with Milankovitch cycles, it is noted that ice-sheets must reach a certain size before they become unstable, and this may be controlled by orbital forcing (Jansen, 1992).

which indicates an Icelandic source for this event. This suggests that the Laurentide ice-sheet and Icelandic ice cap underwent synchronous increases in calving, which implies that the geothermal model cannot apply, and that iceberg discharges result from lowered air temperature. The study suggests that Heinrich events are superimposed on a climate-forced rhythm of ice-rafting events, rather than dominating the North Atlantic ocean record. The notion that injections of fresh water from Heinrich event iceberg discharges alter the conveyor, and subsequently reduce temperatures, is thus challenged.

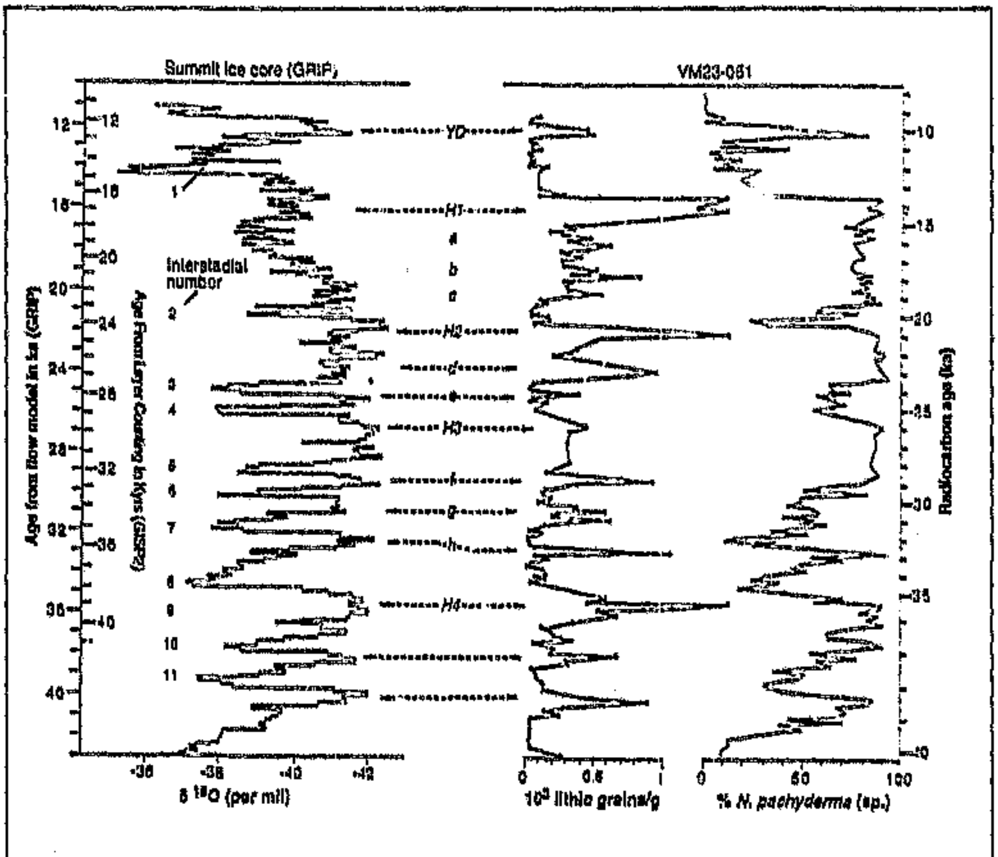

Fig. 3.16 Comparison of the oxygen isotope record and age model for the GRIP ice core, Summit, Greenland, with measurements of lithic concentrations and percentages of the planktic foraminifera *Neogloboquadrina pachyderma* (sinistral). A striking match between the lithic concentration cycles and the temperature cycles in the ice core exists; the match of the lithic cycles to the ocean surface temperatures, however, is much poorer (Bond and Lotti, 1995).

It is possible that the Dansgaard-Oeschger coolings reflect a recurring climate-driven mechanism, where climate seems to be the trigger of the iceberg discharges, (both the smaller frequent discharges and the classical Heinrich events), which is subsequently amplified by the ocean's response to the meltwater input (Bond and Lotti, 1995). Blanchon and Shaw (1995) suggest that thermohaline activation results from air mass expansion during atmospheric reorganisation, and that the atmosphere flips between glacial and interglacial modes, regulating deglaciation by switching the thermohaline circulation from one mode to another. This conclusion is drawn from analysing drowned

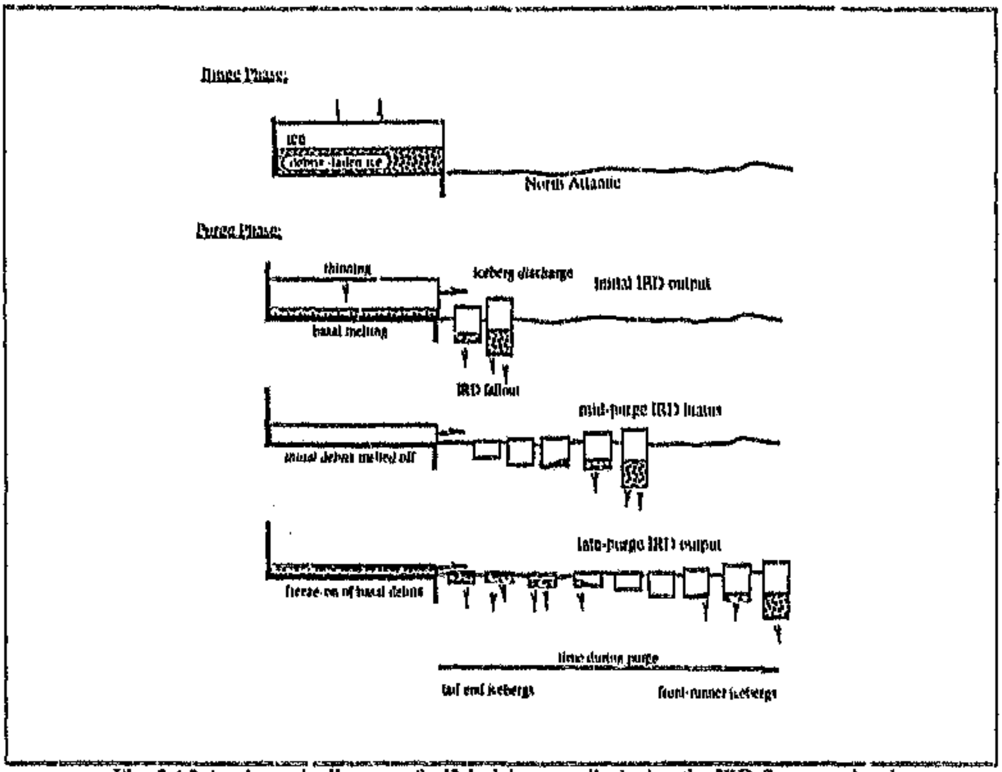

Fig. 3.15 A schematic diagram of a Heinrich event displaying the IRD flux associated with a binge/purge cycle of the Laurentide ice-sheet when debris is entrained into the ice stream by a simple freeze-on mechanism (Alley and MacAyeal, 1994).

Catastrophic ice dam collapse has also been suggested as the cause of the Dansgaard-Oeschger and Heinrich events (Johnson and Lauritzen, 1995). These "jökulhlaups" release vast amounts of meltwater into the oceans, with associated circulation changes. These events cannot, however, be reconciled with Fennoscandian ice-sheet collapse, nor with southern hemisphere temperature correlations.

Paillard (1995) noted a hierarchical structure to the Heinrich events which he subsequently modelled. Every 7 000 - 10 000 years the ice-sheet collapses during temperature minima. Abrupt warming then follows; oscillations lasting between 1 000 and 2 000 years subsequently occur, which correspond to the Dansgaard-Oeschger events in the ice record. The model exhibits internal oscillations embracing ice-sheet growth, basal ice melting and iceberg discharges. Massive fresh water inputs stop the thermohaline circulation causing cooling, which is followed by the reinitiation of the thermohaline circulation and associated warming (Paillard, 1995). This model is in conformity with the work by Bond and Lotti (1995), who identified a linked rhythm between large and smaller discharge events.

A recent study of Dansgaard-Oeschger and Heinrich events by Bond and Lotti (1995) has revealed iceberg calving events at 2 000 to 3 000 year intervals (Figure 3.16). These more frequent events correlate well with the Dansgaard-Oeschger events and are decoupled from SSTs. The study also identified carbonate grains in the H3 IRD layers, but H3 is different from other events in its unusually low concentration of lithic grains, relatively warm and deglaciation was about to begin, but reduced calving subsequent to cooling when the climate was very cold. It was concluded that Heinrich events did not generally reflect a direct response of the Laurentide ice-sheet to climate cooling (Oerlemans, 1993).

In models developed by Nakamura *et al.* (1994), to take into account feedbacks between the thermohaline circulation and atmospheric moisture transport, the "eddy moisture transport-thermohaline circulation (EMT) feedback" was identified. Reduced high-latitude sinking caused a reduction in oceanic heat transport, resulting in an increased meridional temperature gradient. This caused an increase in northward transport of 'ure, wh. increased (decreased) net precipitation in high (low) latitudes causing a decrease in high-latitude salinity and reduced high-latitude sinking. Thus the k. edback results in a higher sensitivity of the thermohaline circulation in the coupled ocean-atmosphere system to destabilising factors (Nakamura *et al.*, 1994).

An alternative explanation of these events is that geothermal heat fluxes cause long periods of ice growth that alternate with short periods of rapid discharge. Ice builds up over a period of about 7 700 years, but geothermal heat slowly warms the glacial bed until the thawed base facilitates the rapid flow and collapse of the ice-sheet into the North Atlantic (Figure 3.15) (Alley and MacAyeal, 1994). This binge/purge model needs no external forcing which could solve the dilemma posed by the observed timings of these events (Oerlemans, 1993). With the collapse of the ice-sheet, cold winds would abate and subsequently evaporation would increase saline deposition, switching the conveyor on and resulting in rapid warming (Kerr, 1993a). Further, as the number of icebergs begins to decrease, salinity would increase and the conveyor would resume (Bond *et al.*, 1993). Although this suggestion is tentative, models of ice-sheet decay under geothermal forcing have produced a 7 000 year cycle.

A serious problem with this hypothesis is that it cannot account for the synchroneity between southern and northern hemispheric climate oscillations, as registered by glacier advances in the Andes (Broecker, 1994b) and other locations. Further, a model proposed by Verbitsky and Saltzman (1994), demonstrates that periodic ice surging can be explained by the internal thermo-hydrodynamical instability of ice-sheets, and concludes that three types of surging could occur. During extremely cold periods, surface conditions of the ice-sheet are very cold, but basal friction is at its maximum, causing melting and surging. During warmer periods, thinner ice allows surface heat to be advected to the base, with resultant melting and surging. During periods of ice-sheet growth, particles of ice can "remember" warmer conditions and basal friction can once again cause melting (Verbitsky and Saltzman, 1994).

A later model by Verbitsky and Saltzman, (1995), which compares ice-sheet collapse due to geothermal fluxes, with collapse due to friction and advection, favours the friction/advection scenario. This implies that ice elevation, atmospheric CO_2, and surface temperature are key elements in determining vuln rability to basal sliding, as these are transmitted to the bottom of the ice through time (Verbitsky and Saltzman, 1995).

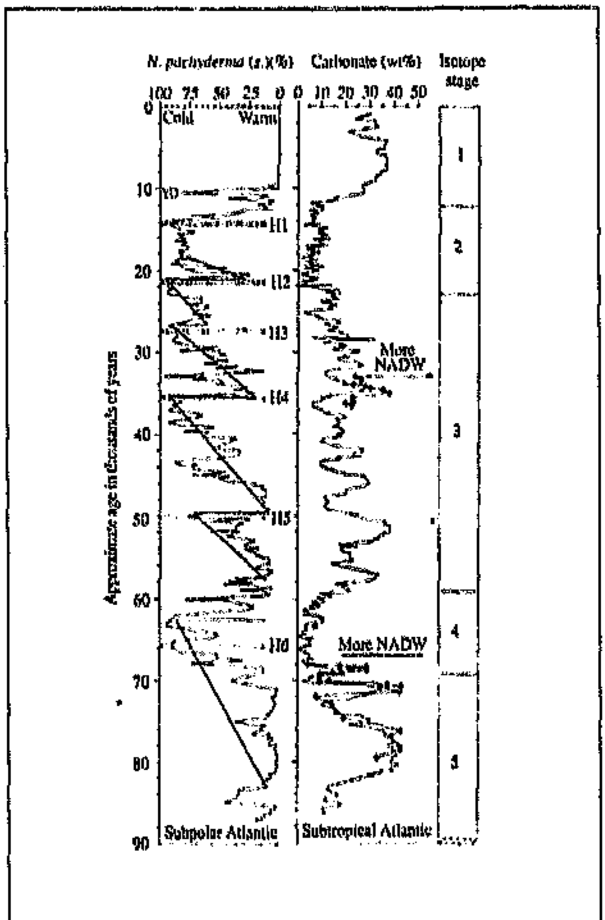

Fig. 3.14 Correlation between millenial SST changes of the subpolar North Atlantic, Dansgaard-Oeschger temperature cycles in the Greenland cores, longer-term saw-toothed temperature cycles (Bond cycles), Heinrich events, and biogenic carbonate changes in the subtropical Atlantic suggesting lowered NADW production during colder periods (Lehman, 1993a).

A model developed by Maslin *et al.* (1995), to calculate sea surface salinities (SSS), and densities (SSD), from SSTs and planktic foraminifera $\delta^{18}O$, reconstructed deepwater formation due to SSD changes between 45 ka and 30 ka, interrupted by H3 and H4 at 27 ka and 38 ka, and from 13 ka to the present. Between 30 ka and 13 ka deepwater could not form owing to the input of meltwater causing reduced SSS. The model indicated climatic rebounds after each Heinrich event, which persisted for 2 000 years. Event H1 seems to be unique, as it occurs during the northern hemisphere insolation increase, coeval with Fennoscandian ice-sheet melting. The input of meltwater during H1 reduced deepwater formation and delayed northern hemisphere deglaciation by 1 500 years (Maslin *et al.*, 1995).

Oerlemans (1993), using a model of the Laurentide ice-sheet driven by orbitally forced insolation variations, argues against a simple temperature - iceberg calving correlation. The model predicted increased calving subsequent to cooling if the climate was

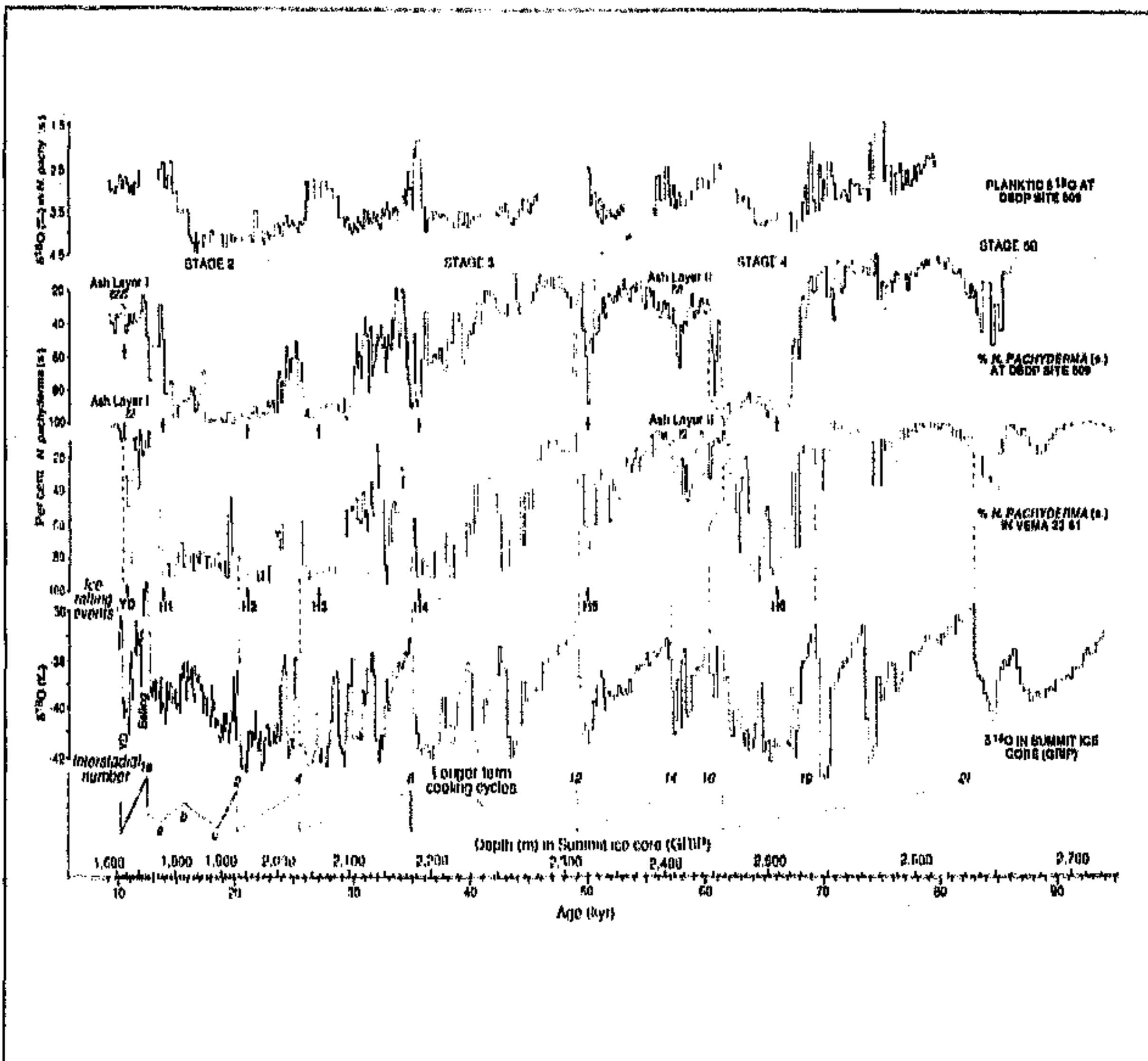

Fig. 3.13 Longer-term cooling cycles, defined by bundling of millenium scale Dansgaard-Oeschger cycles, and abrupt shifts to markedly warm interstadials. Hs refer to Heinrich events (Bond et al., 1993).

Bond *et al.* (1992), and Grousset *et al.* (1993) hypothesised that the Heinrich deposits are the result of a two stage process, firstly a drop in SSTs, and secondly a rapid, massive, discharge of icebergs occurring within, but not spanning, the interval of low SSTs. The melting of the icebergs would result in lowered salinity as suggested by the low planktonic $\delta^{18}O$ values. It is noted that the salinity drop could be sufficient to shut down the North Atlantic thermohaline circulation (Bond *et al.*, 1992).

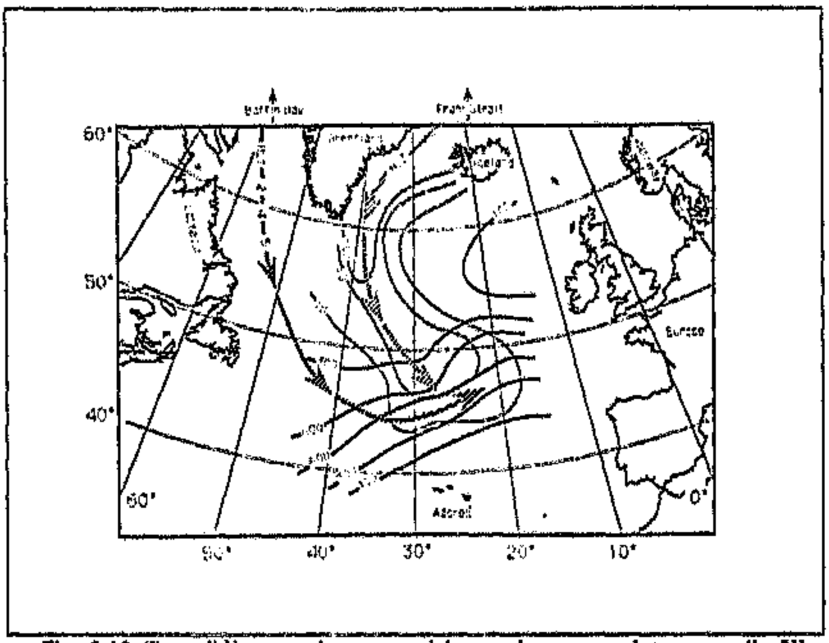

Fig. 3.12 Two different trajectory models can be proposed to reconcile HL patterns and IRD source regions: Durin events 1,2,4 and 5, icebergs were coming from the Baffin Bay, drifting across the Labrador Basin; during event 3, they were coming from the "Arctic" region, drifting across the Irminger Basin (Grousset *et al.*, 1993).

Heinrich events have been equated with the Dansgaard-Oeschger events (Bond *et al.*, 1993). Dansgaard-Oeschger events have been recognised through the analysis of ice-core data and ocean core records and constitute a number of cycles comprising a gradual cooling to full glacial temperature depression, followed by abrupt jumps to warm temperatures on a scale of 500 to 2 000 years. The ice armadas occurred during the coldest phase of the Dansgaard-Oeschger cycles, which were then followed by prominent warming which initiated the next Dansgaard-Oeschger cycle (Broecker, 1994b). These cycles resulted in air and ocean temperature shifts characterised by sharp boundaries, asymmetrical shapes and strong amplitudes of up to 5°C (Kerr, 1993b), and support the notion that the atmosphere and ocean have been a tightly coupled system for at least the last 80 000 years. The events are independent of ice volume changes during glaciation, glacial maxima and the inception of ice-sheets (Bond *et al.*, 1993; Dansgaard *et al.*, 1993). Evidence of reduced surface salinities is recorded in large decreases in planktic $\delta^{18}O$, probably caused by melting icebergs during very cold stadials. Subsequently, after the reduction in iceberg swarms as ice-sheets diminished in size, salinity levels increased causing the thermohaline circulation to commence, resulting in rapid warming of northern latitudes (Bond *et al.*, 1993).

Dansgaard-Oeschger events can be further bundled into longer, progressively cooler cycles termed Bond cycles (Figure 3.13) (Bond *et al.*, 1993), which end with an abrupt shift to warmer temperatures associated with a Heinrich event (Figure 3.14) (Lehman, 1993a; Kerr, 1993a). Bond cycles are probably caused by changes in the strength of the ocean conveyor belt circulation system (Lehman, 1993a).

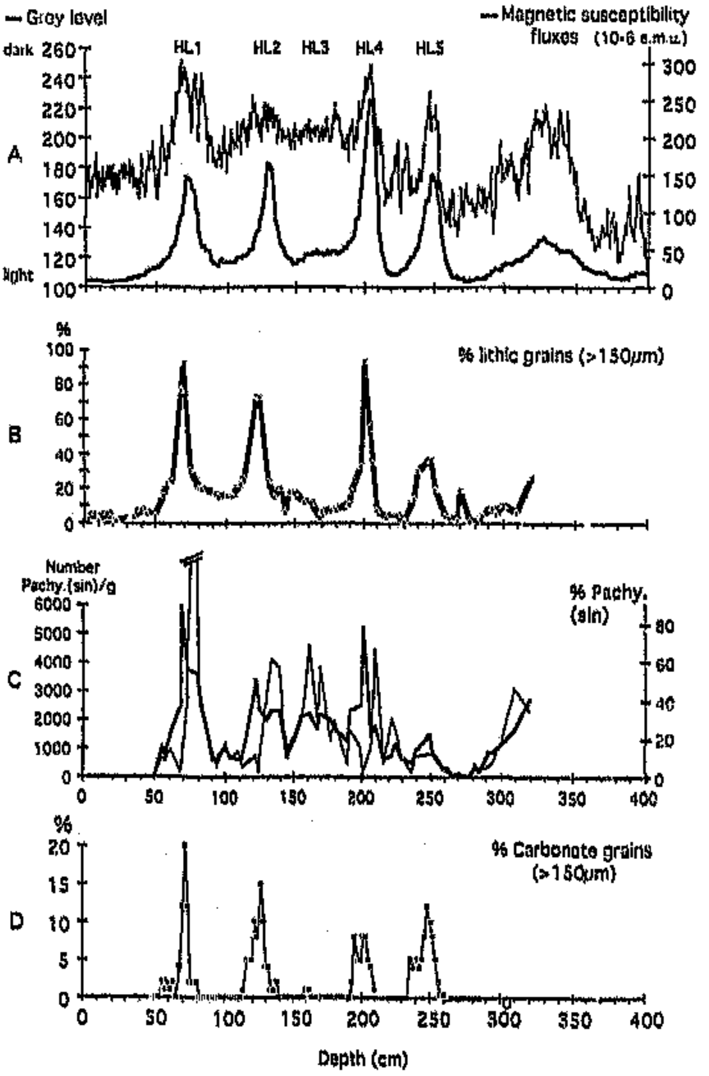

Fig. 3.11 Core SU-9008: Focus on the uppermost 400 cm; (a) grey level pattern along with low-field magnetic susceptibility flux (in 10^{-6} electromagnetic units cm^{-2} ka^{-1}). Dark bands highlight the Heinrich layers (HL); (b) proportion of lithic grains in the >150 µm fraction. (c) number per gram (thin line) and percentage (thick line) of *Neogloboquadrina pachyderma* (sinistral), in the >150 µm fraction. (d) proportion (percent) of detrital carbonate grains in the coarse lithic fraction (>150 µm), counted only between 50 and 320 cm (Grousset *et al.*, 1993).

Greenland. An analysis of the increase in dust in the ice cores on Greenland suggests that the atmospheric circulation during certain stadials expanded in aerial extent. As sea salt levels did not increase concomitantly, increased wind speeds cannot alone account for the dust increase. Important locations for the incorporation of dust are regions of strong cyclogenisis that form along marine and atmospheric thermal gradients. It is argued that atmospheric thermal gradients were significantly steepened by the radiative influence of ice-sheets during the last glaciation, and that the presence of continental ice led to an increase of sea ice production in the North Atlantic. As primary sources for dust would be south of the main ice cover, their incorporation into Greenland ice suggests that the air masses would have covered areas further south (Mayewski *et al.*, 1994).

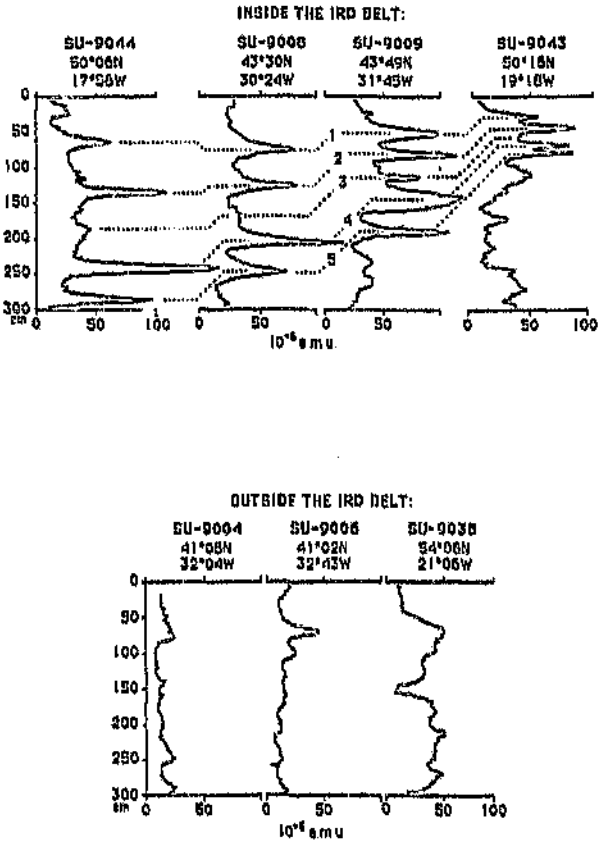

Fig. 3.10 Examples of low-field magnetic susceptibility profiles on uppermost 3 m in cores located inside and outside the ice-rafted detritus belt. Correspondences between peaks can be proposed on the basis of biostratigraphic arguments (dashed numbered lines) (Grousset *et al.*, 1993).

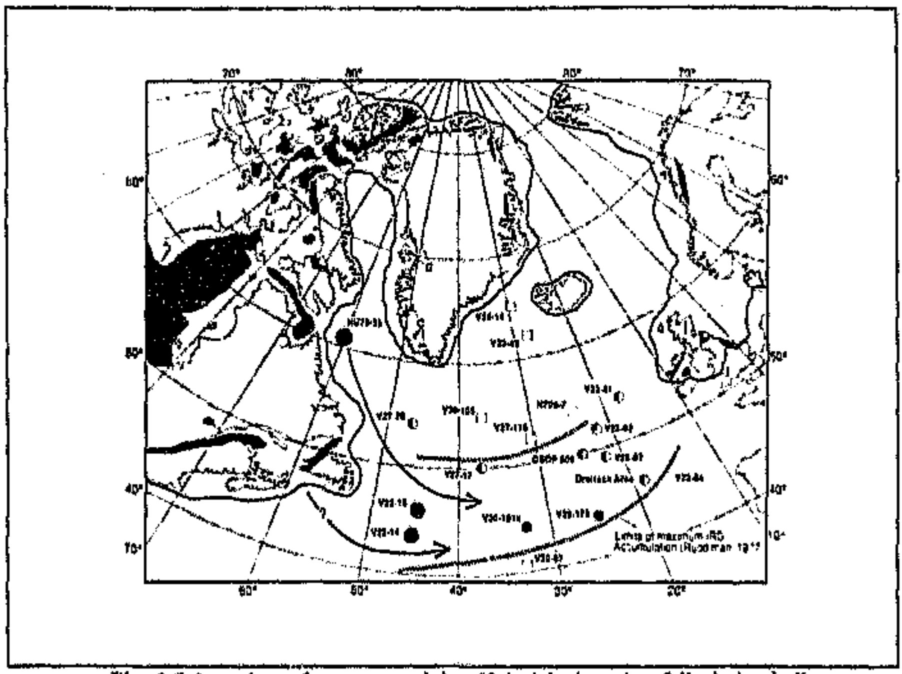

Fig. 3.9 Location of cores containing Heinrich deposits, full circles indicate carbonate-rich IRD is present in all Heinrich deposits identified; half-filled circles that some is present; open squares indicate no presence of carbonate-rich IRD. Solid black shading represents the extent of limestone and dolomite bedrock. Thick solid line represents the maximum extent of ice-sheets during the last glaciation. Arrows represent possible paths of icebergs (Bond et al., 1992).

Heinrich (1988), initially correlated the IRD layers with northern hemisphere precessional insolation minima (precessional angle $\Pi = 90°$ and $\Pi = 270°$), although he did acknowledge a problem in that ice-sheet construction and decay cannot occur simultaneously. A suggested solution was that decreasing stability of continental ice-sheets could occur during enhanced ice accumulation, with faster lateral progression and subsequent discharge into the ocean (Reeh, 1985; Jansen, 1992).

An analysis by Bond *et al.* (1992) produced revised dates viz. 14.3 ka, 21 ka, 2[illegible] ka, 52 ka, and 69 ka. The intervals between these revised dates do not correlate well with insolational cycles, indicating that some other mechanism is responsible for the cooling. Repeated advances of the Laurentide ice-sheet, possibly connected to reduced air temperatures, could be the cause of the events. Reconstructions of the Laurentide ice-sheet suggest that the Hudson Strait drained 3-4 x 10^6 km^2 of the ice producing $10^3 km^3/a$ of meltwater during the deglaciation (Andrews *et al.*, 1994). The analyses pointed to surface water characterised by low temperature and low salinity at the time of deposition. Domination of *Neogloboquadrina pachyderma* (sinistral) in the IRD layers of the cores indicates deep southward penetration of polar water at the time of deposition.

The iceberg discharges have been correlated with expanded sea ice and changes in the size and intensity of the polar circulation index (PCI) (Mayewski *et al.*, 1994). The PCI refers to the size and intensity of the circulation system that transports air masses to

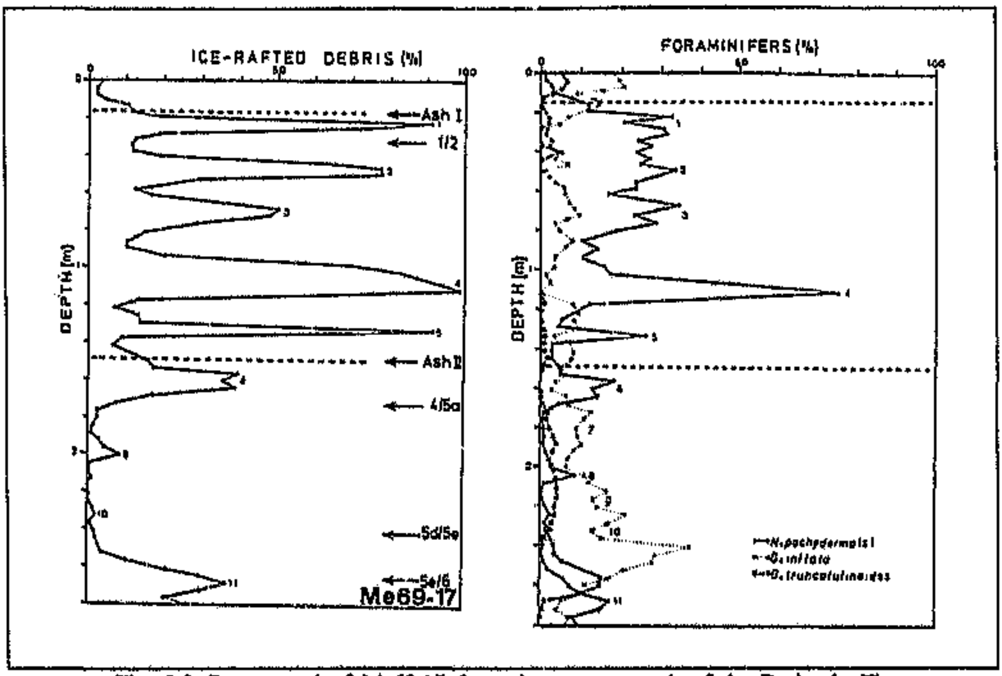

Fig. 3.8 Core record of Me69-17 from the western peak of the Dreizack. The amount of ice-rafted debris is given as part of the total split (IRD + Forams). The amount of one species is given as part of the sum of planktonic forams in a split. The right side of the IRD record shows the stratigraphic markers (Ash I and II, oxygen-isotope stage boundaries) (Heinrich, 1988).

Subsequent work by Bond *et al.*, (1992), traced the Heinrich deposits in cores across the North Atlantic and Labrador Sea (Figure 3.9), using fast digital scanning of the grey reflectance of the sediments. Grousset *et al.* (1993), conducted low-field magnetic susceptibility analysis on the cores and observed well-marked peaks corresponding to the IRD belts (Figures 3.10 and 3.11), which correlate well with the grey levels. McManus *et al.* (1994), discovered a further five Heinrich events which confirms Heinrich's (1988), postulation of eleven events during the last climatic cycle. The spatial extent of the IRD accumulation suggests a zone between 40°N and 55°N stretching across the entire North Atlantic. The pattern is characterised by a west to east gradient, except for event H3 which is orientated north-west to south-east. Analysis of the IRD revealed a layer with abundant detrital carbonate that seems to have accumulated rapidly in the core. A suggested source is the limestone and dolomite bedrock in the Hudson Strait (Figure 3.9). Event H3 could have a different source (Scandinavian) as it contains low levels of detrital carbonate (Figure 3.12) (Grousset *et al.*, 1993).

It seems that Heinrich events are global, as they correlate with cycles evident in the Vostok ice-core and mountain glacier retreat in the southern Andes (Kerr, 1993b). Heinrich events have also been correlated with the Chinese loess climate record, suggesting a link through the westerlies (Porter and Zhisheng, 1995), and are linked with fluctuations in Lake Tulane in Florida (Grimm *et al.*, 1993).

termination of the Last Glacial Maximum, nor account for the Younger Dryas cooling. Veum *et al.* (1992) maintain that strong warming during reduced thermohaline circulation took place, as revealed in a high resolution record obtained from the Norwegian Sea. The record suggests that NADW was only reinstated 1 000 years after the meltwater anomalies in this region had ended. Lowell *et al.* (1995) cite evidence that Nordic deepwater production may have begun causing rapid warming in the far northern Atlantic region 1 300 years before the major North Atlantic thermohaline circulation resumed.

Evidence obtained from the $\delta^{13}C$ benthic record in the Greenland, Iceland and Norwegian (GIN) (Figure 4.10) seas for the Younger Dryas points to a circulation similar to that of the present, and very different from that during the LGM: this was characterised by good ventilation, and high $\delta^{13}C$ (Veum *et al.*, 1992). The strong benthic $\delta^{13}C$ gradient between the Norwegian Sea and the north-east Atlantic before 12.5 ka indicates that the nutrient-poor GIN seas did not ventilate the deep regions of the Atlantic until 12.6 ka (Veum *et al.*, 1992). High values of $\delta^{13}C$ from epibenthic foraminifers indicate that the GIN seas were highly ventilated as opposed to the North Atlantic, which was under the influence of nutrient-enriched, low-$\delta^{13}C$ southern source waters (Veum *et al.*, 1992). Highly ventilated GIN seas were a probable source of nutrient-depleted glacial intermediate water, which did not contribute to the formation of deep water, as is the case at present (Veum *et al.*, 1992).

Models of the thermohaline circulation

The conveyor belt has been successfully modelled (Kerr, 1993d; Weaver and Hughes, 1994), throwing light on the importance of massive ice-sheets in destabilising the conveyor (Kerr, 1993a; Lehman, 1993a; Broecker, 1994a). The postulated effects of this circulation system are in general agreement with the temperature changes inferred over Europe and Asia (Lehman and Keigwin, 1992a). It is maintained that Late Glacial climate oscillations, including the Younger Dryas, can be explained by the models (Alley *et al.*, 1993; Duplessy *et al.*, 1992), and changes in the position of the Arctic frontal system have been linked to these ocean changes (COHMAP Members, 1988).

A simple ocean model coupled to an ice-sheet surging model produced a break down of the thermohaline circulation as surging icebergs caused a meltwater influx, which subsequently resulted in a cooling of the North Atlantic region. Rapid resumption of the circulation followed, leading to abrupt warming (Paillard and Labeyrie, 1994; Bender *et al.*, 1994). In a model by Boyle and Weaver (1994), the conveyor was perturbed by a fresh water input at high latitudes, which briefly reduced convection. Subsequently, the convection was restored, but was characterised by a shallower North Atlantic convection cell, with a stronger deep inflow of AABW beneath it. The associated climate was colder than at present (Figure 4.11) (Boyle and Weaver, 1994).

A model by Rahmstorf (1994) realistically reproduces an AABW cell under the NADW cell caused by colder temperatures in the Southern Ocean (Figure 4.12). A meltwater input at 56°N interrupted the conveyor temporarily, causing temperatures to drop by 2.6°C north of 48°N and by 3°C north of 56°N, and salinity to drop by 1‰ before it recovered. NADW flow had become shallower and AABW filled the abyssal attributed directly to varying strengths of NADW production, and it is proposed that these changes promoted the reorganisation of global climate. Records from the Benguela suggest that post glacial warming was interrupted at 12.5 ka but resumed at 11 ka, reaching a maximum at 10.5 ka - 9 ka (Pether, 1994).

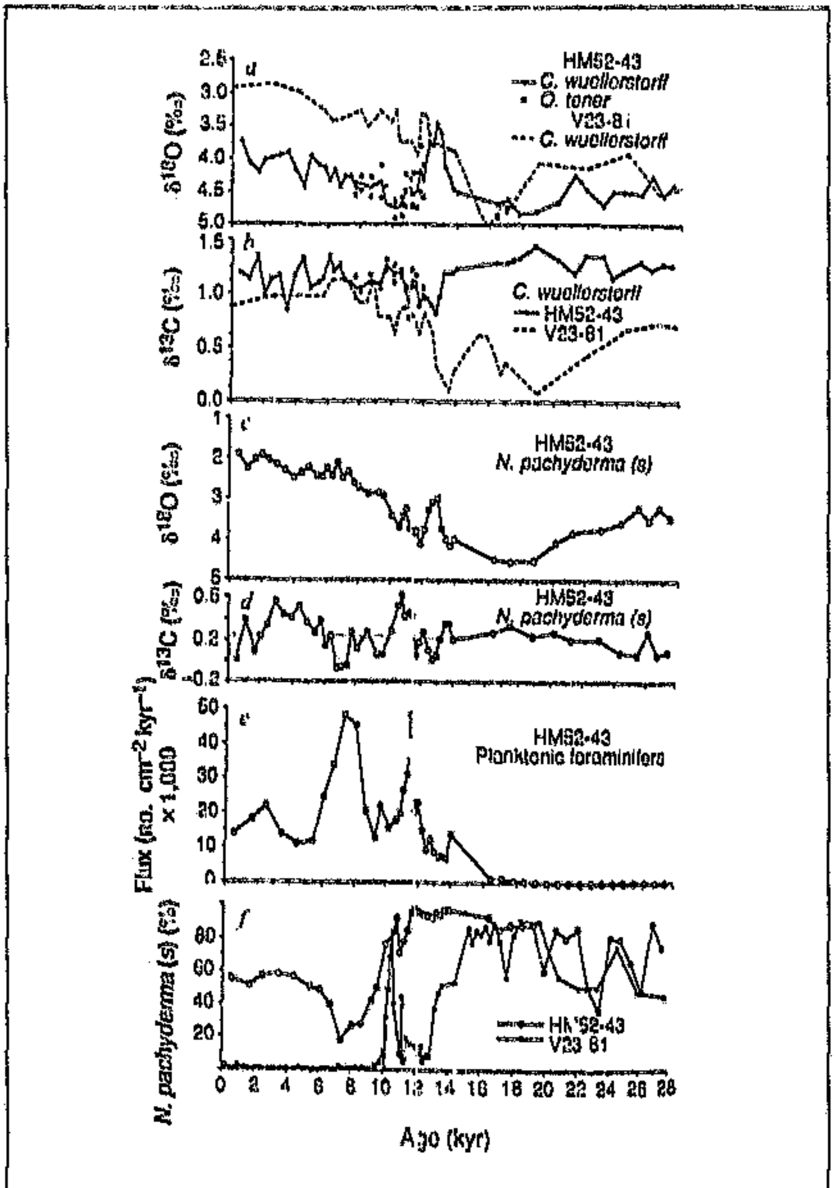

Fig. 4.10 Comparison of (a) $\delta^{18}O$ and (b) $\delta^{13}C$ of benthic foraminifers, (c) $\delta^{18}O$ and (d) $\delta^{13}C$ from analyses of the planktonic foraminifer *Neogloboquadrina pachyderma* (sinistral), (e) total flux of planktonic foraminifers, (f) relative occurrence of *Neogloboquadrina pachyderma* (sinistral), in %. The vertical shaded area marks the Younger Dryas chronozone (Veum *et al.*, 1992).

Not all agree that NADW fluxes are responsible for climate oscillations. It is maintained by some that rapid changes in the thermohaline circulation did not initiate the

100 years (Lehman and Keigwin, 1992a); thereafter the area was influenced by southern water until 9 ka.

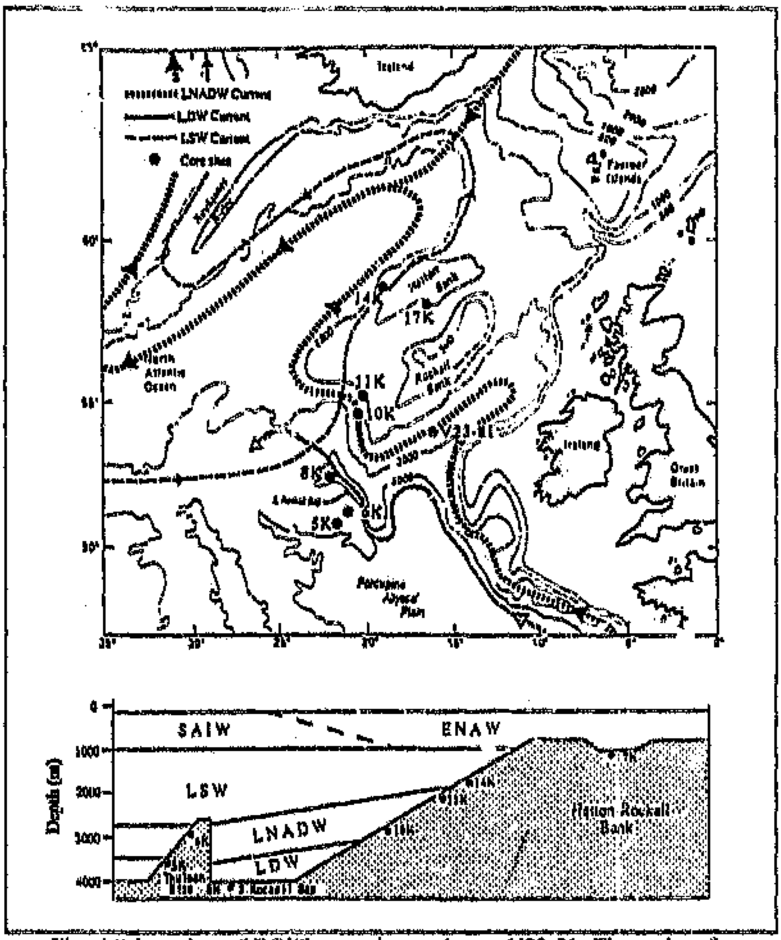

Fig. 4.9 Location of BOFS core sites and core V23-81. The paths of major deep-water currents are shown as dashed and dotted lines (LDW = Lower Deep Water, a derivative of AABW, LSW = Labrador Sea Water, or UNADW) (McCave *et al.*, 1995).

The benthic $\delta^{13}C$ record from core RC 11-83 indicates that deglacial changes in the nutrient chemistry of the deep Southern Ocean were rapid and large. It is suggested that little or no NADW entered the Southern Ocean during the LGM and that the Southern Ocean had a greater influence on the chemistry of the deep Atlantic than today (Oppo and Fairbanks, 1987). A high $\delta^{13}C$ value was recorded at 13.1 ka, followed by a dramatic drop at 12.7 ka. From 12.6 ka to 12.2 ka an abrupt shift in $\delta^{13}C$ from low to high values occurred, interrupted by a return to low values at 11.5 ka. The high $\delta^{13}C$ values for the Younger Dryas period in RC 11-83 could be a record of a shallower NADW flow, which would not reflect reduced LNADW formation (Lehman and Keigwin, 1992a). Between 12.2 ka and 10 ka, a number of oscillations of differing magnitude occurred in $\delta^{13}C$ values (Charles and Fairbanks, 1992). These oscillations are

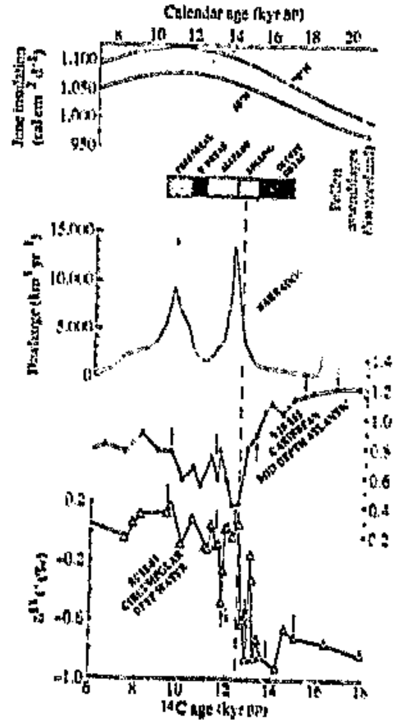

Fig. 4.8 Convergence of deep Southern Ocean and Caribbean $\delta^{13}C$ records, with AMS ^{14}C dated levels indicated by arrows, marks the "turn on" of NADW (dashed line). The timing of this event can be compared with the ice-sheet meltwater discharge curve (calculated as the first derivative of the Barbados sea-level curve), the change in pollen assemblages in Swiss lake sediments, and June insolation at 60°N and 70°N, provided that a common timescale is established. The top scale is calendar years, and the bottom scale is ^{14}C years (Charles and Fairbanks, 1992).

The cores indicate that at 14.5 ka surface waters were fresh with low productivity and cooler conditions than at 18 ka and NADW production was at its lowest since 20 ka (Keigwin and Lehman, 1994). Atlantic water began entering the Norwegian Sea at 13.5 ka and NADW levels rose from their glacial minimum to modern levels; near interglacial levels were reached by 13.1 ka, persisting until 11.7 ka (Lehman and Keigwin, 1992a). A number of brief reductions in flow occurred between 12.6 ka and 12.2 ka, but the major decrease occurred at 11.7 ka and at about 11.5 ka, NADW ebbed to a level only slightly higher than glacial levels (Boyle and Keigwin, 1987). ^{13}C and Cd data suggest that nutrient enriched water of southern origin occurred between 11.5 ka, and 9 ka, in the North Atlantic (Oppo and Fairbanks, 1987). However at 10.5 ka ocean cooling ended, with the resumption of surface inflow from the Atlantic occurring within

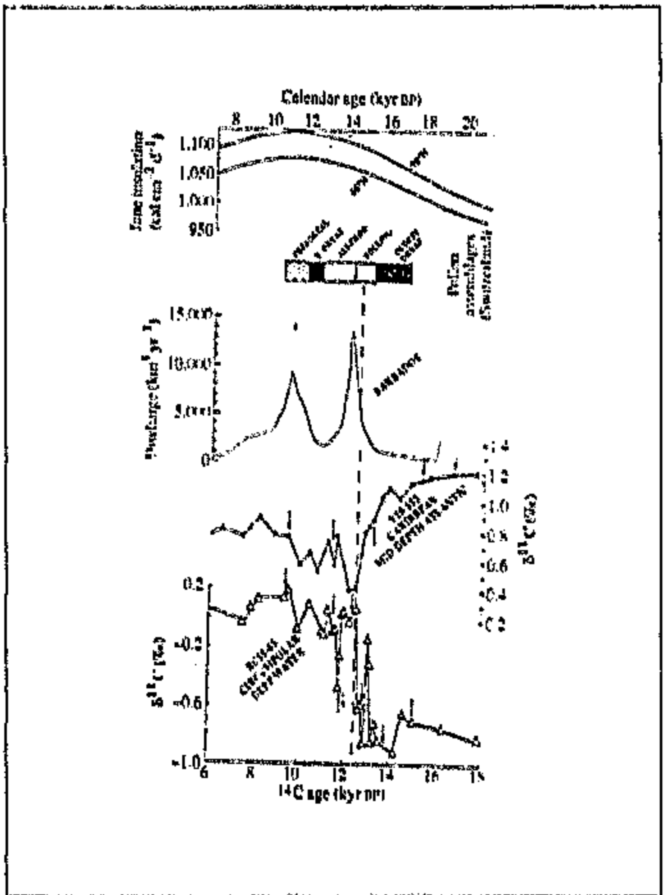

Fig. 4.8 Convergence of deep Southern Ocean and Caribbean $\delta^{13}C$ records, with AMS ^{14}C dated levels indicated by arrows, marks the "turn on" of NADW (dashed line). The timing of this event can be compared with the ice-sheet meltwater discharge curve (calculated as the first derivative of the Barbados sea-level curve), the change in pollen assemblages in Swiss lake sediments, and June insolation at 60°N and 70°N, provided that a common timescale is established. The top scale is calendar years, and the bottom scale is ^{14}C years (Charles and Fairbanks, 1992).

The cores indicate that at 14.5 ka surface waters were fresh with low productivity and cooler conditions than at 18 ka and NADW production was at its lowest since 20 ka (Keigwin and Lehman, 1994). Atlantic water began entering the Norwegian Sea at 13.5 ka and NADW levels rose from their glacial minimum to modern levels; near interglacial levels were reached by 13.1 ka, persisting until 11.7 ka (Lehman and Keigwin, 1992a). A number of brief reductions in flow occurred between 12.6 ka and 12.2 ka, but the major decrease occurred at 11.7 ka and at about 11.5 ka, NADW ebbed to a level only slightly higher than glacial levels (Boyle and Keigwin, 1987). ^{13}C and Cd data suggest that nutrient enriched water of southern origin occurred between 11.5 ka, and 9 ka, in the North Atlantic (Oppo and Fairbanks, 1987). However at 10.5 ka ocean cooling ended, with the resumption of surface inflow from the Atlantic occurring within

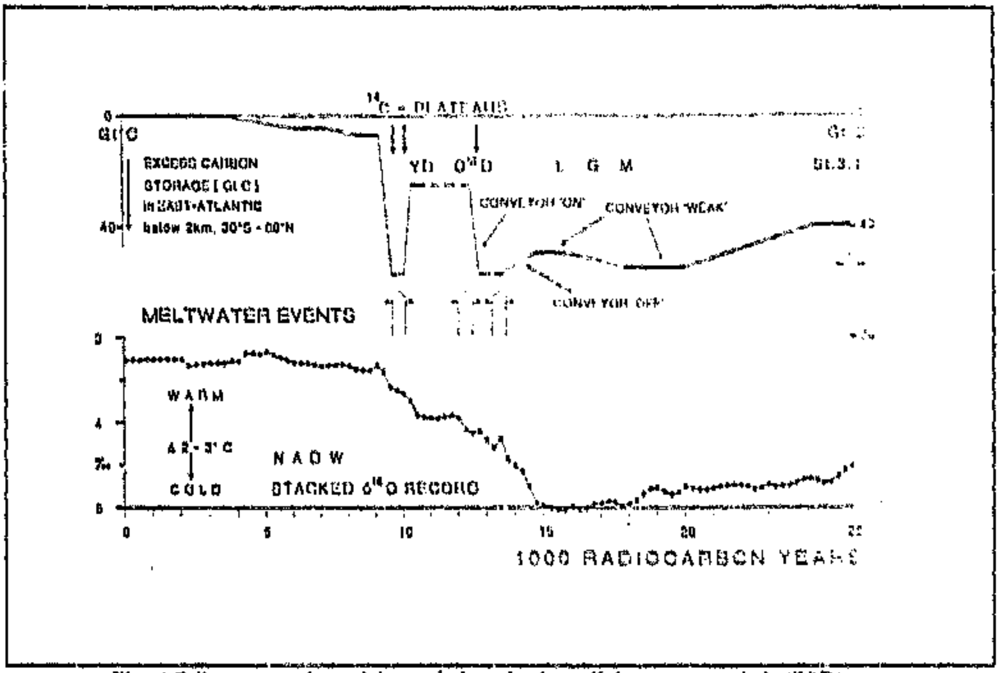

Fig. 4.7 Reconstruction of the variations in the salinity conveyor belt (SCB) over the last 30 ka (calendar) years. SCB intensity is deduced from $\delta^{13}C$ differences between past time slices and the Recent, converted into gigatons of carbon stored in excess of today in the east Atlantic below 2 000 m depth. The $\delta^{18}O$ curve is based on six stacked high-resolution benthic records from the same depth range in the eastern Atlantic. Thin arrows mark positions of ^{14}C plateaus and wide arrows indicate meltwater events (Sarnthein *et al.*, 1994).

One problem with the so called "meltwater mode" is that the mode *precedes* the meltwater pulses at 12 ka and 9.5 ka documented by Fairbanks (1989) (Figure 4.8) in both instances. The prominent low $\delta^{13}C$ value at 13 ka is documented by Jansen and Veum (1990) in core V 23-81; they maintain that the low values indicate reduced NADW formation due to the fresh water input, and increased influence and subsequent replacement by AABW. They acknowledge that the low $\delta^{13}C$ value centred on 13 ka occurs 1 000 years before the large melt water input at 12 ka reflects the reduction of NADW (Jansen and Veum, 1990), but explain this discrepancy as being within the error limits of the timescales for these records.

An analysis of grain sizes in sediments taken from cores in the Rockall Bank area (Figure 4.9) (McCave *et al.*, 1995) as an index of palaeocurrents for the last 25 000 years suggests that glacial intermediate water flowed rapidly at depths of 1 100 m and 2 000 m, but that deep water circulation was sluggish at the LGM. At the start of termination 1A flow speeds decreased to a minimum between 14 ka and 13 ka and were accompanied by a $\delta^{13}C$ minimum, suggesting a reduced influence of northern source water, probably caused by event H1. Subsequently, both grain size and $\delta^{13}C$ values increased reflecting a return to more vigorous deep-water circulation during the Allerød (12 ka) (McCave *et al.*, 1995).

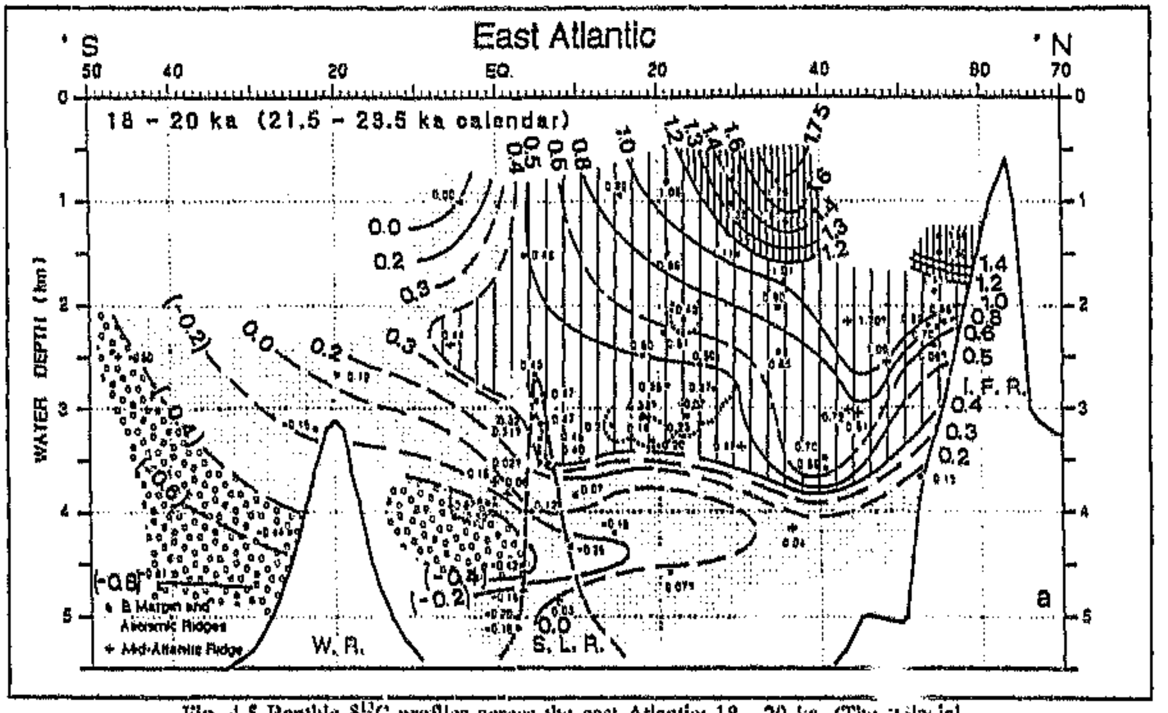

Fig. 4.5 Benthic $\delta^{13}C$ profiles across the east Atlantic: 18 - 20 ka. (The 'Glacial Mode') For abbreviations see Fig. 4.4 (Sarnthein *et al.*, 1994).

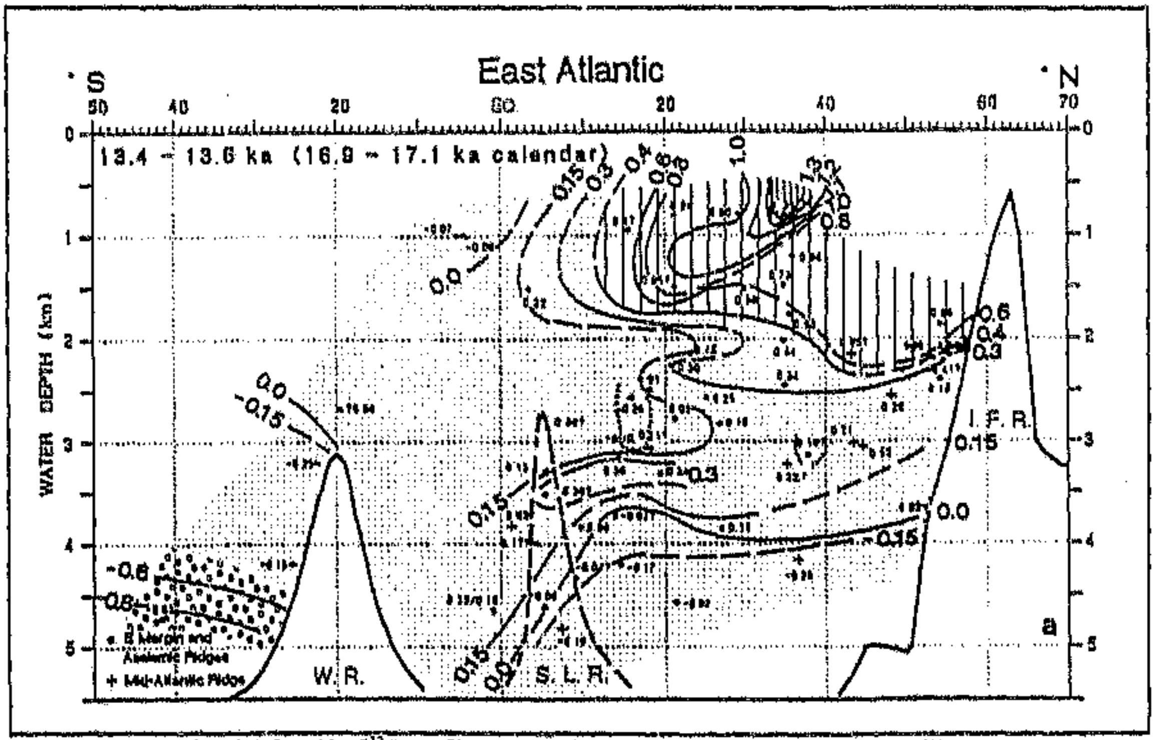

Fig. 4.6 Benthic $\delta^{13}C$ profiles across the east Atlantic: 13.4 - 13.6 ka. (The 'Meltwater Mode') For abbreviations see Fig. 4.4 (Sarnthein *et al.*, 1994).

Atlantic (Sarnthein *et al.*, 1994). The Holocene/interglacial mode (Figure 4.4) is characterised by a strong southward bound flow of NADW, originating in the Norwegian-Greenland Sea, and is similar to that of today. The glacial mode (Figure 4.5), which was active until end of the last glacial, includes a weakened southward bound NADW end-member which forms south of Iceland, underlain by very cold AABW which upwells near the Azores Fracture Zone and markedly dilutes the NADW from below.

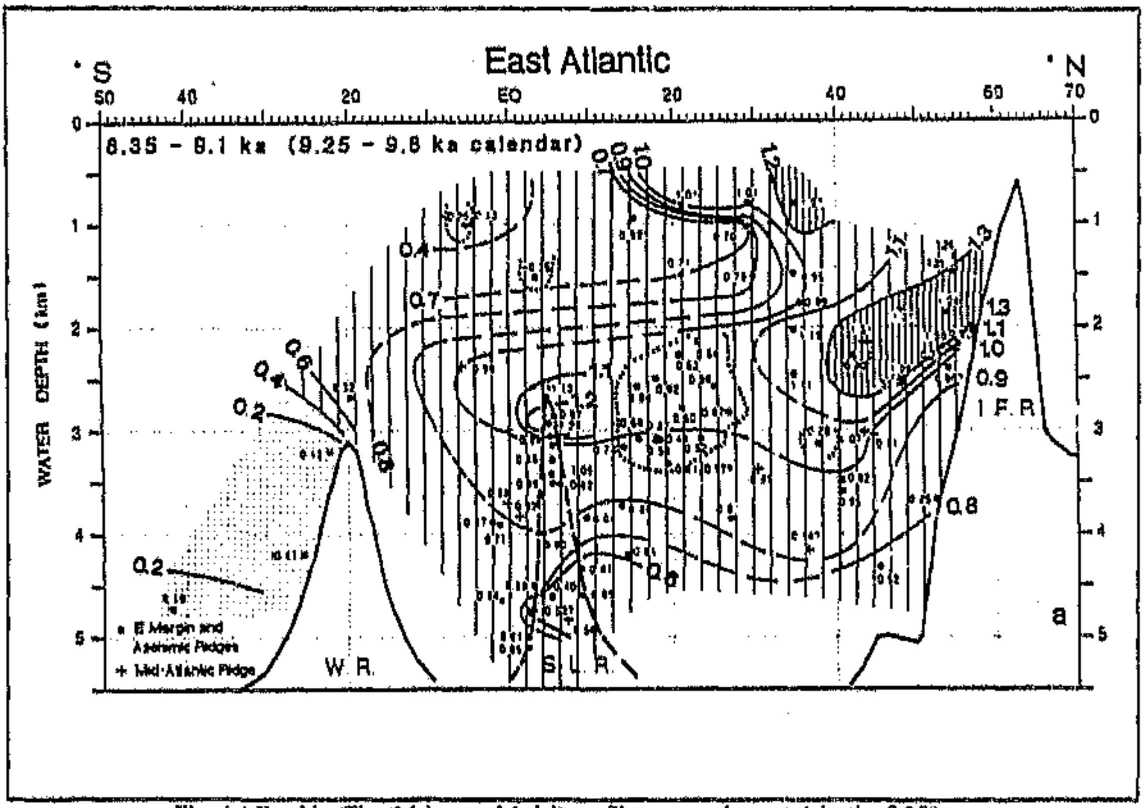

Fig. 4.4 Benthic (The 'Meltwater Mode') profiles across the east Atlantic; 8.350 - 9.100 ka. (The 'Holocene/Interglacial Mode') W.R. = Walvis Ridge, S.L.R. = Sierra Leone Rise, I.F.R. = Island-Faeroe Ridge (Stippled shading = AABW, Vertical wide line shading = NADW, Vertical narrow shading = MOW, Open stippled shading = WSBW) (Sarnthein *et al.*, 1994).

The meltwater mode consists of poorly ventilated AABW up to 2 000 m, above which no NADW or NAIW was formed, overlain by a meltwater lid (Figure 4.6). This third mode is encountered twice; once between 13.6 ka and 13.4 ka, and between 10.3 ka and 9.6 ka. However, this type of circulation is difficult to detect, as it occurs over short periods and is only recorded in a small number of very high resolution cores. The fact that other "meltwater modes" are not documented does not imply that they did not occur. Similar, but very short lived, modes may have occurred, but were too rapid to be observed in the sediments. Further, ^{14}C "plateaus" (defined as intervals when ^{14}C ages remain constant over several hundred calendar years) (Figure 4.7) make absolute dating difficult (Sarnthein *et al.*, 1994).

deep water circulation was sluggish during the last glaciation, but increased after deglaciation. Deep current strengths declined again during termination IA and during the Younger Dryas (McCave *et al.*, 1995). Holocene and glacial carbon isotope data of benthic foraminifera from shallow to mid-depth cores from the north-eastern Atlantic show that this region was highly stratified, with ^{13}C enriched GNAIW overlying ^{13}C depleted SOW (Oppo and Lehman, 1993).

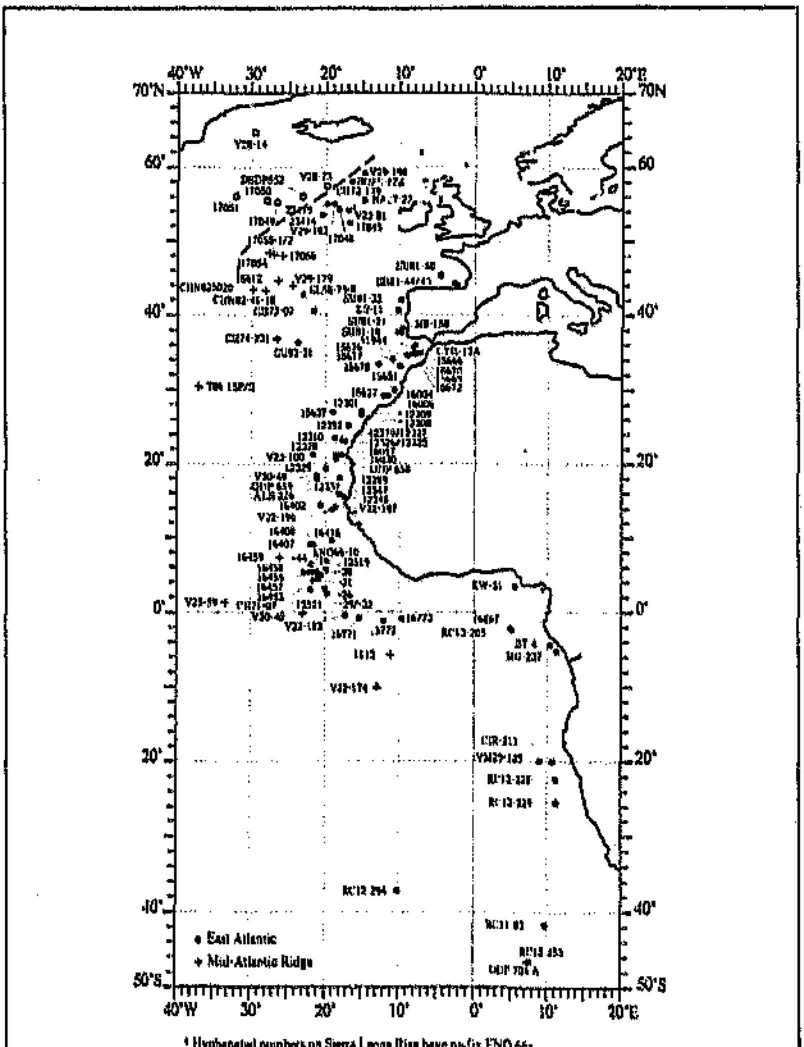

Fig. 4.3 Core locations in the east Atlantic. Dashed line separates core locations north of 40°N below east and west Atlantic water masses. Hyphenated numbers on the Sierra Leone Rise have prefix ENO66- (Sarnthein *et al.*, 1994).

An examination of 95 epibenthic $\delta^{13}C$ records covering the last 30 000 years (Figure 4.3) suggests that there are three distinct modes of deep water circulation in the North

1994). A decrease in salinity would make it more difficult for very dense water to form in the North Atlantic, and the production of intermediate water would occur (Boyle and Keigwin, 1987). An analysis of micropalaeontological records of foraminifera by Duplessy *et al.* (1992), revealed that a primary forcing factor for surface salinity was the injection of meltwater into the North Atlantic, which led to decreasing SSTs and intensified stratification. These two effects resulted in decreased evaporation, increased precipitation and reduced poleward flux of salty, warm water. Broecker *et al.* (1985), recognised that NADW production was reduced during glacial maxima and was rejuvenated during warmer periods. Later work by Broecker (1994b), suggested a shallower conveyor rather than a complete breakdown of the system, as shown from evidence in $^{14}C/^{12}C$ ratios in atmospheric CO_2 for the Younger Dryas. NADW production formation was not completely suppressed, but continued during the Younger Dryas, with variable rates of formation (Edwards *et al.*, 1993), while the source region shifted to lower latitudes (Broecker, 1994b). It is possible that the conveyor is still operative in the "off" mode, but runs much slower and forms a nearly closed circulation loop within the Atlantic itself (Broecker *et al.*, 1990).

Heinrich events could cause the dilution of the salt, resulting in the suppression of NADW formation, and thus cause the associated sharp cooling (Kerr, 1993b). Keigwin and Lehman (1994), analysed a core from the Mid-Atlantic Ridge at about 43°N and noted the existence of Heinrich layer 1 (H1) which was associated with maximum rates of sedimentation, IRD, surface water cooling and minimum rates of NADW production. The most striking feature of the carbon isotope record of the core is the abrupt increase – possibly within a 100 years – of $\delta^{13}C$ at the end of H1, associated with an increase in the percentage of *Neogloboquadrina pachyderma* (sinistral). Keigwin *et al.* (1994), maintain that deep ocean changes occur too frequently (on millennial scales) to be caused solely by Heinrich events, and suggest changes in meltwater flux and evaporation/precipitation budgets over the North Atlantic as forcing agents. An alternative view, based on available proxy nutrient data which indicates a coincidence of minimum NADW and lowered sea surface salinity in the North Atlantic region, suggests that salinity changes could be a product of conveyor variability rather than a cause thereof (Keigwin and Jones, 1994).

Surface organisms take up ^{12}C in preference to ^{13}C and also absorb Cd, resulting in surface waters characterised by high ^{13}C and low Cd levels, while bottom waters are high in Cd and low in ^{13}C (Boyle, 1990). NADW has high $\delta^{13}C$ because it contains a large amount of upper ocean water which has been enriched in ^{13}C as a result of isotopic fractionation by marine plants prior to deep-water formation (Oppo and Fairbanks, 1987; Oppo and Fairbanks, 1990). Benthic data from a core in the northern Atlantic show glacial deep water (4 450 m) to be depleted in ^{13}C and enriched in Cd, suggesting a lower proportion of northern source water relative to southern source water (Boyle and Keigwin, 1987).

High ^{13}C waters over the Rockall Plateau formed north of the glacial polar front, possibly indicating that the deep Norwegian Sea was a source for Glacial North Atlantic Intermediate Water (GNAIW) (Oppo and Lehman, 1993). During the last glaciation, NADW was replaced by Southern Ocean Water (SOW) in the northern and tropical Atlantic and GNAIW filled the ocean above 2 000 m (Oppo and Lehman, 1993). Glacial intermediate water flowed rapidly at depths of between 1 100 m and 2 000 m, whereas with the Younger Dryas may be related to the cessation of LNADW formation, rather than oscillations in NADW rate and depth, which are controlled by meltwater discharge from the Fennoscandian ice-sheet (Edwards *et al.*, 1993). Further support for the importance of the Norwegian seas comes from the work of Cortijo *et al.* (1994), who document sharp decreases in SST and SSS in the Norwegian seas which reduced the ventilation of the region to about 2 300 m, and enhanced the SST gradient between this water mass and the North Atlantic. NADW would still be formed, although LNADW formation would have ceased. This thermal gradient could enhance the formation of major atmospheric depressions associated with winter snow and increased ice-sheet growth (Cortijo *et al.*, 1994).

It is well documented that the lower belt ceased operating during the last glaciation, and was replaced by AABW, while the upper belt persisted but shallowed slightly from its present depth. It is maintained that the history of the lower belt is responsible for the changes in climate in the Greenland region (Lehman and Keigwin, 1992b), and because of the high rate of heat loss during the formation of LNADW, it is suggested that this water mass is the pre-eminent deep water mass in controlling surface climate in the Atlantic region (Lehman and Keigwin, 1992a).

Studies indicate that the conveyor belt is a self-sustaining circulation which can collapse when disturbed and which can have multiple steady states. As the conveyor is density driven, a perturbation in the salt content can destabilise it; thus changes in precipitation, evaporation, or ice-sheet, iceberg or sea ice melting rates, as well as changes in the rates of advection and mixing in the Atlantic Ocean (Duplessy *et al.*, 1992; Kerr, 1993c; Lehman, 1993a; Broecker, 1994a), could act to dampen the conveyor or shut it down (Kerr, 1993c). The density change created by an increase of ~ one salinity unit ($1^0/_{00}$) is enough to tip the balance between the conveyor "off" or "on" situations (Broecker *et al.*, 1990). When the density becomes sufficiently low in the northern Atlantic, the deep water cannot force itself into the Southern Ocean and the conveyor stops (Broecker *et al.*, 1990). Slight decreases in surface water salinity could have slackened deep water formation in the Norwegian sea within a few decades, affecting the thermohaline circulation and deep convection (Cortijo *et al.*, 1994). As the circulation is shut down, the associated entrainment of warmth is suppressed and cooling will set in, halting melting and allowing salt to build up to levels which will allow renewed deep water formation (Lehman and Keigwin, 1992a). A large meltwater input could shut down the conveyor completely, with the resulting difference between the warm and cold conveyor being about 30% in heat transport (Rahmstorf, 1994).

While surrounded by ice-sheets, the Atlantic Ocean's thermohaline circulation was vulnerable to meltwater induced mode switches, which were responsible for large temperature changes in the land surrounding the northern Atlantic (Broecker, 1994a). Since the beginning of the Holocene, when large ice-sheets have been absent, it appears that the global thermohaline circulation has been more stable because of the absence of meltwater induced mode switches (Broecker, 1994a). This conclusion is supported by the work of Keigwin *et al.* (1994), who observed no variations in NADW formation during substage 5e of the Eemian when massive ice sheets were absent.

The trigger for the mode changes is not completely understood, although Heinrich events or Milankovitch cycles have been suggested (Kerr, 1993b; Weaver and Hughes, The rate of NADW production is about 20 Sv (20 000 000 m^3s^{-1}). Surface water cools from 10°C to 0°C as it descends off Greenland, and to about 3.5°C as it descends off Canada. In creat r NADW, 5 x 10^{21} cal of heat are released in northern latitudes, corresponding to 30% of insolation over the Atlantic Ocean north of 35°N (Broecker *et al.*, 1985; Street-Perrott and Perrott, 1990; Lehman and Keigwin, 1992 a,b). In the region of about 55°N, the warm, salty surface flow splits into two subsurface belts of NADW referred to as upper NADW (UNADW) and lower NADW (LNADW) (Figure 4.2). The upper belt is fed primarily by open ocean convection in the Labrador Sea, and the lower by convection in the Norwegian Sea basin. Although SSTs at the two sources are nearly identical, the cooling associated with the LNADW production in the vicinity of 70°N is twice as great as that further south, resulting in a release of 40% more heat per unit flux, making it a more effective climate forcing agent (Lehman and Keigwin, 1992a,b).

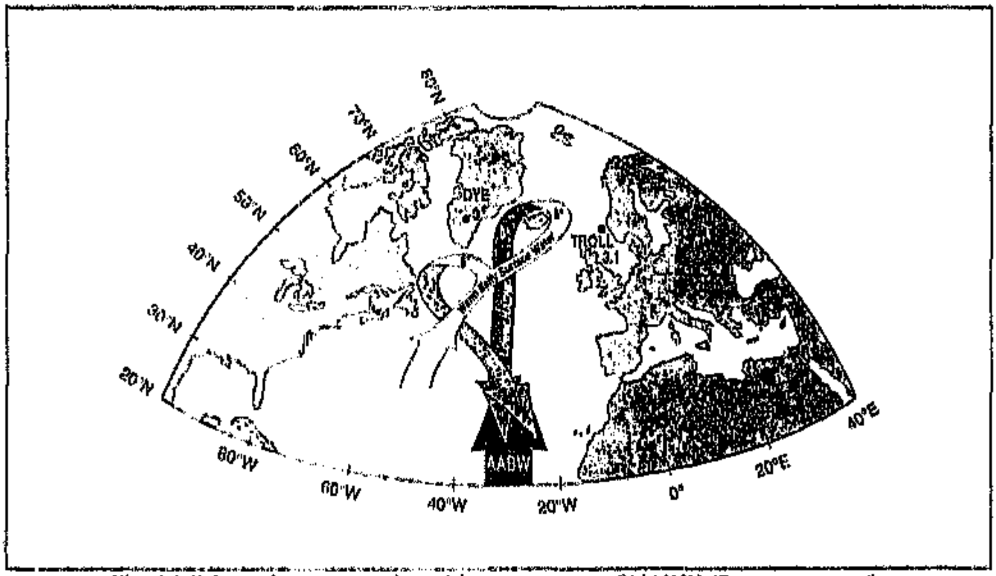

Fig. 4.2 Schematic representation of the components of NADW. Temperatures refer to surface waters before convection, and lower waters after convection. When the NADW ceases to flow, AABW flows north (Lehman and Keigwin, 1992b).

At present, a combination of cold air and restricted sea ice promotes deep water formation in the Norwegian Sea, and drives a compensatory surface flow of warm Atlantic water into the basin. Deep waters formed in the Norwegian Sea flow southwards into the deep Atlantic, forming the densest and deepest component of NADW, LNADW (Lehman and Keigwin, 1992a). It is maintained that during interglacial stages, the Atlantic Ocean is characterised by the formation of high and low density NADW, with LNADW penetrating southward to the equator, while Upper Circumpolar Water (UCPW) and UNADW dominate the mid-depth tropical Atlantic. During full glaciations little or no LNADW is formed, UNADW is restricted to above 2 000 m, and the deep ocean contains a mixture of southern and northern waters (Oppo and Fairbanks, 1990). Deglacial shifts in the poleward flow of warm Atlantic surface waters can occur very rapidly (within 40 years), resulting in SST increases of 5°C; these, in turn, cause rapid changes in atmospheric temperatures, in thermohaline circulation and in ice-sheet melting rates (Lehman and Keigwin, 1992a). The cooling associated circulation was much greater than present (Partridge, 1997) and occurred at a time of increased regional pressure gradients (Lancaster, 1989). Interaction between the South Atlantic and South African anticyclones is cited as a possible explanation to the pattern of alignments of the southwestern Kalahari dunes. The present day October circulation pattern, when the relative strengths of the two anticyclones is about the same, produces winds parallel to the dunes; it appears that a similar circulation regime may have formed the dunes (Lancaster, 1989).

From 30 ka until about 25 ka all regions reflect lower temperatures than present, and except for the Namib and Kalahari, were drier than present (with up to 50% less rainfall) (Partridge, 1995). The Southwestern Cape experienced a 4°C - 5°C drop in temperatures on the basis of an analysis of dissolved gases (N_2 and Ar) in an artesian aquifer near Uitenhage (Heaton *et al.*, 1987) and analysis of a stalagmite from Cango Cave (Talma and Vogel, 1992). Caution has been advised in accepting that the Namib and Kalahari were arid during this interval (Partridge, 1993b), as good evidence for humidity exists at Khommabes and Narabeb between 30 ka and 26 ka (Deacon *et al.*, 1983). Speleothem formation in Rössing Cave occurred between 42 ka and 26.5 ka (Heine and Geyh, 1984), with no subsequent development of the sinter. Tufa deposits in the Kuiseb River at Hudaob and calcified rootcasts and calcretes are further evidence for increased local moisture availability during this period (Vogel, 1989). High water levels in pans in the south-west Kalahari suggest increased rainfall and recharge of aquifers at about 27 ka (Lancaster, 1989), although it must be remembered that precise dating is problematical, as groundwater recharge may lag rainfall by some time (up to thousands of years for large aquifers) (Lancaster, 1986).

Evidence for Isotope Stage 2 (21 ka - 10 ka) is relatively detailed, owing to the improved dating resolution for the period. Although the circulation regimes producing winter and summer rainfall are quite different, the effect of the Glacial Maximum seems to have been similar in both regions, although sites in the winter rainfall region of the country are relatively few. From 20 ka - 16 ka, it appears that the entire subcontinent was uniformly much colder and drier than at present (Scott, 1988) with coldest temperatures occurring between 20 ka and 17 ka, (Figures 6.3 - 6.5), reaching values of about 5°C - 6°C below present. These values for the Last Glacial Maximum come from the Uitenhage aquifer (Heaton *et al.*, 1986) and the Cango Cave speleothem (Talma and Vogel, 1992). During this interval conditions became drier over the whole sub-continent, (Partridge *et al.*, 1990) with estimates of annual rainfall varying from 20% to 80% of the present mean. In the Namib, the Homeb silts occur to heights of 37 m above the Kuiseb river, indicating reduced flow and increased aridity (Vogel, 1989). It has, however, been suggested that conditions may have been somewhat wetter in the Transvaal, based on pollen spectra from Wonderkrater (Scott and Thackeray, 1987).

Although conditions remained cold between 16 and 13 ka, the end of the LGM in Africa is generally placed no later than 16 ka and mesic conditions followed: from 17 ka to 13 ka (Figures 6.6 - 6.9) there is some evidence of increased rainfall over the whole subcontinent, including the Kalahari and Namib (Lancaster, 1981). Kalahari lakes returned to former levels (Shaw *et al.*, 1988), and conditions in the Namib were also wetter. The reach of the Tsondab river was extended westwards, renewed tufa formation occurred in a gorge of the Kuiseb river, and the Homeb silts were extensively incised (Vogel, 1989). Evidence from the south western Cape (Cederberg Range and

CHAPTER SIX

RESULTS

Southern African Palaeoclimate since 40 000 B.P.

The trends shown by the proxy data are mapped below. Although each map represents a time slice of 1 ka, some time slices are grouped to facilitate meaningful discussion. On a number of maps which combine both the newer PASH data and supplementary data derived from a review of post-1986 publications, a number of anomalous sites have emerged (showing opposing trends in proximity to each other). In general, these anomalies have been resolved by examining the weight of evidence from other nearby sites, before deciding the probable dominant component. In some cases the data received or published may in fact be subject to errors, or there may be dating problems. Further, not all the maps have an equal number of sites.

For each of the Arc/Info-generated South Africa maps, the reader is invited to refer to Figure 6.1 which gives the key to the symbols used in the maps, along with estimates of the actual differences they show. There is, on the whole, good agreement between the published data postdating 1986 and those from the PASH database. The material gathered to date will undoubtedly be a valuable resource for climate researchers, both locally and internationally.

Before discussing the patterns revealed by the maps, note should be taken of problems of dating. In Quaternary studies heavy reliance is placed on the use of absolute dating techniques. Although several different techniques are used routinely, the most readily available method is radiocarbon dating, which has a limited range and requires calibration based on both global and regional departures from theoretically and empirically determined relationships. ^{14}C dating is possible only for the last 40 ka of Earth history; this is reflected in the paucity of data for periods beyond 40 ka. A detailed account of dating and other related problems is given in Appendix One, where the data from individual sites are described in detail.

The palaeoclimates of southern Africa have been investigated through the medium of several different disciplines, and a fair understanding of temporal and spatial changes over the subcontinent has been achieved (Deacon and Lancaster, 1988; Vogel, 1984; Tyson, 1986; Partridge *et al.*, 1990). In order to place the analysis of the last 20 ka in proper perspective, it is necessary to review the changes preceding this period. As the emphasis of this work is on the last 20 ka, the period from 40 ka to 21 ka has not been analysed in terms of synthetic maps.

From about 40 ka to 30 ka, the general trend indicates lower temperatures and wetter conditions than at present (Partridge *et al.*, 1990). However, dune formation associated with increased aridity occurred during this period in north-western Botswana, southern Angola, and Namibia. As dunes form only where annual rainfall is less than about 150 mm - 200 mm, palaeodunes in these regions indicate movement of the 150 mm isohyet by up to 1200 km north-east of its present position. Although the inferred extent of the shifts has been revised (Lancaster, 1988), it is clear that the intensity of the anticyclonic

SECTION TWO

CHAPTER FIVE

SOUTHERN AFRICAN PALAEOCLIMATES

DATA and METHODOLOGY

In an attempt to link past responses of southern African environments to global changes, it is essential to know what the conditions in various parts of the country were during selected key time-slices. To this end the gathering of a substantial database is necessary. This objective forms part of the Palaeoclimates of the Southern Hemisphere (PASH) project. Although data from the whole of southern Africa are being accumulated, the present study focuses on Africa south of 22°S. The last twenty thousand years (20 ka) are considered in detail.

Quaternary scientists, who have carried out primary research, have supplied data using a 6-page data capture form which was submitted to the Climatology Research Group at the University of the Witwatersrand. The trends in hydrological and thermal parameters for each period, as interpreted by the generators of the primary data, were then compiled on maps of Africa south of 22°S, using the Arc/Info Geographic Information System. The maps were analysed to determine trends in rainfall and temperature for the different time-slices and regions. This analysis was compared to existing summaries of palaeoenvironmental trends and to possible mechanisms that could account for the observed trends. Modern-day mechanisms were also investigated to determine whether or not they are analogous with those which prevailed in the past.

The data cited here will ultimately be part of a palaeoclimate database for the southern hemisphere, which is currently being assembled under a collaborative international project of the International Union for Quaternary Research. The database uses Oracle software, which allows for the assimilation, manipulation and updating of datasets through the use of multiple spread-sheets. These provide templates for the entry of data into the database and allow the creation of scenarios and the retrieval of information in terms of specified parameters. Spread-sheets are created using object-oriented programming in a Windows environment, thus avoiding the complications of special programme writing. Once all data for a specific palaeoclimatic site are entered, they are saved on a Unix-based system at the University of the Witwatersrand, from which they can be accessed anywhere in the world through the Internet. Those sites which must be embargoed (because their data are currently unpublished) can be hidden from view, and searches can be made for sites using any one of a series of unique, primary keys which define that site, e.g. researcher's name, site number, time-slice and climatic parameters.

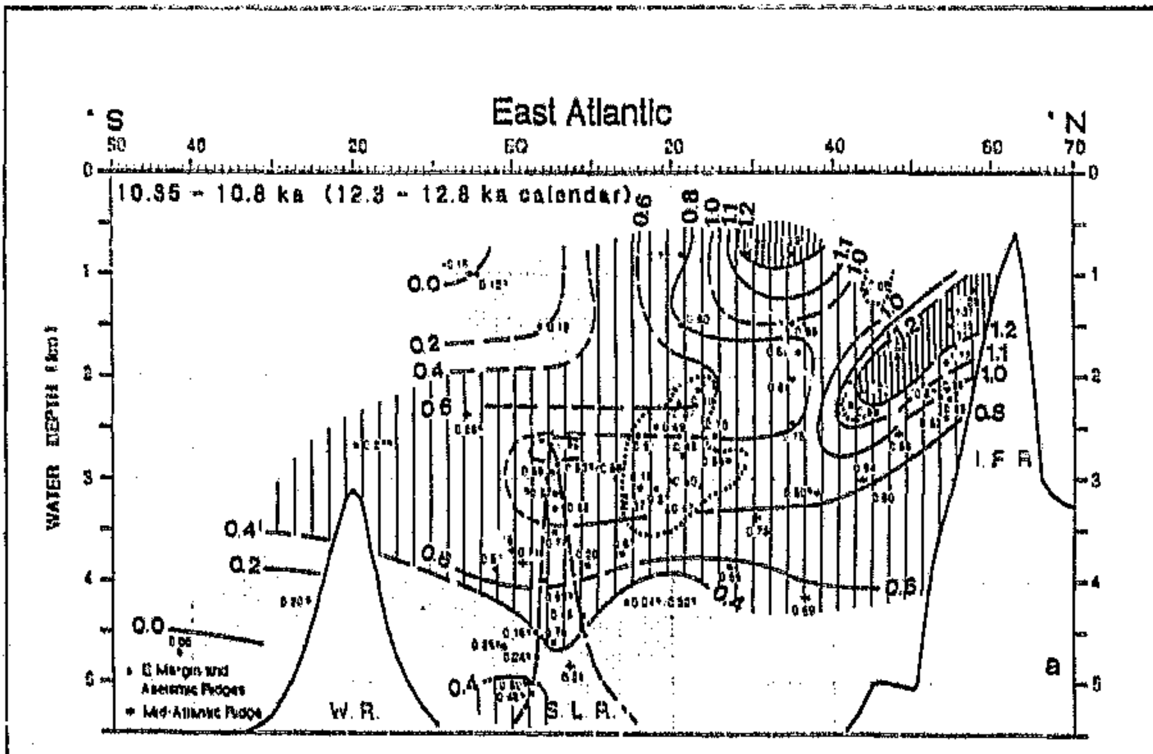

Fig. 4.19 Benthic $\delta^{13}C$ profiles across the east Atlantic; 10.4 -10.8 ka during the Younger Dryas. For abbreviations see Fig. 4.4 (Sarnthein *et al.*, 1994).

Although it is generally argued that melt water pulses result in salinity decreases, an analysis based on dinoflagellate-cyst assemblages in cores recovered from the shelf break at the outlet of the St Lawrence suggests that the melt water pulses did not affect sea-surface salinity (SSS), and the melt water pulse cannot be a trigger for the YD (de Vernal *et al.*, 1996). Work by Duplessy *et al.* (1992) on core NA 87-22 on the Rockall Plateau showed no additional salinity decreases during peaks of meltwater discharge, and sharp negative salinity anomalies were associated with the Younger and Older Dryas cold events. It is argued that these negative anomalies resulted either from a reduction in the strength of the thermohaline circulation, or from a strong freshwater injection owing to changes in the precipitation/evaporation budget. Although these fluxes cannot account for the low salinity values, they can result in a weakening of the thermohaline conveyor by reducing NADW formation. This led to decreased evaporation, increased precipitation and reduced poleward advection of salty subtropical water, which amplified the initial signal resulting in a further decrease in NADW formation (Duplessy *et al.*, 1992). It was concluded that, despite the injection of glacial meltwater during warmer episodes, SSS and SST remained positively correlated during the deglaciation. Cold, low salinity events occurred during the early stages of deglaciation, (14.5 - 13 ka) and the Younger Dryas, but minor injections of meltwater at high latitudes are insufficient to account for the observed salinity changes. It is necessary to invoke an additional feedback from changes in the hydrological cycle and in advection to trigger changes in the thermohaline circulation (Duplessy *et al.*, 1992).

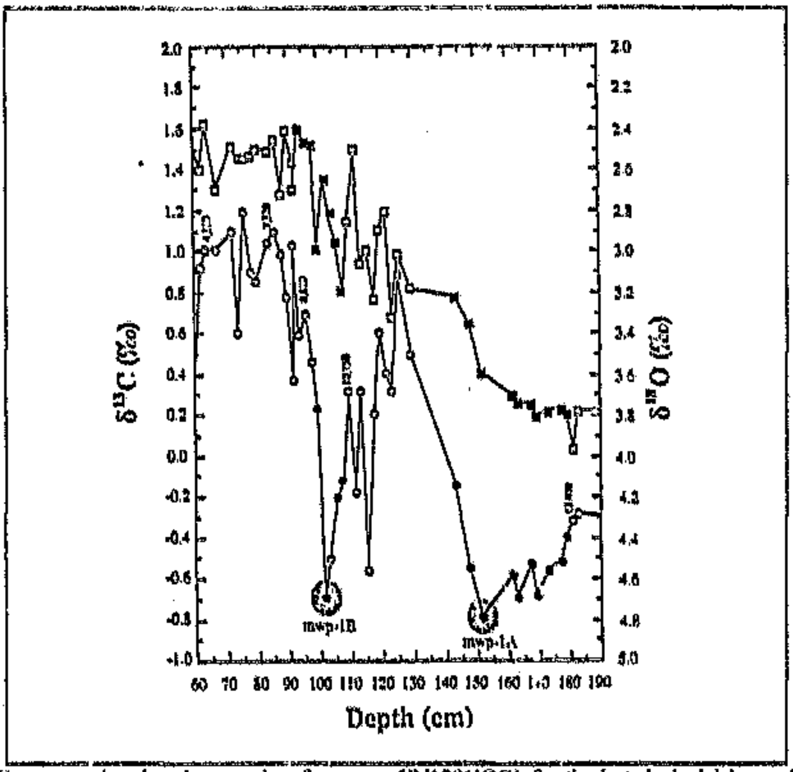

Fig. 4.17 Oxygen and carbon isotope data from core EN120GGC1 for the last deglacial interval. Age assignments are based on four AMS ^{14}C dates from a companion core that has been stratigraphically correlated to EN120GGC1. Using this age model, $\delta^{13}C$ minima are approximately coincident with mwp-1A and mwp-1B. Closed symbols mark the intervals around mwp-1A and mwp-1B and illustrate that $\delta^{13}C$ minima occur during the unidirectional shifts in $\delta^{18}O$ (Fairbanks, 1989).

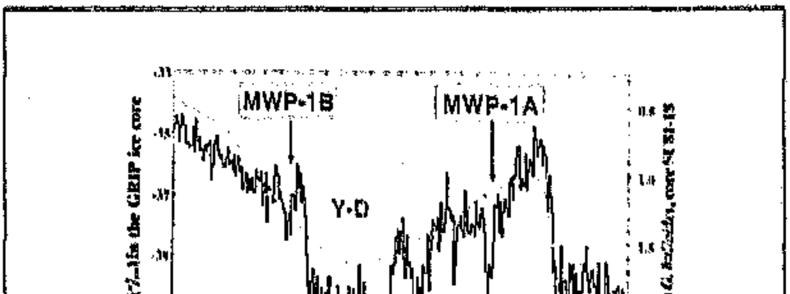

Fig. 4.18 The solid line represents the $\delta^{18}O$ variations measured in the GRIP ice core, open dots show the planktonic foraminifera $\delta^{18}O$ record of deep sea core SU81-18 (raised from 38°N in the north east Atlantic). The strong warming ($\delta^{18}O$ increase at ±14.7 cal ka in the Greenland ice) at the beginning of the Bølling/Allerød (B/A) period is synchronous with the sharp warming in core SU81-18. MWP-1A dated at 14 cal ka is significantly younger than the strong warming at 14.7 cal ka. It corresponds to the first cold reversal of the Bølling/Allerød observed in the GRIP core and GISP2 core (Bard, *et al.*, 1996).

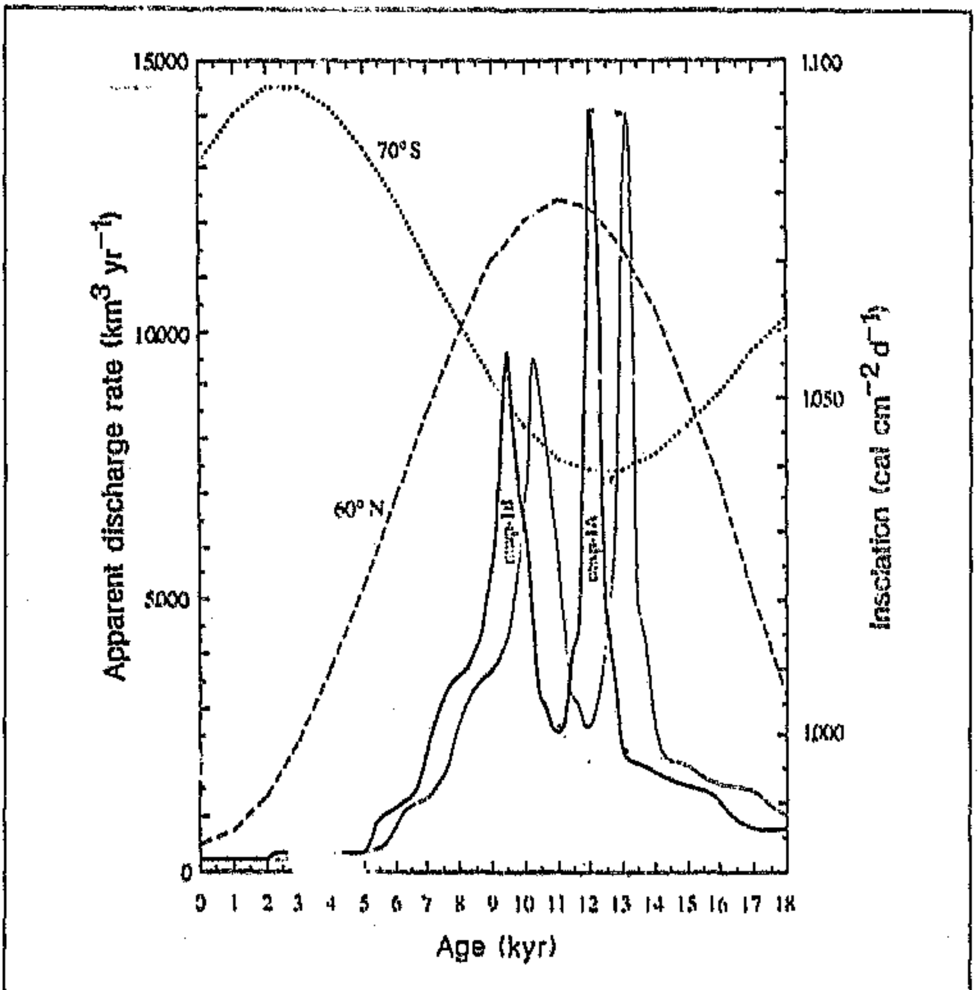

Fig. 4.16 The rate of glacial melt-water discharge calculated from the Barbados sea level curve compared to summer insolation. The discharge curve (thick line) is plotted according to radiocarbon years uncorrected for secular changes in atmospheric ^{14}C. Insolation at 60°N dashed line and 70°S dotted line are plotted against absolute time (Fairbanks, 1989).

Deglaciations and Melt Water Pulses

Deglaciations are triggered by re-organisations of the ocean-atmosphere system. In par'icular they point to the sudden resumption of conveyor circulation in the Atlantic as a 'ey ingredient of such reorganisations. The conveyor brings vast amounts of warm water to the surface of the northern Atlantic, and its resumption would explain the rapidity and magnitude of the change associated with Termination II (Broecker *et al.*, 1990). Recent geochemical data have challenged the view that rapid climate fluctuations in the North Atlantic were caused by the thermohaline circulation being switched on or off. and indicate rather that circulation switches between a warm deep mode and a shallow cold mode were associated with different sites of deep convection. The mechanism for the transition is the rearrangement of convection in the North Atlantic. triggered by brief melt water pulses (Rahmstorf, 1994).

Melt water pulses are characterised by low $\delta^{13}C$ values and reduced flow speeds. It has been inferred that high Cd/Ca ratios in benthic foraminifera deposited on the Bermuda Rise reflected dramatically reduced NADW production at 14.5 ka in response to a widespread flux of meltwater in the Norwegian Sea (Keigwin, and Lehman, 1994). After the start of Termination IA (14 ka) flow speeds abruptly decreased and reached a minimum at between 14 ka and 13 ka, as indicated by a pronounced minimum in $\delta^{13}C$, values which suggests a decreased influence of northern source water. This decline is coincident with Heinrich event 1 and the associated melt water input (McCave *et al.*, 1995). It is maintained that this meltwater pulse at 13,5 ka induced the "meltwater mode", which shut down NADW production, and halted the thermohaline conveyor belt (Sarnthein *et al.*, 1994). The result was a major cooling in Europe, (the Older Dryas). Subsequent renewal of NADW production reversed the cooling in a few hundred years and synchronously released vast amounts (120 Gt) of carbon, which accounts for the carbon "plateaus" at these times (Sarnthein *et al.*, 1994). The melt water pulses centred at 12 ka and 9.5 ka (Figure 4.16) were also characterised by very low $\delta^{13}C$ values, (Figure 4.17) as determined from an accurate chronology of core EN120GGC1, presumably owing to reduced NADW influence at the site (Fairbanks, 1989). The Younger Dryas cold epoch. does not, however, seem to have resulted from a similar oceanic circulation regime. a situation similar to that of the present existed during the event (Figure 4.19). According to the data, a meltwater pulse preceded the YD by 1 ka (Figure 4.18) (Bard, *et al.*, 1996); this pulse, although larger than that at 13.5 ka, seems not to have impacted on the crucial site of deep water production in the GIN seas (Sarnthein *et al.*, 1994). Subsequently, at 10.3 ka, towards the end of the Younger Dryas, a melt water mode occurred (Sarnthein *et al.*, 1994).

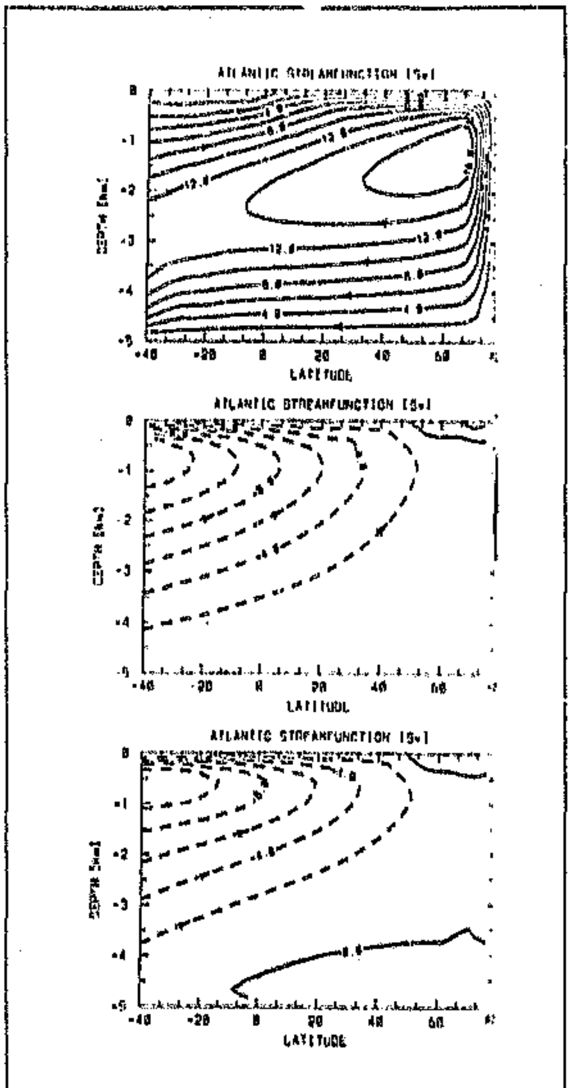

Fig. 4.15 Three states of the Atlantic thermohaline circulation afte. 1000 years of anomalous runoff into the North Atlantic. (a) the slightly perturbed conveyor, (b) The Atlantic circulation has reversed (termed southern sinking) (Stocker *et al.*, 1992b).

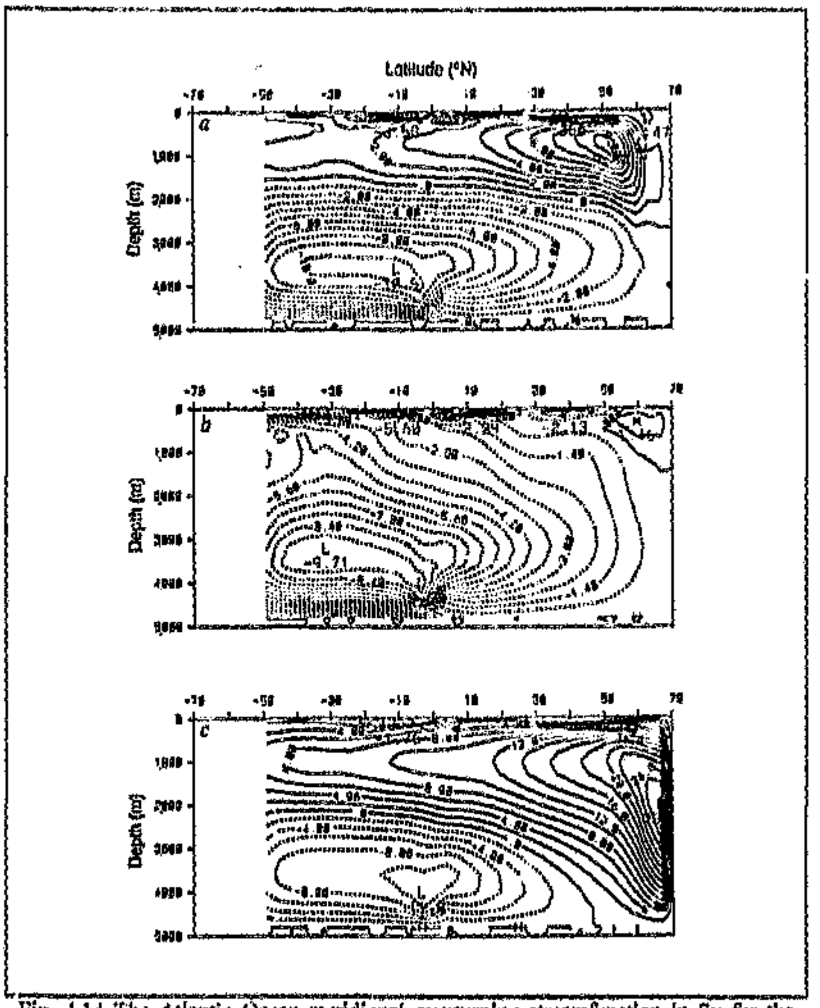

Fig. 4.14 The Atlantic Ocean meridional overturning streamfunction in Sv for the three equilibria. (a) the normal 'present-day' conveyor, (b) the weak 'colder' conveyor, (c) the strong 'warmer' conveyor. The x-axis is the latitude with positive and negative values indicating °N and °S respectively. Positive and negative contours indicate clockwise and counterclockwise circulations, respectively, with H and L indicating local maxima and minima, respectively (Weaver and Hughes, 1994).

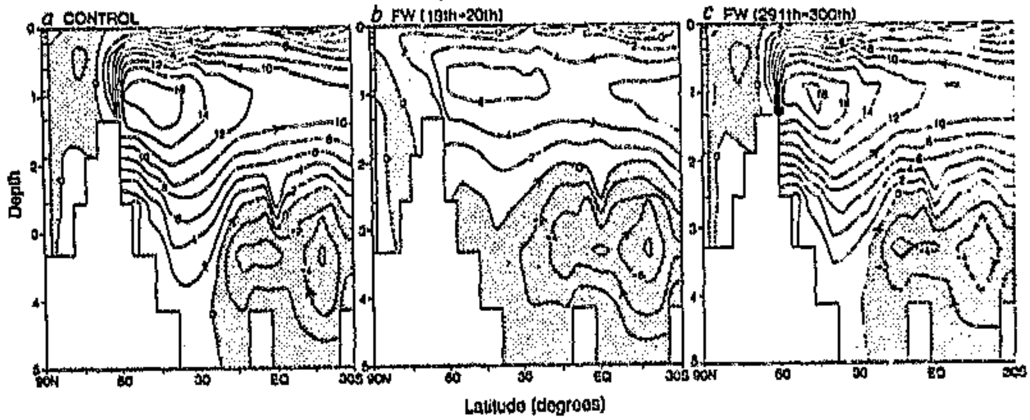

Fig. 4.13 Latitude-depth distribution of the stream function which represents the meridional overturning in the North Atlantic in units of sverdrups averaged over (a) years 501 - 600 of the control experiment, (b) years 19 and 20 and (c) years 291-300 of the freshwater experiment. (Depth is given in km, areas of clockwise circulation are shaded). During the few initial decades, the THC in the North Atlantic markedly weakens and becomes shallower (compare (a) and (b), allowing a stronger deep inflow of AABW. The initial capping of the Atlantic Ocean by the low-density, fresh surface water chokes off the heat exchange between the atmosphere and the ocean and raises the temperature of the subsurface water, rapidly weakening the THC (Manabe and Stouffer, 1995).

medium mode, 25 Sv: strong mode). Cycles involving millenium-long intervals, during which the strong conveyor mode is operative are induced; these terminate in sharp transitions to the weak mode, followed immediately by a more gradual shift to a millenium-long medium mode. The cycle ends with an abrupt shift back to the strong conveyor (Broecker, 1994a).

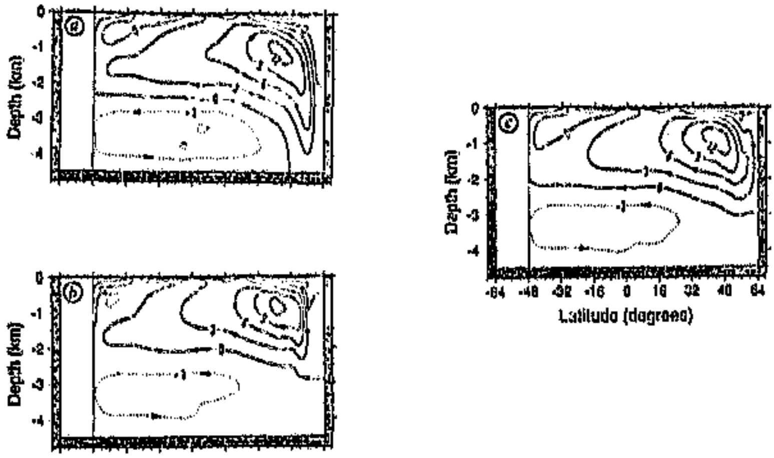

Fig. 4.12 Zonally integrated meridional mass transport in 10^6 m^3 s^{-1} in the Atlantic model basin: (a) for the spin-up conveyor state, (b) for the equilibrium reached after the first fresh water perturbation; (c) for the equilibrium after the second perturbation. These three coupled equilibria exist under the same forcing. Note that in (b) and (c) the NADW cell does not reach down to the bottom of the North Atlantic (Rahmstorf, 1994).

A model by Stocker *et al.* (1992b), (Figure 4.15) produced four steady states of the thermohaline circulation under identical boundary conditions. One of these states is when the Atlantic circulation is reversed, with deep water only being formed in the Southern Ocean. Atlantic SSTs are 4°C cooler in this mode than in the normal conveyor, and result in atmospheric temperature changes of 2.6°C at 70°N.

Common to all the ocean circulation models is the sensitivity of the ocean circulation to small changes in surface forcing, particularly to buoyancy fluxes in regions of deep water formation in high latitudes (Hasselmann, 1991). Differences in the circulation regimes may be attributed to different relative rates of deep water formation in the North Atlantic and in Antarctica. The experiments produce a continuous transition from a circulation regime in which most of the deep water is formed around Antarctica to a circulation regime similar to the conveyor belt circulation, in which deep water is formed mostly in the North Atlantic (Hasselmann, 1991). Further, all models tend to replicate the tight coupling between the strength of the conveyor belt and changes in temperature in the northern hemisphere.

Atlantic to high northern latitudes. The model predicted a drop in SST of up to 5° C within 10 years. The rate of NADW production remained the same, but cold conditions were associated with NADW sinking to intermediate depths only, while AABW pushed north to fill the entire abyssal Atlantic (Rahmstorf, 1994).

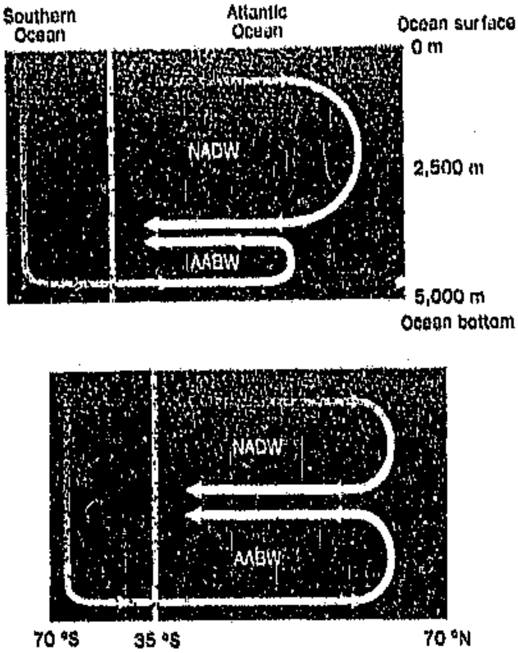

Fig. 4.11 Schematic diagram of North Atlantic Deep Water overlying deeper Antarctic Bottom Water. Top, present-day circulation; bottom, possible circulation in the Last Glacial Maximum, with a shallower North Atlantic conveyor and stronger flow of AABW (Boyle and Weaver, 1994).

Manabe and Stouffer's (1995) coupled model reproduced the abrupt oscillations observed in ice and ocean cores when subjected to fresh water inputs (Figure 4.13). Their model caused the thermohaline circulation to weaken dramatically, and then intensify, followed by a further weakening which subsequently recovered gradually. During the weak thermohaline circulation, AABW moved north and filled the ocean to 60° N up to 2 000m. The oscillations occurred over a time scale of centuries and produced large temperature variations in the northern high latitudes, but had less of an effect on the rest of the world.

Many models exhibit multiple states of operation. Weaver and Hughes' (1994) simple two-basin ocean model, (Figure 4.14) driven by freshwater fluxes in high latitudes exhibits three stable states, all characterised by two Atlantic circulation cells, a shallow conveyor driven by deep water formation at its northern end, and a deep conveyor in the opposite sense driven by deep water formation in the Southern Ocean (Broecker, 1994a). By releasing excess fresh water at the surface of the model's northern Atlantic, sudden swi[illegible]s in circulation from one mode to another occur. The states differ in the relative strengths of the circulation cells (1.5 Sv: - weak mode, 10 Sv:

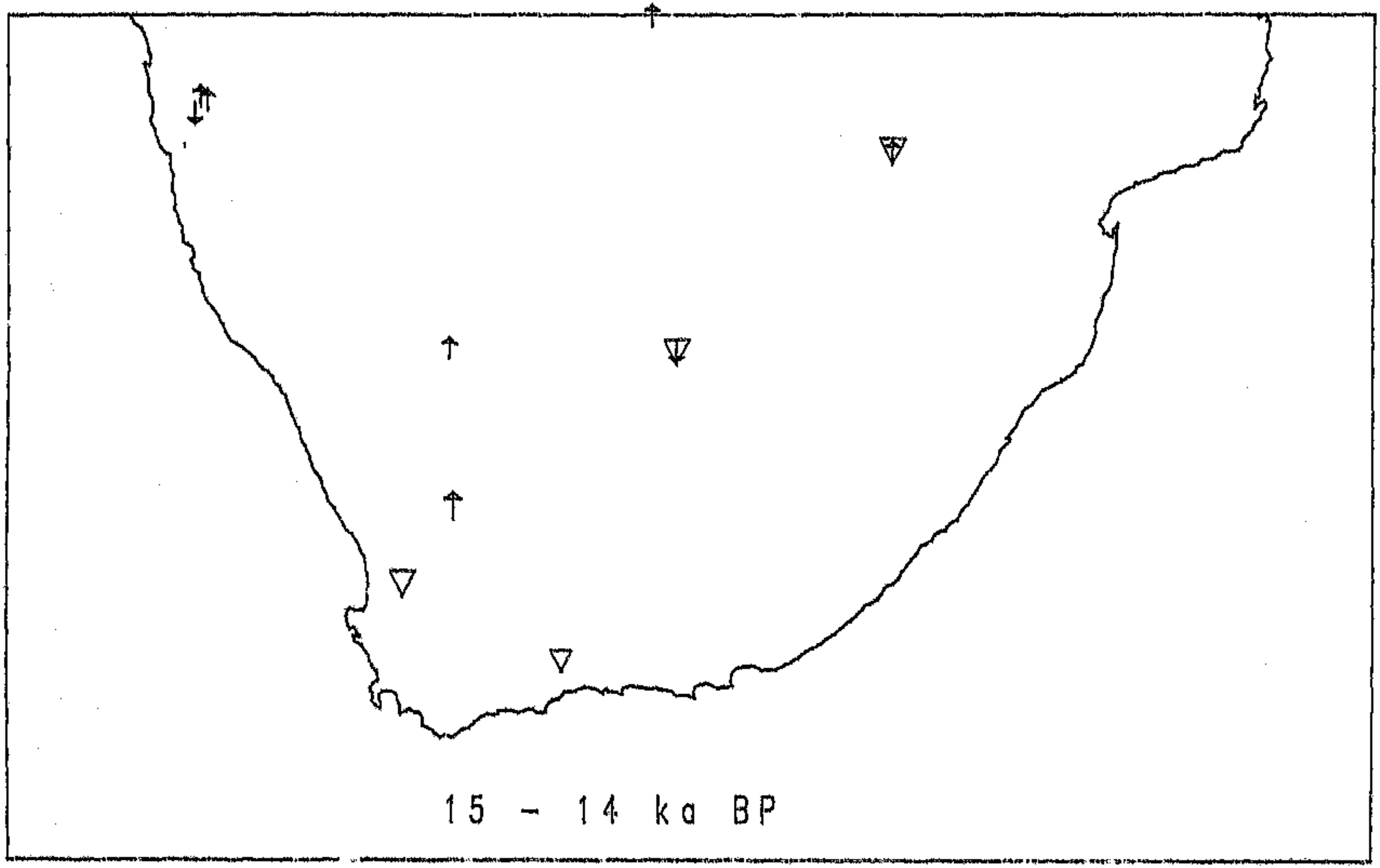

Fig. 6.8 Southern Africa, Temperature and Rainfall: 15 ka.

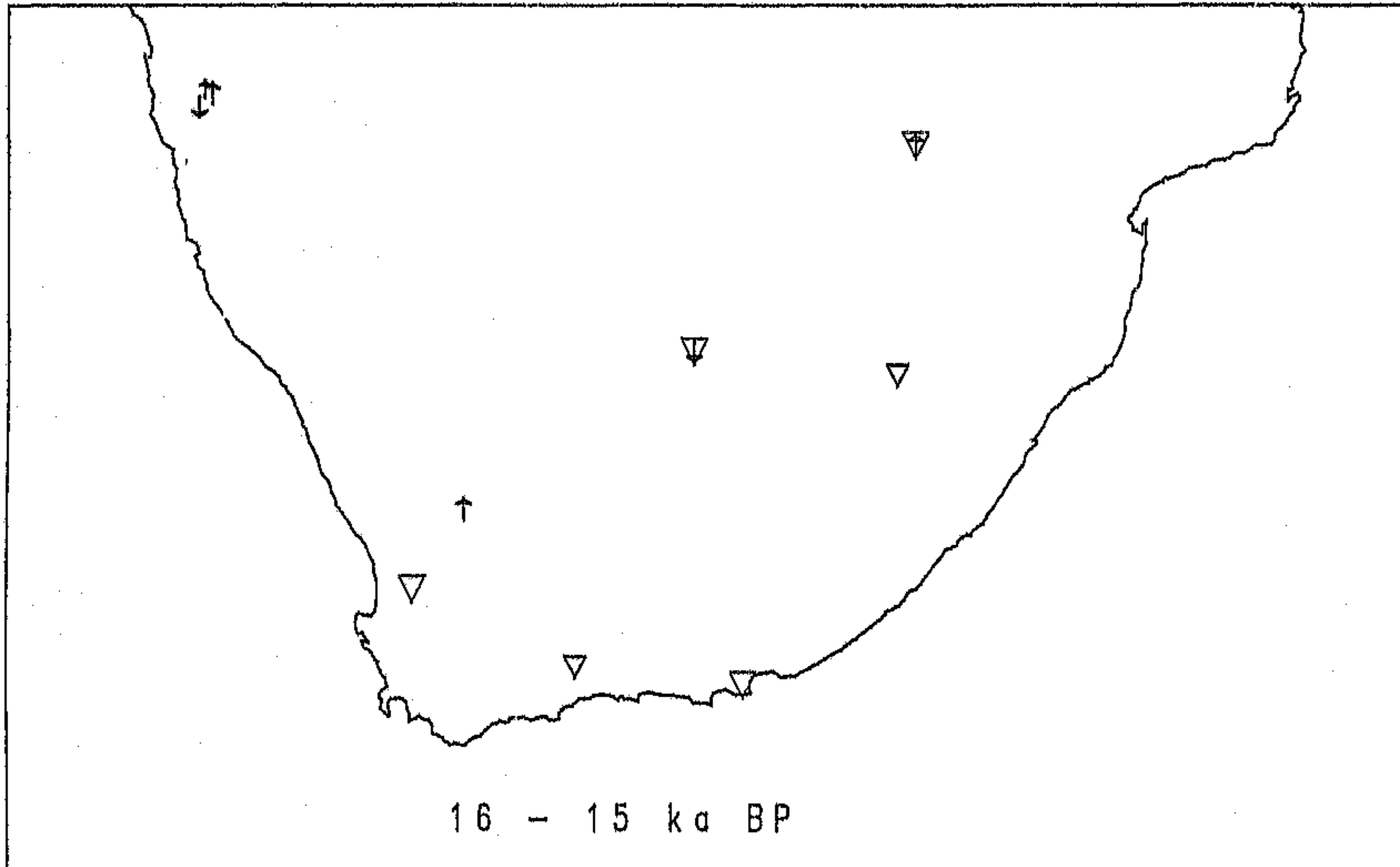

Fig. 6.7 Southern Africa, Temperature and Rainfall: 16 ka.

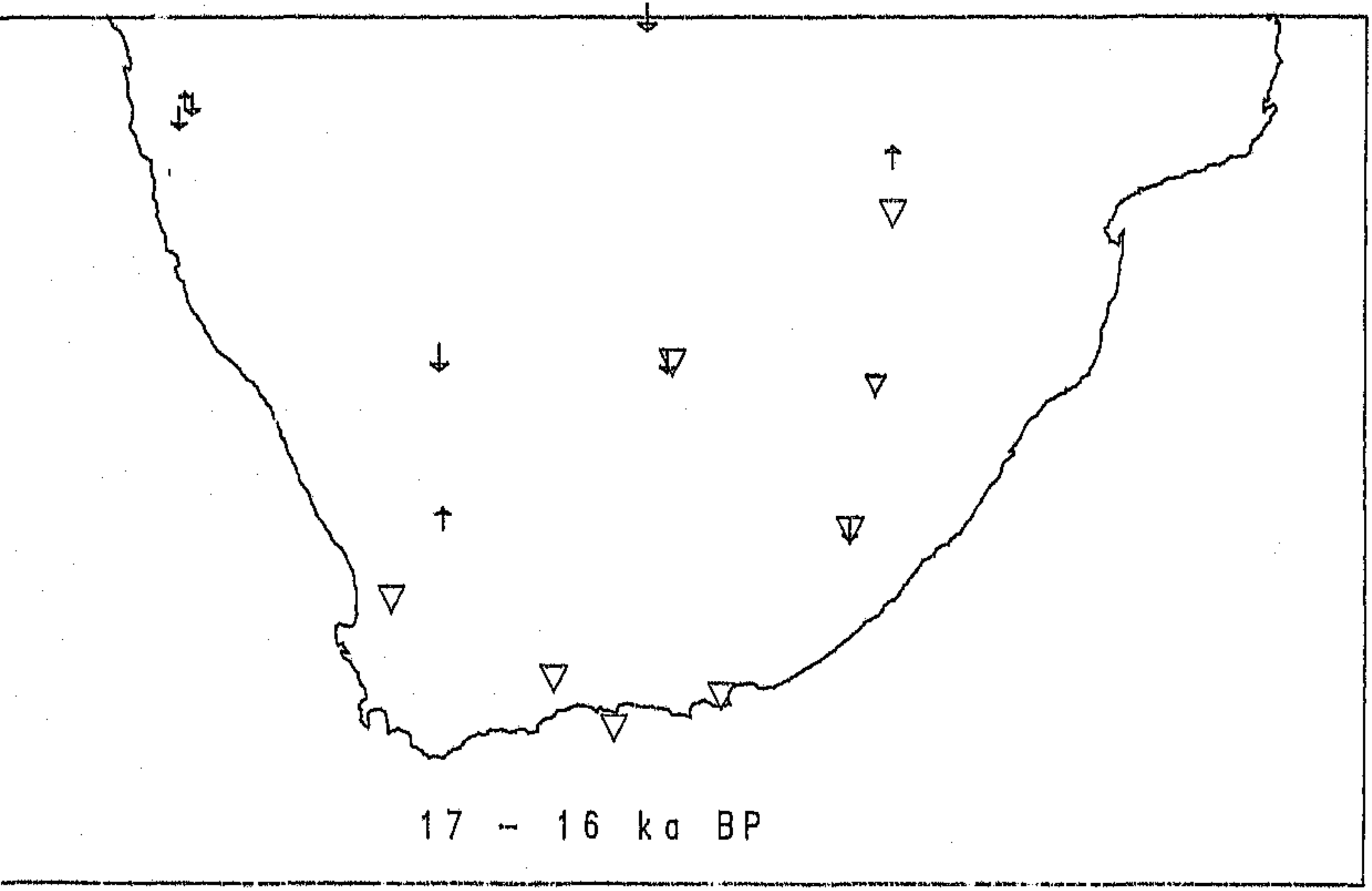

Fig. 6.6 Southern Africa, Temperature and Rainfall: 17 ka.

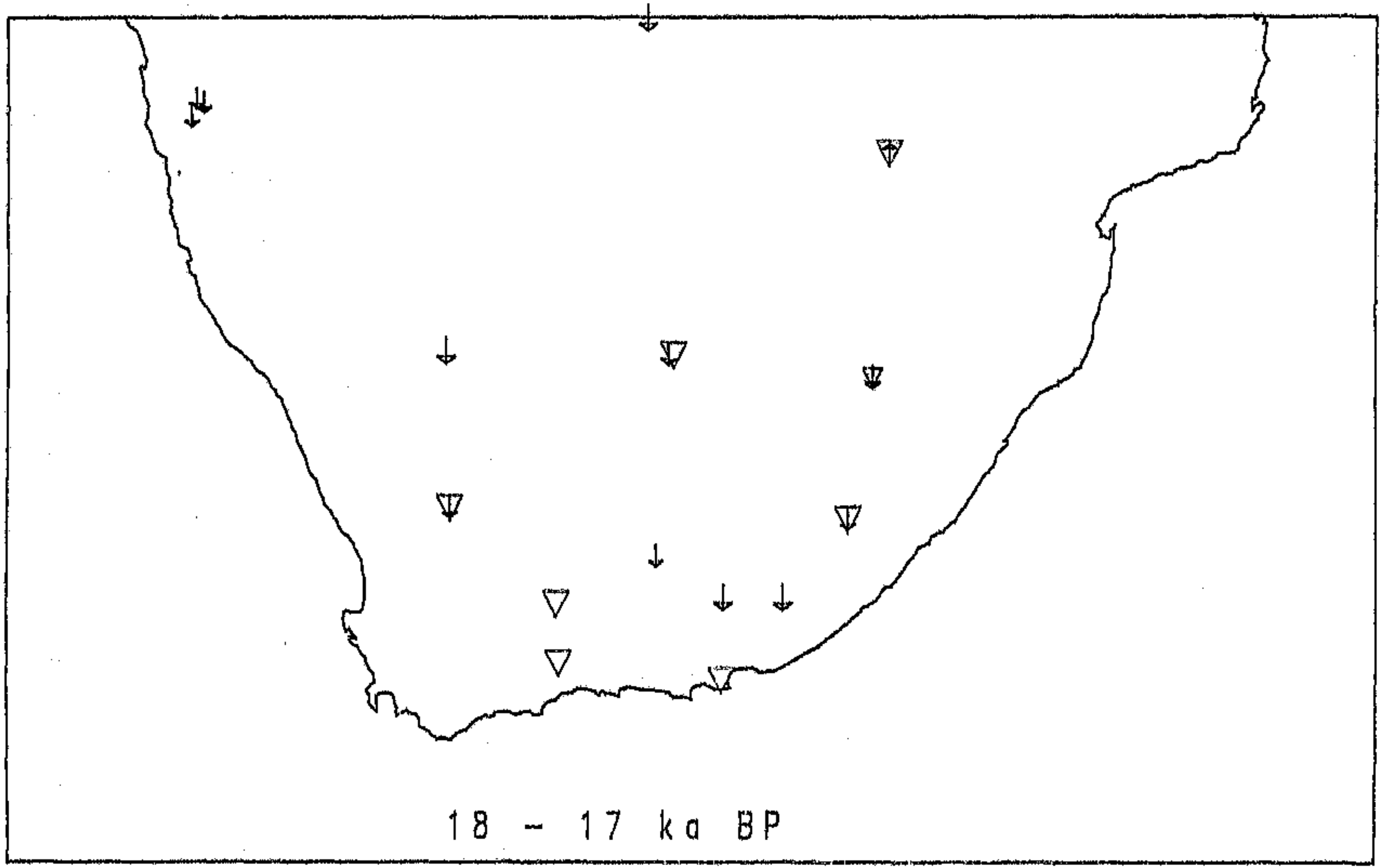

Fig. 6.5 Southern Africa, Temperature and Rainfall: 18 ka.

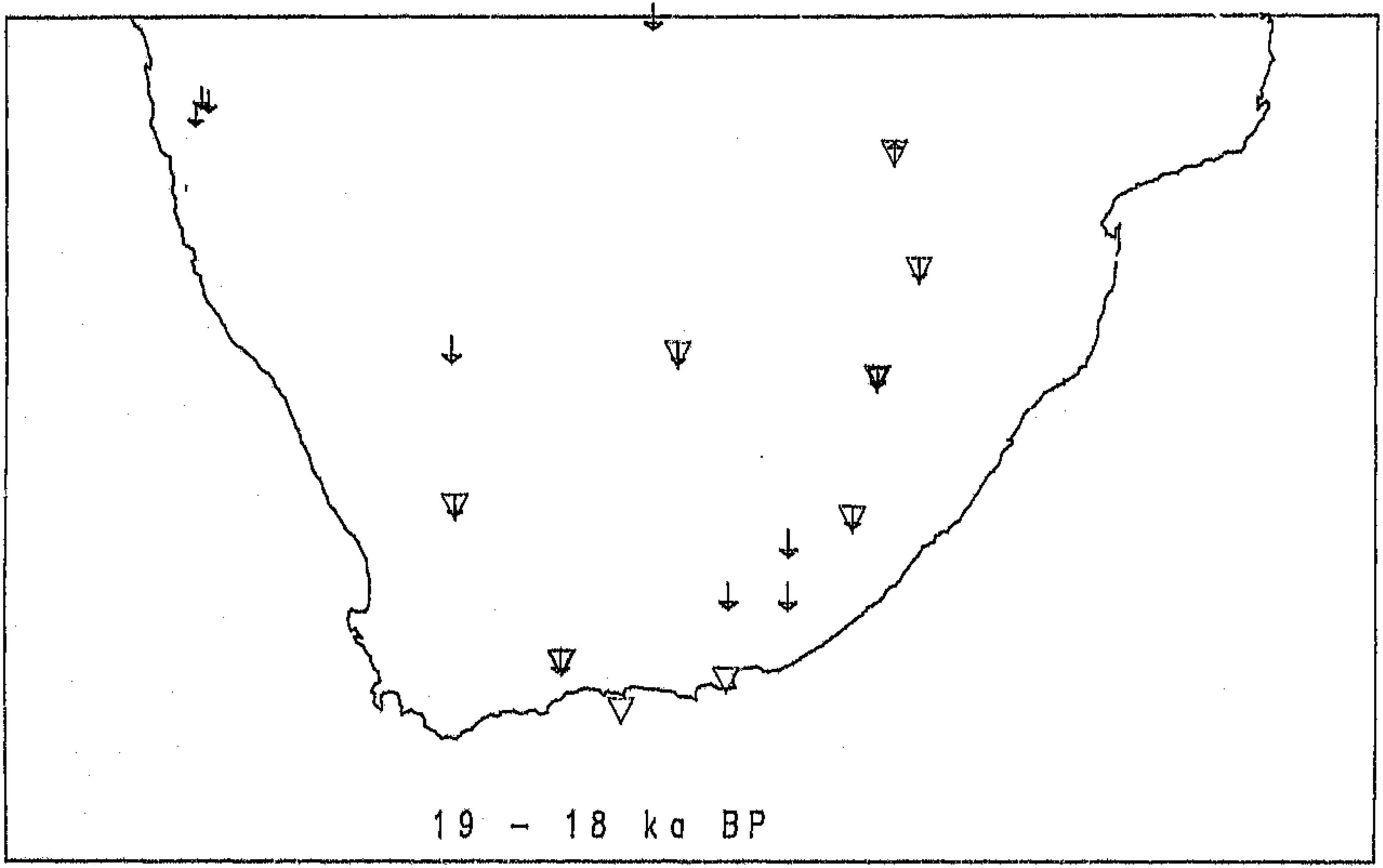

Fig. 6.4 Southern Africa. Temperature and Rainfall: 19 ka.

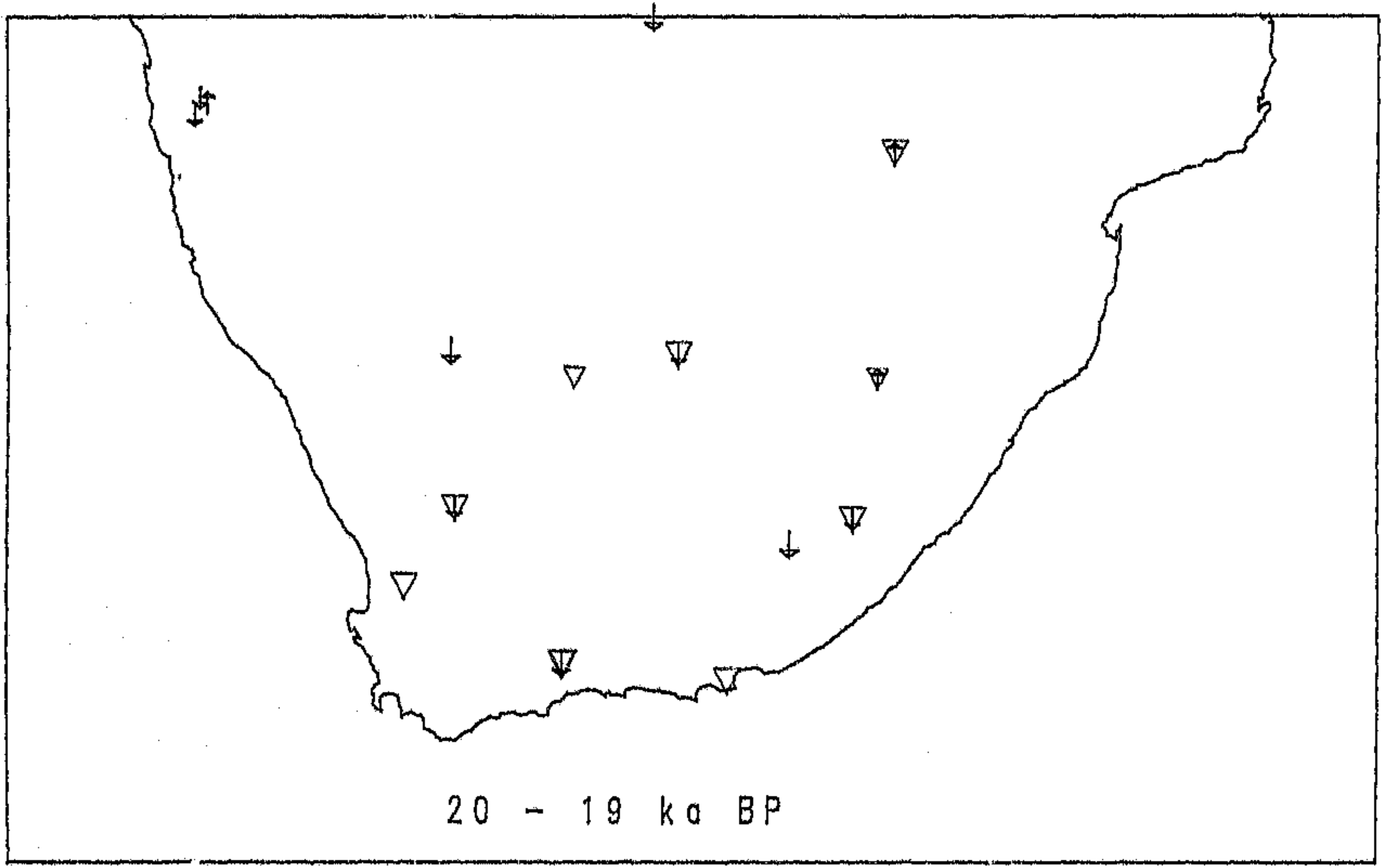

Fig. 6.3 Southern Africa. Temperature and Rainfall: 20 ka.

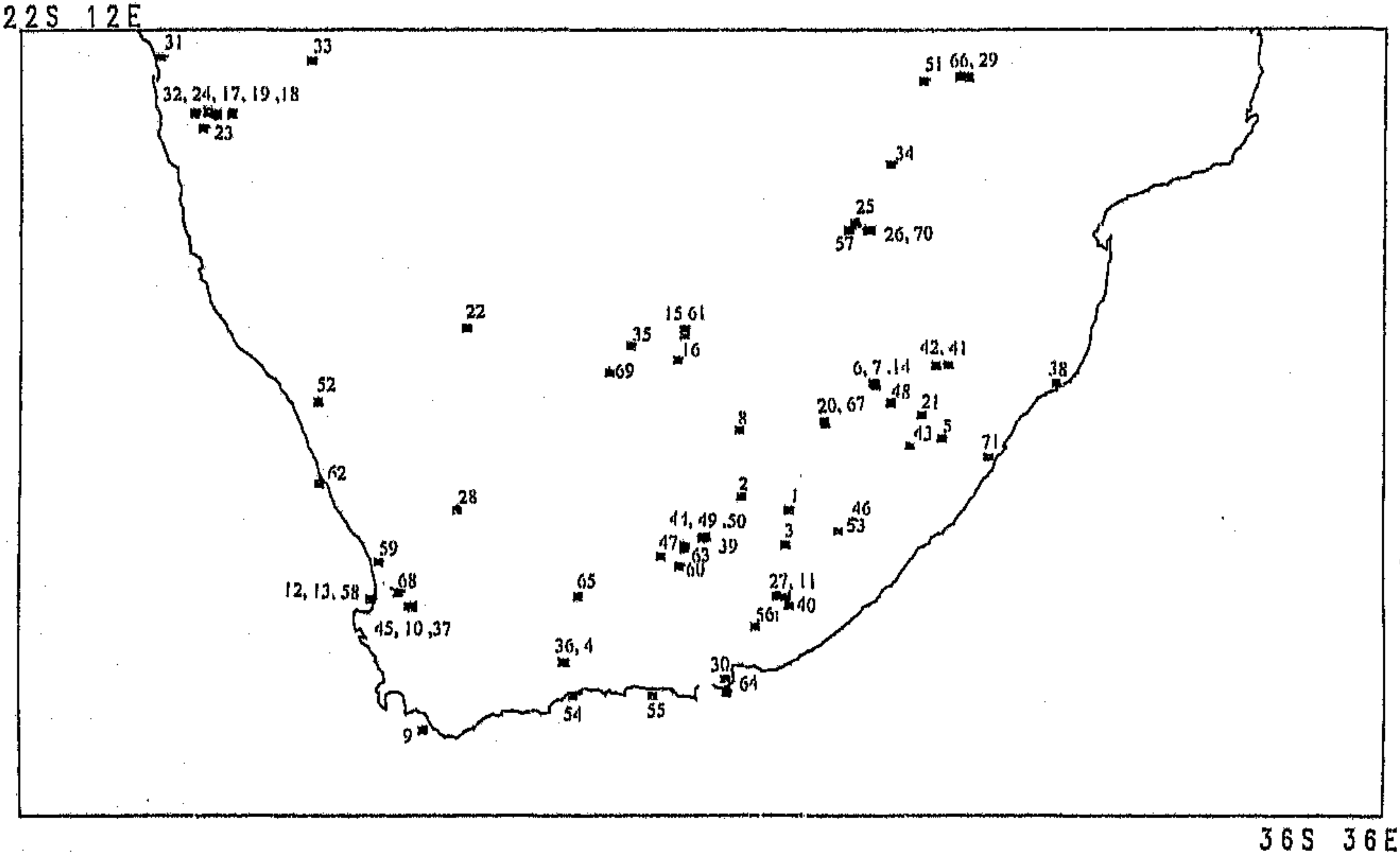

Fig. 6.2 Locations of sites used to generate the PASH maps. Refer to Table 1 in Appendix 3 for details.

PALAEOCLIMATE MAPS OF SOUTHERN AFRICA

Rainfall			Temperature		
↓	> 20%	--	> 2.5°	▽	Decrease from Present
↓	10% - 20%	-	1.5° - 2.5°	▽	
↓	5% - 10%	(-)	0.5° - 1.5°	▽	
□	< 5%	0	< 0.5°	•	
↑	5% - 10%	(+)	0.5° - 1.5°	▵	
↑	10% - 20%	+	1.5° - 2.5°	△	Increase from Present
↑	> 20%	++	> 2.5°	△	

Fig. 6.1 Key to maps generated from the PASH data and the literature review.

In southern Africa, data from 23 sites were compared for signals reflecting the Little Ice Age. The temperature series from Cango Cave speleothem (Talma and Vogel, 1991) and another derived from analyses of planktonic foraminifera off the coast of Walvis Bay suggests that the Little Ice Age started in 1300 AD and ended in about 1850 AD, with a warmer interval at 1550 or 1600 AD. Further palaeonvironmental evidence from shell middens at Elands Bay indicates cooling between 1300 and 1550 AD (Cohen *et al.*, 1992). Evidence from the interior of South Africa suggests that the maximum cooling was at about 1400 AD (Scott, 1991).

The 1400 AD cooling is supported by an analysis of tree ring data from the western Cape (Cedarberg) and Natal (Karkloof). The tree ring series also reflect the warming at about 1600 AD (Tyson and Lindsay, 1992), and indicate that regional differences did exist. Evidence of the Little Ice Age is also forthcoming from Namibia (Vogel and Rust, 1987), where the Amspoort silts buried a riverine forest which grew during the earlier warm period.

Conclusion

The climatic history of southern Africa matches that of other parts of the world in its general characteristics: the cold, arid climates of Isotope Stage 2 were followed by ameliorating conditions during Stage 1 (the Holocene), with temperatures peaking in the Holocene Altithermal. A climate reversal is evident in the record, similar in both temperature and rainfall patterns to the Younger Dryas of the northern hemisphere. It appears, however, to predate its northern hemisphere counterpart by a thousand years in terms of its initiation and termination, although the dating control is less precise than could be wished.

The onset of wetness over Namibia, the Northern Cape and Transvaal dates to between 7.5 ka and 6.5 ka, but south of 29°S it occurs no earlier than 5.5 ka and as late as 3.5 ka in the Southern Cape (Scott, 1993). The influence of the Agulhas current, associated with a southward shift in the Subtropical Convergence, is inferred in controlling this diachronism (Partridge, 1997).

From 5 ka to 3 ka, rainfall throughout the interior of South Africa became higher than at present, while the Namib and southern Kalahari became drier (Figures 6.18 - 6.19). Some caution may be necessary when interpreting certain southern Kalahari sites, as they consistently indicate moisture trends opposite to those from nearby areas, for which no ready climatological explanation is available. Some of these sites rely on dating of pedogenic calcite which may significantly postdate the features in which it has formed. Central sites suggest wetter conditions at 4.5 ka (Scott and Cooremans, 1990), while eastern sites became wetter at 2.4 ka (February, 1993). Temperatures in the summer-rainfall region were higher at 4 ka, but Cape coastal sites reflect lower temperatures at 3 ka (Cohen *et al.*, 1992; Talma and Vogel, 1992). The same temperature regime obtained until 2 ka, except for a possible cooling in the far northern Transvaal. Some sites in the summer-rainfall region show a cooling after 3 ka and rainfall decreased in the winter-rainfall region (Meadows and Sugden, 1991) and in the eastern Cape. This desiccation seems to have spread into Natal before 1 ka.

After 2 ka, the regional differences evident in the previous period continued, but were less marked (Figures 6.20 - 6.22). In the southern part of the winter rainfall region, there was a decline in available moisture, but the western Cape became wetter during this period with a decrease in summer rainfall. A decline in moisture over the Transvaal is also apparent, especially at about 1 ka (Scott and Brink, 1992). Within this interval two periods have been extensively documented: the Mediaeval Warm Epoch, and the Little Ice Age (Tyson and Lindsay, 1992). Although there were climatic fluctuations on even smaller time scales within each period, there is good agreement between several sites with continuous records in western half of the country. The Mediaeval Warm Epoch was characterised by warmer, wetter conditions, while the subsequent Little Ice Age was subject to a climate colder and drier than any since the Younger Dryas.

The Mediaeval Warm Epoch occurred from about 900 to 1300 AD. The Cango Cave temperature series records a peak in temperature at around 900 AD (Talma and Vogel, 1991), while the oxygen isotope analysis and aragonite-to-calcite ratio of *Patella granularis* and *Patella granatina* shells from Elands Bay show a warming from about 1000 to 1300 AD (Cohen *et al.*, 1992). Evidence from the interior at Wonderkrater, Tate Vondo, Scot Spring, and Rietvlei Dam suggests that the warming took place between 900 and 1300 AD (Scott, 1991). Tree ring analyses from Natal suggest that a warm period occurred before 1300 AD (Tyson and Lindesay, 1992).

The Little Ice Age was a globally-extensive cool period, and is well documented in many sites in the southern hemisphere. It is prominent in the ice-core record from Quelccaya in South America, and is evident in other Patagonian glacial series. In New Zealand, the event is recorded in speleothems and glaciers; it is also registered in the Antarctic records from Law Dome (Tyson and Lindesay, 1992).

South Africa some thousand years before the Younger Dryas in the northern hemisphere. This accords well with recent work carried out in the Andes, and New Zealand (Lowell *et al.*, 1995), although the accuracy of the dating control may be questionable in the case of some of the South African sites.

The number of localities for which warmer climates than at present have been inferred increases again between 11 ka and 10 ka (the interval embracing the Younger Dryas in the northern hemisphere), although this period seems to have remained dry (Figure 6.12). The warming seems to have followed the same pattern as the 13 ka - 12 ka interval, i.e. occurring first in the Karoo and Drakensberg, and thus indicating three regions of climate response. After 10 ka, the escarpment and winter-rainfall regions seem to have experienced higher rainfall, while the interior and Eastern Cape remained dry. From 10 ka to 9 ka (Figure 6.13) conditions warmed slightly, possibly interrupted by a brief cooling between 9 ka and 8 ka (Figure 6.14) (Partridge *et al.*, 1990). Evidence of drier, warmer conditions from about 9 ka is forthcoming from the analysis of polleniferous sediments at Wonderkrater (Scott and Thackeray, 1987) and Clarens (Scott, 1988), corroborating the evidence for warming at the Uitenhage aquifer at 9 ka (Heaton *et al.*, 1986). The maps suggest that the warming occurred in the eastern interior accompanied by wetter conditions, while the southern Kalahari remained dry. The Namib experienced a wet interval that ended at about 8 ka; this being inferred from renewed tufa formation in the Kuiseb river at about 9.8 ka and evidence derived from the Natab Silts (Vogel, 1989).

After 8 ka, the north eastern part of the summer rainfall region and the southern Karoo/escarpment became markedly drier, and were characterised by temperatures warmer by 2°C than present (Figures 6.15 - 6.17) (Partridge, 1995). This Holocene Altithermal was associated with protracted aridity in the Namib, based on evidence from the Natab silts and the shorter reach of the Kuiseb river (Partridge, 1993a). Dry conditions continued on the escarpment, the south coast and in the Namib until 5 ka BP, while the interior was wetter, except for the north-east. However, by 6.5 ka, rainfall in the Namib may have increased on the basis of increased grass cover at Mirabib (Avery, 1993); these moist conditions for the high lying areas of Namibia between 7 ka and 5.5 ka are also reflected by waterlogged conditions at a spring in Windhoek (Scott *et al.*, 1991). Evidence from the Pretoria Saltpan suggests wetter conditions over the Transvaal (Partridge *et al.*, 1993) in agreement with pollen analysis from Wonderkrater (Scott and Thackeray, 1987). This evidence is, however, in conflict with micromammalian evidence obtained from Jubilee Shelter further south and Wonderwerk Cave on the Kalahari margin (Avery, 1993). The south western Cape coast (as determined from coastal cave bone fossils) may also have been drier (Klein, 1990). This distinctive patterning of wet and dry regions in South Africa is one of the new findings of this project.

It is argued that the southern part of the region responded differently, with a change in rainfall seasonality (Partridge, 1993b). Thus the southern Cape may have experienced more summer rainfall at about 6.2 ka (Avery, 1993), while year round rain in the rest of the Little Karoo commenced at about 5 ka (based on renewed speleothem growth) and lasted until 2 ka (Talma and Vogel, 1986). A lack of synchroneity between changes in wetness between the northern and southern parts of southern Africa is thus apparent.

coastal caves) suggests moister conditions were initiated at about 14.6 ka (Klein, 1990; Meadows and Sugden, 1991).

After 13 ka, temperatures began to rise to levels higher than present in the Karoo and Drakensberg (Figure 6.10). Although no deposition took place on the Cango Cave stalagmite between 13 ka and 5 ka, proxy data from Boomplaas and Wonderkrater confirm this trend (Partridge, 1995). The Kalahari and Namib became wetter, but dried again after 12 ka. The earliest proxy evidence for temperatures more than a degree above present levels is between 13 and 12 ka, in the Karoo and along the foothills of the Natal Drakensberg Escarpment. Analysis of sediments from Clarens suggest that the warming at 13 ka was accompanied by moist conditions (Scott, 1988). Opposing trends are in evidence in the winter rainfall region. Changes in deep water control were such that NADW and LNADW reached a peak in formation at about 13 ka, while AABW was very much reduced. Current theory holds that when NADW production rates are high, southern hemisphere temperatures increase (Bender *et al.*, 1994; Jouzel *et al.*, 1995); the relatively warm upwelling of NADW promotes sea ice melt back around Antarctica (Crowley, 1992). This may move belts of Antarctic climate southwards and thereby increase the poleward transport of heat through the atmosphere (Bender *et al.*, 1994).

In the period 12 ka - 11 ka (Figure 6.11) all sites show reduced temperatures, suggesting a brief return to near-glacial conditions during that time. Evidence suggesting that one site (Swartkolkvloer) experienced a temperature increase is probably questionable. Cooling associated with a southern African climate reversal is also evident from shell isotopes along the Atlantic seaboard, and from ostrich eggshells from the interior, although this cooling is dated at 11 - 10 ka (Cohen *et al.*, 1992; Partridge, 1997) which is more in keeping with global trends spanning the Younger Dryas interval. (In a later publication, the cold interval along the coast is dated to between 12 ka and 10 ka (Cohen and Tyson, 1995)). NADW suddenly declined, while AABW increased from 12.6 ka to 11.5 ka with a small reversal in the trend around 12 ka. These changes in deep water formation may explain the apparent diachronism between the two hemispheres. The increase in AABW is attributed to increased sea ice formation around Antarctica, owing to decreased insolation at about 12 ka. Increased AABW would subsequently reduce the flow of NADW reaching the southern hemisphere, or reduce its formation rate further north (*vide infra)*. Southern hemisphere cooling would thus precede cooling in the northern hemisphere.

Except for the eastern parts of the country, there is a marked decline in rainfall coincident with the temperature reduction. Sites in the interior (Aliwal North) (Scott and Cooremans, 1990) and vegetation changes near Wonderkrater (Scott and Thackeray, 1987) record drier conditions at this time. Although wetness for the period 14 ka and 10 ka is suggested by a study of calcareous lacustrine sediments at Narabeb and Khommabes in the Namib (Teller *et al.*, 1990), a regional period of dessication between 11.9 ka and 10.7 ka is evident from calcification and desiccation of [illegible]d beds at Conception Bay and Meob Bay in the Namib (Vogel, 1989). Evidence from lakes and caves in the Kalahari suggests aridity at about 11 ka (Shaw *et al.*, 1988), while inner dune formation at pans subjected to falling water tables is apparent at 12 ka (Lancaster, 1986). Two south western Cape sites suggest an increase in moisture over parts of the winter rainfall area. If this interpretation is correct, a climatic reversal occurred in

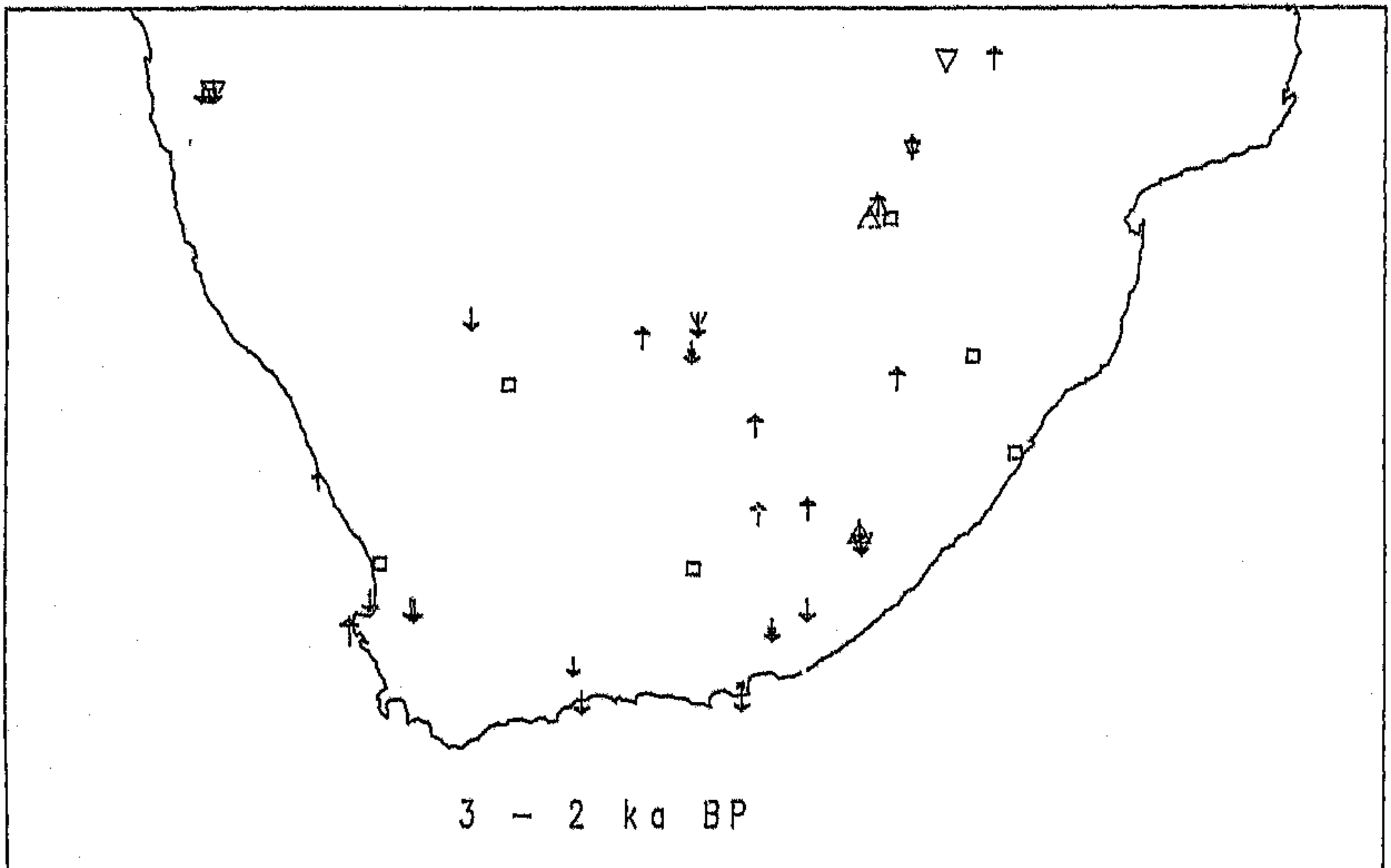

Fig. 6.20 Southern Africa, Temperature and Rainfall: 3 ka.

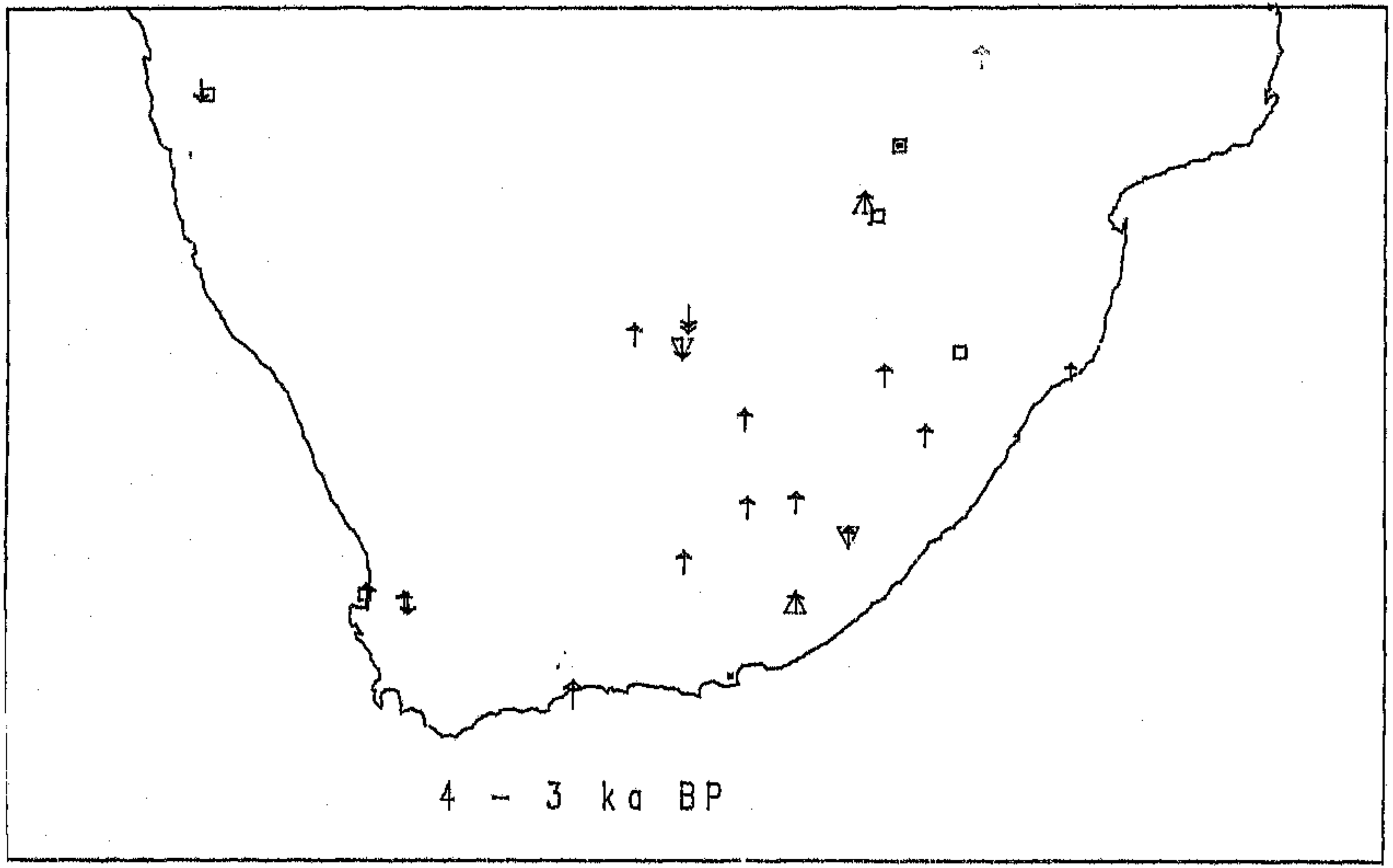

Fig. 6.19 Southern Africa, Temperature and Rainfall: 4 ka.

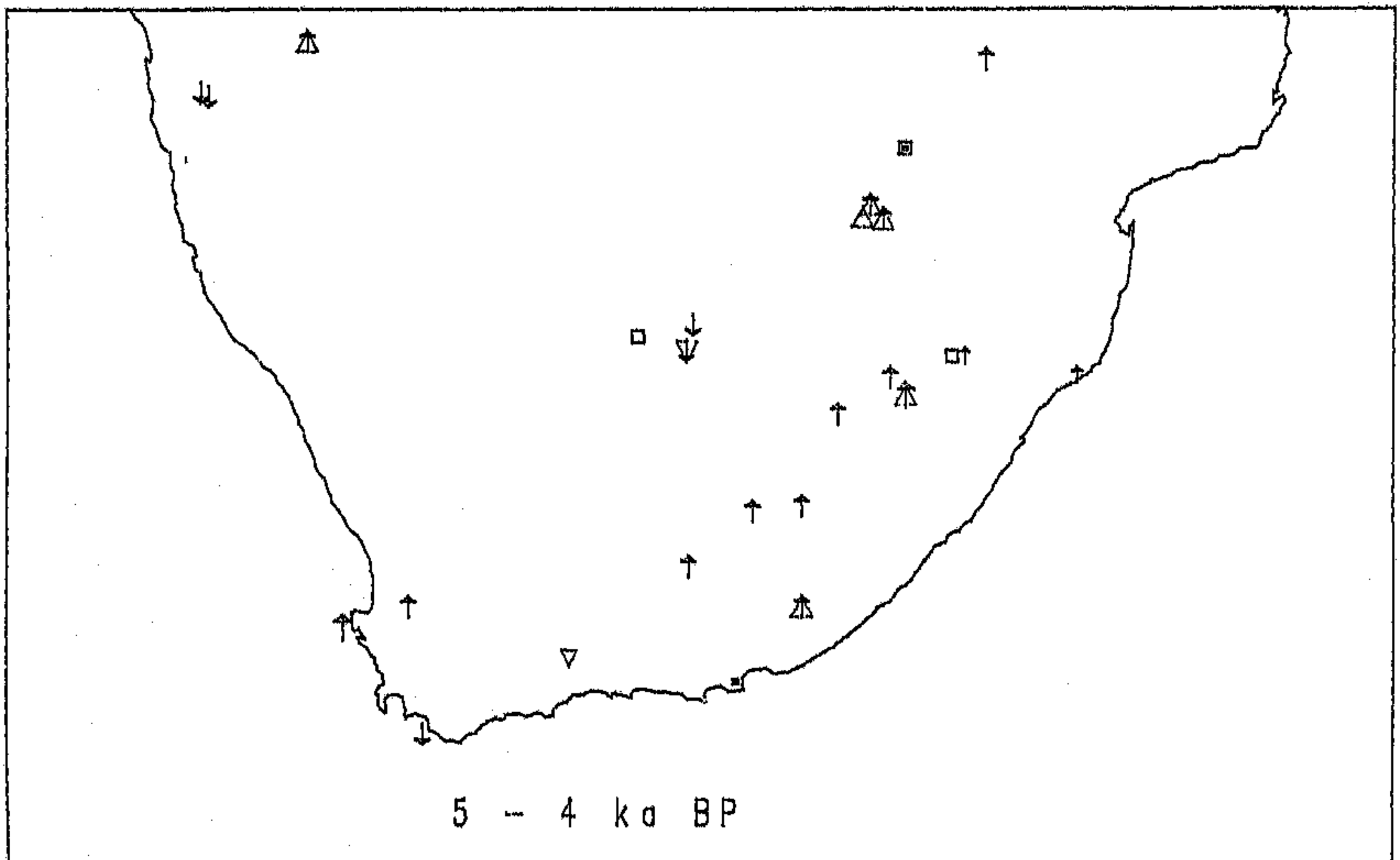

Fig. 6.18 Southern Africa, Temperature and Rainfall: 5 ka.

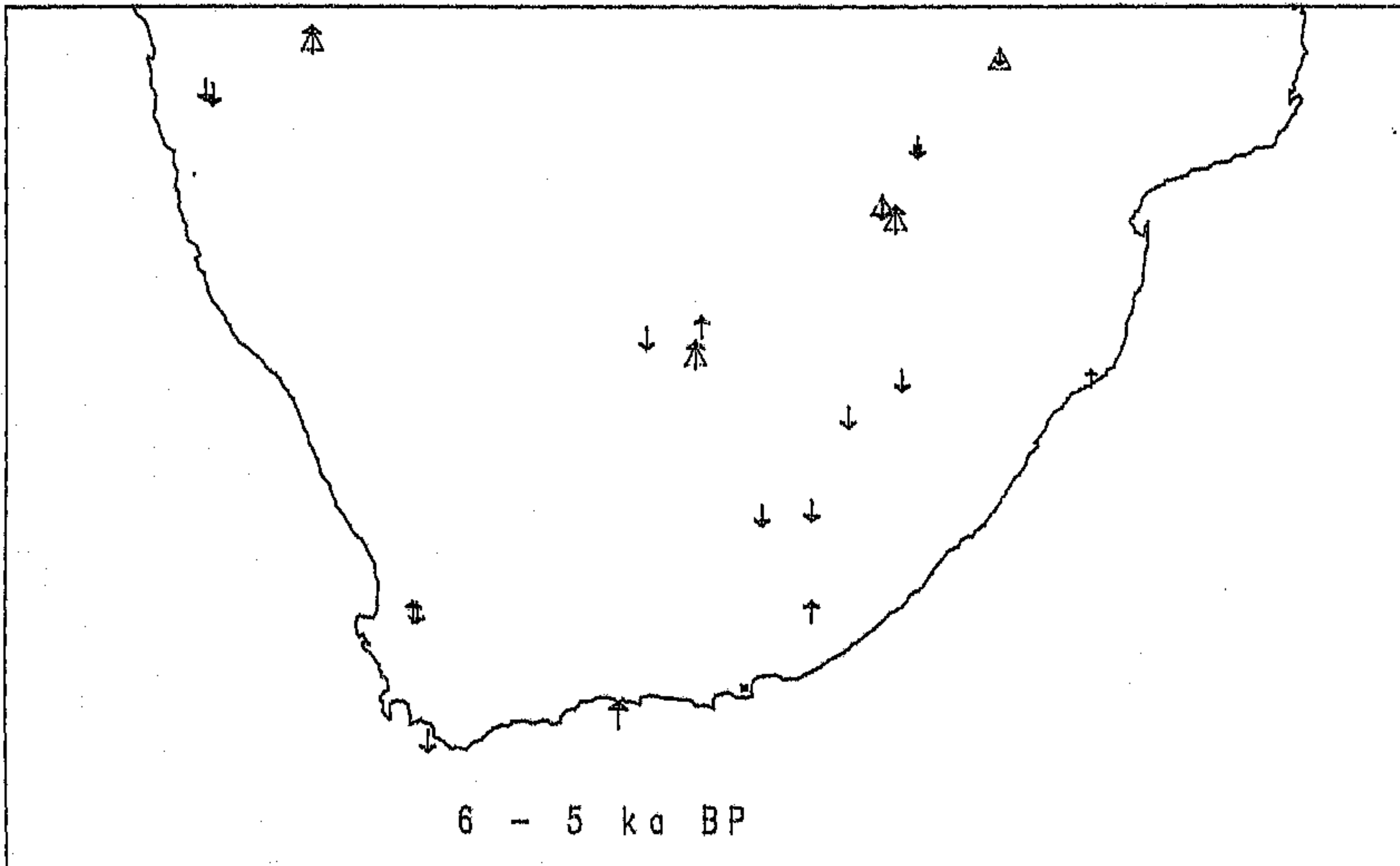

Fig. 6.17 Southern Africa, Temperature and Rainfall: 6 ka.

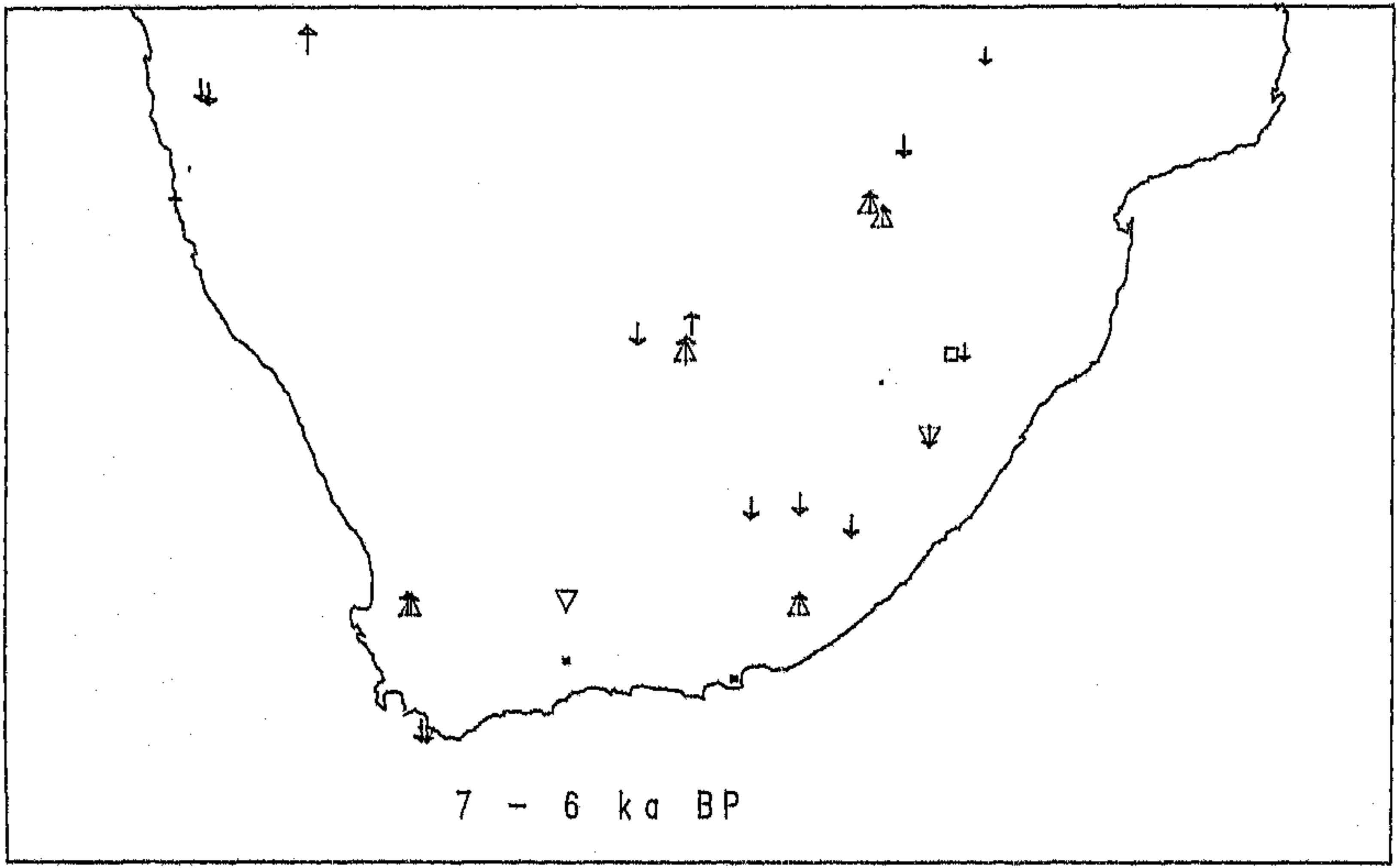

Fig. 6.16 Southern Africa, Temperature and Rainfall: 7 ka.

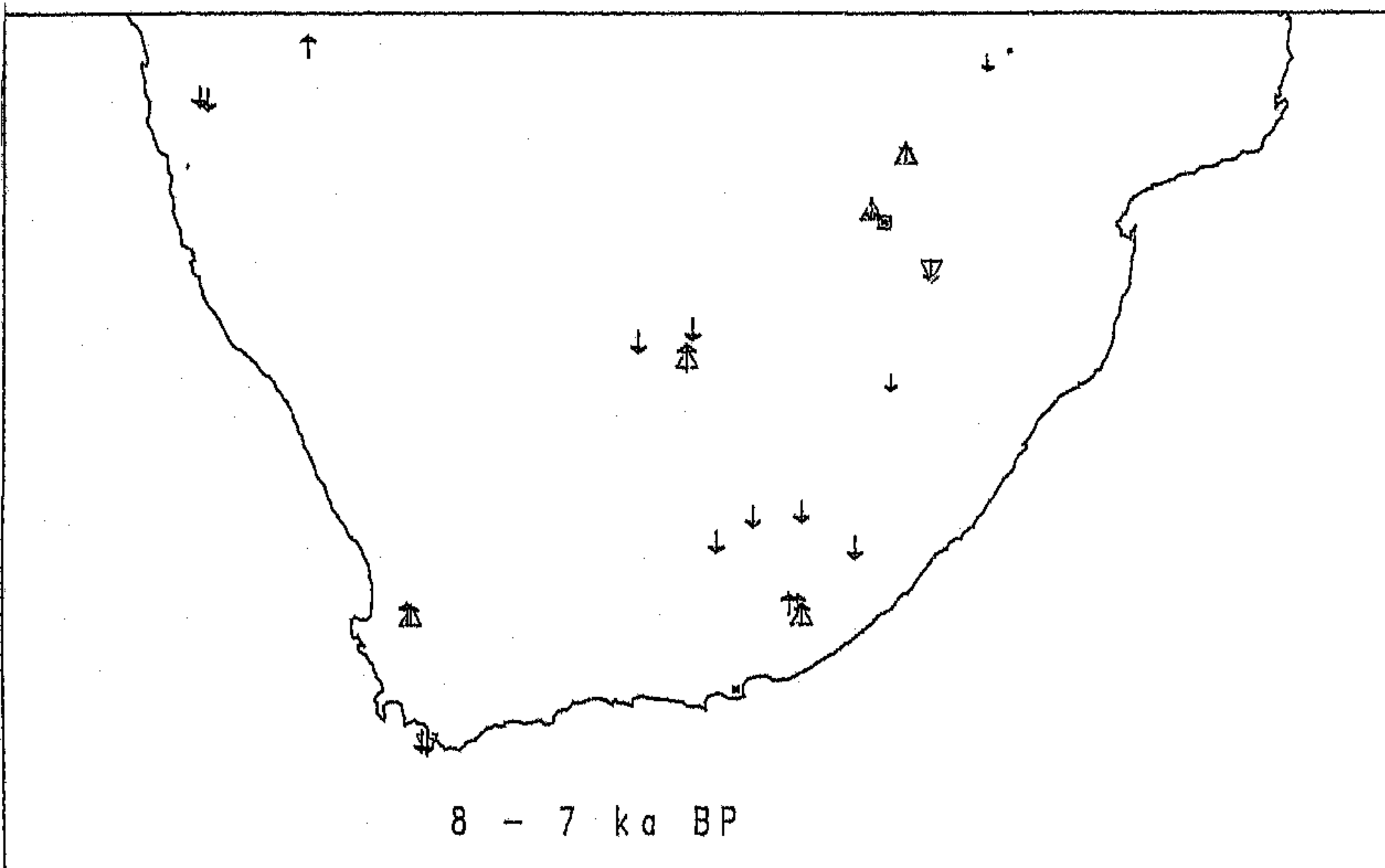

Fig. 6.15 Southern Africa, Temperature and Rainfall: 8 ka.

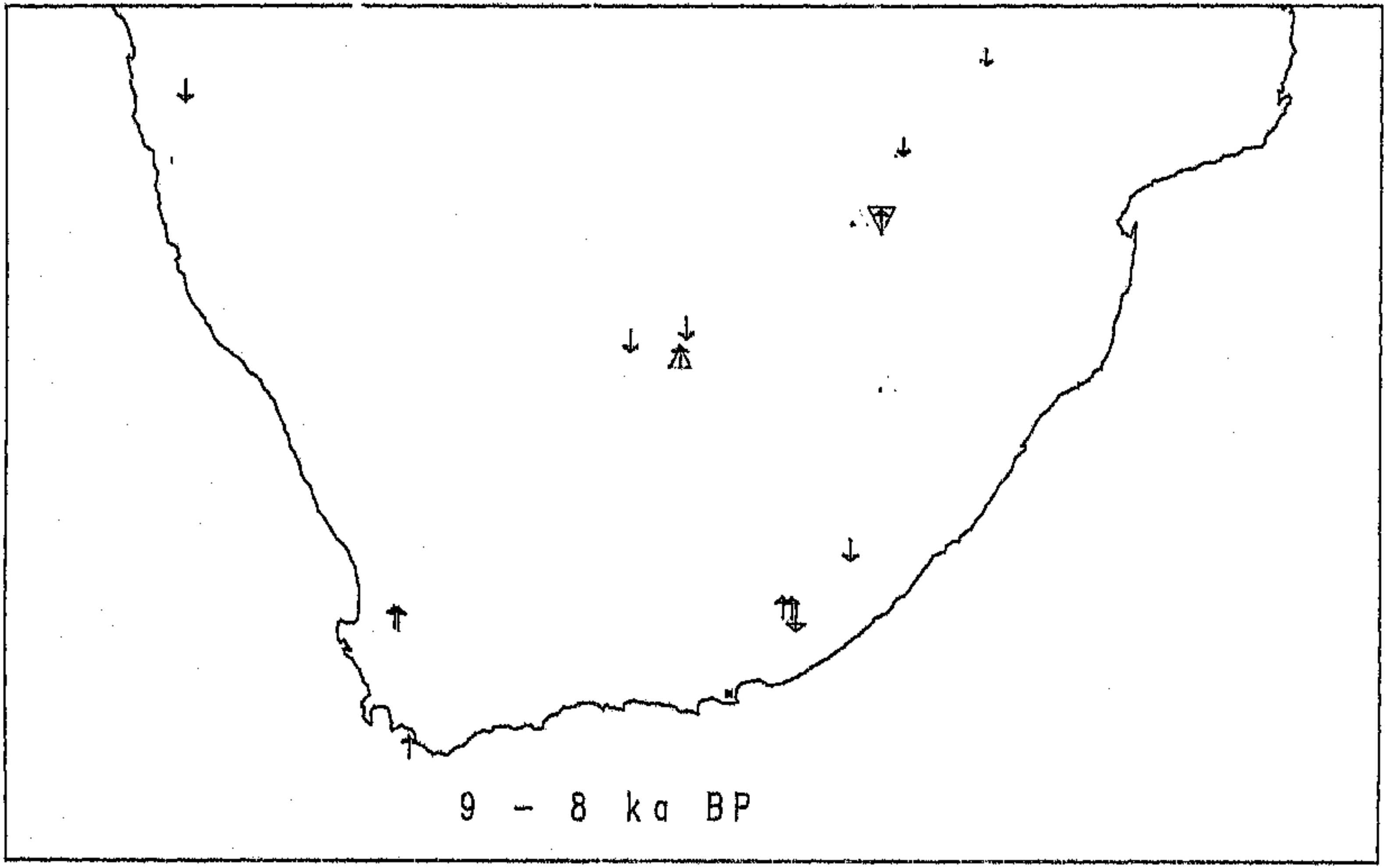

Fig. 6.14 Southern Africa, Temperature and Rainfall: 9 ka.

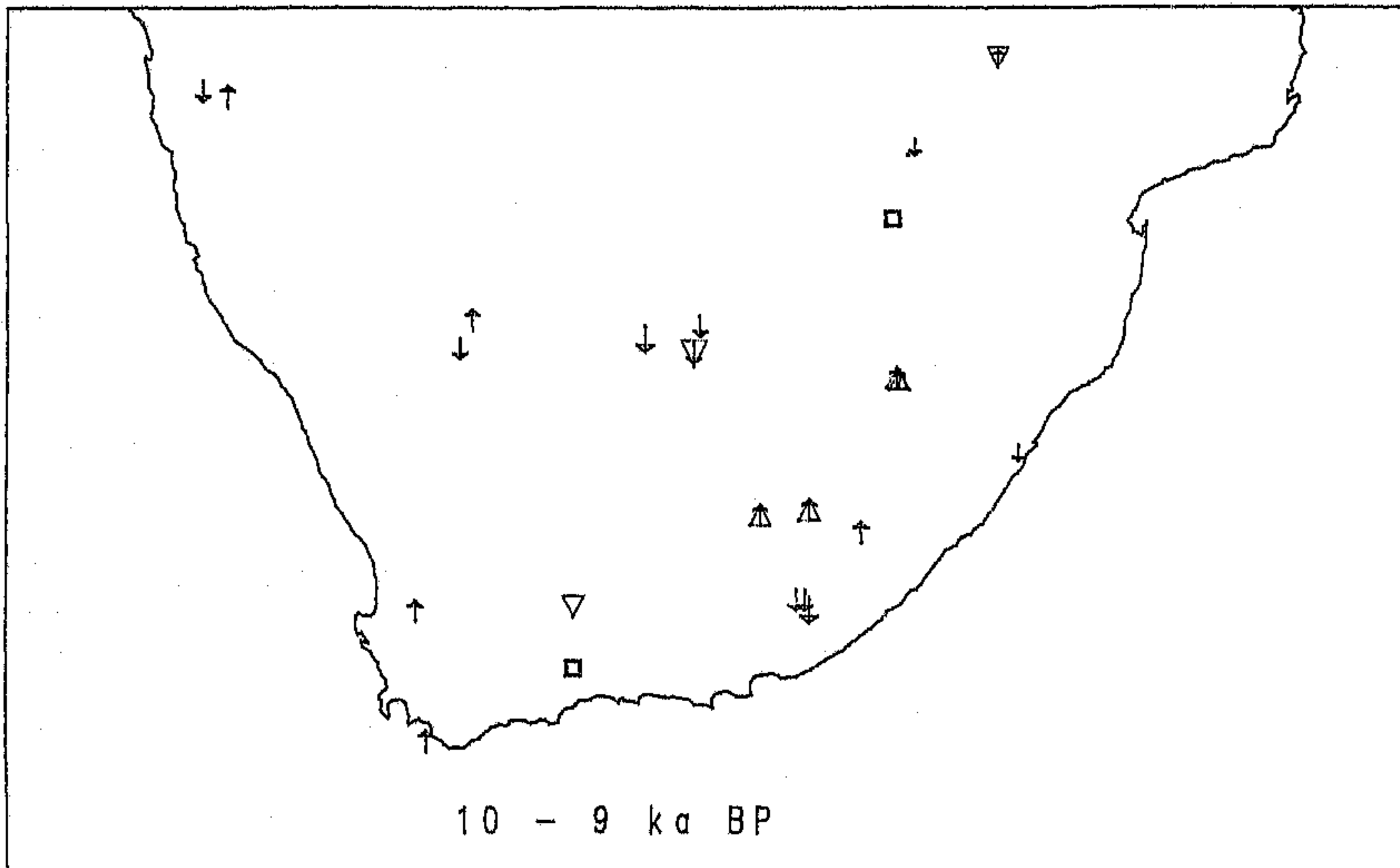

Fig. 6.13 Southern Africa, Temperature and Rainfall; 10 ka.

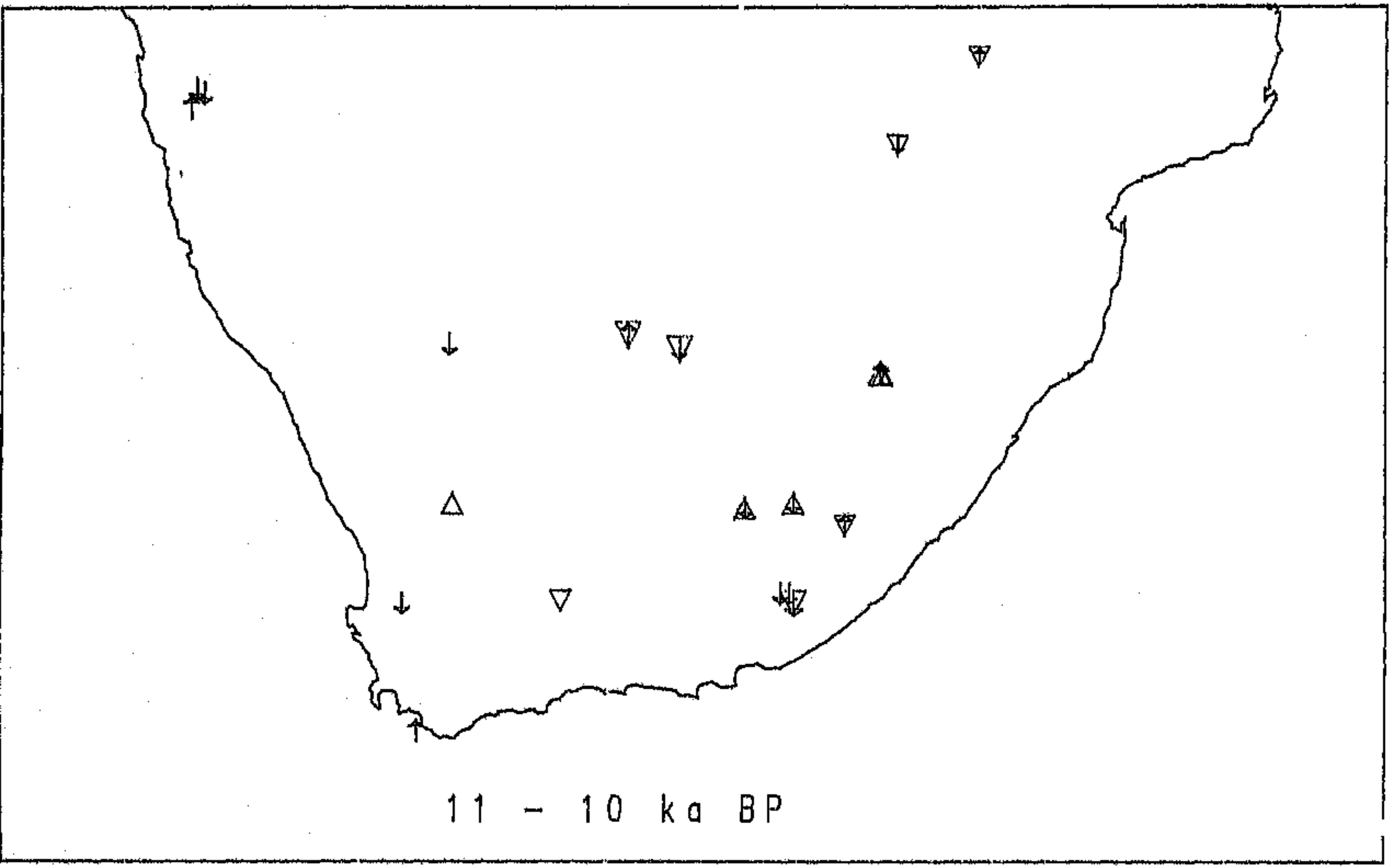

Fig. 6.12 Southern Africa, Temperature and Rainfall: 11 ka.

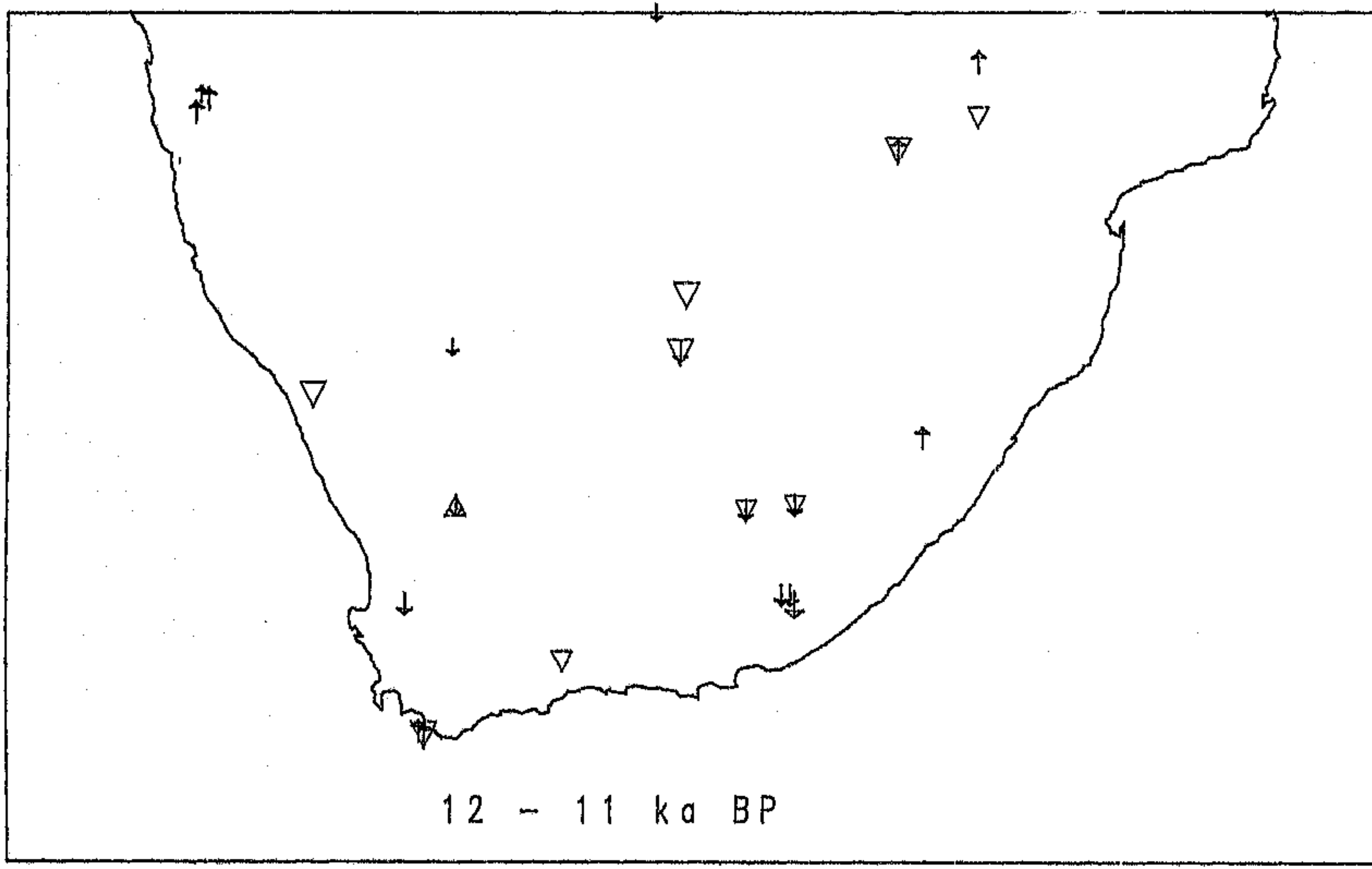

Fig. 6.11 Southern Africa, Temperature and Rainfall: 12 ka.

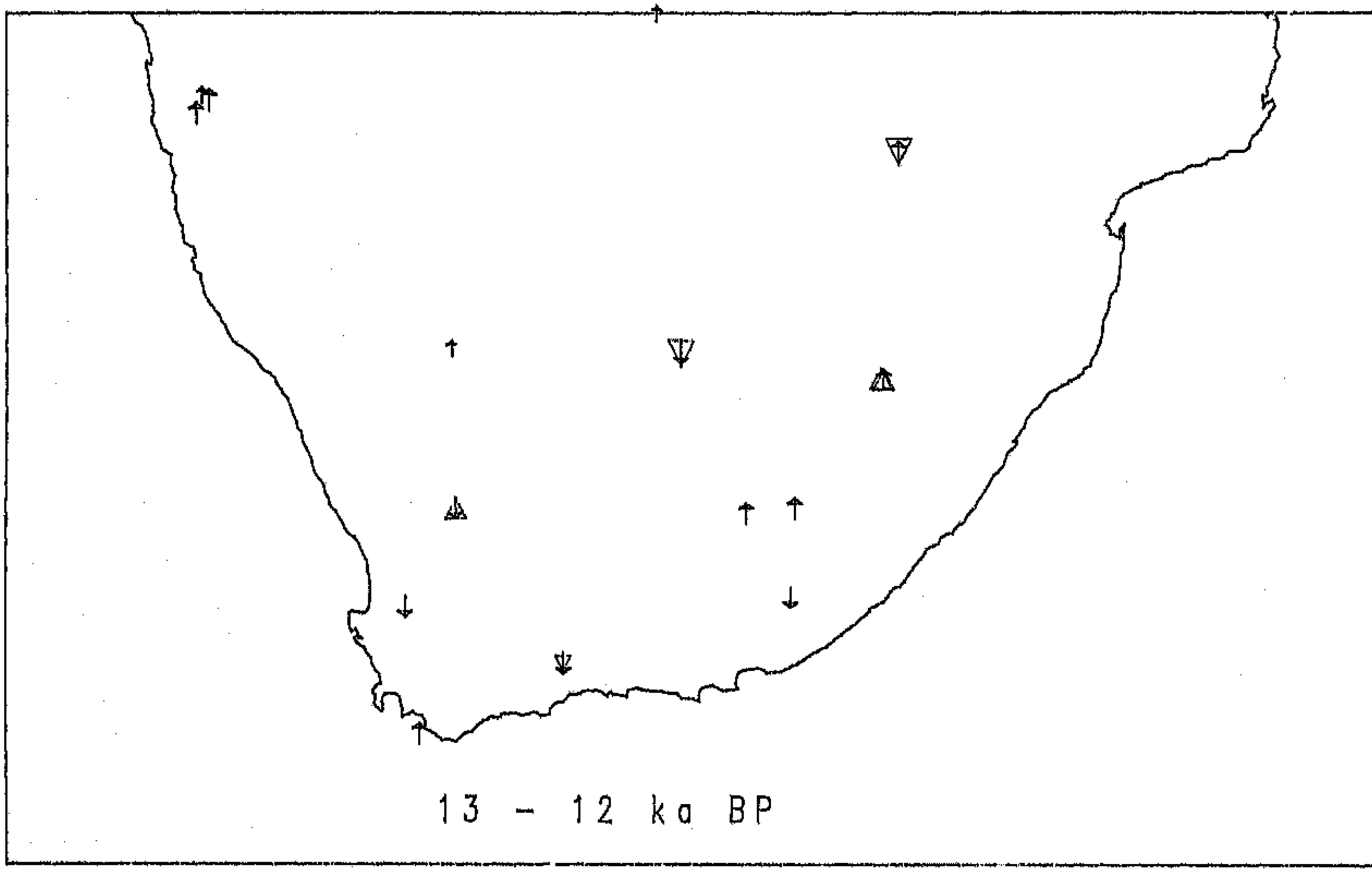

Fig. 6.10 Southern Africa, Temperature and Rainfall: 13 ka.

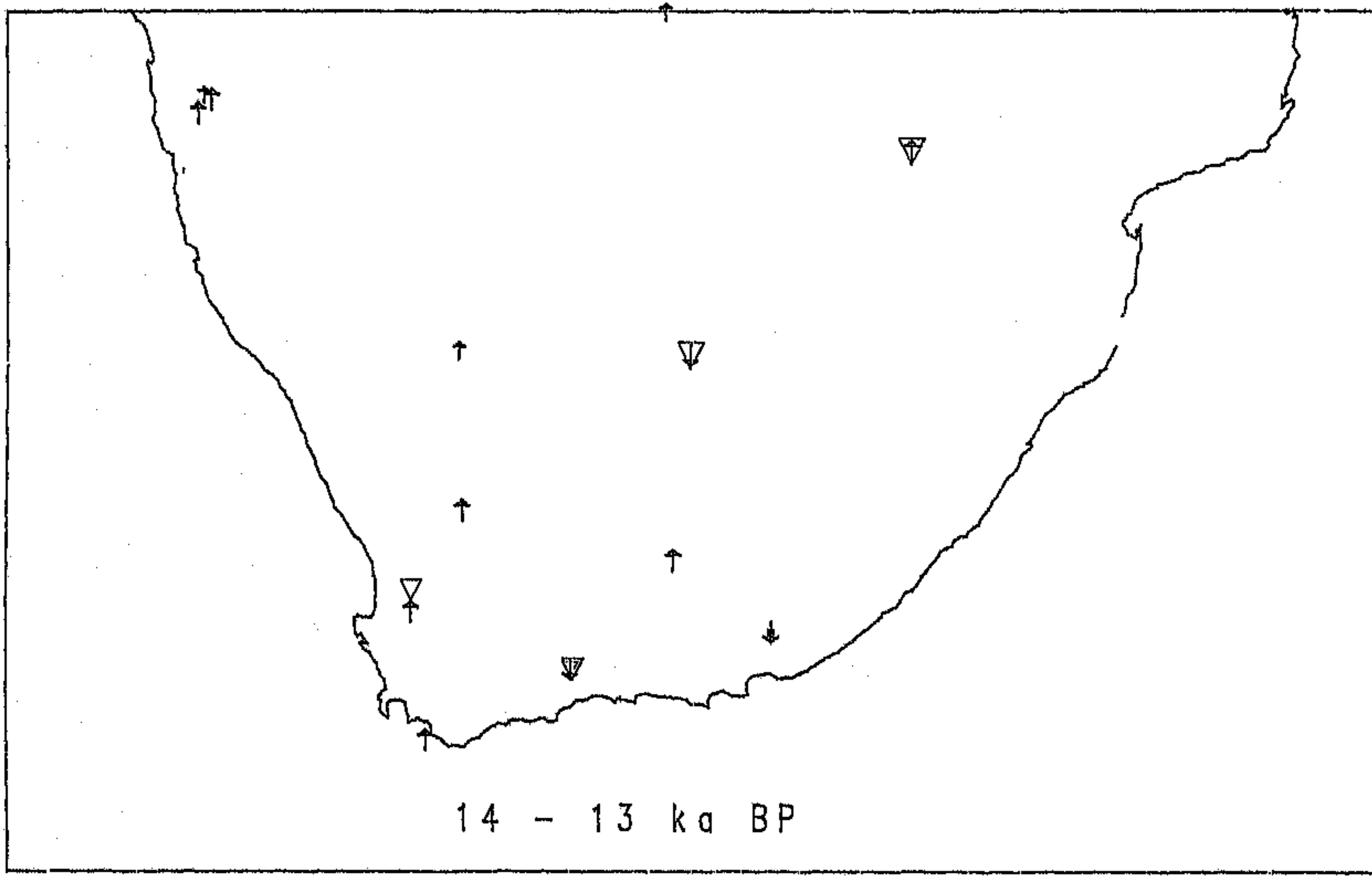

Fig. 6.9 Southern Africa, Temperature and Rainfall: 14 ka.

AABW Formation and the Role of Antarctic Sea Ice

It is generally maintained that northern hemisphere ocean-atmosphere dynamics control the global pattern of climatic change through the interaction of NADW production and the global thermohaline circulation. An analysis of southern hemisphere dynamics follows which demonstrates the vital role played by the southern ocean and Antarctica in modulating global climate change. This analysis also proposes mechanisms that explain southern African climate variability.

Antarctica and its surrounding ocean have a unique influence on global climate, in that the ocean completely surrounds the continent. In contrast to the situation in the northern hemisphere, the Southern Ocean interacts dynamically with the Atlantic, Pacific and Indian oceans (Figure 7.6) (Budd, 1991; White and Peterson, 1996) via the deep water Antarctic Circumpolar Current (extending from the surface to about 4 000 m, (Corliss, 1983)), which flows at 130 Sv. Surface winds over the Southern Ocean have important effects on west coast temperatures (Budd, 1991); some consider the interplay between tropical Australasia and Antarctica to be the key to south Pacific palaeoclimatic dynamics (Markgraf *et al.*, 1992).

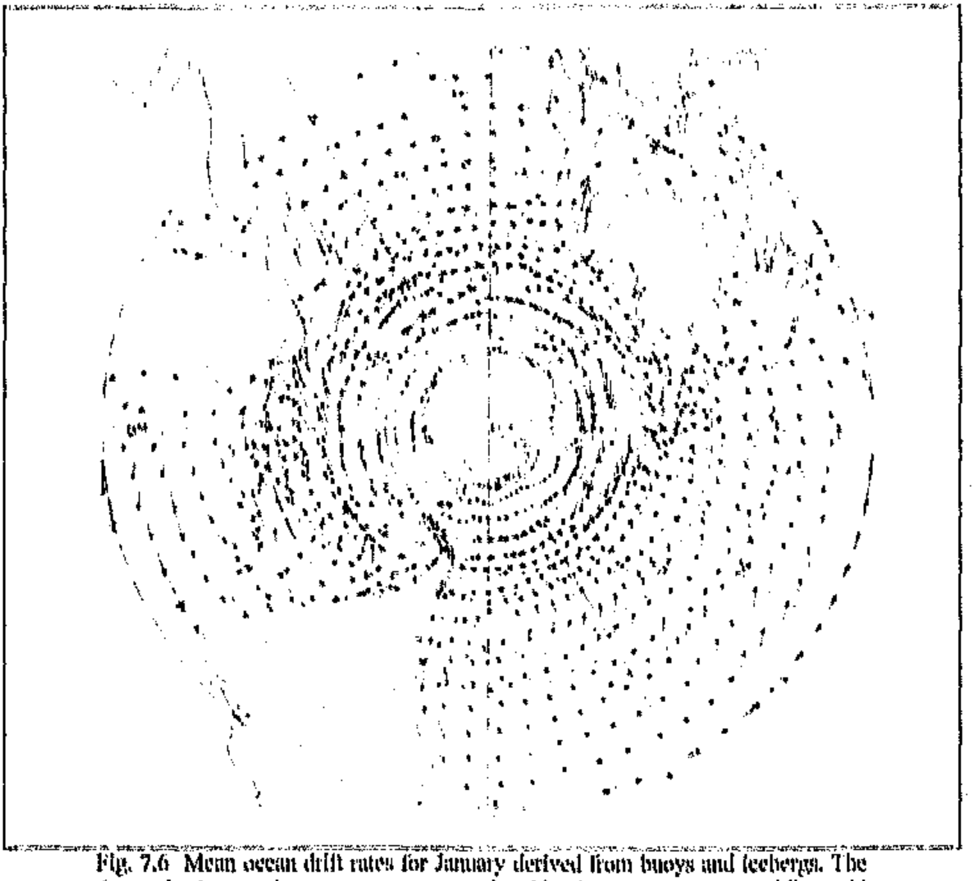

Fig. 7.6 Mean ocean drift rates for January derived from buoys and icebergs. The Antarctic circumpolar current reacts strongly with other ocean gyres, providing cold water on west coasts (Budd, 1991).

eastern regions of the country at about 7 ka. From 5 ka to 3 ka, all sites, except a few in the Kalahari and Namib, reflect a return to wetter conditions in agreement with SST data for the period 4.3 ka to 2 ka (Cohen and Tyson, 1995) and temperatures were higher except in the southern Cape. Unfortunately, a hiatus exists for the period 2.4 ka to 650 a B.P. in the Nelson Bay Cave data, subsequently SSTs at 650 a B.P. were lower suggesting wetter conditions. Conditions below the escarpment in the Namib were consistently drier from 10 ka and remained so until the last millenium. This is at variance with the findings of Cockcroft *et al.*(1987), who report wetter conditions from 9 ka to 4 ka.

Cockcroft *et al.* (1987), conclude that their spatial reconstruction accords well with the theoretical expectations that follow from the Tyson (1986) model. In general, the results of this work do not contradict their conclusions; many of the differences may be an artefact of the time-slices chosen. However, the period between 8 ka and 4 ka shows too many variations to be considered as a single time-slice, and their conclusion that the period between 12 ka and 10 ka was marked by lower rainfall, but otherwise similar climatic conditions, may need re-examination. The results of this work reinforce the concept of southern African climates being closely connected to ENSO events, and the associated Antarctic teleconnection, on time scales varying from decades to millenia. The inferences proposed by the conceptual model of Cohen and Tyson (1995) are generally borne out by the climatic reconstructions based on the PASH data.

According to Cockcroft *et al.*, the interval from 14 ka to 12 ka was wetter, with drier, possibly anomalous, conditions, in the east. The present analysis suggests that from 14 ka to 13 ka, the whole country except for the southern Cape coastal littoral was characterised by wetter conditions. The wetter tendency continued until 12 ka, except that the drying spread further north, and west. The dry Namib postulated by Cockcroft *et al.*, 1987, is not apparent; the Namib sites reflect increased wetness for the whole period under discussion, possibly owing to the warmer SSTs resulting from Agulhas intrusions. The incursions of warm Agulhas water into the Benguela are indicated by occurrences of shells of east coast taxa in the Benguela region between 13.5 ka and 12 ka (Pether, 1994). Considerable agreement is, however, apparent in inferred temperature trends, with a warming trend apparent between the Cape Fold mountains and the central Karoo; this trend tends to recur within the wetter regions. The analysis of Algoa taxa, and the proxy data suggest that this period was characterised by warm, moist conditions, with opposing trends occurring in the winter rainfall area. The model, however, suggests that dry spell conditions should have prevailed at this time.

The return to warmer, wetter conditions was interrupted by a climatic reversal between 12 ka and 11 ka when most sites indicate a return to cooler and drier conditions. Sites in the eastern third of the country and the Namib reflect wetter conditions. This finding is in agreement with that of Cockcroft *et al.*, (1987). Subsequently, between 11 ka and 10 ka, warming similar to that observed from 13 ka to 12 ka is apparent; the corresponding return to wetter conditions did not, however, occur. Since Cockcroft *et al.* (1987), do not map the interval 12 ka to 11 ka as a single time-slice, it is difficult to make meaningful comparisons. The data from Nelson Bay cave dated prior to 9 ka contains no *Patella tabularis* shells, and the area was colonised by cold-water species, suggesting decreased SSTs associated with wet-spell conditions (Cohen and Tyson, 1995).

According to Cockcroft *et al.* (1987), a wet phase characterised the west of the country from 9 ka, while the southern and eastern areas remained dry; from 8 ka to 4 ka the country as a whole, except for the south western Cape, experienced moister conditions than present. These conclusions are corroborated by recent work on SSTs off the south coast. Evidence of SST fluctuations above the Agulhas Bank off South Africa using *Patella tabularis* shell from Nelson Bay Cave was obtained for the period 9 ka to present (Cohen and Tyson, 1995). The record suggests lower SSTs between 8.6 ka and 6.3 ka, and wet-spell conditions are inferred. Evidence from this study suggests that between 9 ka and 8 ka no clear trends are evident; the southern Cape was possibly wetter, and many sites show evidence of warming. Contrary to Cockcroft *et al.* (1987), and Cohen and Tyson (1995), 8 ka to 7 ka was drier, except in the southern Cape. The wet conditions in the western Cape were reversed from 7 ka to 3 ka.

Evidence from this study suggests that the eastern half of the country experienced dry conditions from 7 ka to 5 ka, with some areas showing cooler conditions. Cohen and Tyson (1995) maintain that their results are in conflict with syntheses based on terrestrial proxy rainfall data in earlier reviews (Cockroft *et al.*, 1987; Partridge *et al.*, 1990) As SSTs between 6 ka and 4.7 ka were higher than present, dry-spell conditions are inferred, with a wetter winter rainfall area. The PASH maps corroborate this inference and show drier conditions at many sites for the period 6 ka to 5 ka, with increased wetness at some southwestern Cape sites. The drying trend seems to have started in the

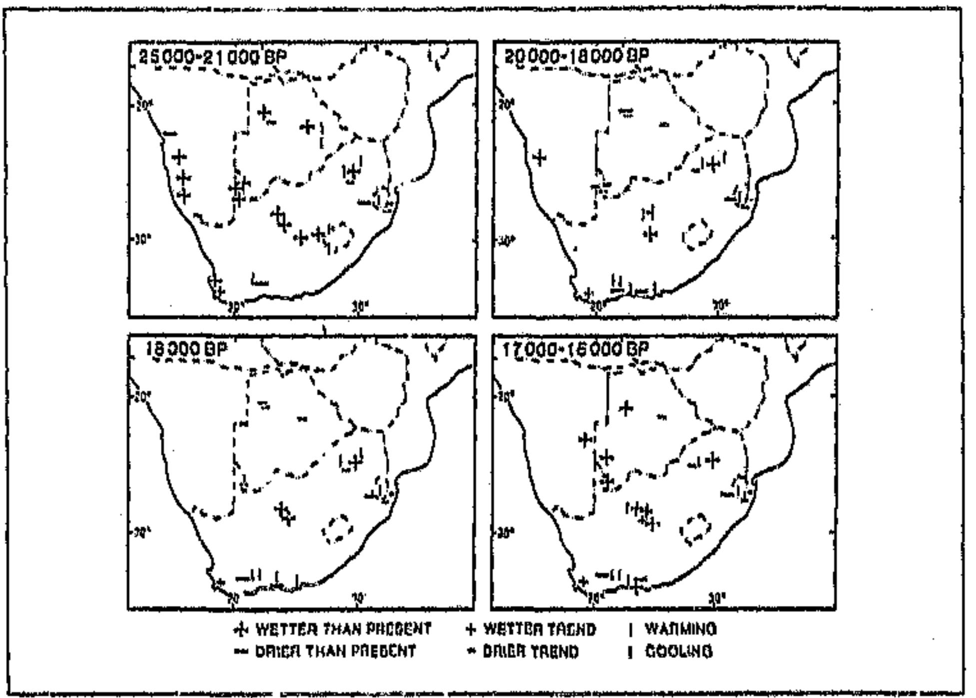

Fig. 7.4 Moisture and temperature conditions in southern Africa at 25 - 21 ka, 20 - 18 ka, 18 ka and 17 -15 ka. Maps based on the work of numerous authors detailed in Cockroft *et al.*, 1987.

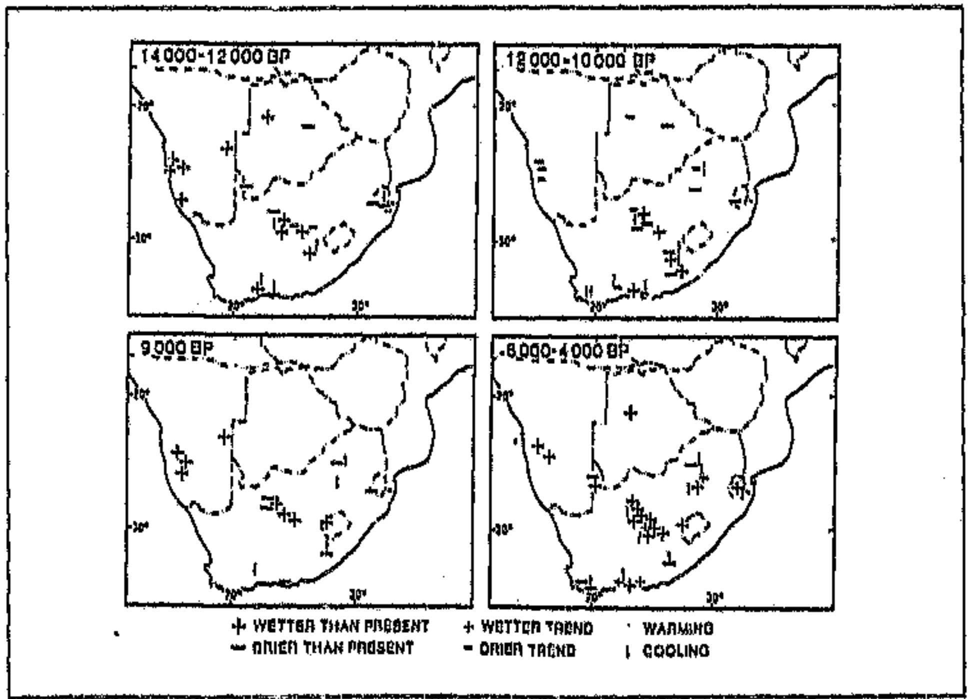

Fig. 7.5 Moisture and temperature conditions in southern Africa at 14 - 12 ka, 12 -10 ka, 9 ka and 8 - 4 ka. Maps based on the work of numerous authors detailed in Cockroft *et al.*, 1987.

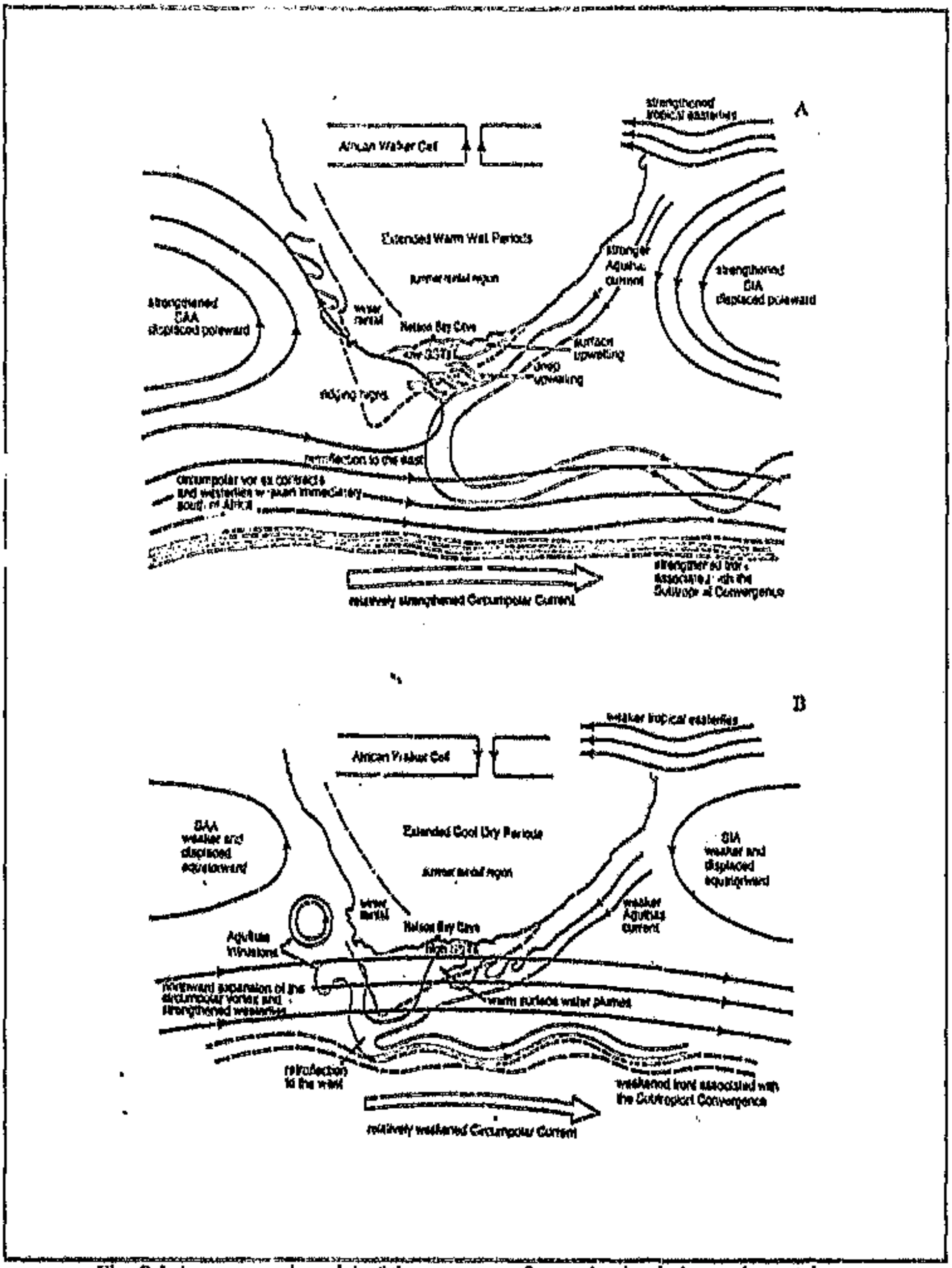

Fig. 7.3 A conceptual model of the response of oceanic circulation and coastal sea surface temperatures to atmospheric circulation anomalies responsible for extended wet spells (A) and extended dry spells (B) in South Africa. All aspects of the atmospheric circulation depicted here are after Tyson (1986) and Cockroft *et al.* (1987). Oceanic conditions in (B) result in anomalously high SSTs in the vicinity of both Nelson Bay Cave and on the southern Cape coast and Elands Bay Cave on the west coast. Holocene SST records have been constructed from isotopic measurements of mollusc shells of both cave sequences (Cohen and Tyson, 1995).

the south west of the continent could be associated with changes in the upper westerly troughs. In recent work highlighting the associations between SSTs around South Africa and rainfall (Mason, 1995), high SSTs, owing to a poleward shift in the zone of surface westerlies, in a broad zonal band between 15°S and 35°S and in an area immediately to the south of southern Africa, are associated with wetter conditions over the summer rainfall area. This is due to enhanced atmospheric baroclinicity and hence cyclogenesis associated with both tropical and temperate synoptic systems (Mason 1995). Although it is maintained that SST variations off the west coast are of minimal climatic significance to South Africa, except locally along the west coast (Mason, 1995), an area in the subtropical latitudes of the eastern South Atlantic Ocean between 15°S and 30°S, and 15°W and 15°W may influence rainfall in that it encompasses an area subject to the leakage of warm Agulhas waters in the form of Agulhas rings, which result in anomalously warm pools of water within this area (Figure 7.2) (Pether, 1994; Mason, 1995). The warm water may result in a weakening of the South Atlantic Anticyclone which has been associated with drier conditions over South Africa (Mason, 1995), and wetter conditions prevailing along the west coast.

Comparison between the PASH maps and contemporary modelling studies.

Cockcroft *et al.* (1987), and subsequently, Cohen and Tyson (1995) have attempted to explain southern African variability using Tyson's (1986) wet and dry spell model. The model proposes that wet-spell conditions (as defined by Tyson 1986), are associated with negative SST anomalies in the eastern Agulhas Bank region caused by upwelling, higher volume transports of the Agulhas Current and reduced influence of winds from the southwest. At the same time, the stronger southeasterly winds along the west coast would enhance southern Benguela upwelling with low SSTs. Dry-spell conditions on the other hand, are associated with positive SST anomalies caused by reduced upwelling, onshore advection of warm surface plumes, and decreased volume transport owing to weakened atmospheric circulation over the southwest Indian Ocean (Figure 7.3) (Cohen and Tyson, 1995). Using the available literature, a number of maps (Figures 7.4 and 7.5) of palaeorainfall and temperature were compiled for significant time slices by theses authors.

The results of the study (Cockcroft *et al.* 1987) suggest that from 25 ka to 20 ka, and from 18 ka to 15 ka, the broad climatic pattern appears to have been cooler and wetter. The findings of the present analysis are in agreement with respect to the temperature tendencies, but suggest the existence of drier conditions at nearly all sites until 17 ka, with the exception of eastern sites between 20 and 19 ka (Figure 6.1). Increased winter rainfall is also not apparent until 17 ka (Figures 6.4 & 6.5). The assertion that the present day dry spell analogue would have prevailed for the period 25 ka to 15 ka, with an equatorward displacement of the circulation is corroborated by this work. The lack of winter rainfall over the western Cape during this period may be an artefact of insufficient data for that period; alternatively, desiccation may have prevented the accumulation of good, datable material such as pollens.

level by Antarctic sea ice variability through the SOI. If this is the case, past climates may have been influenced in a similar way.

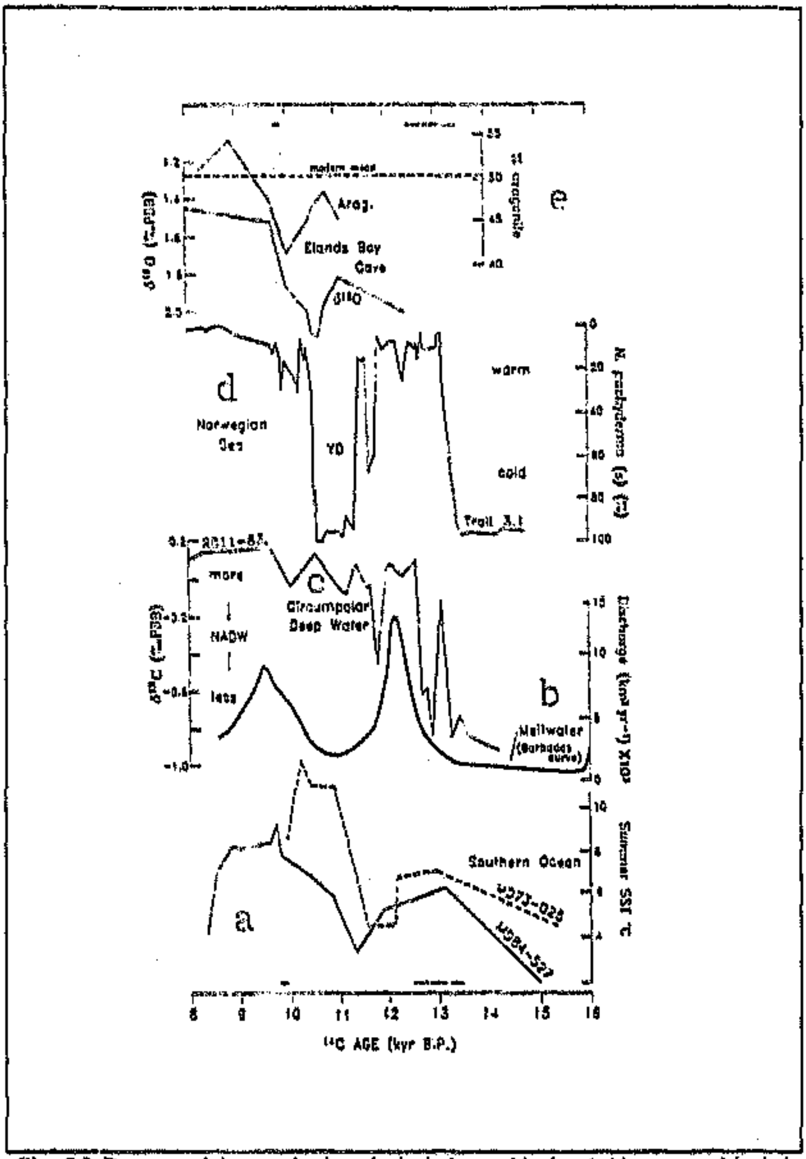

Fig. 7.2 Data pertaining to the last deglaciation, with dated Algoa taxa (shaded columns). (a) Estimated summer SSTs in the Southern Ocean. (b) Meltwater discharge curve. (c) $\delta^{13}C$ record from Southern Ocean core RC11-83 indicating variations of NADW flux. (d) percentages of *Neogloboquadrina pachyderma* (sinistral) in Norwegian Sea core Troll 3.1 as indicator of retreat of Arctic Polar Front. (e) Carbonate mineralogy and oxygen isotope changes in *Patella* shells from Elands Bay Cave (Pether, 1994).

An investigation using spectral analysis of SSTs around South Africa suggest that associations between present day SST fluctuations and rainfall oscillations exist (Mason, 1990). The rainfall variability is thought to be modulated with local SST anomalies through a mid-latitude atmospheric response. Further, the position of the SST gradient to

North of 20°S, the Inter-Tropical Convergence Zone (ITCZ) has a pronounced affect on summer weather patterns; the vertical movement of air in this region produces closed tropical lows, troughs and ridges associated with convective activity. The ITCZ moves in an annual cycle with the passage of the sun, and the rain belts move accordingly. Cyclonic and anticyclonic perturbations in the mean flow occur in all seasons. The core of highest frequency of anticyclones experiences a seasonal meridional displacement of about 4° (Tyson, 1986).

The Southern Oscillation is an important feature of southern hemisphere climates. During the high phase, pressure rises over the eastern Pacific, and falls over Indonesia. Surface easterlies and upper air westerlies complete the cell, termed the Walker Circulation. During the low phase, the circulation weakens, the surface easterlies decrease in intensity, or reverse, and the 200mb westerlies weaken. The sub-tropical jet stream in both hemispheres intensifies during the low phase, while the Pacific Hadley cell weakens during the high phase, resulting in weaker jets and less meridional flow in the Hadley cell. The Southern Oscillation Index (SOI) has been positively correlated with summer rainfall over South Africa, accounting for about 20% of the variance. In general, more wetter years were associated with high phases, than drier years with low phases (Tyson, 1986).

Correlations with circulation indices indicate significant links between the SOI and circulation over South Africa. The SOI modulates tropical easterly flow over low latitudes during summer, and is significantly correlated with changes in summer westerly flow to the south of the country. Geopotential heights over southern Africa are correlated, with lower heights occurring during the low phase, and vice versa. Over the ocean, pressure tends to rise during high phase, and weakens during the low phase. The consequence of these pressure reversals is a weakened poleward and meridional pressure gradient during high-index summers, and an enhanced gradient in low-phase summers. Summer temperature fields show a similar correlation. High-index summers are associated with weakened poleward temperature gradients, and vice versa. A negative correlation between the SOI and the zonal wind component at 200mb exists. During high phase, wind anomalies become easterly, except over Marion Island where westerlies strengthen. During low phase the opposite occurs. Meridional wind components at 200mb during high phase become more southerly over tropical Africa, and more northerly over the sub-tropics. During the low phase, the reverse occurs, with upper air convergence enhancing surface divergence over central southern Africa (Tyson, 1986).

The Southern Oscillation is a quasi-periodic phenomenon, with a mean recurrence interval of 3.2 years, and the length of a typical event is between 18 and 24 months. Peaks in southern African rainfall spectra at 2-3, 3-4, 5-6, and 10-12 years are echoed by identical peaks in the SOI spectral peaks (Tyson, 1986). Recent work has suggested that ENSO signals in the Antarctic sea ice have been previously underestimated (Yuan, 1996). 40.% of variance in Antarctic sea ice anomalies is attributed to ENSO, and the sea ice has high correlations with precipitation over tropical land areas (28°N to 28°S, 85.5°W to 152.5°E) and with SSTs in the equatorial Indian Ocean. However, the physics of the connection is not well understood (Yuan, 1996). It is tempting to speculate that present day climate variability over southern Africa may be influenced at a significant molluscan taxa, are correlated with decreased trade winds and reduced upwelling off the coast of Namibia (Pether, 1994).

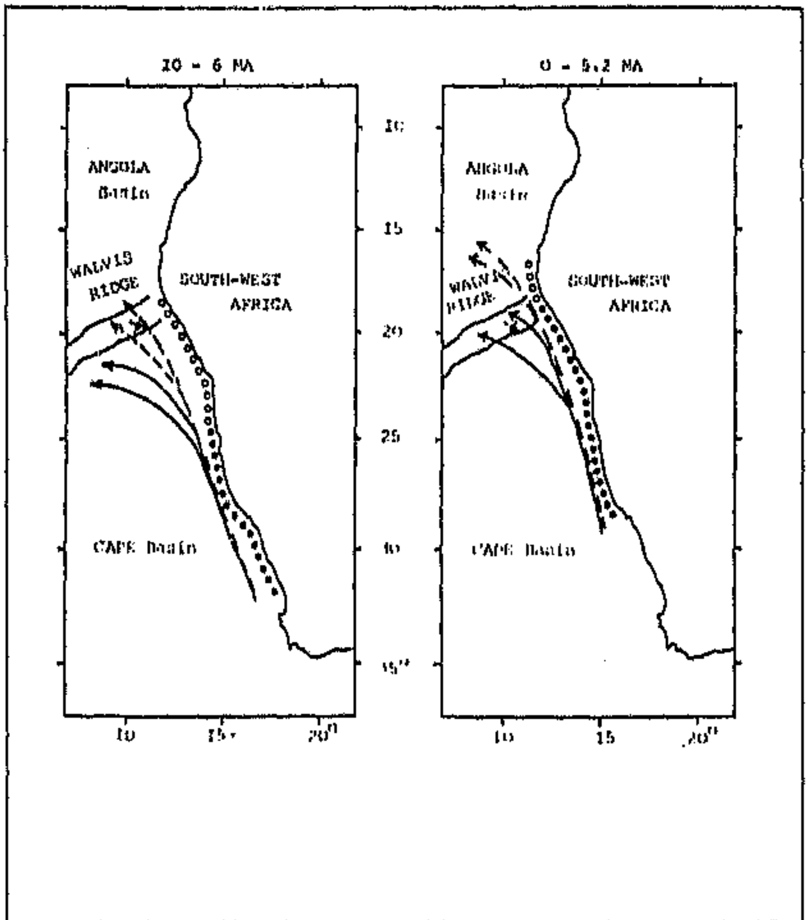

Fig. 7.1 Position of the Benguela Current in the interval 10-6 My and 5.2 My to the present, during glacial (dashed lines) and interglacial (solid lines) periods. Near-coastal upwelling in glacial (open circles) and interglacial (solid circles) periods. Glacial/interglacial shifting of shore-line has not been shown (Diester-Haas, 1987).

Presently, the dominant feature of the southern hemisphere circulation is the large tropospheric circumpolar vortex of westerly winds, and the associated pressure fields. The surface is dominated by large semi-permanent anticyclones which vary in position on a seasonal scale. The South Atlantic Anticyclone and South Indian Anticyclone have a significant influence on South Africa's climate, although it is maintained that anticyclogenesis in a poleward stream of subsiding air originating in the Indian monsoon system affects South African winter weather (Tyson, 1986).

The wind field over southern Africa is dominated by the inter-annual variation of mid-latitude westerlies and tropical easterlies. The westerlies dominate the subtropics (30°S) in winter, and the jet core migrates to 40°S in summer, while the easterlies strengthen and move poleward. The meridional component of the wind field, while not as large as the zonal component, is important in transporting water vapour, mass, heat, and momentum (Tyson, 1986).

CHAPTER SEVEN

Present Day Southern Hemisphere Climates

A number of mechanisms have been invoked to explain the changes outlined above. A short synopsis of the main variables affecting present day southern African climate is necessary before an attempt can be made to explain palaeoclimates of the region in terms of regional atmospheric and oceanic circulations. This synopsis is necessarily brief; the reader is referred to Tyson (1986) for more detail.

In general, southern hemisphere climates are determined principally by the asymmetrical distribution of land and sea. – the small area of land and the very cold polar region (Markgraf *et al.*, 1992). Changes in rainfall over time may result from changes in the frequencies of rain producing systems crossing a region, changes in rainfall receipts from a system, or changes in the type of system affecting the region (Harrison, 1988). These changes are determined by variations in circulation under different boundary conditions.

The three most important boundary conditions uniquely affecting southern Africa are SSTs, ocean currents distributions and Antarctic sea ice extent. At the Last Glacial Maximum (LGM) Southern Ocean SSTs were reduced in conformity with increased Antarctic sea ice. The Agulhas current was weaker, while the Benguela upwelling increased locally, leading to reduced SSTs. Orbitally forced changes in insolation altered the seasonal distribution of radiation (Markgraf *et al.*, 1992). Latitudinal temperature gradients were stronger (Harrison, 1988b; Markgraf *et al.*, 1992) and the westerlies were enhanced and displaced northwards. Easterlies may also have been stronger; aeolian deposits in western Amazonia have been ascribed to enhanced trade winds during colder periods (Thompson *et al.*, 1995), as have the palaeodunes between the Okavango Delta and Etosha Pan (Lancaster, 1981). Evaporation rates over the Indian Ocean would have been reduced in response to decreased SSTs, while increased upwelling along the west coast would have accentuated aridity (Harrison, 1988b). As sea level lowering extended the land area of the Australasian region, the influence of the ENSO phenomenon would have changed (Markgraf *et al.*, 1992).

Since the late Miocene, upwelling along the west coast of Namibia has had an important influence on the coastal hinterland; this followed the development of the East Antarctic ice sheet around 13.7 Ma (Oberhänsli, 1991). During periods of intensified upwelling, the advent of water from greater depths results in cooler SSTs (Oberhänsli, 1991). Fluctuations in upwelling show periodicities at seasonal to Milankovitch frequencies; increased upwelling occurred during stadials, and vice versa. The upwelling also changed in extent, reaching 17°S during glacials, and retracting to 20°S during interstadials, before the cold water retroflected westward (Figure 7.1) (Diester-Haas, 1987). The Benguela current flow is controlled mainly by the trade winds and the position of the ITCZ. Weaker trades in the Indian Ocean result in a reduced flow of the Agulhas current, decreasing south-eastward retroflection and increasing penetration into the Benguela regime: this results in warmer SSTs, and in stronger onshore winds. Incursions of warm Agulhas water into the Benguela, as determined from an analysis of

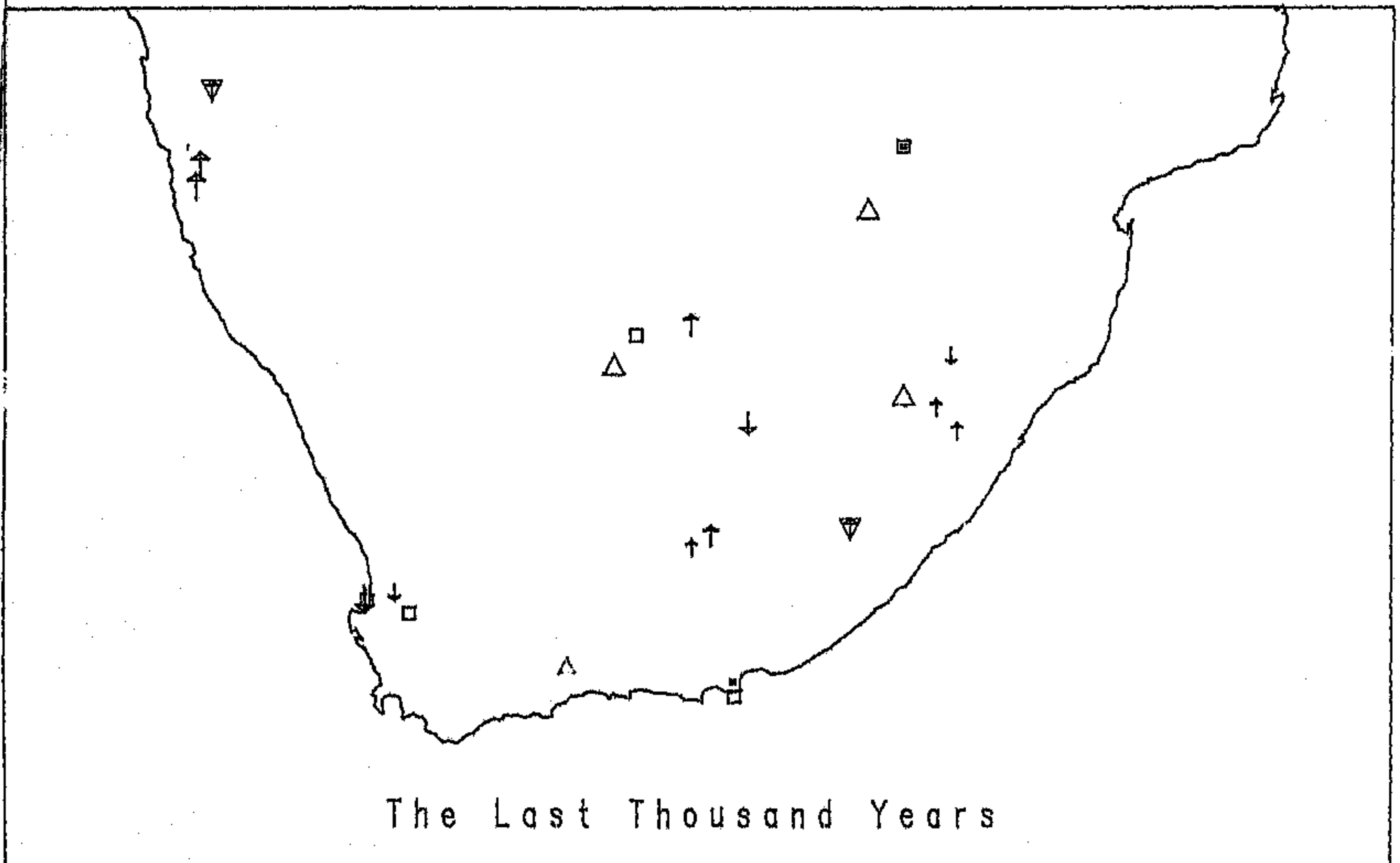

Fig. 6.22 Southern Africa, Temperature and Rainfall: 1 ka.

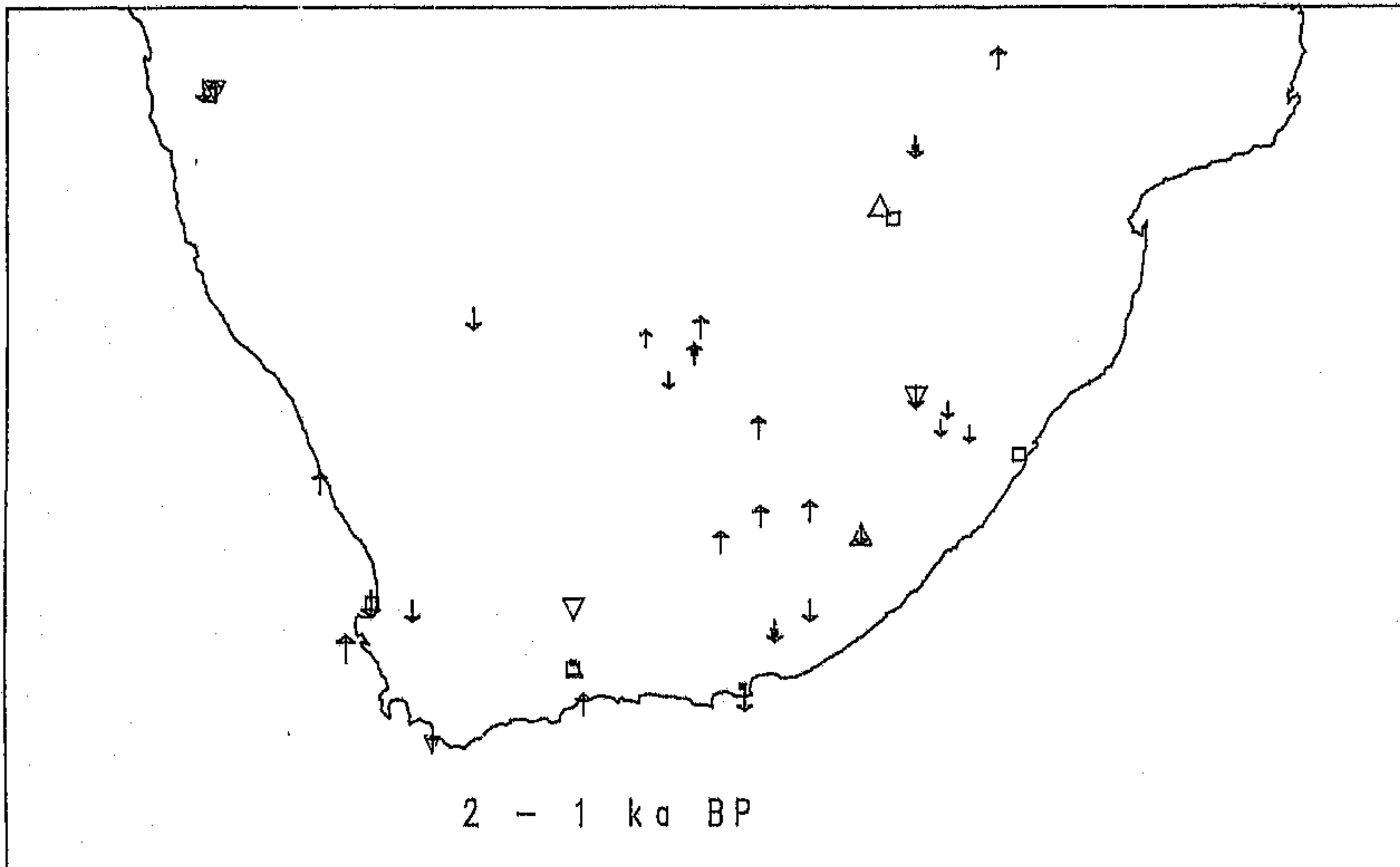

Fig. 6.21 Southern Africa, Temperature and Rainfall: 2 ka.

One possible explanation for the lack of synchroneity between the North Atlantic and elsewhere is that a stationary polar front was located at around 45°N, which effectively insulated areas to the north from global warming. During the last glacial ... fauna, consisting almost exclusively of *Neogloboquadrina pachyderma* (sinist. ...), spread throughout the basin indicating that the polar front had advanced to about 45°N (Lehman, and Keigwin, 1992a). The polar front moved northward at about 14 700 years, just before the onset of the Bølling period. The Barbados coral record indicates melt water pulses associated with ice sheet collapse at 14 500 and 11 500 years, and the migration of the front seems to be synchronous with the renewal of NADW (Sowers and Bender, 1995).

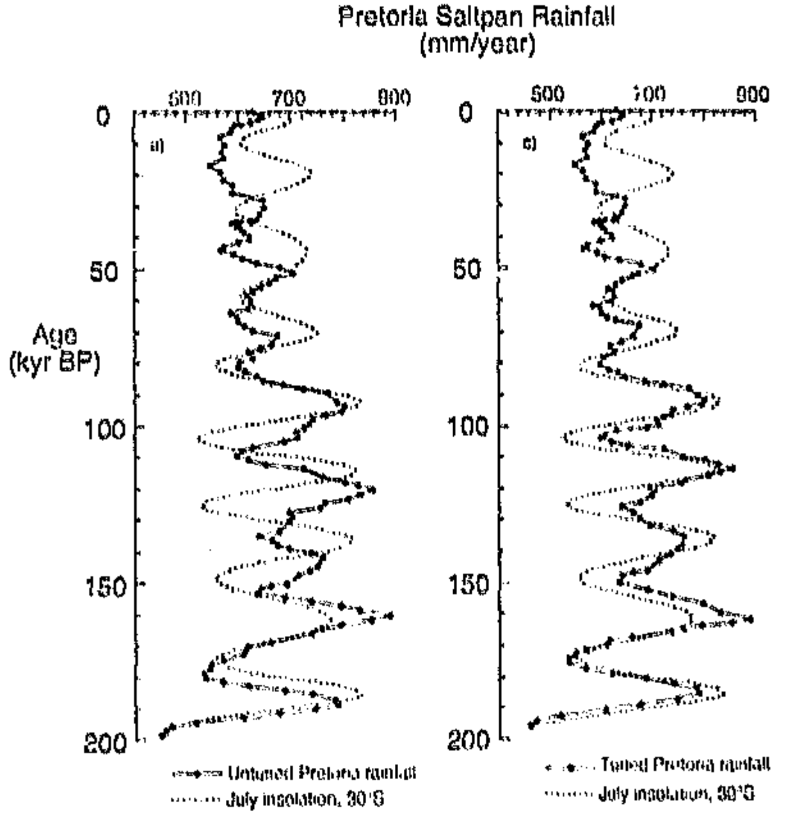

Fig. 7.13 The Pretoria Saltpan rainfall timeseries. Note the dominance of precessional variability in the power spectrum of both the untuned and tuned rainfall time series which accounts for 44% (untuned) and 46% (tuned) of the total variability (Partridge *et al.*, 1997).

(Lorius *et al.*, 1992). The warming trend over Southern Africa identified on the PASH maps for the period 13 ka to 12 ka may be a reflection of an increase in CH_4.

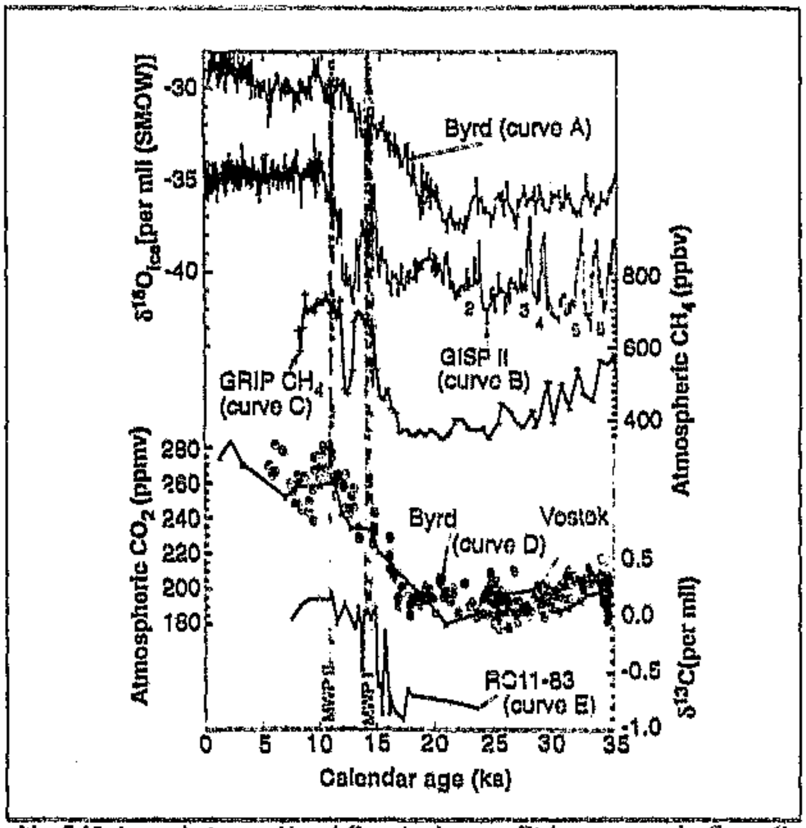

Fig. 7.12 Antarctic (curve A) and Greenland (curve B) isotope records. Curve C plots the atmospheric CH_4 on the GISP 2 time scale showing rapid CH_4 oscillations during the interstadial and Younger Dryas events. Curve D plots the Byrd CO_2 record (circled pluses) and the Vostok CO_2 record (solid line) on the correlated time scale. Curve E shows the benthic foraminiferal $\delta^{13}C$ record from core RC11-83. (Ages are calendar years BP) (Sowers and Bender, 1995).

The interhemispheric symmetry of the abrupt atmospheric event that initiated the last termination about 14 ka is not easily explained by orbital seasonal forcing, which is in the opposite sense at mid-latitudes in the two polar hemispheres (Lowell *et al.*, 1995). Further, the global glacial pulses are not obviously connected with known thermohaline switches in the North Atlantic. The Younger Dryas glacial advance in New Zealand cannot be explained by a NADW flux, as the southern hemisphere chronology implies that the last termination occurred before the switch to modern modes of NADW production in the North Atlantic and could thus not result from this switch. The same difficulty exists for southern hemisphere advances at 14 890, 17 720, 21 000, 23 060, 26 940, 29 600 years (Lowell *et al.*, 1995). The switch to a modern type of deep water formation in the northern Atlantic basin apparently did not occur until after bi-hemispheric glacial collapse, when southern glaciers had already shrunk significantly compared to their extent during the LGM (Lowell *et al.*, 1995).

reduced insolation would reduce water vapour levels in the atmosphere, which would lead to cooling owing to less longwave forcing. The affect of water vapour changes, in concert with CO_2 and thermohaline variations, could account for the interhemispheric synchroneity of global temperature oscillations (Guilderson *et al.*, 1994).

As methane is a very efficient greenhouse gas (molecule for molecule, 21 times as powerful as CO_2), it may also play a significant role in transmitting glacial/deglacial signals across the globe (Peel, 1993). Methane fluctuations may amplify weak orbital forcing, and may constitute the link between the two hemispheres (Lorius *et al.*, 1990); atmospheric water vapour and sea-ice are two fast feedbacks that can be associated with methane forcing (Lorius *et al.*, 1992). Methane concentrations in the atmosphere are limited by photochemically derived OH radicals (Peel, 1993); it is hypothesised that variations in monsoonal rainfall owing to insolation changes control methane concentrations through the expansion or contraction of wetlands and herbaceous swamps (Street-Perrot, 1994).

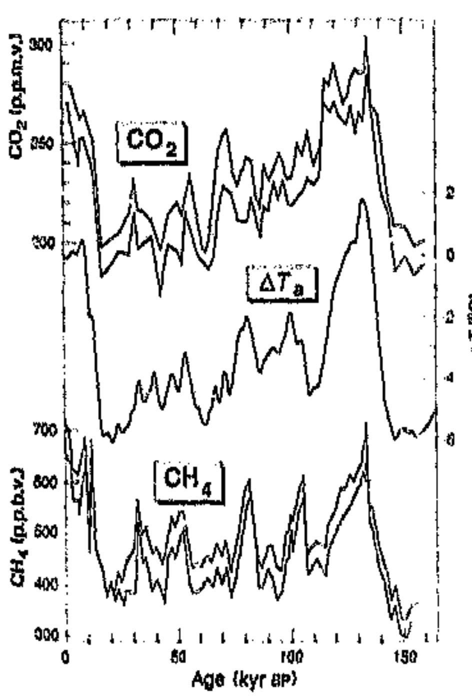

Fig. 7.11 Variation during the last climate cycle, as derived from measurements along the 2,083 m Vostok ice core, of the CO_2 atmospheric concentration, the atmospheric temperature change over Antarctica, and the CH_4 atmospheric concentration. For CO_2 and CH_4 the envelope shown has been plotted taking into account the different sources of uncertainty, whereas the temperature record is a smoothed curve (Lorius *et al.*, 1990).

Methane levels in the GRIP and GISP 2 ice cores do parallel the inferred temperature changes in the cores (Figure 7.11 and Figure 7.12), and a 24 ka and 19 ka periodicity is evident in the Vostok core (Street-Perrot, 1994). It is calculated that CO_2 and CH_4 changes may account for up to 50% of the glacial-interglacial change at a global scale

Southern Hemisphere – Northern Hemisphere Synchroneity

The rapidity and amplitude of glacial-interglacial transitions and the interhemispheric synchroneity of climatic change are difficult to explain in term of solar insolation changes alone (Charles and Fairbanks, 1992). Experiments show that northern hemisphere ice sheets have little influence on atmospheric processes and SSTs in the southern hemisphere, and it is unlikely that regional forcing mechanisms will impact globally (Lowell *et al.*, 1995). It was initially believed that the atmosphere cannot be the link between northern hemisphere insolation fluxes and southern hemisphere climate changes, and that the link must be through oceanic circulation changes (Genthon *et al.*, 1987). Two mechanisms that may link the hemispheres are changes in CO_2 and changes in the flux of NADW. CO_2 fluxes are correlated with orbital variations, and may have important effects on sea ice coverage (Howard and Prell, 1992). However, NADW is not the only regulator of southern hemisphere climates, accounting for only 20% of the Antarctic variance (Crowley, 1992). Evidence from the southern hemisphere implies that southern warming antedated the resumption of NADW (Lowell *et al.*, 1995), and could not therefore be a result of it. Changes in southern hemisphere SSTs are coherent at the Milankovitch orbital frequencies, but precede northern hemisphere ice volume changes, and southern SST warming precedes increases in NADW in the precessional and eccentricity bands (Howard and Prell, 1992).

Work on interhemispheric links by Lowell *et al.* (1995) suggests that interhemispheric coupling implies a global atmospheric control, possibly through variations in atmospheric water vapour, rather than a North Atlantic or Laurentide ice-sheet trigger. Southern hemisphere polar climates have had tight teleconnections to subtropical climates during the periods of early monsoon intensification at 13.5 ka when methane levels increased over the subtropics while Antarctica experienced a concomitant deglacial change in wind trajectories and dust levels (Sirocko *et al.*, 1996). It is suggested that water vapour exports to high latitudes may explain the coeval, but hemispherically asymmetrical evolution of subtropical climates with polar climates.

Recent estimates of tropical SSTs at 16 ka indicate that temperatures were 5°C colder than present. These new estimates, although in conflict with those of CLIMAP, are in agreement with other tropical temperature indices (Thompson *et al.*, 1995) and the present analysis. The recent SST analysis indicates that significant warming occurred between 16 ka and 12.5 ka, and that this was interrupted between 12.5 ka and 11.5 ka by a temporary cooling, possibly of up to 4°C, coincident with melt water pulse 1A (Thompson *et al.*, 1995). The PASH data maps show no discernible warming for the period 16 ka to 13 ka, however, a warming trend is identified at Boomplaas and Wonderkrater from about 16 ka (Partridge *et al.*, 1990; Thackeray, 1990); this warming over Southern Africa may have occurred at a rate of 1°C per millenium (Thackerav, 1990).

Another prominent change in temperature occurs at about 9.5 ka, just after melt water pulse 1B. These temperature variations are ascribed to radiative changes, possibly owing to the equatorward displacement of highly reflective clouds. The resultant cooling could reduce tropical SSTs and amplify the extent of high latitude glaciation (Guilderson *et al.*, 1994). The resulting radiative imbalance in the tropics caused by circulation, and north of 45° N heat transport decreased to zero owing to the southward shift of the polar thermal front. These responses agree with reconstructions of the Atlantic circulation during stadials as derived from measurements of Cd/Ca ratios and carbon isotope ratios in benthic foraminifera shells (Fichefet *et al.*, 1994).

In a simulation where salinities at 62.5°S and 65°N were set at 35 $^0/_{00}$ the Atlantic circulation became weaker and shallower as AABW occupied the entire deep ocean below 3 000 m and penetrated north to about 55°N (Figure 7.9) (Stocker *et al.*, 1992a). Surface forcing of the Southern Ocean not only determines the properties of AABW, but also directly influences the strength and depth of NADW formation (Stocker *et al.*, 1992a). Modelling by Rind *et al.* (1995) indicated that increased southern sea ice does not result in northern hemisphere cooling through atmospheric climatic processes, but the model does not include the affects of alterations in AABW, and thus southern sea ice could affect northern locations through such a mechanism (Rind *et al.*, 1995).

The intensity of the Atlantic thermohaline overturning is controlled by the density differences between surface waters in the northern North. In a model developed by Fichefet *et al.* (1994), deep-water formation in the high-latitude North Atlantic under glacial boundary conditions ceased because of stratification due to the lower salinities. Decreasing the salinity anomalies by 0.4 $^0/_{00}$ in the north Atlantic, or increasing them by the same amount in the south in the vicinity of Antarctic continent, leads to a significant weakening of thermohaline overturning and to a more pronounced intrusion of AABW (Figure 7.10) (Fichefet *et al.*, 1994).

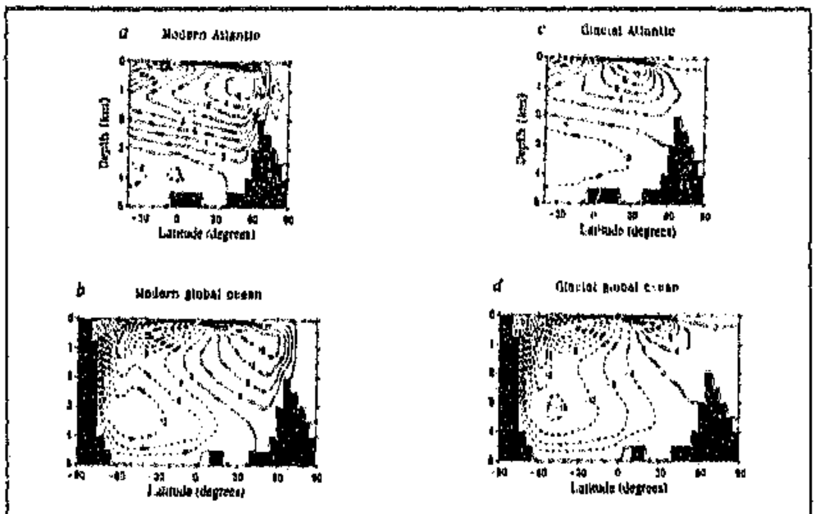

Fig. 7.10 Contours of the annual mean meridional overturning stream-function in the Atlantic basin and in the three basins taken as a whole for the control run (a and b) and for the standard LGM experiment (c and d). The flow of water is parallel to the contours and is greatest where contour spacing is closest. Units are Sv (Fichefet et al., 1994).

Around 50°N, the surface-water salinity was sufficiently high to permit deep convection to a maximum depth of 2 500 m as a source of glacial NADW. Thermohaline overturning of moderate strength (11 Sv) confined to north of 40°S occurred with only 1 Sv of glacial NADW escaping south. Below 2 500 m most of the Atlantic basin filled with AABW. The intensity of the Antarctic thermohaline cell increased by ± 10% and resulted in a deep Atlantic temperature reduction of 2 - 3°C, accompanied by an enhanced northward flow of bottom water in the three ocean basins, with AABW replacing relatively warm NADW (Fichefet *et al.*, 1994). Northward heat transport was reduced as a consequence of the weaker thermohaline attendant upon waxing and waning of the Antarctic sea ice must be considered. Increasing salinity in the formation region for AABW can cause it to flow much further northward into the Atlantic, and can make NADW formation weaker and shallower. NADW during the Last Glacial Maximum (LGM) was shallower than today, and the AABW penetrated much further north. Work by Fichefet *et al.* (1994), suggests that the glacial production of AABW was slightly higher than present, whereas that of NADW was reduced by 40%. Increasing AABW density relative to NADW results in a state similar to that observed during the LGM (Stocker *et al.*, 1992a), as demonstrated in a model in which states of the thermohaline circulation can be varied from NADW control of the deep ocean to AABW dominance.

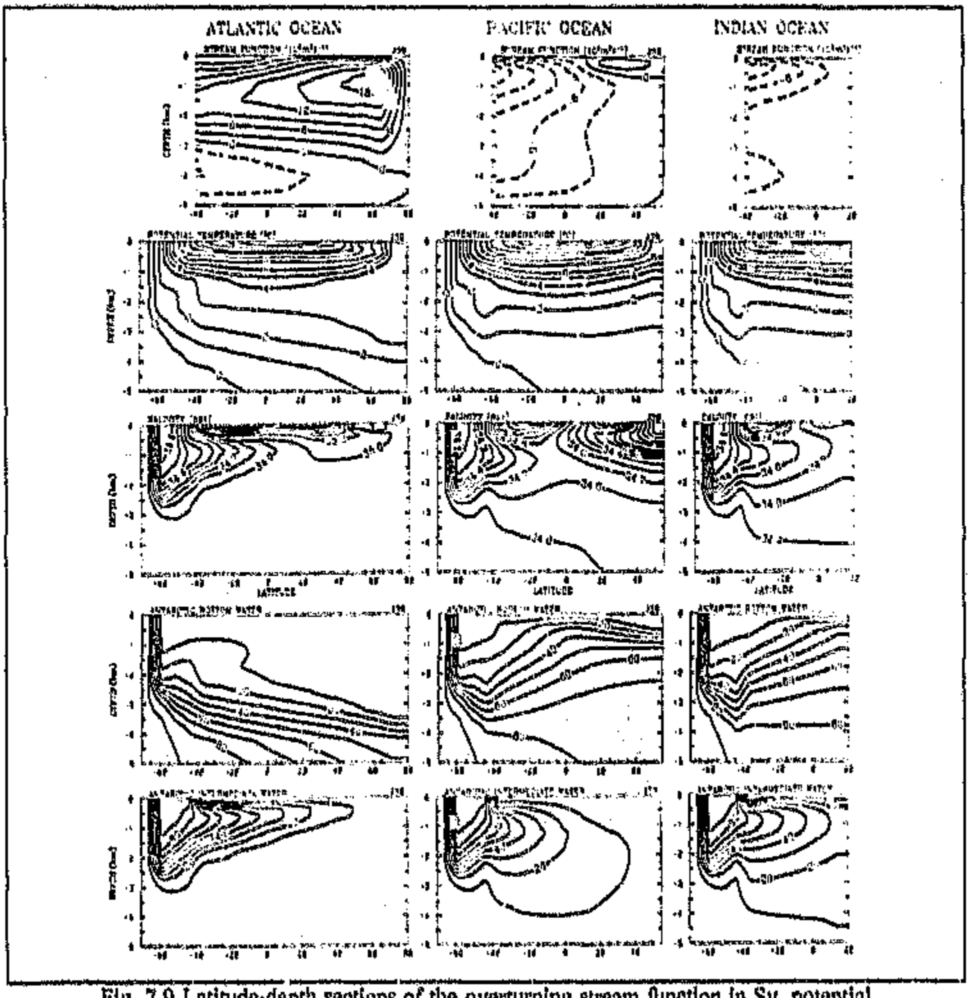

Fig. 7.9 Latitude-depth sections of the overturning stream function in Sv, potential temperature, salinity, percent concentration of AABW, AAIW, and NADW, concentrations exceeding 60% are shaded for the glacial mode of the thermohaline circulation in the world ocean. The deep ocean is cooler and more saline than the modern state because AABW is dominant The influence of NADW in the Pacific and Indian Oceans is reduced, and the deep North Atlantic is occupied by older water originating from the Southern Ocean, and stronger vertical property gradients are present (Stocker *et al.*, 1992a).

AABW forms in the Eckman layer on Antarctic continental shelves by the process of salt rejection during sea ice formation (Kellogg and Kellogg, 1986; Hoffert, 1990; Stocker *et al.*, 1992a), and is not formed from the direct effect of cold surface temperatures. However, open areas in the sea ice (polynyas) can also create bottom water directly (Hoffert, 1990). Salt rejection due to sea ice formation enhances deepwater formation, which acts as a sink for gases, especially CO_2 (Figure 7.8) (Lucas and Lindesay, 1991). As the water freezes, it is calculated that 70% – 80% of the salt is rejected (Hoffert, 1990). The AABW flow rate induced by the seasonal sea ice cycle is of the order of 30 – 40 times the sea ice freezing rate, resulting in between 30 and 40 Sv of AABW for every Sv of sea ice formed (Hoffert, 1990).

There are three significant regions of modern AABW formation: the south west corner of the Weddell gyre, which is the largest contributor and produces the coldest and densest water, the Ross Sea and the Adelie Coast (Johnson, 1985). Eddies from the circumpolar current flow into the Ross and Weddell seas forming clockwise gyres. Water in these gyres is subjected to intense cooling, especially in winter, and is enriched in salt as ice formation occurs. The resulting dense salty water (-1.9°C, >34.52‰) flows down the Antarctic continental slope where it mixes with Circumpolar Deep Water (CDW), attaining an increased density, and subsequently sinks as AABW (Kellogg and Kellogg, 1986). Total present day AABW volume is estimated to be in the vicinity of 13 Sv (Gordon, 1988).

Variable rates of formation of NADW have also been suggested as a mechanism through which changes in the flow in the oceanic conveyor could modulate the amount of sea ice around Antarctica and thus alter southern hemisphere climates (Kerr, 1993b). Faunal data show that the glacial-interglacial oscillations of the Antarctic Circumpolar Current (AACC) are very similar to those of the North Atlantic, and suggest reduced influence of NADW on CDW during glacial intervals (Corliss, 1983). One hypothesis holds that changes in area of Arctic sea ice due to orbital variations reduce NADW production, which leads to an increase in sea ice around Antarctica (Rind *et al.*, 1995). There are some problems with such a simple northern/southern hemisphere link. Modelling studies suggest that the influence of NADW on the sea ice field of the Southern Ocean is modest and NADW can account for only 20% of the observed glacial -to-interglacial change in the South Atlantic (Hodell, 1993). It is thus possible that the observed relationship between NADW and Southern Ocean surface water properties is not one of cause and effect (Hodell, 1993).

Although present day AABW receives much of its salt from NADW, a total shut down of NADW need not lead to a cessation of AABW formation. AABW and NADW do not co-vary, there is evidence of AABW formation when NADW was shut off (Johnson, 1985). An alternative source of salt is available from the western Indian Ocean, and evidence exists that indicates that there was a southward flow of hypersaline water... the Indian Ocean during the Quaternary (Johnson, 1985). During glaciations, the most important area responsible for the formation of cold, global bottom water may have been the Southern Ocean around the glaciated Antarctic continent owing to a gradual build-up of sea ice as the global climate cooled (Hoffert, 1990). However, variations in AABW formation may not have a simple glacial-interglacial signature (Crowley, 1992).

When considering possible influences on the operation of the conveyor belt, effects cycle (Hoffert, 1990). Bottom water is formed very differently in the two hemispheres, with the present day NADW source being the Icelandic and Greenland seas in a region of high salinity created by an excess of evaporation over precipitation (Stocker *et al.*, 1992a). Northern hemisphere seasonal ice formation occurs mostly in the landlocked Arctic Ocean, which communicates very weakly with the North Atlantic (Hoffert, 1990), and unlike the Antarctic is not primarily responsible for bottom water formation.

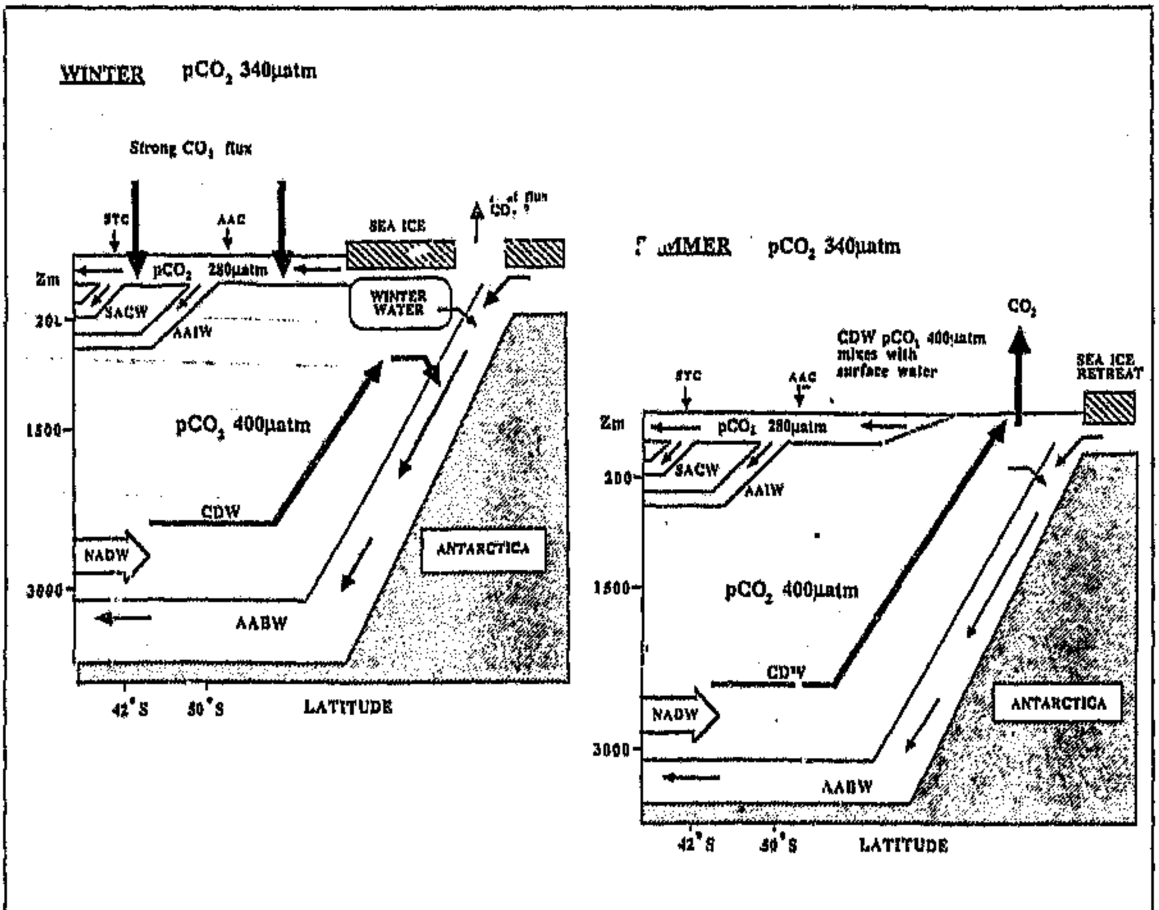

Fig. 7.8 A schematic representation of (a) winter, and (b) summer thermohaline convection and anticipated CO_2 fluxes associated with sea-ice formation and retreat. (Lukas and Lindesay, 1991).

AABW is the densest, coldest and deepest bottom water, underlying all the oceans (Hoffert, 1990). All around Antarctica AABW flows down the Antarctic continental shelf towards the Atlantic Ocean and moves northwards along the bottom (Thurman, 1991). Currently, AABW is a combination of NADW, Circumpolar Water (CPW) and Weddell Sea Shelf Water, in which NADW supplies the salt necessary for the formation of the deep water (Johnson, 1985). The warmer NADW cools as it upwells to the surface layer as a result of contact with the atmosphere and by the Antarctic Circumpolar Current, and subsequently sinks as cold water masses around Antarctica (Gordon, 1988).

sheet; this enhances the growth rate (Squire, 1994; Wadhams, 1994). The most important consequence of sea ice formation, and especially of that in the polynyas, is a salinity increase which causes the dense, cold water to sink along the shelf to form AABW (Figure 7.7) (Gordon, 1988; Wadhams, 1994).

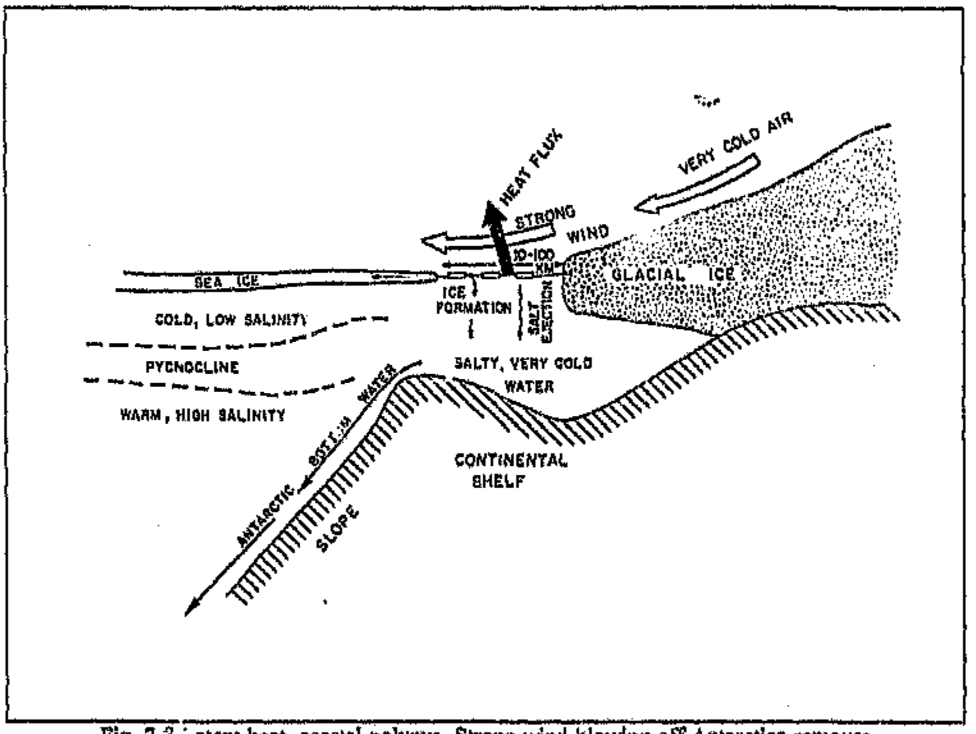

Fig. 7.7 Latent heat, coastal polynya. Strong wind blowing off Antarctica removes sea ice of the coastal region. The open water now exposed to the cold atmosphere, results in formation of new ice. As this ice is also removed by the wind, a persistent coastal polynya forms. These polynyas are maintained by the wind, with the heat flux from ocean to atmosphere supplied by the latent heat of fusion. Massive amounts of sea ice may form within the coastal features. Note the formation of AABW through the process of salt ejection (Gordon, 1988).

During the last glacial, sea ice expanded to 35 x 10^6 km^2 during winter (Hodell, 1993), and summer sea ice may have extended to 55°S as a consequence of a different heat budget induced by polar cooling, which enhanced sea ice formation (Corliss, 1983). Some explanations for the changes invoke CO_2 variations, which are important for the expansion of Antarctic sea ice and orbital insolation variations (Crowley, 1992). Expanded sea ice around Antarctica is supported by the suppression in productivity of open ocean diatoms (*Eucampia antarctica),* as noted in cores from the Southern Ocean (Shemesh *et al.*, 1994). A drastic decrease in this diatom at about 12 ka has been documented (Jouzel et al., 1995). This signifies a major change in the climate of the Southern Ocean between glacial and interglacial periods (Hodell, 1993), and occurs coevally with the southern hemisphere climate reversal suggested by the Southern African proxy data.

The sinking of cold, salty, well ventilated, surface waters to the bottom of the oceans drives the thermohaline circulation and affects dissolved constituents and the carbon has a frequency of between 4-5 years and takes between 8 and 10 years to circle the globe (White and Peterson, 1996).

Sea ice affects the salinity and temperature profiles of the upper ocean layers both in the region of generation and melt (Gordon, 1988; Wadhams, 1994); on longer time scales, sea ice formation influences bottom water formation which is important for global climate change (Lukas and Lindesay, 1991; Yuan *et al.*, 1996). Further, Antarctic Bottom Water (AABW) flows into the northern Atlantic, especially when NADW production is reduced, and this could have an effect on northern hemisphere climate dynamics (Lehman and Keigwin, 1992b).

Present day sea ice formation correlates well with southern hemisphere solar heating cycles, although it is phase-lagged by three months. A 1°C cooling creates about 5 x 10^{12} m^2 of sea ice, and thus 15 x 10^{12} m^2 of sea ice is created between March and September, corresponding to a 3°C cooling of the mean oceanic surface temperature. As sea ice depth varies between 1m and 2 m, about 1 – 1.5 x 10^6 m^3 of ice is produced (Hoffert, 1990). Variations in the area of sea ice from 4 x 10^6 km^2 in February to 20 x 10^6 km^2 in September (Wadhams, 1994) almost double the size of the continent, supplying a high albedo surface to about 60°S by spring (Carleton, 1992). According to the Milankovitch theory, the seasonal and geographical redistribution of insolation is amplified through the affect of albedo (Lorius and Oeschger, 1994), which increases substantially from about 10% to 80% as sea ice is formed (Budd, 1991). Further, models of the northern hemisphere suggest that increased seasonality as a result of the precessional cycle results in colder winters with thicker sea ice (Phillipps and Held, 1994). The southern hemisphere should react in a similar manner.

Sea ice acts as an insulator, reducing air–sea heat exchange (Stocker *et al.*, 1992a), and affects moisture and momentum exchanges between the ocean and atmosphere (Wadhams, 1994). In areas of increased sea ice formation, high cloud formation is suppressed, which leads to greater cooling and maintenance of the sea ice cover (Carleton, 1992). Model simulations show that the affect of sea ice is larger in a cooling climate than in a warming climate, and that if solar irradiance is reduced by 2%, sea ice increases by 150% in the southern hemisphere; its formation can account for 39% of cooling in the model (Rind *et al.*, 1995). When the ice melts, however, it results in a strong positive feedback during subsequent warming (Budd, 1991).

The wave field (Squire, 1994), sea surface temperature and heat flux (Rind *et al.*, 1995) affects the formation of sea ice. In the regions dominated by ocean gyres (Weddell and Ross Seas) annual sea ice production is strongly controlled by winds and currents, and the annual variation of sea ice volume is large (Carleton, 1992). The sea ice zone is a product of air-sea interactions where strong, very cold, dry katabatic winds persistently blow off the continent resulting in the sea ice moving away from the coast (Wadhams, 1994). This process creates coastal polynyas where, owing to latent heat release, more ice is formed rapidly; this is transported away quickly, to allow further freezing and more ice formation (Gordon, 1988; Squire, 1994). The growth rate in coastal polynyas is also enhanced by the fact that the ice grows as frazil which does not cut off the surface water from the atmosphere (Wadhams, 1994). The wave field of the Southern Ocean is the most intense in the world and causes the advancing winter ice edge to exist as a belt of high concentration pancake ice more than 250 km wide, rather than as a continuous

Poleward of the current lies 30 x 10^6 km^2 of ocean exposed to the harsh polar atmosphere and isolated from exposure to warm surface water from the subtropics.
The position of Antarctica influences atmospheric circulation as masses of cold air spread away from the centre (Gordon, 1988; White and Peterson, 1996) and plays a critical role in the global climate system via its continental ice-sheets, floating ice shelves and sea ice zone. Variability in the Antarctic may change the rate of formation of deep and bottom waters, and affect the heat transfer between the ocean and atmosphere (Yuan *et al.*, 1996).

High surface altitudes of ± 3000 m, a high surface albedo (0.85), low atmospheric water vapour content, and lack of cloud cover, (< 4 -5 tenths), results in the area having a net radiation deficit of about $-28Wm^{-2}$. The intense radiative cooling results in mean temperatures of between -60°C and -70°C and strong surface based inversions of up to 25°C. The radiation deficits, slope of the ice surface, and semi-permanent inversions promote a persistent gravitational katabatic flow in the lowermost 100 m of the atmospheric boundary layer, with directional consistency at most coastal areas around Antarctica (Carleton, 1992). These cold winds impose temperature and salinity alterations on the surrounding surface ocean water as sea ice forms, releasing heat into the atmosphere (Gordon, 1988).

The Antarctic sea ice is a sensitive component of the global climate system and amplifies temperature changes by strong positive feedbacks (Budd, 1991). Since there are no constraints on the equatorward extent of the ice, the Antarctic is involved thermodynamically in the oceanic and atmospheric circulations of the middle and lower southern latitudes (Carleton, 1992). The influence of the formation of sea ice around Antarctica is one of the most climatically important features of the southern hemisphere (Denton, 1985; Wadhams, 1994), as is the formation of polynyas (large ice free areas along the coast or within the sea ice) (Gordon, 1988). Antarctic sea ice is linked to the Subtropical Convergence (STC) and the Antarctic Polar Front (APF) through its affect on the circumpolar westerly winds (Howard and Prell, 1992). Reduced sea ice extent results in weaker westerlies in adjacent latitudes (Carleton, 1992).

The advance of sea ice may reinforce baroclinic conditions near the ice edge, intensifying synoptic scale cyclones. Sea ice extent variations influence the frequency of mid-latitude cyclones, and the meridional extension of the subtropical high in the South Pacific; this high being a function of the intensity of the Hadley circulation. The Hadley cell shows close associations with SST zonal anomalies in the Pacific (Carleton, 1992). Sea ice circulation anomalies may manifest a larger climate teleconnection such as ENSO; evidence suggests that the efficiency of Southern Ocean cyclones in transporting eddy sensible heat may vary according to the phase of the SOI (Carleton, 1992). It has been suggested that in contrast to the view that ENSO forces the sea ice, ENSO may be a result of forcing from Antarctic latitudes (Carleton, 1992).

Recently, it has been suggested that the sea ice is linked to El Nino/Southern Oscillation (ENSO) events through the Antarctic Circumpolar Wave (ACW), an interannual wave comprising a disturbance in sea ice extent, SSTs, surface wind speeds, and sea level atmospheric pressure. The propagation speed of the ACW is the same in all three media, suggesting strong interannual coupling (Yuan *et al.*, 1996). This two-wavelength wave above, by an increase in AABW owing to increased Antarctic sea ice, or some combination of both, cannot be determined for certain.

Incursions of Agulhas water into the Benguela based on the occurrence of Algoa molluscan taxa probably occurred during the period 13.5 ka to 12 ka and just after 10 ka (Pether, 1994). The interval 12 ka to 10 ka is characterised by a hiatus in the Algoa molluscan taxa recorded near Kleinzee (Figure 7.2) (Pether, 1994) coincident with cooler SSTs as suggested from the analysis of *Patella granularis* along the west coast (Cohen and Tyson, 1995). The west coast cooling could be a result of stronger trade winds and increased upwelling (Cohen *et al.*, 1992) caused by increased austral winter insolation (Pether, 1994). Both Agulhas intrusions and upwelling may have occurred during the period 12 ka to 11 ka, with upwelling occurring preferentially during the winter, while reduced austral summer insolation associated with reduced trades would allow for the Agulhas intrusions (Pether, 1994). This would explain the increases in local moisture along the west coast during this time. Warm water species are absent from the Nelson Bay Cave deposits prior to 9 ka (Cohen and Tyson, 1995); this may infer that SSTs between 12 ka and 11 ka were too low for their survival along the Algoa coast and thus in the Agulhas intrusions, explaining the observed hiatus (Pether, 1994).

Subsequent Younger Dryas cooling in the northern hemisphere may, in fact have been triggered by events around Antarctica. Amplified AABW formation, following the accelerated development of sea ice, may have caused AABW to wedge in under NADW, reducing the strength and depth of the thermohaline circulation. If the AABW pulses were sufficiently large, LNADW formation may have been halted (Lehman and Keigwin, 1992a), resulting in the dramatic temperature decreases recorded in the ice cores. It is therefore suggested that decreases in the NADW index could be driven by increases in the flux of ^{13}C depleted southern waters (Howard and Prell, 1994). This could explain a reduction in NADW independent of melt water pulses: these occurred too early (12 ka) or too late (9.5 ka) to be the direct trigger for the northern climatic reversal (Fairbanks, 1989). It is, in any case, likely that melt water discharge was reduced by 80% during the Younger Dryas (Jansen and Veum, 1990) and the isotope record off the St Lawrence shows no shift that could be attributed to dilution through a meltwater pulse (de Vernal *et al.*, 1996). Enhanced sea ice formation would restrict CO_2 outgassing in the Southern Ocean (Figure 7.8) (Lucas and Lindesay, 1991), and upwelling of AABW would increase oceanic productivity and subsequent CO_2 absorption.

When insolation increased in the southern hemisphere, sea ice melting would reduce AABW production, and NADW formation would be rapidly enhanced, reversing the temperature trends. Southern African rainfall and temperature patterns would subsequently revert to interglacial mode as temperature gradients decreased. The above argument may help to resolve some of the enigmas that have bedevilled attempts to explain the Younger Dryas; these include the southern hemisphere lead in temperature decline, the need for a source of cooling during a peak in solar insolation receipts, and the postulation of an unambiguous trigger of the oceanic circulation fluxes. The difference in $\delta^{13}C$ values between the GIN seas and the North Atlantic (Veum *et al*, 1992) may also be explained by an increase in bottom water production in the southern hemisphere.

It is proposed that the diachronistic Southern African "Younger Dryas" coolings are a direct result of the insolational minimum that occurred between 13 ka and 9.5 ka when the aphelion occured in the southern summer. Austral summer insolation was 4% lower than at present, while winter insolation was between 3% and 6% higher at 40°S (Markgraf *et al.*, 1992). Decreased insolation at high latitudes owing to increased axial tilt (Liu, 1992), and reduced summer melting owing to aphelion at the southern summer solstice, may have enhanced Antarctic sea ice development. Increased areas of sea ice would have steepened the thermal gradient and increased the strength of the westerlies, as well as that of semi-permanent anticyclones and could be the cause of lower Southern Ocean SSTs (Harrison, 1988b; Markgraf *et al.*, 1992).

A southern hemisphere precessional trigger could also account for the asymmetrical hemispheric teleconnections between subtropical monsoons and high latitudes, as the monsoonal frequencies observed in an Arabian sea core are harmonic tones of the precessional cycle which tie in with global climate oscillations (Sirocko *et al.*, 1996). A precessional covariation of the African monsoonal systems and summer rainfall over South Africa has recently been documented (Partridge *et al.*,1997).

The cooling suggested from the Vostok cores, SSTs and other southern hemisphere data is apparent in the PASH data for the period 12 ka to 11 ka. All sites except one indicate reduced temperatures, the majority of summer rainfall sites concomitantly experienced reduced rainfall; exceptions include northeastern sites and Namib sites. In agreement with theoretical models (Cockroft *et al.*, 1987; Cohen and Tyson, 1995), the winter rainfall sites record increased rainfall. Excluding the localised Algoa upwelling (Cohen and Tyson, 1995), low SSTs to the south of the country, coeval with low Indian Ocean SSTs, are associated with drier conditions over the summer rainfall area (Mason, 1995) owing to reduce evaporation rates (Harrison, 1988b) resulting in less rainfall over the subcontinent from the suppression of both tropical and temperate synoptic systems. Reduced SSTs off the east coast of Southern Africa have been associated with a weaker Agulhas Current, limited to subtropical latitudes (Prell *et al* 1980).

The strength of the Agulhas Current is determined by the strength of easterlies blowing out of the South Indian Anticyclone (Cohen and Tyson, 1995). A return to glacial conditions characterised by a steeper meridional temperature gradient, stronger westerlies, intensified Hadley cells, extended subtropical anticyclones (Cockroft *et al.*, 1987) and reduced SSTs in the Southern Ocean (Labracherie *et al.*, 1989; Pichon *et al.*, 1992), would result in a weaker Agulhas Current. Displaced easterlies would affect summer rainfall patterns over southern Africa, while winter rainfall would increase under the influence of more frequent mid-latitude disturbances (Markgraf *et al.*, 1992). Further, the weaker Agulhas results in a more westward retroflection (Lutjeharms and van Ballengooyen, 1984), allowing Agulhas rings to intrude into the Benguela. Reduced Agulhas heat input to the southern Benguela has been associated with a reduction in NADW production (Cohen *et al.*, 1992). core evidence suggests that NADW increased from a minimum at 13 ka to a maximum at 12 ka, coeval with Southern African warming, followed by a decrease centred on 11.5 ka. Thus the association of increased (decreased) NADW and southern warming (cooling) is confirmed, however, whether the NADW reduction is a result of meltwater inputs (Fairbanks, 1989), or, as suggested

$\delta^{13}C$ values from core RC11-83 in the Southern Ocean record rapid oscillations in water mass composition. Besides the general glacial/interglacial signature, small scale but significant oscillations occurred, with an increase in $\delta^{13}C$ values occurring from 13.1 ka - 12.7 ka, and decreases at about 11.5 ka (Charles and Fairbanks, 1992). Similar oscillations are also recorded in other cores from the Southern Ocean (RC13-229 (Oppo and Fairbanks, 1987, 1990)), as well as the north Atlantic (EN120GGC1 (Fairbanks, 1989); V23-81 (Jansen and Veum, 1990) HM52-43 (Veum *et al.*, 1992) and CHN82-20 (Keigwin and Lehman, 1994)) (Figure 8.4) (Figure 4.10) (Figure 4.9) (Jansen and Veum, 1990). The period covering the Younger Dryas is not characterised by any strong anomaly, but small scale variations do occur in the cores. Comparison of the ice core records from Greenland and Antarctica with those from ocean cores do, however, indicate that temperature minima accord with $\delta^{13}C$ minima, even though the amplitude of the $\delta^{13}C$ variations is not very large (Figure 8.5) (Jouzel *et al.*, 1995).

SSTs from the Indian sector of the Southern Ocean suggest a lead in cooling of 1 ka, compared to the northern hemisphere, occurring between 12 ka and 11 ka (Figure 8.6) (Labracherie *et al.*, 1989). Further, the SST fluxes documented at 12 ka are large (up to 6°) and rapid (Labracherie *et al.*, 1989), and occur coevally with the Dome B temperature reductions, the RC11-83 $\delta^{13}C$ minimum at about 11.5 ka (Figure 8.5) Jouzel *et al.*, 1995) and the insolation minimum in the southern hemisphere. This evidence points to a period lasting for a thousand years when the warming trend in the southern hemisphere was reversed, coincident with an unstable thermohaline circulation.

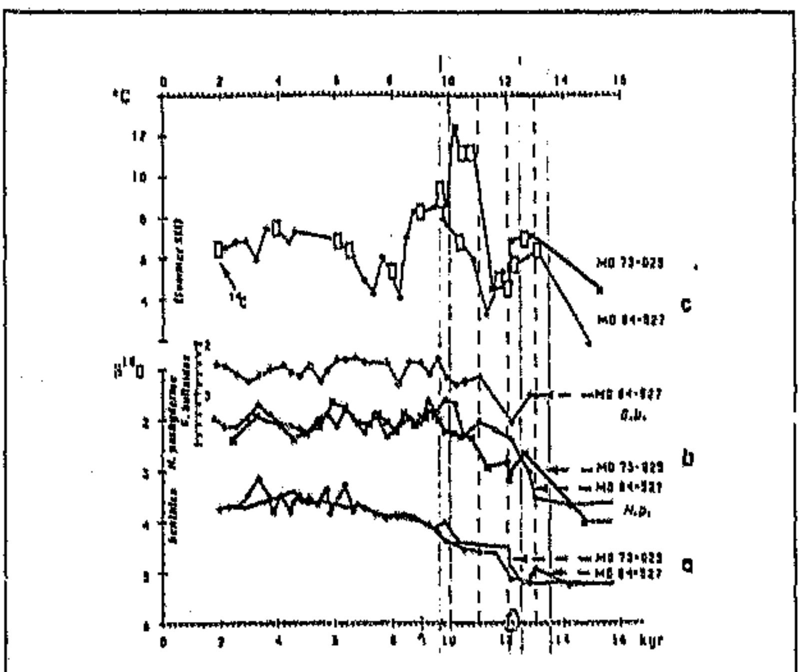

FIG. 8.6 Distribution versus calculated ages in cores MD 84-527 and MD 73-025, of a) $\delta^{18}O$ of the benthic foraminifera, b) $\delta^{18}O$ of the planktonic foraminifera (*N.p.- Neogloboquadrina pachyderma* sinistral; *G.b- Globigerina bulloides*), and c) summer SST (Labracherie *et al.*, 1989).

Although southern hemisphere cooling corresponding to the Younger Dryas has a low amplitude in the Vostok core, (indicating a smaller magnitude of cooling), it is dated 1 ka before the northern hemisphere climatic reversal in Greenland (Genthon *et al.*, 1987; Sowers and Bender, 1995). Analyses of a new core at Dome B also demonstrate the existence of an Antarctic cold reversal antedating the northern cooling. This reversal is not as large as that in Greenland during the Younger Dryas (Jouzel *et al.*, 1995). It may, however, been characterised by a rapid change in temperature (Mayewski *et al.*, 1996).

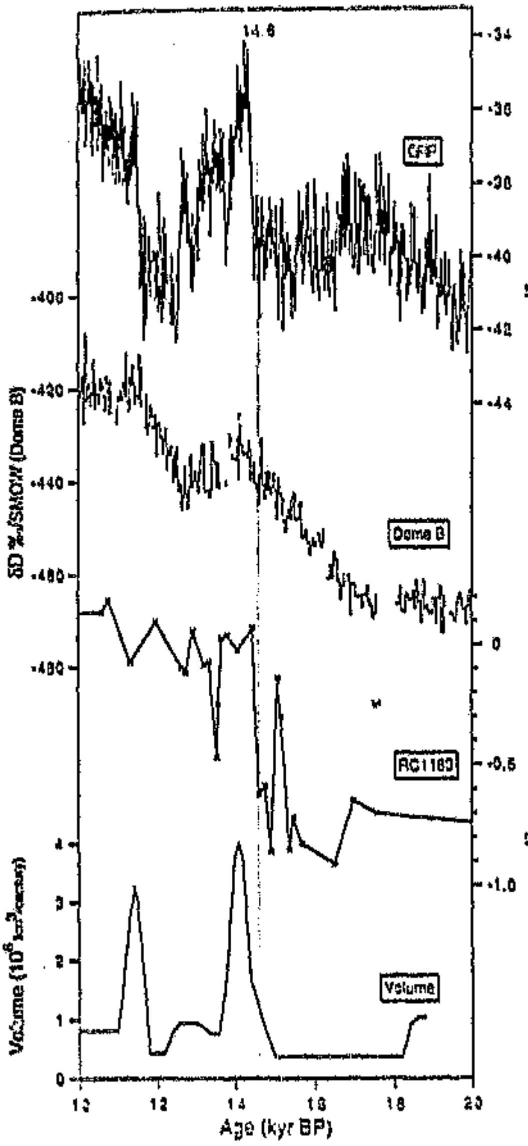

Fig. 8.5 Age profiles of (from top to bottom) the $\delta^{18}O$ GRIP profile, the Dome B profile, the $\delta^{13}C$ profile in RC 11-83 South Atlantic deep-sea core and the deglaciation rate. The vertical line corresponds to the end of the dust peak at Dome B (Ages in CAL years) (Jouzel *et al.*, 1995).

The SST rise documented in cores in the Southern Ocean (Labeyrie *et al.*, 1986) started at about 14.2 ka, coincident with temperature rises over Antarctica, but preceded northern deglaciation signals by up to 3 300 years (Sowers and Bender, 1995).

At about 14 ka southern hemisphere glacial readvances to new limits occurred subsequent to the retreat which began at 18 ka, as shown in data from New Zealand and the Andes (Lowell *et al.*, 1995). Soon after 14 ka, retreat again occurred, but was interrupted by a readvance between 12 ka and 10 ka as revealed in data from Africa, New Zealand, New Guinea and the Andes. In South Georgia wastage of the Antarctic full-glacial ice cap between 12 ka and 10 ka was interrupted by a readvance of outlet and valley glaciers of between 2 km and 6.5 km, the largest since the LGM (Clapperton *et al.*, 1989). Data from the lower latitudes of South America (Colombia, Ecuador, and Peru) suggest colder climates and cooling associated with glacier advance from 12 ka to 10 ka (Heusser and Rabassa, 1987). Antarctic sea ice extension may have caused the cooling over the Fuegian archipelago, as indicated by moraine formation between 11 850 years and 10 510 years (Heusser and Rabassa, 1987). This cooling manifests a number of fluctuations documented by morainic assemblages which indicate glacier advance on three or four occasions (Clapperton, 1990). The readvances are coincident with evidence of cooling from Antarctic cores as seen in the dust, ^{18}O and deuterium profiles (Clapperton, 1990). Between 12 ka and 10.5 ka a small oscillation towards colder conditions is evident in the Byrd record as well as other Antarctic records (Sowers and Bender, 1995).

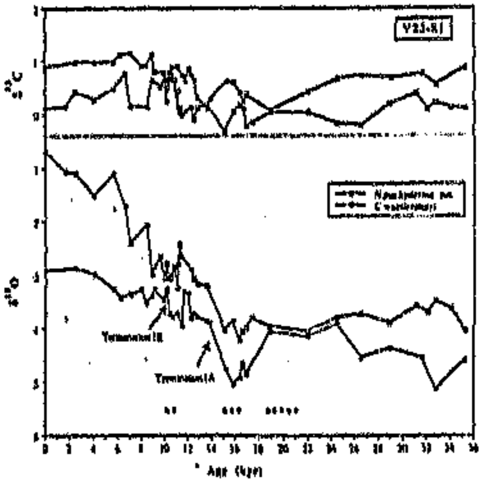

Fig. 8.4 Oxygen and carbon isotope records for the planktonic foraminifer *Neogloboquadrina pachyderma* sinistral, and the benthic foraminifer *Cibicides wuellerstorfi* from core V23-81 plotted against age. Asterisks indicate peak abundance of the polar planktonic foraminifer *Neogloboquadrina pachyderma* sinistral (Jansen and Veum, 1990).

water mass differences at time of deposition may compromise the conclusions (Jansen and Veum, 1990) and the rapid abrupt changes observed in deep water composition could mean that changes in Cd/Ca ratios and $\delta^{13}C$ values in the cores are not being accurately recorded in the sediments (Sarathein *et al.*, 1994). From the perspective of benthic $\delta^{13}C$ data, Southern Ocean mechanisms that create the depleted $\delta^{13}C$ values do not seem to affect the values of Cd/Ca; this discrepancy is not yet understood (Imbrie *et al.*, 1992).

In Antarctica, the initial temperature increase associated with Termination I began at 17 ka, (Sowers and Bender, 1995). Analysis of deuterium (δD) from the Dome B, Dome C and Vostok cores, and analysis of $\delta^{18}O$ from the Byrd core in Antarctica reveals a warming trend from 15. ka to 12 ka and from 10.8 ka to 9.5 ka, interrupted by a cooling lasting about 1 ka (Figure 8.3 and 8.5) (Jouzel *et al.*, 1995). At Byrd the first rise in $\delta^{18}O$ ice levels above the highest glacial level was at 15 ka (Sowers and Bender, 1995).

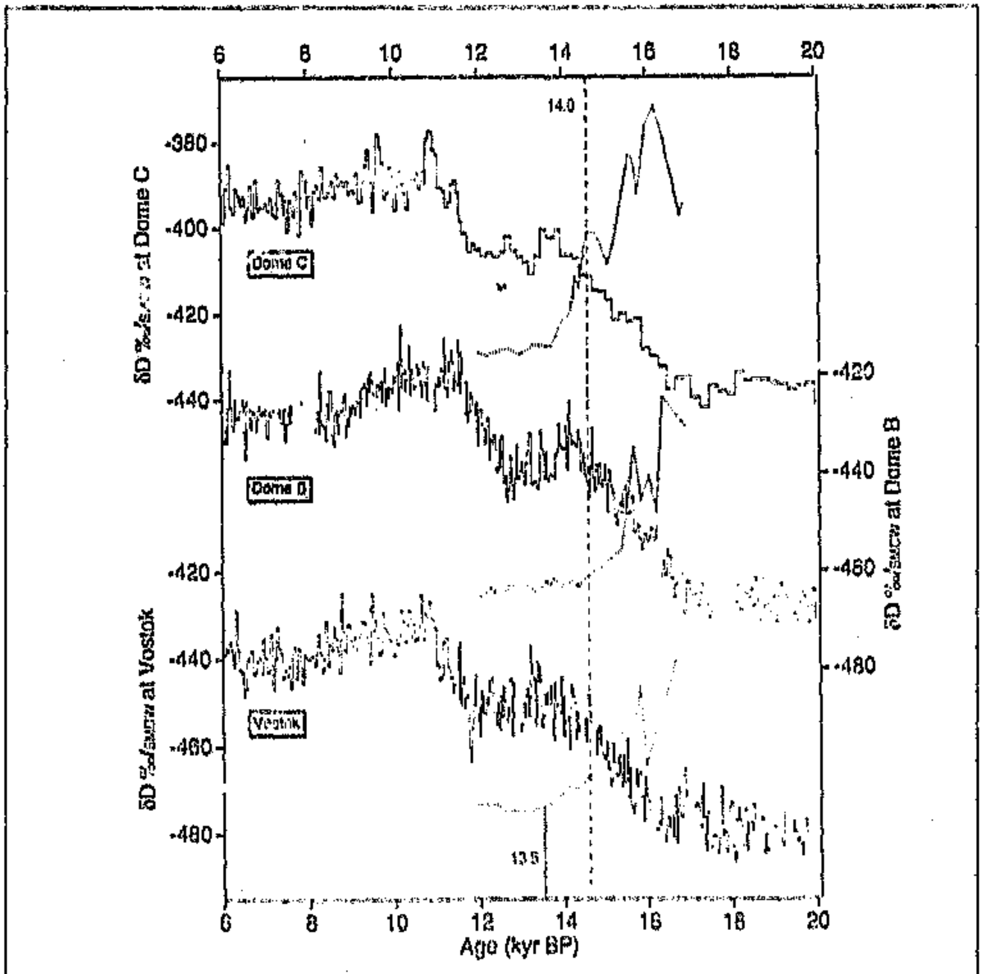

Fig. 8.3 Deuterium and dust profiles against age for Dome B, Dome C and Vostok. The dust profiles (dotted line, arbitrary scale) are given only for the deglaciation part. Ages are in Cal yrs. Note the cooling trend in all records centred on 12-11 (^{14}C) ka (13.5 - 12 Cal) (Jouzel *et al.*, 1995).

suggesting that the glacial Atlantic was vigorously ventilated may not be unequivocal, however, because of changes in the preformed nutrient content of surface water, atmosphere water CO_2 equilibrium and carbon inventory (McCave *et al.*, 1995).

Two minima in $\delta^{13}C$ values in core V23-81 occur, however, at 11.5 ka and 10 ka (Jansen and Veum, 1990), and Cd data from EN120GGC1 suggest that nutrient enriched water of southern origin characterised the ocean between 11.5 ka and 9 ka (Boyle and Keigwin, 1987). Current strengths, as inferred from particle size data, also decreased from Allerød values at the start of the Younger Dryas; these changes are coincident with the $\delta^{13}C$ decreases (McCave *et al.*, 1995).

Notwithstanding the above, it is therefore postulated that rapid changes in the thermohaline circulation did not initiate Younger Dryas cooling, nor can circulation changes account for the termination of the Last Glacial Maximum (Veum *et al.*, 1992). NADW formation did not stop during the Younger Dryas (Jansen and Veum, 1990) but LNADW may have been suppressed, as indicated by high Cd/Ca ratios and low $\delta^{13}C$ values in core EN120GGC1 even though there are some oscillations to higher $\delta^{13}C$ values (Figure 8.2) (Fairbanks, 1989; Lehman and Keigwin, 1992a).

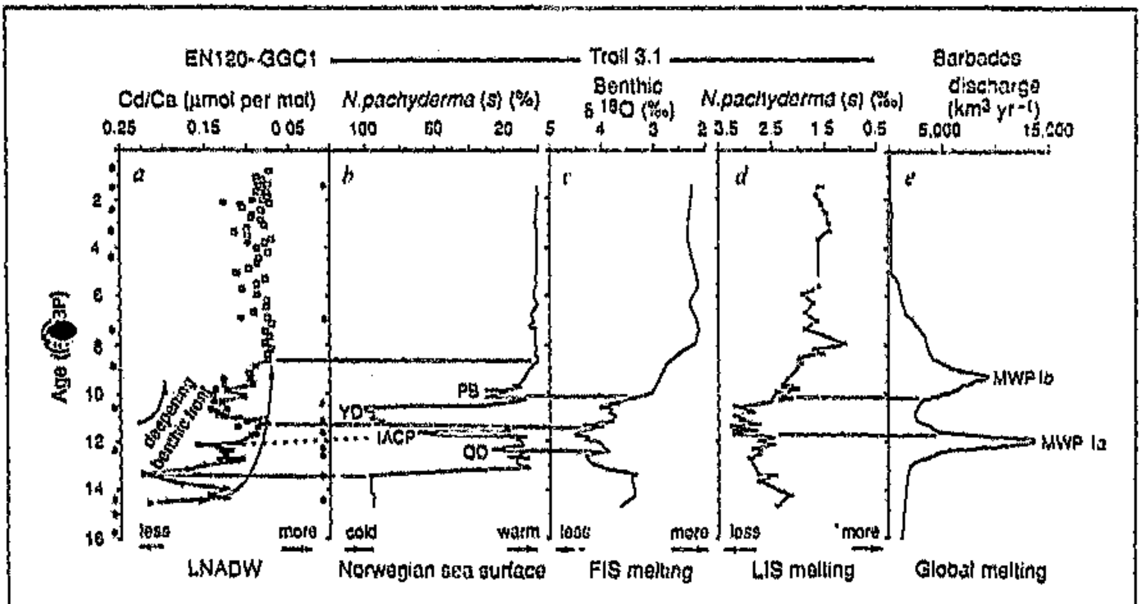

Fig. 8.2 Cd/Ca ratio (µmol per mol) in benthic foraminifera from Bermuda Rise core EN120-GGC1 a) correlated to Troll faunal results, b) showing that after 13.5 ka the flow of LNADW was restricted when the Norwegian Sea was cold. c) Benthic $\delta^{18}O$ in Troll 3.1 mainly reflects the melting history of the Fennoscandian ice-sheet. The solid lines between b) and c) shows that evidence for increased melting immediately precedes faunal evidence for cooling. d) Planktonic $\delta^{18}O$ results for Troll 3.1 reflect primarily the impact of Laurentide ice-sheet melting on the $\delta^{18}O$ of the open Atlantic; e) the record of global ice-sheet melting rate (Lehman and Keigwin, 1992a).

High $\delta^{13}C$ values are not easily reconciled with high Cd/Ca ratios, as they indicate opposite water types. This implies that imprecise dating, core depth differences, and

Younger Dryas, salt levels would have increased until the conveyor was reinitiated and warming recommenced (Broecker *et al.*, 1990).

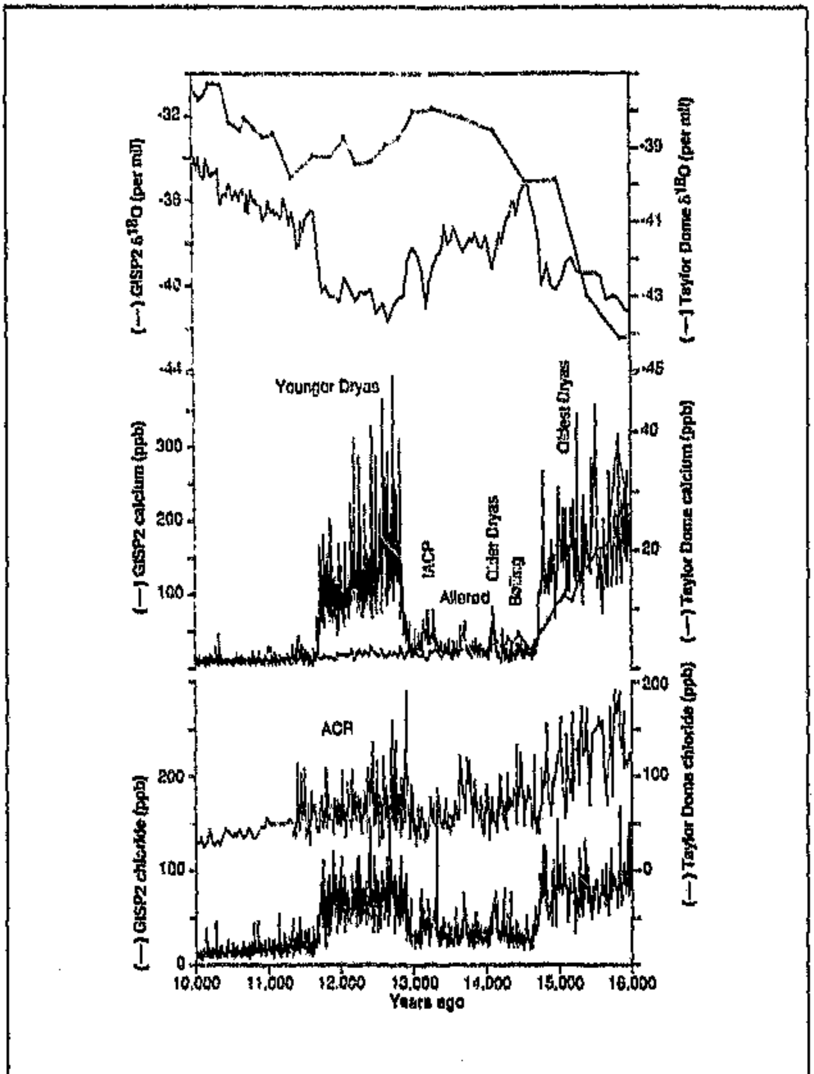

Fig. 8.1 The $\delta^{18}O$ (per mil), calcium (parts per billion) and chlorine (parts per billion) series covering the period 16 ka to 10 ka from Taylor Dome and GISP 2 (Mayewski *et al.*, 1996).

Work by Broecker (1994b) has suggested a switch to a shallower conveyor, rather than a complete breakdown of the system; this inference is supported by dramatically lowered $\delta^{14}C$ in atmospheric CO_2 during the Younger Dryas (11 -10 ka). The low atmospheric $\delta^{14}C$ is cited as evidence of increased ventilation of the ocean during this period, which is consistent with high rates of NADW formation within a shallow layer (Edwards *et al.*, 1993) and with a source region shifted to lower latitudes (Broecker, 1994b). This is substantiated by the occurrence of low $\delta^{13}C$ values at 13 ka - 12 ka and 10 ka -9 ka in the Norwegian benthic and planktonic records from core HM52-43 in the Norwegian Sea, in contrast to higher $\delta^{13}C$ values during the Younger Dryas. The conclusions

CHAPTER EIGHT

The Younger Dryas Cold Epoch and its Southern Hemisphere Counterpart

The Younger Dryas was a dramatic reversal of the general warming after the Last Glacial Maximum. Temperatures dropped to glacial values and glacial retreat was halted and often reversed. Analyses of *Globigerina bulloides* (a cool water planktonic foraminifer) during the Younger Dryas indicate that $\delta^{18}O$ values were lower than at the LGM (Bard *et al.*, 1987). The polar front moved southwards during the Younger Dryas (Lehman, and Keigwin, 1992a), before retreating to its present position. This change could have taken place in less than 400 years, although the ice core record indicates that it may have taken less than 40 years (Lehman, and Keigwin, 1992a).

The Younger Dryas is marked by an increase in *Neogloboquadrina pachyderma* (sinistral) in cores, indicating reduced inflow of warm Atlantic water (Lehman, and Keigwin, 1992a). The *Neogloboquadrina pachyderma* (sinistral) dominance also indicates SST drops of ≤ 5°C in less than 40 years, which would have resulted in marked surface air temperature reductions over Europe. Recent work in the southern hemisphere indicates that a climate reversal, although similar in length, but not coeval with the northern hemisphere cooling, occurred. Coolings were documented in South America, New Zealand, Antarctica, and the Southern Ocean; recent studies suggest that there may have been regional differences (Labracherie *et al.*, 1989; Jouzel *et al.*, 1995; Lowell *et al.*, 1995; Mayewski *et al.*, 1996). This work confirms its existence in South Africa. The cooling in Antarctica, and subsequent fluctuations, have been shown to be possibly as rapid as that documented in the Greenland cores (Figure 8.1) (Mayewski *et al.*, 1996).

No single hypotheses satisfactorily explains the enigma of the Younger Dryas, or its southern hemisphere counterpart called the Antarctic Cold Reversal (ACR) (Mayewski *et al.*, 1996). Evidence from the ice cores indicates that the changes in temperature were large and very rapid. The occurrence of a synchronous insolation maximum rules out a northern hemisphere orbital trigger. One of the first explanations involves a meltwater diversion from the Mississippi into the St Lawrence River; the onset of the Younger Dryas was associated with the resulting lowering of northern Atlantic salinity which suppressed NADW formation and heat entrainment from lower latitudes (Edwards *et al.*, 1993). This hypotheses has been questioned as recent evidence argues against such a scenario (de Vernal *et al.*, 1996).

Most modern hypotheses invoke oceanic explanations, in which oscillations in the thermohaline conveyor belt and NADW fluxes are linked to changing melt water inputs from receding ice sheets (Keigwin and Jones, 1994). During the preceding warm interval a combination of meltwater input and salt export steadily reduced the salt content of the Atlantic, culminating in a conveyor shutdown which resulted in depressed temperatures. Slight decreases in surface water salinity could have slackened deep water formation in the Norwegian sea in a few decades, affecting the thermohaline circulation and deep convection (Cortijo *et al.*, 1994). Cd/Ca analysis suggest that the NADW reduction that occurred during the Younger Dryas was similar in magnitude to the NADW reduction that occurred at 70 ka (Keigwin and Jones, 1994). During the

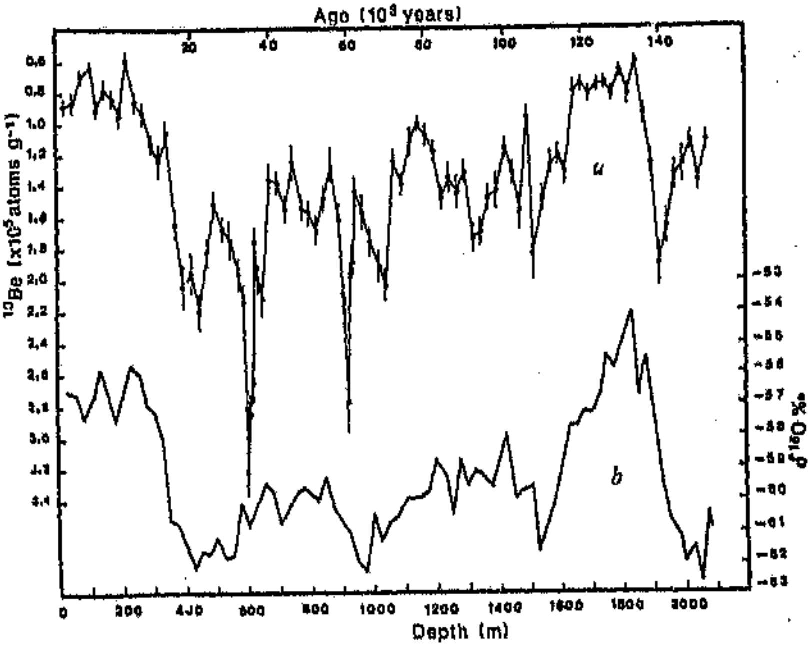

Fig. 7.15 a) The ^{10}Be concentration and b) $\delta^{18}O$ as a function of depth in Vostok ice core. Note inverted scale for ^{10}Be to facilitate comparison between the two curves (Raisbeck *et al.*, 1987).

energy balances, sea ice leads and sea ice transport, among other atmospheric interactions, shows that it is possible to initiate large scale ice sheet growth at periods of very low summer solstice solar radiation because of the dominance of the decrease in summer ablation of the ice over changes in ice accumulation (Ledley and Chu, 1995). Although it is maintained by Pichon *et al* (1992) that the qualitatively apparent southern insolation influence on Vostok air temperatures cannot be demonstrated on statistical grounds, high frequency fluctuations of SSTs and planktonic foraminifera $\delta^{18}O$ observed in southern ocean cores suggest that SSTs are influenced locally by changes in southern summer insolation which may drive part of the sea ice distribution. Investigations of the sensitivity of climate models to solar radiation changes have shown that the climatic response is always greatest during summer, as orbitally induced radiation changes are most profound at this time (Felzer *et al.*, 1995).

Good covariance exists between air temperature changes at Vostok and SSTs, as derived from radiolarian transfer functions obtained from core RC11-120 (Pichon *et al.*, 1992). The oceanic core indicates that large changes in ice accumulation rates occurred between warm and cold periods (Pichon *et al.*, 1992). The Vostok dust record was also compared to the magnetic susceptibility of the marine core RC11-120. Three well marked peaks occur in the marine core that agree with the Vostok dust record. The higher magnetic susceptibility of the marine core could be attributed to increased erosion of the ocean floor and more efficient transport of material by enhanced AABW formation. Erosion of smectite from volcanic areas such as the Kerguelen plateau by AABW could produce the higher magnetic susceptibility seen in the marine core (Figure 7.14) (Petit *et al.*, 1990).

Further evidence suggesting a strong insolation influence in southern climatic oscillations comes from an analysis of cosmogenic ^{10}Be in ice cores. The Dome C and Vostok cores contain two peaks in cosmogenic ^{10}Be, probably associated with low precipitation during glacial troughs at around 60 ka and 35 ka; each spans a period of about 2 000 years (Raisbeck *et al.*, 1987). Although controversy surrounds the two ^{10}Be spikes (Beer *et al.*, 1990; Raisbeck *et al.*, 1990), it has been argued that the two spikes could result from a significant supply of aerosols from lower latitudes (Thouveny *et al.*, 1993). The two intervals of enhanced ^{10}Be deposition, which may be interpreted as reflecting changes in solar modulation, occur when the precessional angle $\Pi=270°$, i.e. during a southern hemisphere summer insolation minimum when the earth is at aphelion (Heinrich, 1988). The precessional angle for the Younger Dryas, and the ^{10}Be peaks at 35 ka and 60 ka is $\Pi= 270°$ (Heinrich, 1988), which suggests a similarity in forcing for these three periods. Recent rainfall data from the Pretoria saltpan (Partridge, 1995) show well defined, periodic (23 ka) variations with rainfall minima that correspond with insolation peaks and troughs for the 200 ka covered by the core. Significant, well defined minima in the rainfall record occur at 35 ka and 60 ka coeval with the ^{10}Be deposition (Figure 7.15) (Raisbeck *et al.*, 1987).

It is possible that southern hemisphere climatic oscillations are strongly influenced by southern insolational variations, indicating astronomical forcing as the initial cause of the cycles (Lorius *et al.*, 1992). Rainfall oscillations in South Africa, as reconstructed from the Pretoria Saltpan data, are coherent with precessional frequencies (Figure 7.13) (Partridge, *et al.*, 1997). Spectral analysis of the Vostok core shows that temperature fluctuations are dominated by a strong 40 ka component, and to a lesser degree a 20 ka component (Jouzel *et al.*, 1987; Lorius *et al.*, 1992), and that the Vostok dust record revealed a 90% confidence level for a precessional signal suggesting orbital forcing associated with increased wind intensity and increased aridity (Petit *et al.*, 1990). Changes in total insolation at 78°S correlate with the Vostok isotope record, while November insolation at 60°S is thought to be important in controlling sea ice extent around Antarctica (Genthon *et al.*, 1987). A precessional signal may be evident in Arctic ice formation since Isotope stage 4 (Mangerud *et al.*, 1996).

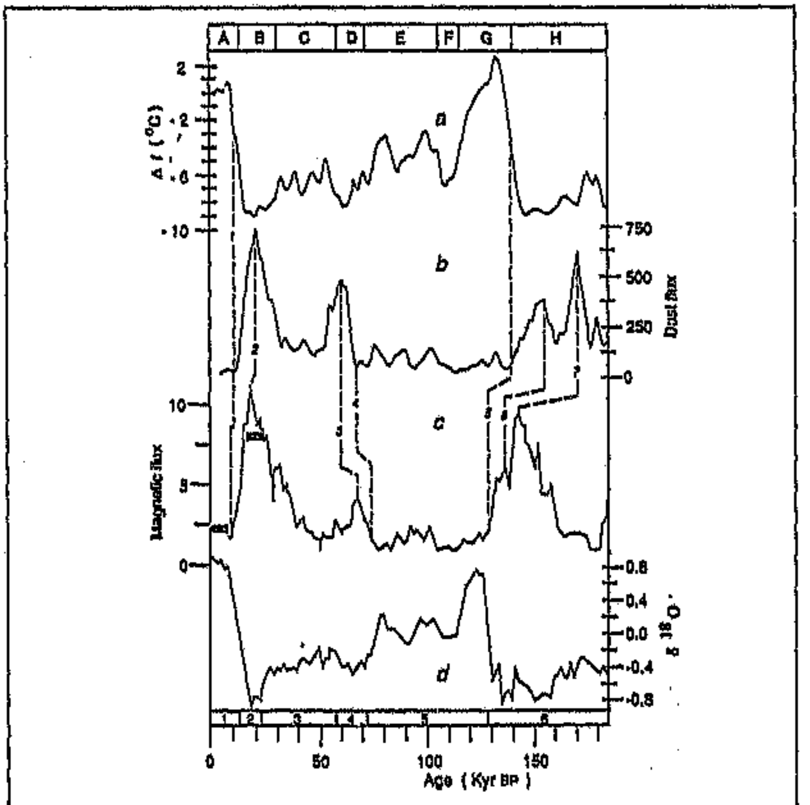

Fig. 7.14 Comparison between the Vostok and RC11-120 records over the last 180 ka and the possible correspondence through the dust events. (a) Vostok temperature as derived from stable-isotope measurements, (b) Vostok dust flux ($\times 10^{-9}$ cm a^{-1}) after smoothing by a cubic spline function, (c) RC11-120 magnetic-susceptibility 'flux' and the estimated quartz flux variation for the Holocene and the LGM (in relative units). (d) SPECMAP normalized oxygen isotope curve (Petit *et al.*, 1990).

A coupled energy balance climate-thermodynamic sea ice model that considers conduction within the ice and snow, penetration of solar radiation into the ice, surface palaeorainfall regimes were deduced. Cool, moderately humid conditions prevailed during the late Pleistocene. The early Holocene was characterised by warmer, drier conditions, but from 7.5 ka climatic conditions were similar to today, although some variation in conditions is apparent. (See: Klein, R.G., 1986: Quat. Res. 26, 153-170 and Klein, R.G, *et al.*, 1991: Quat. Res. 36, 94-119) (Scott, 1987).

The Gorrokop site comprises a succession of tufas located on the Ghaap escarpment. Dating of the tufa supplied a history of its development, and inferences about the palaeoenvironmental conditions were possible. There is, however, some debate on the conditions associated with intervals of rapid tufa growth. It is argued that rapid tufa growth occurs under mesic cycles, the waning phases of pluvial cycles, semiarid intervals or periods similar to the present. Further, ^{14}C dating of tufa is problematical due to its sponge-like structure when fresh. This makes the material susceptible to contamination by lime subsequently introduced, or by means of moisture permeating through the formation.

Notwithstanding the above caveats, 'reliable' ^{14}C ages for the Gorrokop tufas are available. These include the 3-4 m thick Tufa 4 laid down between 12 ka and 11 ka, with some addition at 8 ka and after 1 ka. Relating this evidence to that from Kathu Pan, Equus Cave and Wonderwerk Cave, a palaeoenvironmental history has been deduced. From 19 ka to 14 ka, low rainfall resulted in tufa accretion being impeded or interrupted. From 13 ka to 11 ka an acceleration of tufa formation suggests increased rainfall and rising water tables. From 10 ka, increased rainfall associated with storms masked the spring-seep contribution and resulted in net erosion of the formation.

The tendency for this site's data to often contradict the balance of evidence on the maps may indicate a problem with some of the conclusions drawn, but the analysis does support the theory that tufa accretion occurs during the waxing phase of a mesic cycle in an otherwise arid environment.

SITE 35: WONDERWERK CAVE 27°50'00"S, 23°33'00"E
Site Description: CAVE
Data Source: EQUID TEETH
Thackeray, J.F.& Lee-Thorp, J.A., 1992: Pal.3 99,141-150

Wonderwerk Cave is a large cave in the Kuruman Hills on the western edge of the Ghaap plateau and contains well preserved fauna in a continuous sequence of deposits. Mammalian microfauna were examined to reveal palaeoclimatic trends through an analysis of oxygen isotope ratios in bone phosphate. Specifically, an isotopic analysis of the $^{13}C/^{12}C$ and $^{15}N/^{14}N$ ratios in equid teeth was undertaken.

Modern equid samples were analysed to determine a frame of reference, against which fossil samples could be compared. Factors that influence the carbon isotope ratios in equid teeth include the type of grass consumed; C_4 grasses are enriched in ^{13}C, and are found mainly in summer rainfall areas, whereas C_3 grasses are depleted in ^{13}C, and are found mainly in winter rainfall areas. Variability in rainfall affects nitrogen ratios in the collagen; the teeth become enriched in ^{15}N during times of water stress. It is bones at a number of sites in the southern Cape was undertaken to determine palaeorainfall patterns. (A number of other locations, *viz.* Spoeg Rivier Shelter, Elands Bay Cave, Tortoise Cave, Sea Harvest, Elandsfontein Main, and Byneskranskop Caves 1&3 were also examined by the author. Owing to the close proximity of the sites, and the similar palaeorainfall results, only Die Kelders Cave 1, and Elands Bay Cave were used in the preparation of the climate maps). It is argued that size variations in dune molerats is a function of moisture rather than temperature. Evidence along the west coast of South Africa, where rainfall ranges from 750 mm in the south to 125 mm in the north, supports this hypothesis. Dunerat size, along with vegetation density, increases (decreases) with increasing (decreasing) precipitation receipts. The molerat inhabits sandy, near-coastal habitats in this area where temperature variations are limited to about 1°C.

As dune molerat size and rainfall are shown to be meaningfully correlated, rainfall fluctuations can be inferred from mean bone size in fossil sites. It is thus argued that conditions from 14 ka to 8 ka were moist, with a drier interval occurring between 8 ka and 4 ka. It must be noted that fossil dune molerat size is more useful in detecting moist intervals, as very dry periods are often characterised by depositional gaps in the fossil record.

Note that Elands Bay Cave has also been studied by other researchers examining mollusc shells, and charcoal. (Refer to Cohen, A.L., *et al.*, 1992: Quat. Res. 38, 379-385 and February, E.C., 1992: SAJS, 88, 291-292)

SITE 15: EQUUS CAVE 27°37'00'S, 24°37'00"E
Site Description: CAVE
Data Source: COPROLITES
Scott, L., 1989: Palaeo 3. 70,345-353, and Scott, L., 1987:Quat.Res. 28, 144-156

SITE 16: GORROKOP 28°05'00"S, 24°30'00"E
Site Description: TUFA DEPOSIT
Data Source: CALCIUM
Beaumont, P.B.&Vogel, J.C., 1993: SAJS, 89,195-198

Equus cave is located on the Ghaap Escarpment near Taung in the southern Kalahari. The escarpment is a Precambrian dolomite cuesta with a face averaging between 70 to 120 m in height. In many places it is covered by sheets or lobes of tufa originating from the evaporation of carbonate-charged spring waters during times of accelerated spring discharge or conditions no moister than the present (Klein *et al.*, 1991). Caves are located within the tufa and these contain sediments rich in fossils. Climate at the site is semi-arid, with most rainfall derived from thunderstorms during summer. Precipitation in this region varies from 100 mm to 1000 mm, with an average of 450 mm (Klein *et al.*, 1991).

The site, contains 2.5m of sediments, rich in bones and hyena coprolites. There is little pollen except for that derived from coprolites. Pollen from coprolites reflects diet as well as vegetation over the large areas frequented by hyenas. In contrast, pollen from the cave sediments reflect the local vegetation. From this, palaeotemperatures and between linear dunes. The underlying bedrock comprises Ecca shales and sandstones of the Karoo system. In the lower Molopo valley, in the southwestern Kalahari, a concentration of pans exists. Low, fluctuating ground water levels promoted the deflation of clays and sands to form lunette dunes; this process only occurs during periods of high salinity and evaporation in hot, windy climates. It is argued that phases of deflation may be associated with higher, but fluctuating groundwater levels in this area; this would keep pan surfaces free of vegetation and promote rapid salt weathering of pan surface sediments. Ground water conditions are determined by rainfall regimes, although aquifer recharge lags rainfall changes by periods of up to thousands of years for large aquifers.

SITE 10: DRIEHOEK VLEI 32°26'00"S, 19°05'00"E
Site Description: SWAMP
Data Source: CEDAR POLLEN
Meadows, M.E.&Sugden, J.M.,1990: Pal. Afr. 21,269-281; Meadows, M.E.,&
Sugden, J.M., 1991: SAJS,87,34-43

Driehoek Vlei lies in the Cedarberg Range in the south western Cape. Rainfall occurs in winter; vegetation is largely determined by underlying geology (quartzites of the Table Mountain Group). The altitude of the site is about 1 100m. There is marked local relief, with broad linear valleys separated by high ridges. In the largest of these valleys, in the headwaters of the Driehoek River, deep organic sediments are located; these have been sampled for pollen analysis. According to radiocarbon analysis of the core, (and of a companion core at Sneeuberg vlei), the cores are stratigraphically consistent, suggesting that no major hiatus or disturbance has occurred during the period of sedimentation. The base of the Driehoek Vlei core is dated to 14.6 ka. Sedimentation rates vary; 25 cm/ka for the period 14.6 ka to 3.2 ka, and 80 cm/ka from then on.

The initiation of sedimentation at 14.6 ka suggests a shift to moister conditions, possibly as a response to the general climate amelioration after the LGM. The pollen diagram derived for Driehoek suggests no major changes in the vegetation history at the site, although xeric conditions are identified at 3.2 ka.

SITE 9: DIE KELDERS CAVE 1 34°32'00"S,19°22'00"E
Site Description: MIDDENS
Data Source: MOLERAT BONES
Klein, R.G., 1991: Quat. Res. 36, 243-256

SITE 13: ELANDS BAY CAVE 32°18'00"S, 18°20'00"E
Site Description: COASTAL CAVE
Data Source: MOLERAT BONES
Klein, R.G., 1991: Quat. Res. 36, 243-256

Die Kelders Cave 1 is a large coastal cave with Middle and Late Stone Age middens rich in molerat bones and other fossils. Elands Bay Cave is a coastal cave with fossiliferous deposits spanning the interval 20 ka to 300 a. An analysis of molerat

The Elim site is a swamp near the upper reaches of the As River in the Rooiberge. Two distinct sediment units exist, situated on a north facing slope: a basal unit about 6 m thick consisting of dark coloured silts and an upper channel fill of light coloured coarse grained sediment about, 1.3 m thick. Dates from the lower sequence covers the interval from 23.4 ka to 20.4 ka. The analysis of pollens from this sequence suggest that conditions in this area were cold and dry at 18 ka, and that warming at 13 ka was accompanied by moist conditions.

SITE 8: DEELPAN 29°20'00"S,25°45'00"E
Site Description: PAN
Data Source: POLLEN
Scott, L.&Brink, J.S., 1992: SA Geographer,19,22-34

It is argued that although pans are not ideal sites for the preservation of organic material, fossils of plants and animals may be found in deposits associated with them. Most pans in South Africa are deflation features, and sediments trapped in them are often removed or recycled by wind or erosion, resulting in young strata in relation to the basin in which they occur (Scott and Brink, 1992). Pans contain pollen from a variety of plant communities in and around the pan, as well as wind born pollen from the surrounding areas. Fossils in pans also document the fauna of the wider environment, being a source of water and salt for migratory ungulates and their predators. Pans also provided a specialized local habitat for aquatic and non-migratory animals (Scott and Brink, 1992).

The pans that have the highest potential for palynological research are those containing with peaty deposits associated with local springs or high water tables. Unfortunately, fresh roots associated with spring environments can contaminate peats and prevent accurate dating. Sandy and clayey deposits may contain bones, but are usually poor in pollens (except when found in coprolites). Calcretes associated with pans lack pollen or have concentrations too low for reliable dating. Pan floor deposits do not preserve pollen if subjected to seasonal wetting and drying, but pan floors in wetter areas can be pollinferous (Scott and Brink, 1992).

Deelpan is a pan in the Orange Free State where analysis was undertaken on pollen, molluscs, ostrich shells and vertebrate remains. Results from analysis of pollen in one metre organic deposits reflect environmental changes since 4 ka. At 4 ka good grass cover existed, which was interrupted by drier conditions at about 1 ka. Further, bone assemblages contain the clawless otter, suggesting wetter conditions at this time (Scott and Brink, 1992).

SITE 22: MOLOPO PANS 27°30'00"S, 20°15'00"E
Site Description: PANS
Data Source: CALCITE DEPOSITS
Lancaster, N., 1986: Palaeecol. Afr. 17, 59-67

Pan development in the southwestern Kalahari seems to be strongly influenced by changes in groundwater conditions. The pans occur within the interdune corridors

Botswana, and the western Orange Free State. All these deposits are interpreted as having accumulated during periods of stronger anticyclonic circulation.

SITE 6: CORNELIA 28°30'00"S, 28°25'30"E
Site Description: EROSION CHANNEL
Data Source: POLLEN
Scott, L., 1989: S.Afr.J.Bot , 55,107-116

SITE 7: CRAIGROSSIE 28°31'45"S, 28°28'15"E
Site Description: RIVER BANK
Data Source: POLLEN
Scott, L., 1989: S.Afr.J.Bot., 55,107-116

SITE 14: ELIM 28°28'45"S, 28°25'00"E
Site Description: SWAMP
Data Source: POLLEN
Scott, L., 1989: S.Afr.J.Bot., 55,107-116

Clarens in the Orange Free State is located in a mountainous area in the foothills of the Drakensberg. Current rainfall is about 700 mm, occurring in summer, and severe frost occurs in winter. The topography of the area is controlled by the bedrock, which consists mostly of sandstone of the Clarens Formation, overlain by peaks of basaltic lava of the Drakensberg Group. Mudstones and sandstones of the Elliot Group underlie these formations, and these have been exposed along deep valleys into which Quaternary alluvium has been deposited.

Some caution must be exercised when using surface pollen spectra as a control for the interpretation of fossil spectra. Studies of modern vegetation dynamics in the area show that marked changes in vegetation have occurred in twenty years.

Cornelia is a swamp deposit north of Clarens near the top of a drainage line. The site is situated in a channel which is deeply incised into Pleistocene alluvial sediments. The sediments studied are part of a 3.5m terrace in this channel. Radiocarbon dates show that the organic sediments range in age between 20 ka and 12.6 ka. Unfortunately, the poor resolution of the sequence here between 17 ka and 13 ka precludes reliable deductions concerning that period.

Craigrossie is situated about 20 km west of the source of the Little Caledon River, in the foothills of the Drakensberg. Sediments contain pollen from local swamps, and potentially from flood or slack water. The upper drainage basin includes slopes above 2500 m in altitude. The pollens were obtained from an anomalously wet organic sequence of sediments belonging to a 10 m terrace on the south of the stream. The saturated sediments do not seem to be the result of reworked organic material from upstream deposits, as these are largely inorganic. The Craigrossie site can be divided into 8 sedimentary units dating from about 10 ka. It is suggested that conditions before 10 ka were wet with intermediate temperatures. After 9.5 ka, conditions warmed, but remained dry, although the author advises caution as few spectra are available.

SITE 2: BADSFONTEIN 30°50'00"S, 25°48'00"E
Site Description: HOT SPRINGS
Data Source: POLLEN
Scott. L.& Cooremans, B.,1990: SAJS, 86,154-156

Badsfontein is a warm sulphur spring located in mudstones of the Karoo sequence associated with dolerite intrusions. It is located at Venterstad in the Orange Free State, where rainfall is about 500 mm occurring in summer; frost is common in winter. As the peat has been disturbed by fire, a core was recovered about 30 m west of the spring eye, which could be divided into a sequence commencing with a base of hard green silt, overlain by yellowish clayey-silt, grey spring silts, and 130 cm of black peat. The base of the peat provided a radiocarbon age of 4.45 ka at about 112 cm depth. It is suggested that drier conditions occurred at this site from about 8 ka to 4.5 ka, which were replaced by wetter conditions in the late Holocene.

Even though Aliwal North and Badsfontein are in close proximity, it is not possible to view the two sites as one composite profile, because dating at Badsfontein is inadequate and does not provide a good link between the two profiles. The Aliwal North sequence suggests cooler and moister conditions than the oldest part of the Badsfontein section.

SITE 3: BUFFELSFONTEIN 31°23'00"S, 26°41'00"E
Site Description: SAND DEPOSIT
Data Source: LITHOLOGY
Marker, M.E.,& Holmes, P.J., 1993:J.Afr. Earth.Sci.17,479

Inland localities of red sands are uncommon outside of the Kalahari and the isolated outlier of red sand located near Buffelsfontein in the northeastern Cape is unique in the region, and is not a product of current geomorphic processes. It is at a altitude of 1 800m above the Great Escarpment, on the southern margin of an upland basin ringed by hills. The deposit forms a narrow pseudo-terrace extending 2000 m along the foot of an arcuate ridge of Elliot Formation sandstone capped by Clarens Formation sandstone. The sands extend north downslope beyond the topographic terrace for about 1000 m (Marker and Holmes, 1993). The deposit consists of two parts, the upper of which forms a topographic bench, sloping at 8° which subsequently flattens to between 4° and 5°. The northern part extends as a footslope fan at 4° which has bee modified by cultivation and erosion. The deposit topography does not mirror the underlying bedrock slope, and has a distinct topographic form of its own (Marker and Holmes, 1993). This partly lithified red sand deposit is in an incipient state of diagenesis.

In vertical section, the main deposit consists of horizontally, well-bedded sandstone with incipient joints. All beds dip at 4° parallel to the surface. Occasionally cross-bedding occurs. The deposit was dated using thermoluminescence, and is about 20.5 ka old. The physical location of this deposit precludes a fluvial origin, and it is argued that the sand is an aeolian deposit dating from the hypothermal. The sand texture suggests that it is not from the local Clarens formation, and that it is a remnant of a former more extensive aeolian deposit. The red colour suggests that the sand is similar to that found further west, similar to deposits in Namibia, the northwest Cape, two cores suggest that conditions prior to 12.5 ka at Dunedin, and 11.8 ka at Salisbury were much drier than present (possibly 50% less precipitation); this arid phase was subsequently reversed and at 8 ka moister conditions than present prevailed.

SITE 28: SWARTKOLKVLOER 30°45'00"S, 20°05'00"E
Site Description: PAN
Data Source: SHELLS
Kent, L.E.& Gribnitz, K.H., 1985: SAJS, 81, 361-370

Swartkolkvloer is a large pan (10 km by 8 km) near Brandvlei in the north west Cape. It is one of the southernmost pans of a group which occupies a large ill-defined interfluve between the Fish and Sak river system to the east, and the smaller rivers that drain directly into the Atlantic to the west. Although it is presently linked to the Fish river, the outlet is has been cut in recent times, and the pan was probably a closed system for most of its existence. The pan lies on flat-lying shales of the Ecca Series which are cut by dykes and sills of Karoo dolerite. From an analysis of surrounding topography, it is suggested that the pan is quite old. It contains many gastropod shells and reveals evidence of high water stands at 6 m, 9 m and 15 m. The shells date to about 13.7 ka and the species (*Tomichia ventricosa*) are very sensitive to moisture changes in seasonal cycles, but are adaptable to any environment from fresh water to hyper saline, as long as calcium is available.

The sequence of events suggested by this site is that conditions prior to 17 ka were cold and dry with some amelioration at 15 ka. By 13.7 ka rainfall had increased, resulting in the lake level reaching a +6 m level. Subsequently dessication was initiated in this area. Temperatures increased between 12 ka and 11 ka, although conditions remained dry.

SITE 1: ALIWAL NORTH 30°45'00"S, 26°45'00"E
Site Description: HOT SPRINGS
Data Source: POLLEN
Scott, L.& Cooremans, B.,1990: SAJS, 86,154-156

Four peat cores were recovered from hot springs near Aliwal North, these were between 10.2m and 7.5m in depth. Rich pollen spectra could only be obtained from levels below 5 m; the overlying black peaty clay and upper fibrous peat (dated at 4.3 ka) were generally barren. Pollen in the organic loams and silts were analysed; these dated from 9 ka to 12.6 ka, and revealed six stages of alternating cool, moist and warm, dry events associated with shifts in the grassland/shrubland border. The sequence suggests that before 12.6 ka, cool moist conditions prevailed, gradually becoming warmer and dry between 12 ka and 11 ka before recovering at about 9.6 ka. The period between 12 ka and 11 ka in the Aliwal North sequence is the most prominent of the dry cycles in the record, but seems to be of low intensity when compared with the lower section of Badfontein.

two cores suggest that conditions prior to 12.5 ka at Dunedin, and 11.8 ka at Salisbury were much drier than present (possibly 50% less precipitation); this arid phase was subsequently reversed and at 8 ka moister conditions than present prevailed.

SITE 28: SWARTKOLKVLOER 30°45'00"S, 20°05'00"E
Site Description: PAN
Data Source: SHELLS
Kent, L.E.& Gribnitz, K.H., 1985: SAJS, 81, 361-370

Swartkolkvloer is a large pan (10 km by 8 km) near Brandvlei in the north west Cape. It is one of the southernmost pans of a group which occupies a large ill-defined interfluve between the Fish and Sak river system to the east, and the smaller rivers that drain directly into the Atlantic to the west. Although it is presently linked to the Fish river, the outlet is has been cut in recent times, and the pan was probably a closed system for most of its existence. The pan lies on flat-lying shales of the Ecca Series which are cut by dykes and sills of Karoo dolerite. From an analysis of surrounding topography, it is suggested that the pan is quite old. It contains many gastropod shells and reveals evidence of high water stands at 6 m, 9 m and 15 m. The shells date to about 13.7 ka and the species (*Tomichia ventricosa*) are very sensitive to moisture changes in seasonal cycles, but are adaptable to any environment from fresh water to hyper saline, as long as calcium is available.

The sequence of events suggested by this site is that conditions prior to 17 ka were cold and dry with some amelioration at 15 ka. By 13.7 ka rainfall had increased, resulting in the lake level reaching a +6 m level. Subsequently dessication was initiated in this area. Temperatures increased between 12 ka and 11 ka, although conditions remained dry.

SITE 1: ALIWAL NORTH 30°45'00"S, 26°45'00"E
Site Description: HOT SPRINGS
Data Source: POLLEN
Scott, L.& Cooremans, B.,1990: SAJS, 86,154-156

Four peat cores were recovered from hot springs near Aliwal North, these were between 10.2m and 7.5m in depth. Rich pollen spectra could only be obtained from levels below 5 m; the overlying black peaty clay and upper fibrous peat (dated at 4.3 ka) were generally barren. Pollen in the organic loams and silts were analysed; these dated from 9 ka to 12.6 ka, and revealed six stages of alternating cool, moist and warm, dry events associated with shifts in the grassland/shrubland border. The sequence suggests that before 12.6 ka, cool moist conditions prevailed, gradually becoming warmer and dry between 12 ka and 11 ka before recovering at about 9.6 ka. The period between 12 ka and 11 ka in the Aliwal North sequence is the most prominent of the dry cycles in the record, but seems to be of low intensity when compared with the lower section of Badsfontein.

SITE 5: COLLINGHAM SHELTER 29°27'35"S, 29°47'45"E
Site Description: CAVE
Data Source: CHARCOAL
February, E.C., 1993: Quat. Res. 42, 100-107.

SITE 21: MHLWAZINI CAVE 29°02'52"S, 29°23'23"E
Site Description: CAVE
Data Source: CHARCOAL
February, E.C., 1993: Quat. Res. 42, 100-107.

Climatic conditions can be reconstructed from an analysis of the measurement of xylem vessel size and frequency in archaeological charcoal samples. Wood maintains its anatomical structure when burned and can be identified to genus or species level by the characteristic arrangement of different cell types. It is assumed that the charcoal assemblage in a site should reflect the woody vegetation in the vicinity of the site, and that the types of vegetation reflect the climate of the region. Further, the vessel diameter increases with increased moisture, while vessel frequency decreases.

Collingham shelter and Mhlwazini Cave are located at a height of 1 800 m in the Drakensberg foothills in Natal, and were occupied by hunter-gatherers for 1 500 years before 1 600 AD. Six assemblages of charcoal were chosen for analysis from each cave. The study revealed a wetter phase at 2.4 ka becoming drier towards 1.3 ka. A return to moist conditions occurred between 600 a and 200 a.

SITE 11: DUNEDIN 32°17'00"S, 26°40'00"E
Site Description: MARSH
Data Source: POLLEN
Meadows, M.E. & Meadows, K.F., 1988: SAJS,84,253-259

SITE 27: SALISBURY 32°16'00"S, 26°30'00"E
Site Description: MARSH
Data Source: POLLEN
Meadows, M.E.&Meadows, K.F., 1988: SAJS,84,253-259

The Winterberg escarpment is made up of a number of dolerite peaks containing vlei areas in the undulating plateau. While much of the south-eastern Cape is too arid for the accumulation of sediments, the climate of the Winterberg is cooler and wetter, allowing the development of polleniferous sediments. Most precipitation is orographic and exceeds 1000 mm.

Vleis on the farm Salisbury and Dunedin in the Winterberg mountains were cored for polleniferous sediments. A 175 cm core was recovered from the marsh at Dunedin, and a 300 cm core was recovered from Salisbury. Pollen recovered from the cores was analyzed and dated. Three main zones were identified; a grassy open community indicative of drier conditions, followed by a community dominated by sedges suggesting moister conditions. The third zone comprises elements of montane forests, but is still dominated by grass and sedge pollen. The palaeoclimates inferred from the

Appendix 1

Site Descriptions - Literature

The sites documented below are not in numerical or alphabetical order. Where possible, similar types of sites have been grouped together to facilitate more reasonable discussion. A table listing the sites in alphabetical order is attached below (Table 1).

SITE 4: CANGO CAVE 33°23'00"S, 22°13'00"E
Site Description: CAVE
Data Source: STALAGMITE
Talma, A.S. & Vogel, J.C., 1992: Quat. Res. 37, 203-212

The temperature at which calcium carbonate is precipitated can be inferred from an examination of the oxygen isotopic composition of the carbonate deposits. This is because the isotopic fractionation that occurs during precipitation is temperature dependent. Valid results can be obtained if the carbonate precipitate was in isotopic equilibrium with the water at time of deposition, and the oxygen isotopic content of the water is known. Further, no diagenic alteration of the isotope record must have occurred, and the deposit must be properly datable. Stalagmites are most likely to fulfill the above conditions. In a poorly ventilated cave, equilibrium precipitation would occur as the release of CO_2 from cave drip water would be sufficiently slow. If the stalagmite is compact and nonporous, subsequent isotopic alteration is unlikely. To determine the isotopic composition of the water at the time of deposition, an examination of confined and dated groundwater was undertaken. The stalagmite was dated using radiocarbon and ionium dating.

Cango Cave is a cave system formed in limestone in the foothills of the Swartberg mountains. The stalagmite was located 1 100 m from the opening where temperature remains constant (17.5°C) and relative humidity exceeds 95%. The temperature recorded reflects the average outside temperature, and the position of the stalagmite is such that it conforms to the conditions necessary for it to be a suitable specimen for meaningful palaeotemperature analysis. The stalagmite sampled also consisted of large, compact crystals with no evidence of resolution or diagenesis or cavities likely to contain fluid inclusion water. Unfortunately, no development occurred between 13.8 ka and 5 ka, and it is suggested that this is a result of a local, or regional hiatus in cave drip water supply. The study suggests that temperatures between 30 ka and 13.8 ka were between 4° and 7° C cooler than present, with the coldest interval between 19 ka and 17 ka. From 5 ka, temperatures varied within +1°C to -2°C of present temperatures with lower temperatures between 5 ka and 2 ka and warmer temperatures from 2 ka. No conflicting data are available to contradict the results of this study.

Holocene Altithermal, characterised by warmer, drier conditions from 8 ka to possibly 6 ka. Subsequently, moisture indexes increased from 5 ka to about 2 ka, when conditions reflect the typical wet spell situation. Although some sites reflect cooler conditions, temperature variations remained small or localised until the Mediaeval Warm Epoch and subsequent Little Ice Age cooling. The diachronism identified in the onset of wetness in the higher Southern African latitudes may well be a function of variations in the strength of the Agulhas Current. The Younger Dryas in Europe may have been initiated by the cooling in the southern hemisphere, the signal being transferred through reduced CH_4, CO_2, and increased AABW formation and decreased LNADW formation.

General agreement between the results of this study and the conceptual models developed to account for southern African climate variability exists, although some anomalies remain. Southern African moisture trends seem to be tightly coupled to SSTs, the relative strength of the westerly and easterly winds, (which may be controlled to some degree by Antarctic sea ice fluctuations) and the associated insolation forcing. Changes in southern Africa's climate are generally coeval with switches from a dominance of NADW to a dominance of AABW in the deep ocean: warmer, wet spells are associated with NADW influence, and colder, dry periods with AABW influence.

The results of this study demonstrate the pivotal role of orbital variations in controlling glacial cycles in both hemispheres through the interplay of insolation receipts, and oceanic and atmospheric responses, especially in relation to fluxes in CO_2 and CH_4. The importance of North Atlantic ocean variations modulated by Dansgaard-Oeschger cycles and Heinrich events is confirmed; however, southern hemisphere climates may be influenced to a significant degree by local insolation receipts, through the formation of sea ice, and subsequently increased AABW. This in turn may impact on global climate, and challenges the view that glacial cycles are controlled solely by northern hemisphere dynamics. The forcing behind the change from NADW to AABW control of the deep ocean cannot as yet be conclusively demonstrated; a southern hemisphere control through Antarctic sea ice fluctuations has been hypothesised, since southern African climates seem to be tightly coupled to these variations. Further, the fluxes in the formation of NADW and LNADW and the occurrence of Heinrich events may be the consequence of atmospheric or oceanic processes occurring in both hemispheres, as suggested by the $CaCO_3$, $\delta^{13}C$ and Ca/Cd fluxes in the Southern Ocean. As meltwater pulses may not necessarily control NADW fluxes, the assertion that the thermohaline circulation is stable in the absence of these pulses may require re-examination; the benign climate of the Holocene may unleash some unexpected cold periods, as did the Eemian 115 000 years ago. Global warming may yet revert to global cooling in an unexpected and unforeseen way.

Conclusion

The major trends from 20 ka to present comprise a general warming over Southern Africa which may have been initiated at about 16 ka subsequent to the global cooling phase of the LGM. The cold, dry conditions typical of the glacial climate at 17 - 18 ka were replaced by moister and increasingly warm conditions which reached a local maximum at about 13 ka to 12 ka. The Southern African proxy data is in agreement with the general global tendencies recorded by CO_2, ^{18}O, CH_4, SSTs and sea level fluctuations. An interhemispheric diachronism, whereby the southern hemisphere leads this deglacial phase by at least 1 ka, is apparent.

The period 13 ka to 12 ka is characterised by evidence suggesting opposite climatic trends. On the one hand, the terrestrial PASH proxy data suggests warm, moist summer rainfall conditions typical of a wet spell situation coincident with reduced winter rainfall. Increases in CH_4 documented over the subtropics (Sirocko *et al.*, 1996) and a warming maximum documented at Wonderkrater at 13 ka (Partridge, *et al.*, 1990) support this inference. The oceanic evidence suggests that regional lowering of SSTs only commenced at 12 ka (Labracherie *et al.*, 1989). In contrast, molluscan evidence off Kleinzee (Pether, 1994), and increased localised west coast moisture argues for the intrusions of Agulhas rings from 13.5 ka to 12.5 ka, typical of a dry spell situation. It has been suggested that reduced summer insolation would reduce the meridional temperature gradient, resulting in weaker trade winds. This would reduce the volume flux of the Agulhas Current, enhancing its tendency to round the Cape, and suppress summer Benguela upwelling, thus allowing the Algoa taxa to colonise the west coast (Pether, 1994). To reconcile the apparent inconsistencies, it is possible that Agulhas intrusions can occur during both wet and dry spell conditions.

The warming was suddenly and dramatically reversed, in agreement with the northern hemisphere Younger Dryas reversal, with a return to near glacial conditions being recorded in most records, but especially in SSTs, $\delta^{13}C$ fluxes in the oceans (suggesting a change in NADW production) and the proxy terrestrial data. Once again, a lead in warming in the Southern Hemisphere is apparent, in that the southern hemisphere cooling appears to antedate its northern hemisphere counter part by up to 1 ka. Good evidence for this is found in palaeo-SSTs and oceanic $\delta^{13}C$ fluxes; the terrestrial southern African proxy data are in agreement, but caution is necessary as dating control is insufficient to permit unambiguous conclusions. The cause of the southern hemisphere climate reversal is attributed directly to the reduced southern hemisphere insolation that occurred between 13 ka and 9 ka, and the subsequent increases in sea ice, and reductions in Southern Ocean SSTs and LNADW (caused possibly by enhanced AABW formation, coincident with meltwater pulses), reduced trades and stronger westerlies.

Subsequently, while Europe returned to the neo-glacial conditions associated with the Younger Dryas, conditions in the southern hemisphere improved, as indicated by the terrestrial proxy data, SSTs and $\delta^{13}C$ evidence. Temperatures increased until the

RAINFALL																				
NAME	20-19	19-18	18-17	17-16	16-15	15-14	14-13	13-12	12-11	11-10	10-9	9-8	8-7	7-6	6-5	5-4	4-3	3-2	2-1	1-0
ALIWAL NORTH								+	-	-	+		-	-	-	+	+	+	+	
BADSFONTEIN								+	-	-	+		-	-	-	+	+	+	+	
BUFFELSFONTEIN	=	=																		
COLLINGHAM SHELTER																			(-)	(+)
CORNELIA	(+)	-	-							+	+									
CRAIGROSSIE								+		(+)	(+)		(-)		(-)	+	+	+		
DEELPAN																	+	+	+	-
DIE KELDERS CAVE I							+	+	+	+	+	+	-	-	-	-				
DRIEHOEK VLEI							+	-	-	-		+	+	+	+	+	+	-	-	
DUNEDIN		=	=					-	-	-	-	+	+							
ELANDS BAY																	0	-	0	-
ELIM	(+)	-	-																	
EQUUS CAVE											-	-	-	+	+	-	-	-	+	+
GORROKOP	-	-	-	-	-	-	-	-	-	-	-	+	++	++	++	-	-	-	+	
HOMEB SILTS	+	-	-	-	+	+	+	+	+	-										
GUDAOB CALC-TUFA											+									
KALAHARI DUNES	=	=	=	=		(+)	(+)	(+)	(-)	-	-									
KHOMMADES	-	-	-	(+)	(+)	(+)	(+)	(+)	(+)	-	-	-	-	-	-	-	-	-	-	
LELIEHOEK SHELTER															-	+				
MHLWAZINI CAVE																			(-)	(+)
MOLOPO PANS											+							-	-	
NARABEB	-	-	-	-	-	-	+	+	+	+										
NATAB SILTS													-	-	-	-	0	0	0	
PRETORIA SALTPAN													-	+	-	+	+	+		
RIETVLEI DAM											0	+	0	+	++	+	0	0	0	
SALISBURY		=	=						-	-	-	+	+							
SWARTKOLKVLOER	-	-	-	+	+	+	+	-	-											
TATE VONDO									(+)	(+)	(+)	(-)	(-)	(-)	(-)	+	+	+	+	
WINDHOEK														++	++	+				
WONDERKRATER	+	+	+	+	+	+	+	+	+	(-)	(-)	(-)	(+)	-	-	0	0	+	(-)	0
WONDERWERK CAVE											=	-	-	-	-	0	+	+	(+)	0

Tab.2. Rainfall changes over the last 20 ka

WALVIS BAY	22°30'00"S,14°04'00"E	OFFSHORE SEDIMENTS	FORAMINIFERA	Thackeray, J.F.&Herbert, R.S., 1991: SAJS, 87,611-613
WEST PAN A	23°33'15"S,14°45'00"E	LAKE DEPOSIT	SEDIMENTS	Teller, J.T., *et al.*, 1990: Quat. Sci. Rev. 9, 343-364
WINDHOEK	22°34'00"S,17°06'00"E	SPRING DEPOSIT	POLLEN	Scott, L., *et al.*, 1991: The Holocene, 1, 8-13
WONDERKRATER	24°30'00"S,28°45'00"E	CAVE	POLLEN	Scott, L., 1989: Palaeo 3, 70,345-353
WONDERKRATER	24°30'00"S,28°45'00"E	CAVE	POLLEN	Scott, L.& Thackeray, J.F., 1987: SAJS, 83, 93-98
WONDERWERK CAVE	27°50'00"S,23°33'00"E	CAVE	EQUID TEETH	Thackeray, J.F.& Lee-Thorp, J.A., 1992: Pal.3 99,141-150

Tab. 1. Alphabetical listing of sites from the literature review

NAME	POSITION	SITE DESCRIPTION	ANALYSIS	REFERENCE
ALIWAL NORTH	30°45'00"S,26°45'00"E	HOT SPRINGS	POLLEN	Scott, L.& Cooremans, B.,1990: SAJS, 86,154-156
BADSFONTEIN	30°50'00"S,25°48'00"E	HOT SPRINGS	POLLEN	Scott, L.& Cooremans, B.,1990: SAJS, 86,154-156
BUFFELSFONTEIN	31°23'00"S,26°41'00"E	SAND DEPOSIT	LITHOLOGY	Marker, M.E.,& Holmes, P.J., 1993:J.Afr. Earth.Sci.17,479
CANGO CAVE	33°23'00"S, 22°13'00"E	CAVE	STALAGMITE	Talma, A.S. & Vogel, J.C., 1992: Quat. Res. 37, 203-212
COLLINGHAM SHELTER	29°27'35"S,29°47'45"E	CAVE	CHARCOAL	February, E.C., 1993: Quat. Res. 42, 100-107.
CORNELIA	28°30'00"S,28°25'30"E	EROSION CHANNEL	POLLEN	Scott, L., 1989: S.Afr.J.Bot., 55,107-116
CRAIGROSSIE	28°31'45"S,28°28'15"E	RIVER BANK	POLLEN	Scott, L., 1986: Palaeecol. Afr. 17, 113-122
CRAIGROSSIE	28°31'45"S,28°28'15"E	RIVER BANK	POLLEN	Scott, L., 1989: S.Afr.J.Bot., 55,107-116
DEELPAN	29°20'00"S,25°45'00"E	PAN	POLLEN	Scott, L.&Brink, J.S., 1992: SA Geographer,19,22-34
DIE KELDERS CAVE I	34°32'00"S,19°22'00"E	MIDDENS	MOLERAT BONES	Klein, R.G., 1991: Quat. Res. 36, 243-256
DRIEHOEK VLEI	32°26'00"S,19°05'00"E	SWAMP	CEDAR POLLEN	Meadows, M.E.&Sugden, J.M.,1990: Pal. Afr. 21,269-281
DRIEHOEK VLEI	32°26'00"S,19°05'00"E	SWAMP	CEDAR POLLEN	Meadows, M.E.,& Sugden, J.M., 1991: SAJS,87,34-43
DUNEDIN	32°17'00"S,26°40'00"E	MARSH	POLLEN	Meadows, M.E.&Meadows, K.F., 1988: SAJS,84,253-259
ELANDS BAY	32°18'00"S, 18°18'00"E	OPEN MIDDEN	MOLLUSC SHELL	Cohen, A.L., *et al.*, 1992: Quat. Res. 38, 379-385.
ELANDS BAY	32°18'00"S, 18°18'00"E	OPEN MIDDEN	CHARCOAL	February, E.C., 1992: SAJS, 88, 291-292
ELANDS BAY CAVE	32°19'00"S,18°20'00"E	COASTAL CAVE	MOLLUSC SHELL	Cohen, A.L., *et al.*, 1992: Qu[illegible]. Res. 38 379-385.
ELANDS BAY CAVE	32°18'00"S,18°20'00"E	COASTAL CAVE	MOLERAT BONES	Klein, R.G., 1991: Quat. Res. 36, 243-256
ELIM	28°28'45"S,28°25'00"E	SWAMP	POLLEN	Scott, L., 1989: S.Afr.J.Bot., 55,107-116
EQUUS CAVE	27°37'00'S, 24°37'00"E	CAVE	BONES	Klein, R.G, *et al.*, 1991: Quat. Res. 36, 94-119
EQUUS CAVE	27°37'00'S, 24°37'00"E	CAVE	COPROLITES	Scott, L., 1987:Quat.Res. 28, 144-156
EQUUS CAVE	27°37'00'S, 24°37'00"E	CAVE	CARNIVORE BONES	Klein, R.G., 1986: Quat. Res. 26, 153-170
EQUUS CAVE	27°37'00'S, 24°37'00"E	CAVE	COPROLITES	Scott, L., 1989: Palaeo 3, 70,345-353
GORROKOP	28°05'00"S,24°30'00"E	TUFA	CALCIUM	Beaumont, P.B.&Vogel, J.C., 1993: SAJS, 89,195-198
HOMEB SILTS	23°33'15"S,15°10'00"E	SILT DEPOSITS	CALCIUM DEPOSITS	Vogel, J.C., 1989: Palaeo 3, 70, 355-366
HUDAOB CALC-TUFA	23°35'00"S,15°30'00"E	TUFA	CALCIUM DEPOSITS	Vogel, J.C., 1989: Palaeo 3, 70, 355-366
KALAHARI DUNES	28°S TO 16°30'S	FIXED DUNES	DUNE ALIGNMENTS	Lancaster, N., 1981: Palaeo 3, 33, 327-346
KHOMMABES	23°30'00"S,15°02'00"E	LAKE DEPOSIT	SEDIMENTS	Teller, J.T., *et al.*, 1990: Quat. Sci. Rev. 9, 343-364
LELIEHOEK SHELTER	29°10'00"S,27°27'00"E	SANDSTONE CAVE	CHARCOAL/MICRO	Esterhuysen, A.B., 1992: Palaeecol.Afr.23, 193-201
MHLWAZINI CAVE	2[illegible] 02'52"S,29°23'23"E	CAVE	CHARCOAL	February, E.C., 1993: Quat. Res. 42, 100-107.
MOLOPO PANS	27°30'00"S,20°15'00"E	PANS	CALCIUM DEPOSITS	Lancaster, N., 1986: Palaeecol. Afr. 17, 59-67
NARABEB	23°49'24"S,14°55'00"E	LAKE DEPOSIT	SEDIMENTS	Teller, J.T., *et al.*, 1990: Quat. Sci. Rev. 9, 343-364
NARABEB	23°49'24"S,14°55'00"E	LACUSTRINE MUDS	CALCIUM DEPOSITS	Teller, J.T.&Lancaster, N., 1986: Palaeo 3, 56,177-195
NATAB SILTS	23°33'15"S,15°10'00"E	SILT DEPOSITS	CALCIUM DEPOSITS	Vogel, J.C., 1989: Palaeo 3, 70, 355-366
PRETORIA SALTPAN	25°34'30"S,28°04'59"E	CRATER LAKE	POLLEN	Partridge, T.C., *et al.*, 1993: Palaeo 3,,101, 317-[illegible]37
RIETVLEI DAM	25°45'00"S,28°20'00"E	SPRING	POLLEN	Scott, L., 1989: Palaeo 3, 70,345-353
SALISBURY	32°16'00"S,26°30'00"E	MARSH	POLLEN	Meadows, M.E.&Meadows, K.F., 1988: SAJS,84,253-259
SWARTKOLKVLOER	30°45'00"S,20°05'00"E	PAN	SHELLS	Kent, L.E.& Gribnitz, K.H., 1985: SAJS, 81, 361-370
TATE VONDO	22°53'45"S,30°19'36"E	SPRING	POLLEN	Scott, L., 1989: Palaeo 3, 70,345-353
TATE VONDO	22°53'45"S,30°19'36"E	MARSH	POLLEN	Scott, L., 1987: Rev. Palbot/Palynology,53, 1-10
UITENHAGE	33°40'00"S,25°28'00"E	ARTESIAN AQUIFER	INERT GASES	Heaton, T.H.E., *et al.*, 1986: Quat. Res. 25, 79-88

Tab. 1. Alphabetical listing of sites from the literature review

This site is a peat deposit near Tate Vondo in Venda which lies at a height of 1 100 m in a high rainfall area. Average temperatures exceed 25° C and the area is virtually frost free. The large peat deposit, covering an area of 30 000 m^2, is located in a swamp fed by a spring which drains to a river. A peat profile of 2.1 m was examined for pollen. The base of the boring is dated to about 12 ka, and three time zones were identified; a grassland with fynbos elements interspersed with forests in mountain ravines comprise the oldest from 12 ka -10 ka; the second is indicative of a dry savanna environment with reduced forest and fynbos dating from 10 ka - 6.5 ka, while the third is made up of swamps and woodland elements suggesting moister conditions from 6.5 ka to present. The general conclusions are in accordance with other Transvaal sites, such as Wonderkrater, Rietvlei and Moreletta River.

SITE 12: ELANDS BAY CAVE 32°18'00"S,18°20'00"E
Site Description: COASTAL CAVE
Data Source: MOLLUSC SHELL
Cohen, A.L., *et al.*,1992: Quat. Res. 38, 379-385.

An analysis of marine mollusc shells from coastal middens on the west coast was undertaken to determine the thermal history of the southern Benguela region. The middens are located in and near Elands Bay Cave. Two techniques to determine paleaotemperatures were used: oxygen isotopes and aragonite-calcite ratios. The ambient seawater isotope composition and the sea temperature during shell accretion will determine the oxygen isotope composition of skeletal carbonates. The aragonite-calcite ratio is temperature dependent, as the percentage of aragonite is directly proportional to temperature. In the limpet species *Patella granularis*, discrete aragonite and calcite layers are easily identified and can be measured.

Three discrete periods of isotope enrichment in the shells were recognised covering the periods 11 ka to 10 ka, 3 ka to 2 ka and the Little Ice Age. The arogonite/calcite ratios suggest a drop in temperature of between 1°C and 2°C at the site during the cooler periods. A hiatus in the midden covers the period from 7.9 ka and 4.3 ka.

dunes were formed under a circulation pattern similar to that of the modern July pattern further south. It is suggested that the year-round circulation was similar to the present winter circulation.

The southern dunes were formed as the result of the interaction of the South Atlantic anticyclone, which may have been stronger, and South African anticyclone. A modern analogue would be the present October circulation pattern, a circulation pattern common during modern drought years, when the relative strengths of the two anticyclones are equal.

These conditions, resulting in expanded aridity over southern Africa, have probably occurred repetitively during the Quaternary. Wetter periods when the dunes became fixed by vegetation, and eroded by runoff, intervened. It is maintained that the dune patterns visible today represent the most recent arid episodes. Dating dunes is difficult, but three periods of dune formation can be identified. The oldest, associated with the Group A northern dunes, probably predates 30 ka, and may have been as early as 38 ka. The second period associated with southern dune and north-eastern Botswana dune activity, postdates a major fluvial and lacustrine period in the northern Kalahari. Conditions from 20 ka to 16 ka were dry, followed by a cool, humid phase between 15 ka and 12 ka. Although conditions in the northern Kalahari may have ameliorated at 12 ka, the southern Kalahari became arid and windy and the inner dunes of the pans were probably formed at this time, associated with falling water tables (Lancaster, 1986). The southern dunes were probably reformed at this time, a process which continued into the early Holocene.

SITE 20: LELIEHOEK SHELTER 29°10'00"S, 27°27'00"E
Site Description: SANDSTONE CAVE
Data Source: CHARCOAL/MICROMAMMALS
Esterhuysen, A.B., 1992: Palaecol.Afr.23, 193-201

Leliehoek Shelter is located at a height of 1 640 m in the montane belt, formed in the cave sandstone of the Clarens formation near Ladybrand. A mountain stream flowed through the back of the shelter. It was occupied, as many stone tools, bone and ostrich shells are present. Once leached to remove contaminating resin, the ostrich shells were dated and the charcoal and micro-fauna were analysed to reveal palaeoclimatic trends. It is suggested that at about 4.5 ka increased rainfall enhanced the flow of the stream with an attendant change in vegetation. Results tend to concur with those for neighboring areas, and suggest mesic conditions during the Holocene with dense vegetation capable of supporting humans, while much of the interior of South Africa was uninhabited.

SITE 29: TATE VONDO 22°53'45"S, 30°19'36"E
Site Description: MARSH
Data Source: POLLEN
Scott, L., 1987: Rev. Palbot/Palynology,53, 1-10, and Scott, L., 1989: Palaeo 3. 70,345-353

SITE 31 KALAHARI DUNES 28°S TO 16°30'S
Site Description: FIXED DUNES
Data Source: DUNE ALIGNMENTS
Lancaster, N., 1981: Palaeo 3. 33, 327-346

The Kalahari sands cover a large part of the southern African interior, extending from 16°30' S to 28°S. Through the years they have been formed into an extensive system of fixed, parallel, linear dunes, with local areas of transverse dunes. As the pattern of dune alignments at a regional scale reflects the regional pattern of sand-moving winds, the alignment and morphologies of the dunes may be used to infer palaeowind directions, and palaeomoisture indices associated with the palaeocirculation patterns may also be deduced. This is based on the assumption that linear dunes extend parallel to the dominant wind direction. Active continental sand dunes occur in areas with less than 100 mm rain per annum, where sand conditions permit. Vegetated dunes indicate that the former arid environments have been replaced by wetter climates, as vegetation takes hold once rainfall exceeds 150 mm. The Kalahari dunes form a large semicircular arc with a radius of 1000 km, corresponding approximately to the pattern of winds around the South African anticyclone. Two distinct subsystems exist, separated by the Ghanzi ridge and the central Kalahari watershed (Figure A1)(pg340 fig9).

The northern dunes, comprising two groups, A and B are aligned E-W to ENE-WSW. The group A dunes are remarkably straight, and continuous up to 200 km in some cases. The dunes are extensively degraded, and are covered in open tree savanna or savanna woodland associated with precipitation ranging from 600 mm to 800 mm. The dunes are comparable to the linear dunes of the Namib sand sea in size and spacing and were formed by easterly winds. The group B dunes consist of low sand ridges aligned ENE-WSW, commonly 50 km long and are covered by open tree savanna under a rainfall of 500 - 600 mm.

The southern dunes are located in area extending from the highlands of Namibia to the Orange river at Upington and cover a belt between 100 km and 200 km in width. The dunes comprise parallel linear ridges with NW or NNW to SE or SSE alignments. The dunes are covered in vegetation comprising grasses, scattered trees and shrubs. The dunes resemble those in the Simpson Desert of Australia, which is marginally arid with rainfall between 150 mm and 200 mm.

The extent of the dunes described above indicates that the 100 mm isohyet must have been located 1 000 - 1 200 km northeast of its present position in order for the northern dunes to have formed. The southern dunes would have needed a 250 - 300 km shift of the 100 mm isohyet. This suggests that considerable change in the atmospheric circulation took place, including an expansion of aridity and latitudinal displacements of circulation patterns.

The northern dunes, comprising group A, were probably deposited under a regime of southeasterly winds that penetrated further into the subcontinent that at present. This implies a stronger anticyclone with a greater circulation radius. A modern analogue is when the South African anticyclone occasionally assumes a more southerly, continental position; this may have occurred more frequently in the past. The group B subsequently from 7 ka to 2 ka, conditions were wet and relatively warm. The previous period may have been dry.

SITE 23: NARABEB 23°49'24"S, 14°55'00"E
Site Description: LAKE DEPOSIT
Data Source: SEDIMENTS
Teller, J.T., *et al.*, 1990: Quat. Sci. Rev. 9, 343-364

SITE 19: KHOMMABES 23°30'00"S, 15°02'00"E
Site Description: LAKE DEPOSIT
Data Source: SEDIMENTS
Teller, J.T., *et al.*, 1990: Quat. Sci. Rev. 9, 343-364

SITE 32: WEST PAN A 23°33'15"S, 14°45'00"E
Site Description: LAKE DEPOSIT
Data Source: SEDIMENTS
Teller, J.T., *et al.*, 1990: Quat. Sci. Rev. 9, 343-364

Narabeb, West Pan A, and Khommabes refer to eleven sites in the Namib sand sea. These sites containing calcareous lacustrine sediment located in the interdune areas were studied. Samples were analysed for minerology, grain size, water-soluble content, and acid-soluble content. Calcified reed casts, gastropods, diatoms and ostrocods are present in some places, which were analysed for $\delta^{13}C$ and $\delta^{18}O$. Dating of the sites was achieved through an analysis of the carbonate in the playas, and although there is some uncertainty as to the accuracy of the dates, it is maintained that they do reflect the age of sedimentation at the playa sites.

The beds are typically less than a metre thick, and comprise calcareous sandstones, mudstones and sandy limestones. At the Narabeb site, six calcareous mudstones represent six long periods of ponding, allowing precipitation of calcite along with the clastic muds. It is maintained that the deposits are indicative of increased moisture in this hyper-arid environment. The intervening thick sands represent aeolian deposition during dry phases. The water responsible for the deposits may be the result of ponding at the end of the Tsondab river, flooding by the Kuiseb river, ground water seepage or increased rainfall. There is no evidence of major increases in rainfall in the area, but small increases in the headwaters of the rivers may recharge aquifers, cause flooding or extend the end points of some rivers further west.

The sequence of moisture fluxes in this area suggests that the period between 14 ka and 10 ka may have been wetter than today (Teller *et al.*, 1990), although it is generally held that wet conditions ceased at about 11 ka (Teller and Lancaster, 1986). It is maintained that the terminus of the Tsondab River retreated from Narabeb by 14 ka, and maintained its present position soon after 13 ka.

The Natab Silts are a number of fluvial units occurring at various locations between Gobabeb and Homeb along the Kuiseb River in the Namib Desert. Some of the silts indicate valley filling of up to 10 m above the present river bed, representing a stage that post-dates the removal of the Homeb silt accumulation from the river channel. They are overlain by a thin layer of pebbles (the Gobabeb gravels), which suggest increased flood energies prior to the re-excavation of the silts to their present levels. Analysis of any dateable material was undertaken, as well as interpretation of sedimentological and pedological features to determine palaeoenvironmental conditions. The silts suggest that a dry spell from 8.3 ka to 4.2 ka occurred after which run-off increased producing the Gobabeb gravels. (Other sites in close proximity to the Natab Silts, which have longer records, were included in the Natab Silts data set).

Great Hudaob is located 55 km upstream from Gobabeb on the Kuiseb river. It is a tufa deposit formed from seepage draining out of a side gully. Its formation documents local changes in moisture availability, which peaked at 34 ka to 30 ka and later at 9.8 ka.

Evidence at the coast at Conception Bay and at Meob Bay, where remnants of a flat elevated surface capped by an extensive calcareous crust exist, provide evidence of elevated groundwater and vlei conditions. A drop in the water table associated with regional dessication occurred between 12 ka and 10 ka, resulting in calcification of the surface. The calcified crusts give dates of between 10.7 and 11.9 ka.

SITE 25: PRETORIA SALTPAN 25°34'30"S, 28°04'59"E
Site Description: CRATER LAKE
Data Source: POLLEN
Partridge, T.C., *et al.*,1993: Palaeo 3.,101, 317-337

The Pretoria Salt Pan is a circular crater 1130 m in diameter near Pretoria. The maximum rim elevation above the crater floor is 119 m and its height above the surrounding plain averages no more than 60 m. Presently, largely owing to excavations, the crater floor is slightly below the level of the local water table, and a shallow (3 m) lake covers the base. Before exploitation of the soda brines, a shallow seasonal pool occupied the crater. The crater has an infilling of 90 m of fine lacustrine sediments, resting on 61 m of coarse clastic debris. The sequence covers about 200 ka and a high-resolution palaeoenvironmental record has been reconstructed for the site through pollen and sediment analyses.

The presence of an unbroken, raised rim around the crater, and its occurrence within a uniform granite lithology have ensured that the crater has functioned as a closed system, from a surface hydrological viewpoint, containing a homogeneous source of clastic sediment. Unfortunately, no pollen is preserved between 70 and 34 m, and again between 12 and 6.5m; thus no reconstructions of vegetation at these times is possible, although the authors intend studying the phytoliths in the core, which may shed some light on grass cover at these times. Thus fluctuations in the principal constituents of the lacustrine sequence are a function climatic changes, and record local aridity indexes. From 8 ka to 7 ka, conditions were dry and moderately warm,

SITE 24: NATAB SILTS 23°33'15"S, 15°10'00"E
Site Description: SILT DEPOSITS
Data Source: CALC DEPOSITS
Vogel, J.C., 1989: Palaeo 3. 70, 355-366

SITE 17: HOMEB SILTS 23°33'15"S, 15°10'00"E
Site Description: SILT DEPOSITS
Data Source: CALC DEPOSITS
Vogel, J.C., 1989: Palaeo 3. 70, 355-366

SITE 18: HUDAOB CALC-TUFA 23°35'00"S, 15°30'00"E
Site Description: TUFA DEPOSIT
Data Source: CALC DEPOSITS
Vogel, J.C., 1989: Palaeo 3. 70, 355-366

The Namib Desert is a hyper-arid coastal desert along the west coast of Namibia covering a distance of about 2 000 km from north of the Orange River (31°S) to beyond Moçamedes in Angola (14°S). The desert is quite narrow in lateral extent, about 100 km at its widest, and experiences advection fog, which provides about 32 mm of precipitation annually near coastal sites, but this decreases to zero at the base of the escarpment. A number of dry river beds traverse the desert, which occasionally carry floodwater to the sea. Most of the water carried sinks into the sandy riverbeds as the rivers tend to drop their loads along specific stretches of the river beds; this corresponds to the average reach of the floods. Small changes in flood intensity caused by changes in precipitation lead to a redistribution of sediment along the river course and relicts of these fluvial sediments document such changes accurately. Past environmental conditions are especially well preserved in the Namib Desert because of the extreme aridity of this area. Fluvial silt deposits show virtually no secondary alteration by weathering, and dead trees hardly decay over centuries.

Reliable dates were obtained from plant material, but often less reliable sample material had to be dated such as calcified crusts or calcretes. Here caution is necessary in the interpretation as calcium carbonate may have an initial apparent age of 2 ka, and all ages related to calcium carbonate may have errors of about 500 a, even after a correction of 1 ka has been made. Secondly, host material may be contaminated by lime of much older age.

The Homeb silts comprise a number of remnants of fine-grained silts and are located in embayments of the Kuiseb river between Homeb and Gomkaeb. They are horizontally bedded deposits interdigitated with small aeolian sand lenses, and some levels contain desiccation cracks and calcified crusts. Formation of these silts took place under a regime of low energy deposition over a long period. At Homeb, the silts are 37 m above the present river bed. Radiocarbon dates were obtained from calcified crusts, snails, and interbedded plant material, suggesting that the sediments accumulated between 23 ka and 19 ka. This has been interpreted as representing ephemeral flooding, or ponding during this interval (Teller *et al.*, 1990) with reduced competence of the Kuiseb River resulting in the silt load being deposited at this location (Vogel, 1989).

of the spring area, it became more accessible, or was in greater demand, especially when conditions became regionally drier.

SITE 30: UITENHAGE 33°40'00"S, 25°28'00'E
Site Description: ARTESIAN AQUIFER
Data Source: INERT GASES
Heaton, T.H.E., *et al.*, 1986: Quat. Res. 25, 79-88

The temperature at which water entered the ground may be determined through the measurement of inert gases such as N_2 or Ar in groundwater, and thus palaeotemperatures may be determined if the water can be dated. Water in contact with the atmosphere has concentrations of gases dissolved in it related to solubility, a function of temperature, and partial pressure in the atmosphere. Below the water table the groundwater is isolated from the atmosphere, and gas concentrations will remain constant until sampled. The calculated recharge temperature represents the earth temperature at the base of the unsaturated zone, i.e. the point at which the ground water was last in contact with the atmosphere. At this depth, (few tens of metres) the seasonal temperature fluctuations are completely damped and the temperatures reflect the mean annual temperature, regardless of season of rainfall. Temperatures of the earth a few metres below the surface are typically 1° - 2°C warmer than the air temperature.

N_2 and Ar dissolved in groundwater from an artesian aquifer near Uitenhage in the eastern Cape were analysed and reliable palaeotemperatures for the region were obtained. The geology of the area comprises fractured Ordovician quartzites which outcrop on high ground, but are overlain and confined to the east by impermeable Jurassic-Cretaceous shales and sandstones. The quartzites contain low salinity groundwater which was sampled from deep boreholes in the confined artesian section of the aquifer. The aquifer is recharged at the quartzite outcrop area, and the water flows slowly through the artesian section reaching ages of up to 28 ka at the coast. Contamination of the water by N_2 derived from denitrification, or radiogenically derived Ar by ^{40}K in the aquifer rocks, is low enough to be considered unimportant. The results of this analysis suggest that between 28 ka and 15 ka, recharge temperature was about 14°C, while temperatures between 9 ka and 300 a were about 19.5°C.

suggested that C_4 grasses predominated during the Holocene at this location, indicating increased moisture during this period.

SITE 26: RIETVLEI DAM 25°45'00"S, 28°20'00"E
Site Description: SPRING
Data Source: POLLEN
Scott, L., 1989: Palaeo 3. 70,345-353

SITE 34: WONDERKRATER 24°30'00"S, 28°45'00"E
Site Description: CAVE
Data Source: POLLEN
Scott, L. & Thackeray, J.F., 1987: SAJS, 83, 93-98, and Scott, L., 1989: Palaeo 3. 70,345-353.

Pollens from the Rietvlei Dam spring site were analysed to determine palaeoenvironmental conditions. It is located in grassland adjacent to the Bushveld Basin. Springs may be contaminated by younger roots. Wonderkrater is a thermal spring near Naboomspruit containing a long, particularly well preserved sequence of pollen samples dating back to 35 ka. Ten zones were identified, supplying a detailed temporal record of palaeoclimates in terms of both temperature, and moisture. Mesic conditions are inferred from Rietvlei Dam and Wonderkrater at the end of the Pleistocene (11 ka??). Dry conditions occurred at 8 ka while temperatures continued to rise. Wetter climates returned after maximum temperatures were reached at about 6,5 ka.

SITE 33: WINDHOEK 22°34'00"S, 17°06'00"E
Site Description: SPRING DEPOSIT
Data Source: POLLEN
Scott, L., *et al.*, 1991: The Holocene, 1, 8-13

The town of Windhoek is located in the Khomas Hochland at 1700 m, and receives about 365 mm of rainfall. Before the development of the town, a deep circulating hot groundwater spring supplied water from a north-south running fault to a swamp with lush vegetation, in contrast to the dry Hochland savanna in the surrounding hills. During recent excavations, a number of spring deposits comprising 40 cm of light grey sand, overlain by 140 cm of dark grey spring silts, 120 cm of grey diatomaceous material, including 35 cm of black and dark grey silts, were unearthed.

The age of the present hot spring water is about 20 ka, as determined by carbon in the water. Aquatics living in the water would thus reveal similar apparent ages, complicating the dating of the sediments. However, the ^{13}C content of the dated material is not derived from aquatics, and the dates are considered reliable. Analysis of the pollens derived from the sediments reveals the following succession of events. The base of the sediments are dated to about 7 ka and the pollens suggest waterlogged conditions until 6 ka. Between 6 ka and 5.5 ka, drying is evident. Disturbance by grazers and their hunters is evident at the site, suggesting that owing to partial drying

Berger, A., Imbrie, J., Hays, J., Kukla, G. and Saltzman, B., eds., 1984: *Milankovitch and Climate*, D. Reidel, Dordrecht.

Berger, A., Tricot, C., Gallée, H. and Loutre, M.F., 1993: Water vapour, CO_2 and insolation over the last glacial-interglacial cycles, *Philosophical Transactions of the Royal Society of London*, Vol. 341, 253 - 261.

Berger, W.H. and Labeyrie, L.D., 1987, eds., Abrupt Climatic Change, D. Reidel, Dordrecht.

Blanchon, P. and Shaw, J., 1995: Reef drowning during the last deglaciation: Evidence for catastrophic sea-level rise and ice-sheet collase, *Geology*, Vol. 23, 4 -8.

Bond, G. and Lotti, R., 1995: Iceberg discharges into the North Atlantic on millennial time scales during the last glaciation, *Science*, Vol. 267, 1005 - 1009.

Bond, G., Broecker, W., Johnson, S., McManus, J., Labeyrie, L., Jouzel, J. and Bonani, G., 1993: Correlations between climate records from North Atlantic sediments and Greenland ice, *Nature*, Vol. 365, 143 - 147.

Bond, G., Heinrich, H., Broecker, W., Labeyrie, L., McManus, J., Andrews, J., Huon, S., Jantschik, R., Clasen, S., Simet, C., Tedesco, K., Klas, M., Bonani, G. and Ivy, S., 1992: Evidence for massive discharges of icebergs into the North Atlantic during the last glacial period, *Nature*, Vol. 360, 245 - 249.

Boulton, G.S., 1993: Two cores are better than one, *Nature*, Vol. 366, 507 - 508.

Boyle, E. and Weaver, A., 1994: Conveying past climate, *Nature*, Vol. 372, 41 - 43.

Boyle, E.A. and Keigwin, L., 1987: North Atlantic thermohaline circulation during the past 20 000 years linked to high-latitude surface temperature, *Nature*, Vol. 330, 35 - 40.

Boyle, E.A., 1990: Quaternary deepwater palaeoceanography, *Science*, Vol. 249, 863 - 870.

Broecker W.S., Bond, G., Klas, M., Bonani, G. and Wolfli, W., 1990: A salt oscillator in the glacial Atlantic? 1. The concept, *Paleoceanography*, Vol. 5, 469 - 477.

Broecker, W.S. and Denton G.H., 1989: The role of ocean-atmosphere reorganisations in glacial cycles, *Geochima et Cosmochimica Acta*, Vol. 53, 2465 - 2501.

Broecker, W.S., 1987: Unpleasant surprises in the greenhouse?, *Nature*, Vol. 328, 123 - 126.

Broecker, W.S., 1994a: An unstable superconveyor, *Nature*, Vol. 367, 414 - 415.

Broecker, W.S., 1994b: Massive iceberg discharges as triggers for global climate change, *Nature*, Vol. 372, 421 - 424.

References

Alley, R.B. and MacAyeal, D.R., 1994: Ice-rafted debris associated with binge/purge oscillations of the Laurentide ice-sheet, *Paleoceanography*, Vol. 9, 503 - 511.

Alley, R.B., Meese, D.A., Shuman, C.A., Gow, A.J., Taylor, K.C., Grootes, P.M., White, J.W.C., Ram, M., Waddington, E.D., Mayewski, P.A. and Zielinski, G.A., 1993: Abrupt increase in Greenland snow accumulation at the end of the Younger Dryas event, *Nature*, Vol. 362, 527 - 529.

Andrews, J.T., Erlenkeuser, H., Tedesco, K., Aksu, A.E. and Jull, A.J.T., 1994: Late Quaternary (stage 2 and 3) meltwater and Heinrich events, northwest I dor Sea, *Quaternary Research*, Vol.41, 26 -34.

Appenzeller, T., 1993: Ancient climate coolings are on thin ice, *Science*, Vol. 362, 124 - 125.

Archer, D. and Maier-Reimer, E., 1994: Effect of deep-sea sedimentary calcite preservation on atmospheric CO_2 concentration, *Nature*, Vol. 367, 260 -263.

Avery, D.M., 1993: Last Interglacial and Holocene altithermal environments in South Africa and Namibia: Micromamalian evidence, *Palaeogeography, Palaeoclimatology, Palaeoecology*, Vol. 101, 221-228.

Bard, E., Hamelin, B., Arnold, M., Montaggioni, L., Cabioch, G., Faure, G. and Rougerie, F., 1996: Deglacial sea-level record from Tahiti corals and the timing of global meltwater discharge, *Nature*, Vol. 382, 241 - 244.

Barnola, J-M., Pimienta, P., Raynaud, D. and Korotkevich, Y.S., 1991: CO_2-climate relationship as deduced from the Vostok ice core: a re-examination based on new measurements and on a re-evaluation of the air dating, *Tellus*, Vol. 43B, 83 - 90.

Barnola, J.M., Raynaud, D., Korotkevich, Y.S. and Lorius, C., 1987: Vostok ice core provides 160 000 year record of atmospheric CO_2, *Nature*, Vol. 329, 408 - 414.

Beaumont, P.B. and Vogel, J.C., 1993: What turned the young tufas on at Gorrokop?, *South African Journal of Science*, Vol. 89, 196 - 204.

Bender, M., Sowers, T., Dickson, M-L., Orchardo, J., Grootes, P., Mayewski, P.A. and Meese, D.A., 1994: Climate correlations between Greenland and Antarctica during the past 100 000 years, *Nature*, Vol.372, 663 - 666.

Berger, W.H and Vincent, W., 1986: Sporadic shutdown of North Atlantic deep water production during the Glacial-Holocene transition?, *Nature*, Vol. 324, 53 - 55.

Scott, L, 1984: Late Quaternary palaeoenvironments in the Transvaal on the basis of palynological evidence, *in:* Vogel, JC (ed.), *Late Cainozoic palaeoenvironments of the Southern Hemisphere*, Balkema, Rotterdam, pp 317-327.

Scott, L, 1993: Palynological evidence for Late Quaternary warming episodes in Southern Africa, *Palaeogeography, Palaeoclimatology, Palaeoecology*, 101, 229-235.

Scott, L, 1994: Palynology of late Pleistocene hyrax middens, southwestern Cape Province, South Africa: a preliminary report, *Historical Biology*, 9, 71-81.

Scott, L. And Bousmann, CB, 1990: Palynological analysis of hyrax middens from southern Africa, *Palaeogeography, Palaeoclimatology, Palaeoecology*, 76, 367-379.

Scott, L, Steenkamp, M and Beaumont, PB, 1995: Palaeoenvironmental conditions in South Africa at the Pleistocene-Holocene Transition, *Quaternary Sci. Reviews*, (in press)

Sealy, J and Yates, R, 1994: The chronology of the introduction of pastoralism to the Cape, South Africa, *Antiquity*, 68, 58-67.

Thackeray, JF, 1987: Late Quaternary environmental changes inferred from small mammalian fauna, southern Africa, *Climatic Change*, 10, 285-305.

Tusenius, M, 1989: Charcoal analytical studies in the north-eastern Cape, South Africa, *south African Archaeological Society Goodwin Series*, 6, 77-83.

Wadley, L, 1986: Segments of time: A mid-Holocene site in the Transvaal, *South African Archaeological Bulletin*, 41, 54-62.

Wadley, L, 1992: Rose Cottage Cave: The later Stone Age levels with European and Iron Age artefacts, *South African Archaeological Bulletin*, 47, 8-12.

Wadley, L and Verhagen, BT, 1986: Filling the Gap: A new Holocene chronology for the Transvaal Stone Age, *SA Journal of Science*, 82, 271.

Wadley, L and Vogel, JC, 1991: New dates from Rose Cottage Cave, Ladybrand, eastern Orange Free State, *SA Journal of Science*, 87, 605-607.

Webley, L, 1992: Early evidence for sheep from Spoeg River Cave, Namaqualand, *Archaeology*, 1, 3-13.

Mazel, AD, 1988: Nkupe Shelter: Report on excavations in the eastern Biggarsberg, Thukela Basin, Natal, South Africa, *Annals of the Natal Museum*, 29, 321-377.

Meadows, ME, Baxter, AJ and Adams, TG, 1994: The late Holocene vegetation history of lowland fynbos, Verlorenvlei, SW Cape Province, S Africa, *Historical Biology*, 9, 47-59.

Meadows, ME, Baxter, AJ, Parkington, J and Adams, T, 1994: Late Holocene environments at Verlorenvlei, W Cape Province, S Africa, *Quaternary International*.

Meadows, ME, and Meadows, KF, 1988: Late Quaternary vegetation history of the Winterberg Mountains, E. Cape, S. Africa, *SA Journal of Science*, 84, 253-259.

Meadows, ME and Sugden, JM, 1988: Late Quaternary environmental changes in the Karoo, S Africa, *in:* Dardis, GF and Moon, BP (eds.), *Geomorphological studies in S Africa*, Balkema, Rotterdam, 337-353.

Meadows, ME and Sugden, JM, 1989: Late Quaternary Vegetation History of the Cedarberg, SW Cape, *Palaeoecology of Africa*, 21, 269-281.

Meadows, ME and Sugden, JM, 1991: A vegetation history of the last 14 000 years on the Cedarberg, SW Cape Province, *SA Journal of Science*, 87, 34-43.

Meadows, ME and Sugden, JM, 1992: The late Quaternary palaeoecology of a floristic kingdom: the SW Cape , South Africa, *Palaeogeography, Palaeoclimatology, Palaeoecology*, 101, 271-281.

Partridge, TC, Kerr, SJ., Metcalfe, SE, Scott, L., Talma, AS and Vogel, JC, 1993: The Pretoria Saltpan: A 200 000 year lacustrine sequence, *Palaeogeography, Palaeoclimatology, Palaeoecology*, 101, 237-244.

Sampson, CG, Hart, T, Wallsmith, DL and Blagg, JD, 1989: The ceramic sequence in the upper Seacow Valley: Problems and implications, *South African Archaeological Bulletin*, 44, 3-16.

Sampson, CG and Vogel, JC, 1989: A painted pebble and associated C-14 date from the upper Karoo, *Pictogram*, 2, 1-3.

Schweitzer, FR and Wilson, ML, 1982: Byneskranskop I. A late Quaternary living site in the southern Cape Province, South Africa, *Annals of the South African Museum*, 88,1-203.

Scott, L., 1983: A 5000 year old pollen sequence from spring deposits in the Bushveld at the north of the Soutpansberg, South Africa, *Palaeoecology of Africa*, 14, 45-55.

Bousman *et al.*, 1988, Palaeoenvironmental implications of late Pleistocene and Holocene valley fills in Blydefontein Basin, Noupoort, CP, South Africa, *Palaeoecology of Africa*, 19, 43-67.

Bousman, CB an Scott, L, 1994: Climate and overgrazing? The palynological evidence for vegetation change in the eastern Karoo, *S.Af. J. Sci*, 90, 575-578.

Deacon, HJ, 1979: Excavations at Boomplaas Cave - A sequence through the Upper Pleistocene and Holocene in South Africa, *World Archaeology*, 10, 241-297.

Deacon, HJ, 1984: The LaterStone Age of southernmost Africa *Bar International Series*, 213, 1-441.

Deacon, HJ, Deacon, J and Brooker, M 1976: Four painted stones from Boomplaas Cave, Oudtshoorn District, *South African Archaeological Bulletin*, 31, 141-145.

Deacon, J, 1978: Changing patterns in the late Pleistocene/early Holocene prehistory of southern Africa as seen from the Nelson Bay Cave stone artifact sequence, *Quaternary Research*, 10, 84-111.

Deacon, J 1984: The later Stone Age of southernmost Africa, *Bar International Series*, 213, 1-441.

February, EC, 1992: The analysis of xylem anatomy of wood charcoal in archaeological deposits as a tool in climatic reconstruction, *WRC Report*, no. 222/1/92.

Humphreys, AJB and Thackeray, AI, 1983: Ghaap and Gariep, *South African Archaeological Society Monograph Series*, 2, 1-328.

Kaplan, J, 1990: The Umhlatuzana Rock Shelter sequence: 100 000 years of Stone Age history, *Natal Museum Journal of Humanities*, 2, 1-94.

Marker, ME, 1994: Late Quaternary environmental implications from sedimentary sequences at two high-altitude Lesotho sites (in press at the time), *SA Journal of Science*.

Marker, ME and Hanvey, PM, 1994: Sedimentary sequences in the Tlaeeng Pass area, Lesotho (in press at the time), *SA Geographical Journal*.

Marker, ME and Holmes, PJ, 1993: A pleistocene sand deposit in the north eastern Cape, South Africa: palaeoenvironmental implications, *Journal of African Earth Sciences*, 17, 479-485.

Mazel, AD, 1986: Mgede Shelter: A mid- and late-Holocene observation in the western Biggarsberg, Thukela Basin, Natal, South Africa, *Annals of the Natal Museum*, 27, 357-387.

Appendix 3

References for PASH data only

Avery, DM, 1981: Holocene micromammalian faunas from the northen. Cape Province, South Africa, *SA Journal of Science*, 77, 265-273.

Avery, DM, 1982: Micromammals as palaeoenvironmental indicators and an interpretationof the late Quaternary in the southern Cape Province, South Africa. *Annals of the South African Museum*, 85, 183-377.

Avery, DM, 1987: Micromammalan evidence for natural vegetation and the introduction of farming during the Holocene in the Magaliesberg, Transvaal, *SA Journal of Science*, 83, 221-225.

Avery, DM, 1991: Micromammals, owls and vegetation change in the eastern Cape Midlands, South Africa, during the last millennium, *Journal of Arid Environments*, 20, 357-369.

Avery, DM, 1992: Man and/or climate? Environmental degradation and micromammalian community structure in South Africa during the last millennium, *SA Journal of Science*, 88, 483-489.

Avery, DM, 1992: Micromammals and the environment of early pastoralists at Spoeg River, Western Cape province, South Africa, *South African Archaeological Bulletin*, 47, 116-121.

Avery, DM, 1993: Last Interglacial and Holocene Altithermal environments in South Africa and Namibia: Micromammalian evidence, *Palaeogeography, Palaeoclimatology, Palaeoecology*, 101, 221-228.

Baxter, AJ and Davies, BR, 1994: Palaeoecological insights for the conservation of aquatic ecosytems in dryland environments: A case stusy from the Verlorenvlei system, SW Cape Province, S Africa, *Aquatic Conservation: Marine and Freshwater Ecosystems*, 4, 255-271.

Baxter, AJ, and Meadows, ME, 1994: Palynological evidence for the impact of colonial settlement within lowland fynbos: A high resolution study from the Verlorenvlei, SW Cape Province, S Africa, *Historical Biology*, 9, 61-70.

Beaumont, PB and Vogel, JC, 1972: A new radiocarbon chronology for Africa south of the equator. Part I, *African Studies*, 31, 5-89.

Bickerton, IB, 1981: Estuaries of the Cape, Part II: Synopsis f available information on individual systems, Report no.1 Spoeg (CW5), *CSIR Research Report 400*, Stellenbosch: Estuarine and Coastal Research Unit.

SITE 66: DZATA 22°52'10'S, 30°08'30"E
Site Description: ARCHEOLOGICAL SITE
Data Source: CHARCOAL
Height: 850m, Rainfall: 482mm
February, E.C.

SITE 67: ROSE COTTAGE CAVE 29°13'00"S, 27°28'00"E
Site Description: CAVE
Data Source: MICROMAMMALS
Avery, D.M.

SITE 68: ADRIESGROND CAVE 32°12'00"S, 18°52'00"E
Site Description: ARCHEOLOGICAL SITE
Data Source: MICROMAMMALIAN REMAINS
Height: 327mm, Rainfall: 1370m
Avery, D.M.,

SITE 69: BLINK KLIP KOP 28°18'00"S, 23°07'00"E
Site Description: ARCHEOLOGICAL SITE
Data Source: MICROMAMMALIAN REMAINS
Height: 327mm, Rainfall: 1370m,
Avery, D.M.

SITE 71: UMHLATUZANA ROCK SHELTER 29°48'00"S, 30°45'00"E
Site Description: ARCHEOLOGICAL SITE
Data Source: MICROMAMMALIAN REMAINS
Height: 867mm, Rainfall: 530m
Avery, D.M

SITE 58: VERLOREVLEI 23°49'24"S, 14°55'00"E
Site Description: SWAMP/MARSH
Data Source: POLLEN
Height: 0m, Rainfall: 329mm
Haman, R, Meadows, M,

SITE 59: STEENBOKFONTEIN 31°40'52"S, 18°29'23"E
Site Description: ARCHEOLOGICAL SITE
Data Source: MICROMAMMALIAN REMAINS
Height: 50m, Rainfall: 145mm
Avery, D.M

SITE 60: COMPASSBERG 31°45'37"S, 24°32'22"E
Site Description: SWAMP/MARSH
Data Source: POLLEN
Height: 2000m, Rainfall: 329mm
Haman, R, Meadows, M,

SITE 61: POWER HOUSE CAVE 27°32'00"S, 24°38'00"E
Site Description: CAVE
Data Source: MICROMAMMALIAN REMAINS
Height: 1220m Rainfall: 440mm
Avery, D.M

SITE 62: SPOEG RIVER CAVE 30°17'00"S, 17°16'00"E
Site Description: CAVE
Data Source: MICROMAMMALIAN REMAINS
Height: 10m, Rainfall: 630 mm
Avery, D.M

SITE 63: ABBOT'S CAVE 31°27'00"S, 24°39'00"E
Site Description: ARCHEOLOGICAL SITE
Data Source: MICROMAMMALIAN REMAINS
Height: 1450m, Rainfall: 360mm
Avery, D.M

SITE 64: LAKE FARM 34°00'00"S, 25°30'00"E
Site Description: STREAM DEPOSIT
Data Source: POLLEN
Height: 150m, Rainfall: 780mm
Haman, R, Meadows, M

SITE 65: BOKKRAAL 32°15'55"S, 22°19'40"E
Site Description: MARSH
Data Source: POLLEN
Height: 304mm, Rainfall: 1820 m
Haman, R, Meadows, M

SITE 50: OPPERMANSKOP 31°15'00"S, 25°02'00"E
Site Description: HYRAX MIDDEN
Data Source: POLLEN
Height: 1650m
Scott, L,

SITE 51: SCOT 22°57'00"S, 29°24'00"E
Site Description: SPRING DEPOSIT
Data Source: POLLEN
Height: 823 m
Scott, L

SITE 52: EKSTEENFONTEIN 28°50'00"S, 17°15'00"E
Site Description: HYRAX MIDDEN
Data Source: POLLEN
Height: 600m,
Scott, L.

SITE 53: COLWINTON & RAVENSCRAIG SHELTERS 31°07'45"S, 27°44'22"E
Site Description: ARCHEOLOGICAL SITE
Data Source: CHARCOAL
Height: 1800m, Rainfall: 638mm
February, E.C.

SITE 54: NORGA PEAT 33°57'00"S, 22°23'00"E
Site Description: PEAT /MARSH DEPOSIT
Data Source: CHARCOAL
Height: 200m, Rainfall: 1142mm
February, E.C.

SITE 55: LIMEROCK 28°33'00"S, 24°00'00"E
Site Description: CAVE
Data Source: MICROMAMMALIAN REMAINS
Height: 330mm, Rainfall: 1200m
Avery, D.M

SITE 56: FLORISBAD 32°46'00"S, 26°04'00"E
Site Description: MARSH
Data Source: POLLEN
Height: 1272m, Rainfall: 482mm
Brink, J.S.

SITE 57: JUBILEE SHELTER 25°42'00"S, 27°55'00"E
Site Description: ARCHEOLOGICAL SITE
Data Source: MICROMAMMALIAN REMAINS
Height: 1350m, Rainfall: 550mm
Avery, D.M

SITE 41: NKUPE SHELTER 28°09'00"S, 29°56'00"E
Site Description: CAVE
Data Source: MICROMAMMALS
Rainfall: 924mm.,
Avery, D.M.

SITE 42:MGEDE SHELTER 28°10'00"S, 29°41'00"E
Site Description: CAVE
Data Source: MICROMAMMALS
Avery, D.M.

SITE 43: SANI TOP 29°36'00"S, 29°15'00"E
Site Description: VALLEY SEDIMENTARY SEQUENCE
Data Source: POLLEN
Height: 2950m Rainfall:1095mm
Marker, M.E.,

SITE 44: BONAWE 31°20'37"S, 27°46'30"E
Site Description: ARCHAEOLOGICAL SITE
Data Source: CHARCOAL
Height: 1450m Rainfall:761 mm
February, E.C.

SITE 45: PAKHUIS PASS SHELTER 32°05'00"S, 19°05'00'E
Site Description: HYRAX MIDDEN
Data Source: POLLEN
Height: 450m
Scott,L.,

SITE 46: KILLMORE BOKSPRUIT 30°57'00"S, 27°56'20"E
Site Description: PERIGLACIAL FORMATIONS
Data Source: GEOMORPHOLOGICAL ANALYSIS
Height: 2000m, Rainfall: 686mm
Lewis, C.,

SITE 48: TLAEENG PASS 29°50'00"S, 28°46'00"E
Site Description: CUTTING SEDIMENTARY SEQUENCE
Data Source: POLLEN
Height: 3100m, Rainfall: 1334mm
Marker, M.E.,

SITE 49: MEERKAT SHELTER 31°15'00"S,25°05'00"E
Site Description: CAVE HYRAX MIDDEN
Data Source: POLLEN
Height: 1650m,
Scott, L.

Appendix 2

Site Descriptions - From PASH Data

For the full references for the PASH data, see Appendix 3.

SITE 26: RIETVLEI DAM 25°45'00"S, 28°20'00"E
Site Description: SPRING
Data Source: POLLEN
Scott, L., 1989: Palaeo 3. 70, 345-353

SITE 36: BOOMPLAAS 32°23'00"S, 22°11'00"E
Site Description: CAVE
Data Source: POLLEN
Thackeray, F

SITE 37: SNEEUBERGVLEI32°26'48"S, 19°0828'55"E
Site Description: SWAMP
Data Source: POLLEN
Height: 1440m, Rainfall:1000mm
Haman, R, Meadows, M

SITE 38: LAKE TEZA 28°29'00"S,32°07'00"E
Site Description: COASTAL LAKE
Data Source: POLLEN
Height: 30m,
Scott, L.

SITE 39: BLYDEFONTEIN STREAM 33°15'00"S, 25°05'00"E
Site Description: VALLEY DEPOSIT
Data Source: POLLEN
Height: 1650 m, Rainfall: 330mm
Scott, L.

SITE 40: WINTERBERG MOUNTAINS 32°26'00"S, 26°45'00"E
Site Description: MARSH
Data Source: POLLEN
Height: 1400m, Rainfall: 940mm
Haman, R, Meadows, M,

TEMPERATURE																				
NAME	20-19	19-18	18-17	17-16	16-15	15-14	14-13	13-12	12-11	11-10	10-9	9-8	8-7	7-6	6-5	5-4	4-3	3-2	2-1	1-0
ALIWAL NORTH									-	+	+									
BADSFONTEIN									-	+	+									
CANGO CAVE	=	=	=	=	-	-	-									(-)	(+)	(+)	(+)	(+)
CORNELIA	-	-	-	-				+		+	+									
CRAIGROSSIE								+		+	+	(+)		(+)						
ELIM	-	-	-	-																
GORROKOP	=	=	=	=	=	=	=	=	=	=	=	+	+	+	+	-	-	0	0	
PRETORIA SALTPAN													+	+	+	+	+	+	+	+
RIETVLEI DAM											0	=	0	+	+	+	(+)			
SWARTKOLKVLOER	=	=	=					+	+	+										
TATE VONDO									-	-	-				+					
UITENHAGE	=	=	=	=	=							0	0	0	0	0	0	0	0	0
WINDHOEK															+	+				
WONDERKRATER	=	=	=	=	=	=	=	=	=	-	(+)	(+)	(+)	(+)	0	0	0	(-)	0	0

Tab. 3. Temperature changes over the last 20 ka

Pether, J., 1994: Molluscan evidence for enhanced deglacial advection of Agulhas water in the Benguela current, off southwestern Afric. *Palaeogeography, Palaeoclimatology, Palaeoecology*, Vol. 111, 99 - 117.

Petit, J.R., Mounier, L., Jouzel, J., Korotkevich, Y.S., Kotlyakov, V.I. and Lorius, C., 1990: Palaeoclimatological and chronological implications of the Vostok core dust record, *Nature*, Vol. 343, 56 - 58.

Phillipps, J.P. and Held, I.M., 1994: The response to orbital perturbations in an atmospheric model coupled to a slab ocean, *Journal of Climate*, Vol.7, 767 - 782.

Pichon, J-J., Labeyrie, L.D., Bareille, G., Labracherie, M., Duprat, J. and Jouzel, J., 1992: Surface water temperature changes in the high latitudes of the southern hemisphere over the last glacial-interglacial cycle, *Paleoceanography*, Vol. 7, 289 - 318.

Porter, S.C. and Zhisheng, A., 1995: Correlation between climate events in the North Atlantic and China during the last glaciation, *Nature*, Vol. 375, 305 - 308.

Prell, W.L., Hutson, W.H., Williams, D.F., Be, A.W., Geitzenauer, K. and Molfino, B., 1980: Surface circulation for the Indian Ocean during the last glacial maximum, approximately 18 000 years B.P., *Quaternary Research* Vol. 14, 309 - 336.

Prell, W.L. and Kutzbach, J.E., 1987: Monsoon variability over the past 150 000 years, *Journal of Geophysical Research*, Vol. 92 (D7), 8411 - 8425.

Rahmstorf, S., 1994: Rapid climate transitions in a coupled ocean-atmosphere model, *Nature*, Vol. 372, 82 - 85.

Raisbeck, G.M., Yiou, F., Bourles, D., Lorius, C., Jouzel., J. and Barkov, N.I., 1987: Evidence for two intervals of enhanced ^{10}Be deposition in Antarctic ice during the last glacial period, *Nature*, Vol. 326, 273 - 277.

Reeh, N., 1985: Was the Greenland ice-sheet thinner in the late Wisconsin than now?, *Nature*, Vol. 317, 797 - 799.

Rind, D., 1987: Components of the Ice Age Circulation, *Journal of Geophysical Research*, Vol. 92, 4241 - 4281.

Rind, D., Healey, R., Parkinson, C. and Martinson, D., 1995: The role of sea ice in 2 x CO_2 climate model sensitivity. Part 1: the total influence of sea ice thickness and extent, *Journal of Climate*, Vol. 8, 449 - 463.

Ruddiman, W.F., McIntyre, A., Niebler-Hunt, V. and Durazzi, J.T., 1980:, Oceanic evidence for the mechanism of rapid Northern Hemisphere glaciation, *Quaternary Research*, Vol. 13, 33 - 64.

Oppo, D.W. and Fairbanks, R.G., 1990: Atlantic ocean thermohaline circulation of the last 150 000 years: relationship to climate and atmospheric CO^2, *Paleoceanography*, Vol. 5, 277 - 288.

Paillard, D. and Labeyrie, L., 1994: Role of the thermohaline circulation in the abrupt warming after Heinrich events, *Nature*, Vol. 372, 162 - 164.

Paillard, D., 1995: The hierarchical structure of glacial climatic oscillations: interactions between ice-sheet dynamics and climate, *Climate Dynamics*, Vol. 11, 162 - 177.

Partridge, T.C., 1990: Cainozoic environmental changes in Southern Africa, *South African Journal of Science*, Vol. 86, 315 -317.

Partridge, T.C., 1993a: Warming phases in Southern Africa during the last 150 000 years: an overview, *Palaeogeography, Palaeoclimatology, Palaeoecology*, Vol. 101, 237 - 244.

Partridge, T.C., 1993b: The evidence for Cainozoic aridification in Southern Africa, *Quaternary International*, Vol. 17, 105 - 110.

Partridge, T.C., and Williams, M.A.J., 1993 - Proface to: Palaeogeography, Palaeoclimatology, Palaeoecology, Vol 10., 185-187.

Partridge, T.C., Avery, D.M., Botha, G.A., Brink, J.S., Deacon, J., Herbert, R.S., Maud, R.R., Scholtz, A., Scott, L., Talma, A.S. and Vogel, J.C., 1990: Late Pleistocene and Holocene climatic change in Southern Africa, *South African Journal of Science*, Vol. 86, 302 - 306.

Partridge, T.C., Kerr, S.J., Metcalfe, S.E., Scott, L., Talma, A.S. and Vogel, J.C., 1993: The Pretoria Saltpan: a 200 000 year southern African lacustrine sequence, Vol. 101, 317 - 337.

Partridge, T.C., 1995: Palaeoclimates of the arid and semi-arid zones of southern Africa during the last climatic cycle, *Memoire Societé Géologique du France*, Vol. 167, 73 - 83.

Partridge, T.C., de Menocal, P.B., Lorentz, S.A., Paiker, M.J. and Vogel, J.C., 1997: Orbital forcing of climate over South Africa: a 200 000 - year rainfall record from the Pretoria Saltpan, *Quaternary Science Reviews*, Vol. 16, 1 - 9.

Partridge, T.C., 1997: Cainozoic environmental change in southern Africa, with special emphasis on the last 200 000 years, *Progress in Physical Geography*, Vol.21, 3 - 22.

Peel, D.A., 1992: Merely the tip of the ice core, *Nature*, Vol. 359, 274 - 275.

Peel, D.A., 1993: Cold answers to hot issues, *Nature*, Vol. 363, 403 - 404.

Mayewski, P.A., Twickler, M.S., Whitlow, S., Meeker, L.D., Yang, Q., Thomas, J., Kreutz, K., Grootes, P.M., Morse, D.L., Steig, E.J., Waddington, E.D., Saltzman, E.S., Whung, P.-Y. and Taylor, K.C., 1996: Climate change during the last deglaciation in Antarctica, *Science*, Vol. 272, 1636 - 1638.

McCave, I.N., Manighetti, B. and Beveridge, N.A..S., 1995: Circulation in the glacial North Atlantic inferred from grain-size measurements, *Nature*, Vol. 374, 149 - 152.

McManus, J.F., Bond, G.C., Broecker, W.S., Johnsen, S., Labeyrie, L. and Higgins, S., 1994: High-resolution climate records of the North Atlantic during the last interglacial, *Nature*, Vol. 371, 326 - 329.

Meadows, M.E. and Meadows, K.F., 1988: Late Quaternary vegetation history of the Winterberg Mountains, eastern Cape, South Africa, *South African Journal of Science*, Vol., 84, 253 - 259.

Meadows, M.E. and Sugden, J.M., 1990: Late Quaternary vegetation history of the Cederberg, south-western Cape, *Palaeoecology of Africa*, Vol. 21, 269 -281.

Meadows, M.E. and Sugden, J.M., 1991: The vegetation history of the last 14 000 years on the Cederberg, south-western Cape Province, *South African Journal of Science*, Vol. 87, 34 - 43.

Mortlock, R.A., Charles, C.D., Froelich, P.N., Zibello, M.A., Saltzman, J., Hays, J.D., and Burckle L. H., 1991: Evidence for lower productivity in the Antarctic Ocean during the last glaciation, *Nature*, Vol. 351, 220 - 221.

Muller, R.A. and MacDonald, G.J., 1995: Glacial cycles and orbital inclination, *Nature*, Vol. 377, 107 - 108.

Nakamura, M., Stone, P.H. and Marotzke, J., 1994: Destabilization of the thermohaline circulation by atmospheric eddy transports, *Journal of Climate*, Vol. 7, 1870 - 1882.

Oberhänsli, H., 1991: Upwelling signals at the northeastern Walvis Ridge during the past 500 000 years, *Paleoceanography*, Vol. 6, 53 - 71.

Oerlemans, J., 1993: Evaluating the role of climate cooling in iceberg production and the Heinrich events, *Nature*, Vol. 364, 783 - 786.

Oppo, D.W and Fairbanks, R.G., 1987: Variability in the deep and intermediate water circulation of the Atlantic Ocean during the last 25 000 years: Northern hemisphere modulation of the Southern Ocean, *Earth and Planetary Science Letters*, Vol. 86, 1 -15.

Oppo, D.W. and Lehman, S.J., 1993: Mid-depth circulation of the Subtropical North Atlantic during the Last Glacial Maximum, *Science*, Vol. 259, 1148 - 1152.

Lutjeharms, J.R.E. and van Ballengooyen, R.C., 1984: Topographic control of the Agulhas Current system, *Deep Sea Research*, Vol. 31, 1321 - 1337.

Manabe, S. and Stouffer, R.J., 1995: Simulation of abrupt climate change induced by freshwater input to the North Atlantic ocean, *Nature*, Vol. 378, 165 - 167.

Mangerud, J., Jansen, E. and Landvik, J.Y., 1996: Late Cenozoic history of the Scandinavian and Barents ice sheets, *Global and Planetary Change*, Vol. 12, 11 -26.

Markgraf, V., Dodson, J.R., Kershaw, A.P., McGlone, M.S. and Nicholls, N., 1992: Evolution of late Pleistocene and Holocene climates in the circum-South Pacific land areas, *Climate Dynamics*, Vol. 6, 193 - 211.

Marker, M.E. and Holmes, P.J., 1993: A Pleistocene sand deposit in the northeastern Cape, South Africa: palaeoenvironmental implications, *Journal of African Earth Sciences*, Vol. 17, 479 - 485.

Maslin, M.A., Shackleton, N.J. and Pflaumann, U., 1995: Surface water temperature, salinity, and density changes in the northeast Atlantic during the last 45 000 years: Heinrich events, deep water formation, and climatic rebounds, *Paleoceanography*, Vol. 10, 527 - 544.

Mason, S.J., 1990: Temporal variability of sea surface temperatures around Southern Africa: a possible forcing mechanism for the 18-year rainfall oscillation?, *South African Journal of Science*, Vol. 86, 243 - 252.

Mason, S.J., 1992: *Sea surface temperatures and South African rainfall variability*, Unpublished PhD thesis, University of the Witwatersrand, Johannesburg.

Mason, S.J., 1995: Sea-Surface Temperature: South African Rainfall Associations, 1910 - 1989, *International Journal of Climatology*, Vol. 15, 119 - 135.

Mayewski, P.A., Meeker, L.D., Whitlow, S., Twickler, M.S., Morrison, M.C., Bloomfield, P., Bond, G.C., Alley, R.B., Gow, A.J., Grootes, P.M., Meese, D.A., Ram, M., Taylor, K.C. and Wumkes, W., 1994: Changes in Atmospheric circulation and ocean ice cover over the North Atlantic during the last 41 000 years, *Science*, Vol. 263, 1747 - 1751.

Mayewski, P.A., Meeker, L.D., Whitlow, S., Twickler, M.S., Morrison, Alley, R.B., Bloomfield, P. and Taylor, K.C., 1993: The atmosphere during the Younger Dryas, *Science*, Vol. 261, 195 - 197.

Mayewski, P.A., Meeker, L.D., Whitlow, S., Twickler, M.S., Morrison, M.C., Bloomfield, P., Bond, G.C., Alley, R.B., Gow, A.J., Grootes, P.M., Meese, D.A., Ram, M., Taylor, K.C. and Wumkes, W., 1994: Changes in Atmospheric circulation and ocean ice cover over the North Atlantic during the last 41 000 years, *Science*, Vol. 263, 1747 - 1751.

Lehman, S, 1993a: Ice sheets, wayward winds and sea change. *Nature*, Vol. 365, 108 - 110.

Lehman, S., 1993b: Flickers within cycles, *Nature*, Vol. 361, 404 -405.

Lehman, S.J. and Keigwin, L.D., 1992a: Sudden changes in North Atlantic circulation during the last deglaciation, *Nature*, Vol. 356, 757 - 762.

Lehman, S.J. and Keigwin, L.D., 1992b: Deep circulation revisited, *Nature*, Vol. 358, 197 - 198.

Lindesay, J.A., 1990: Mechanisms, of climatic change: a review, *South African Journal of Science*, Vol. 86, 340 - 349.

Lindstrom, D.R., 1990: The Eurasian ice sheet formation and collapse resulting from natural atmospheric CO_2 concentration variations, *Paleoceanography*, Vol. 5, 207 - 227.

Liu, H-S., 1992: Frequency variations of the Earth's obliquity and the 100 kyr ice-age cycles, *Nature*, Vol. 358, 397 - 399.

Liu, H-S., 1995: A new view on the driving mechanism of Milankovitch glaciation cycles, *Earth and Planetary Science Letters*, Vol. 131, 17 - 26.

Lorius, C. and Oeschger, H., 1994: Palaeo-perspectives: Reducing uncertainties in global change?, *Ambio*, Vol. 23, 30 -36.

Lorius, C., Jouzel, J. and Raynaud, D., 1992: The ice core record: archive of the climate and signpost to the future, *Philosophical Transactions of the Royal Society of London*, Vol. 338, 227 - 234.

Lorius, C., Jouzel, J., Raynaud, D., Hansen, J. and Le Treut, H., 1990: The ice-core record: climate sensitivity and future greenhouse warming, *Nature*, Vol. 347, 139 - 145.

Lorius, C., Jouzel, J., Ritz, C., Merlivat, L., Barkov, N.I., Korotkevich, Y.S. and Kotlyakov, V.M., 1985: A 150 000 year climatic record from Antarctic ice, *Nature*, Vol. 316, 591 - 596.

Lowell, T.V., Heusser, C.J., Andersen, B.G., Moreno, P.I., Hauser, A., Heusser, L.E., Schlüchter, C., Marchant, D.R., and Denton, G.H., 1995: Interhemispheric correlation of Late Pleistocene glacial events, *Science*, Vol. 269, 1541 - 1549.

Lukas, M.I. and Lindesay, J.A., 1991: Global climate change: Environmental and climatic links between Antarctica and South Africa, *The South African Journal of Antarctic Research*, Vol. 21, 199 - 207.

Kent, L.E. and Gribnitz, K.-H, 1985: Freshwater shell deposits in the northwestern Cape Province: further evidence for a widespread wet phase during the late Pleistocene in southern Africa, *South African Journal of Science*, Vol. 81, 361 - 370.

Kerr, R.A., 1993a: How Ice Age climate got the shakes, *Science*, Vol. 260, 890 - 892.

Kerr, R.A., 1993b: The whole world had a case of the Ice Age shivers, *Science*, Vol. 262, 1972 - 1973.

Kerr, R.A., 1993c: Even warm climates get the shivers, *Science*, Vol. 261, 292.

Kerr, R.A., 1993d: Ocean-in-a-machine starts looking like the real thing, *Science*, Vol. 260, 32 - 33.

Kerr, R.A., 1993e: Pinatubo global cooling on target, *Science*, Vol. 259, 594.

Klein, R.G., 1991: Size variation in the Cape dune molerat (*Bathyergus suillus*) and Late quaternary climatic change in the southwestern Cape Province, South Africa, *Quaternary Research*, Vol., 36, 243 - 256.

Klein, R.G., Cruz-Uribe, K. and Beaumont, P.B., 1991: Environmental, ecological, and palaeoanthropological implications of Late Pleistocene mammalian fauna from Equus Cave, northern Cape Province, South Africa, *Quaternary Research*, Vol. 36, 94 - 119.

Labeyrie, L.D., Pichon, J.J., Labracherie, M., Ippolito, P., Duprat, J. and Duplessy, J.C., 1986: Melting history of Antarctica during the past 60 000 years, *Nature*, Vol. 322, 701 - 706.

Labracherie, M., Labeyrie, L.D., Duprat, J., Bard, E., Aarnold, M., Pichon, J.J., Duplessy, J.C., 1989: The last deglaciation in the Southern Ocean, *Paleooceanography*, Vol. 4, 629 - 638.

Lancaster, N., 1981: Palaeoenvironmental implications of fixed dune systems in Southern Africa, *Palaeogeography, Palaeoclimatology, Palaeoecology*, Vol. 33, 327 - 346.

Lancaster, N., 1986: Pans in the southwestern Kalahari: a preliminary report, *Palaeoecology of Africa*, Vol. 17, 59 -67.

Lancaster, N., 1988: Development of linear dunes in the south western Kalahari, southern Africa, *Journal of Arid Environments*, Vol. 14, 233 - 244.

Lancaster, N., 1989: Late Quaternary palaeoenvironments in the southwestern Kalahari, *Palaeogeography, Palaeoclimatology, Palaeoecology*, Vol. 70, 367 - 376.

Ledley, T.S. and Chu, S., 1995: The initiation of ice sheet growth, Milankovitch solar radiation variations, and the 100 ky cycle, *Climate Dynamics*, Vol. 11, 439 - 445.

glacial interstadials recorded in a new Greenland ice core, *Nature*, Vol. 359, 311 - 313.

Johnson, D.A., 1985: Abyssal teleconnections II. Initiation of Antarctic Bottom Water flow in the southwestern Atlantic, in: K.J. Hsü and H.J. Wiessert, *South Atlantic Paleoceanography*, Cambridge University Press, Cambridge.

Johnson, R.G. and Lauritzen, S.-E., 1995: Hudson Bay – Hudson Strait jökulhlaups and Heinrich events: a hypothesis, *Palaeogeography, Palaeoclimatology, Palaeoecology*, Vol. 117, 123 -137.

Johnson, S.J., Clausen, H.B., Dansgaard, W., Fuhrer, K., Gundestrup, N., Hammer, C.U., Iversen, P., Jouzel, J., Stauffer, B. and Steffensen, J.P., 1992: Irregular glacial interstadials recorded in a new Greenland ice core, *Nature*, Vol. 359, 311 - 313.

Jones, P.D., Wigley, T.M.L. and Raper, S.C.B., 1985: The rapidity of CO_2 - induced climatic change: observations, model results and palaeoclimatic implications, in Berger, W.H. and Labeyrie, L.D., 1987, eds., Abrupt Climatic Change, D. Reidel, Dordrecht.

Jouzel, J., Lorius, C., Petit, J.R., Genthon, C., Barkov, N.I., Kotlyakov, V.M. and Petrov, V.M., 1987: Vostok ice core: a continuos isotope record over the last climatic cycle (160 000) years, *Nature*, Vol. 329, 403 - 408.

Jouzel, J., Vaikmae, R., Petit, J.R., Martin, M., Duclos, Y., Stievenard, M., Lorius, C., Toots, M., Mélières, M.A., Burckle, L.H., Barkov, N.I. and Kotlyakov, V.M., 1995: The two-step shape and timing of the last deglaciation in Antarctica, *Climate Dynamics*, Vol. 11, 151 - 161.

Keigwin L.D. and Jones, G.A., 1994: Western North Atlantic evidence for millennial-scale changes in ocean circulation and climate, *Journal of Geophysical Research*, Vol. 99, 12 397 - 12 410.

Keigwin, L.D. and Lehman, S.J., 1994: Deep circulation linked to Heinrich event 1 and Younger Dryas in a middepth North Atlantic core, *Paleoceanography*, Vol. 9, 185 - 194.

Keigwin, L.D., Curry, W.B., Lehman, S.J. and Johnsen, S., 1994: The role of the deep ocean in North Atlantic climate change between 70 and 130 kyr ago, *Nature*, Vol. 371, 323 - 326.

Keller, A.A. and Goldstein, R.A., 1995: Oceanic transport and storage of carbon emissions, *Climatic Change*, Vol. 30, 367 - 395.

Kellogg, T.B. and Kellogg, D.A., 1986: Glacial-interglacial changes in Antarctic bottom water, *South African Journal of Science*, Vol. 82, 501 -503.

Heinrich, H., 1988: Origin and consequences of cyclic ice rafting in the Northeast Atlantic Ocean during the past 130 000 years, *Quaternary Research*, Vol. 29, 142 - 152.

Heusser, C.J. and Rabassa, J., 1987: Cold climatic episode of Younger Dryas age in Tierra del Fuego, *Nature*, Vol. 328, 609 - 611.

Hodell, D.A., 1993: Late Pleistocene palaeoceanography of the South Atlantic sector of the Southern Ocean: Ocean Drilling Program Hole 704A, *Paleoceanography*, Vol. 8, 47 - 67.

Hoffert, M.I., 1988: Climatic change and ocean bottom water formation: Are we missing something?, in: M.E. Schlesinger, (ed.), *Climate - Ocean interaction*, Kluwer Academic Publishers, Dordrecht.

Hoffert, M.I. and Covey, C., 1992: Deriving global climate sensitivity from palaeoclimate reconstructions, *Nature*, Vol. 360, 573 - 576.

Howard, W.R. and Prell, W.L., 1984: A comparison of radiolarian and foraminiferal palaeoecology in the Southern Indian Ocean: new evidence for the interhemispheric timing of climatic change, *Quaternary Research*, Vol. 21, 244-263.

Howard, W.R. and Prell, W.L., 1992: Late Quaternary surface circulation of the southern Indian Ocean and its relationship to orbital variations, *Paleoceanography*, Vol. 7, 79 -117.

Howard, W.R. and Prell, W.L., 1994: Late Quaternary $CaCO_3$ production and preservation in the Southern Ocean: implications for oceanic and atmospheric carbon cycling, *Paleoceanography*, Vol. 9, 453 - 482.

Imbrie, J., Mix, A.C. and Martinson, D.G., 1993: Milankovitch theory viewed from Devils Hole, *Nature*, Vol. 363, 531 - 533.

Ingmanson, D.E. and Wallace, W.J., 1989: *Oceanography, an Introduction*, Wadsworth Publishing Company, Belmont.

Jansen, E. and Veum, T., 1990: Evidence for a two-step deglaciation and its impact on North Atlantic Deep-Water circulation, *Nature*, Vol. 343, 612 - 616.

Jansen, E., 1992: Following iceberg footpaths, *Nature*, Vol. 360, 212 - 2..

Johnsen, S.J., Clausen, H.B, Dansgaard, W., Gundestrup, N.S., Hammer, C.U. and Tauber, H., 1995: The Eem stable isotope record along the GRIP ice core and its interpretation, *Quaternary Research*, Vol. 43, 117 - 124.

Johnsen, S.J., Clausen, H.B., Dansgaard, W., Fuhrer, K., Gundestrup, N., Hammer, C.U., Iversen, P., Jouzel, J., Stauffer, B. and Steffensen, J.P., 1992: Irregular

Grimm, E.C., Jacobson, G.L., Jr., Watts, W.A., Hansen, B.C.S. and Maasch, K.A., 1993: A 50 000 year record of climate oscillations from Florida and its temporal correlation with the Heinrich events, *Science*, Vol. 261, 198 - 200.

Grootes, P.M., Stuiver, M., White, J.W.C., Johnsen, S. and Jouzel, J., 1993: Comparison of oxygen isotope records from the GISP2 and GRIP Greenland ice cores, *Nature*, Vol. 366, 552 -554.

Grousset, F.E., Labeyrie, L, Sinko, J.A., Cremer, M., Bond, G., Duprat, J., Cortijo, E.and Huon, S., 1993: Patters of ice-rafted detritus in the glacial North Atlantic (40° - 55°N), *Paleoceanography*, Vol. 8, 175 - 192.

Guilderson, T.P., Fairbanks, R.G. and Rubenstone, J.L., 1994: Tropical temperature variations since 20 000 years ago: modulating interhemispheric climate change, *Science*, Vol. 263, 663 - 665.

Harrison, M.S.J., 1988a: The components of analogue concepts of southern African Quaternary climate variations: a critique, *Palaeoecology of Africa*, Vol. 19, 283 - 292.

Harrison, M.S.J., 1988b: The status of general circulation model simulations of southern African Quaternary climates, *Palaeoecology of Africa*, Vol. 19, 293 - 302.

Harrison, S.P., Kutzbach, J.E. and Behling, P., 1991: General circulation models, palaeoclimatic data and last interglacial climates, *Quaternary International*, Vol. 10, 231 - 242.

Harrison, S.P., Prentice, I.C. and Bartlein, P.J., 1992: Influence of insolation and glaciation on atmospheric circulation in the North Atlantic sector: implications of general circulation model experiments for the Late Quaternary climatology of Europe, *Quaternary Science Reviews*, Vol. 11, 283 - 299.

Hasselmann, K., 1991: Ocean circulation and climate change, *Tellus*, Vol. 43 AB, 82 - 103.

Hays, J.D., Imbrie, J. and Shackleton, N.J., 1976: Variations in the Earth's orbit: pacemaker of the Ice Ages, *Science*, Vol. 194, 1121 - 1132.

Heaton, T.H.E., Talma, A.S. and Vogel, J.C., 1986: Dissolved gas palaeotemperatures and ^{18}O variations derived from groundwater near Uitenhage, South Africa, *Quaternary Research*, Vol. 25, 79 -88.

Heine, K. and Geyh, M.A., 1984: Radiocarbon dating of speleothems from Rössing Cave, Namib Desert, and palaeoclimatic implications, in: J.C., Vogel, ed., 1984: *Late Cainozoic Palaeoclimates of the Southern Hemisphere*, A.A. Balkema, Rotterdam.

Emiliani, C., 1993: Milankovitch theory verified, *Nature*, Vol. 364, 583 - 584.

Esterhuysen, A.B., 1992: Charcoal from Leliehoek shelter, eastern Orange Free State, South Africa, *Palaeoecology of Africa*, Vol. 23, 193 - 200.

Fairbanks, R.G., 1989: A 17 000 - year glacio-eustatic sea level record: influence of glacial melting rates on the Younger Dryas event and deep-ocean circulation, *Nature*, Vol. 342, 637 - 642.

Fairbanks, R.G., 1993: Flip-flop end to last ice age, *Nature*, Vol. 362, 495.

February, E.C. and van der Merwe, N.J., 1992: Stable carbon isotope ratios of wood charcoal during the past 4 000 years: anthropogenic and climatic influences, *South African Journal of Science*, Vol. 88, 291 - 292.

February, E.C., 1994: Rainfall reconstruction using wood charcoal from two archaeological sites in South Africa, *Quaternary Research*, Vol. 42, 100 - 107.

Felzer, B., Oglesby, R.J., Shao, H., Webb III, T., Hyman, D.E., Prell, W.L. and Kutzbach, J.E., 1995: A Systematic study of GCM sensitivity to latitudinal changes in solar radiation, *Journal of Climate*, Vol. 8, 877 - 887.

Fichefet, T, Hovine, S. and Duplessy, J.C., 1994: A model study of the Atlantic thermohaline circulation, during the Last Glacial Maximum, *Nature*, Vol. 372, 252 - 255.

Fronval, T., Jansen, E., Bloemendal, J. and Johnsen, S., 1995: Oceanic evidence for coherent fluctuations in Fennoscandian and Laurentide ice-sheets on millennium timescales, *Nature*, Vol. 374, 443 - 446.

Ganeshram, R S., Pedersen, T.F., Calvert, S.E. and Murray, J.W., 1995: Large changes in oceanic nutrient inventories from glacial to interglacial periods, *Nature*, Vol. 376, 755 - 758.

Genthon, C., Barnola, J.M., Raynaud, D., Lorius, C., Jouzel, J., Barkov, N.I., Korotkevich, Y.S. and Kotlyakov, V.M., 1987: Vostok ice core: climatic response to CO_2 and orbital forcing changes over the last climatic cycle, *Nature*, Vol. 329, 414 - 418.

Gingele, F.X., 1996: Holocene climatic optimum in southwest Africa - evidence from the marine clay record, *Palaeogeography, Palaeoclimatology, Palaeoecology*, Vol.122, 77 -87.

Gordon, A.L., 1988: The Southern Ocean and global climate, *Oceanus*, Vol. 31, 39 - 46.

GRIP (Greenland Ice-core Project) Members, 1993: Climate instability during the last interglacial period recorded in the GRIP ice core, *Nature*, Vol. 364, 203 - 207.

Cortijo, E., Duplessy, J.C., Labeyrie, L., Leclaire, H., Duprat, J. and van Weering, T.C.E., 1994: Eemian cooling in the Norwegian Sea and North Atlantic ocean preceding continental ice-sheet growth, *Nature*, Vol. 372, 446 - 449.

Crowley, T.J. and Kim, K-Y., 1992: Complementary roles of orbital insolation and North Atlantic Deep Water during Late Pleistocene interglacials, *Paleoceanography*, Vol. 7, 521 - 528.

Crowley, T.J., 1992: North Atlantic deep water cools the southern hemisphere, *Paleoceanography*, Vol. 7, 489 - 497

Cuffey, K.M., Clow, G.D., Alley, R.B., Stuiver, M., Waddington, E.D. and Saltus, R.W., 1995: Large Arctic temperature change at the Wisconsin- Holocene glacial transition, *Science*, Vol. 270, 455 - 458.

Dansgaard, W., Johnsen, S.J., Clausen, H.B., Dahl-Jensen, D., Gundestrup, N.S., Hammer, C.U., Hvidberg, C.S., Steffensen, J.P., Sveinbjörnsdottir, A.E., Jouzel, J. and Bond, G., 1993: Evidence for general instability of past climate from a 250 kyr ice-core record, *Nature*, Vol. 364, 218 - 220.

Deacon, H.J., Deacon, J., Scholtz, A., Thackeray, J.F., Brink, J.S. and Vogel, J.C., 1984: Correlation of Palaeoenvironmental data from the Late Pleistocene and Holocene deposits at Boomplaas cave, Southern Cape, in: J.C., Vogel, ed., *Late Cainozoic Palaeoclimates of the Southern Hemisphere*, A.A. Balkema, Rotterdam.

Deacon, J. and Lancaster, N., 1988: *Late Quaternary Palaeoenvironments of Southern Africa*, Clarendon Press, Oxford.

Denton, G.H., 1985: Did the Antarctica Ice-sheet influence Late Cainozoic climate and Evolution in the southern Hemisphere?, *South African Journal of Science*, Vol. 81, 224-229.

de Vernal, A., Hillaire-Marcel, C. and Bilodeau, G., 1996: Reduced meltwater outflow from the Laurentide ice margin during the Younger Dryas, *Nature*, Vol. 381, 774 -777.

Diester-Haas, L., 1987: History of the Benguela current off SW Africa (DSPD sites 362 and 532), *Palaeoecology of Africa*, Vol. 18, 55 - 70.

Duplessy, J.C., Labeyrie, L., Arnold, M., Paterne, M., Duprat, J. and van Weering, T.C.E., 1992: Changes in surface salinity of the North Atlantic Ocean during the last deglaciation, *Nature*, Vol. 358, 485 - 487.

Edwards, R.L., Beck, J.W., Burr, G.S., Donahue, D.J., Chappell, J.M.A., Bloom, A.L., Druffel, E.R.M. and Taylor, F.W., 1993: A large drop in atmospheric $^{14}C/^{12}C$ and reduced melting in the Younger Dryas, documented with ^{230}Th ages of corals, *Science*, Vol. 260, 962 - 967.

Broecker, W.S., Peteet, D.M. and Rind, D., 1985: Does the ocean-atmosphere system have more than one stable mode of operation?, *Nature*, Vol. 315, 21 - 25.

Budd, W.F., 1991: Antarctica and Global Change, *Climatic Change*, Vol. 18, 271-299.

Carleton, A.M., 1992: Synoptic interactions between Antarctica and lower latitudes, *Australian Meteorological Magazine*, Vol. 40, 129 - 147.

Chahine, M.T., 1992: the hydrological cycle and its influence on climate, *Nature*, Vol.359, 373 - 380.

Charles, C.D. and Fairbanks, R.G., 1992: Evidence from Southern Ocean sediments for the effect of North Atlantic Deep Water flux on climate, *Nature*, Vol. 355, 416 - 419.

Charles, C.D., Rind, D., Jouzel, J., Koster, R.D. and Fairbanks, R.G., 1994. Glacial-interglacial changes in moisture sources for Greenland: Influences on the ice core record of climate, *Science*, Vol. 263, 508 - 511.

Clapperton, C.M., 1990: Quaternary glaciations in the southern hemisphere: an overview, *Quaternary Science Reviews*, Vol. 9, 299 - 304.

Clapperton, C.M., Sugden, D.E., Birnie, J. and Wilson, M.J., 1989: Late-Glacial and Holocene glacier fluctuations and environmental change on South Georgia, Southern Ocean, *Quaternary Research*, Vol. 31, 210 - 228.

Clarke, A., 1992: Global warming, Ocean cooling, *Nature*, Vol. 360, 17 - 18.

Cockcroft, M.J., Wilkinson, M.J. and Tyson, P.D., 1987: The application of a present-day climatic model to the Late Quaternary in southern Africa, *Climatic Change*, Vol. 10, 161 - 181.

Cohen, A.L., Parkington, J.E., Brundit, G.B. and van der Merwe, N.J., 1992: Holocene marine climate record in mollusc shells from the southwest African coast, *Quaternary Research*, Vol. 38, 379 - 385.

Cohen, A.L. and Tyson, P.D., 1995: Sea-surface temperature fluctuations during the Holocene off the south coast of Africa: implications for terrestrial climate and rainfall, *The Holocene*, Vol. 5, 304 - 312.

COHMAP Members, 1988: Climatic changes of the last 18 000 years: Observations and model simulations, *Science*, Vol. 241, 1043 - 1052.

Corfield, R.M., 1994: Palaeocene oceans and climate: an isotopic perspective, *Earth-Science Reviews*, Vol. 37, 225 - 252.

Corliss, B.H., 1983: Quaternary circulation of the Antarctic Circumpolar Current, *Deep-Sea Research*, Vol. 30, 47 - 61.

Vogel, J.C., 1989: Evidence of past climatic change in the Namib Desert, *Palaeogeography, Palaeoclimatology, Palaeoecology*, Vol. 70, 355 - 366.

Vogel, J.C. and Rust, U., 1987: Environmental changes in the Kaokoland Namib Desert during the present millenium, *Madoqua*, Vol. 15, 5 - 16.

Wadhams, P., 1994: Antarctic sea ice, in Hempel, (ed), *Antarctic Science*, Springer-Verlag, Berlin.

Weaver, A.J. and Hughes, T.M.C., 1994: Rapid interglacial climate fluctuations driven by the North Atlantic ocean circulation, *Nature*, Vol. 367, 447 - 450.

Weaver, A.J., 1993: The oceans and global warming, *Nature*, Vol. 364, 192 - 193.

White, J.W.C., 1993: Don't touch that dial, *Nature*, Vol.364, 186.

White, J.W.C., Ciais, P., Figge, R.A., Kenny, R. and Markgraf, V., 1994: A high-resolution record of atmospheric CO_2 content from carbon isotopes in peat, *Nature*, Vol. 367, 153.

White, W.B. and Peterson, R.G., 1996: An Antarctic circumpolar wave in surface pressure, wind, temperature and sea-ice extent, *Nature*, Vol. 380, 699 - 702.

Williams, M.A.J., Dunkerley, D.L., De Deckker, P., Kershaw, A.P., and Stokes, T., 1993: *Quaternary Environments*, Edward Arnold, London.

Yuan, X., Cane, M.A. and Martinson, D.G., 1996: Cycling around the South Pole, *Nature*, Vol. 380, 673 - 674.

Zahn, R., 1994: Core correlations, *Nature*, Vol. 371, 289 - 290.

Taylor, K.C., Lamorey, G.W., Doyle, G.A., Alley, R.B., Grootes, P.M., Mayewski, P.A., White, J.W.C. and Barlow, L.K., 1993a: The 'flickering switch' of late Pleistocene climate change, *Nature*, Vol. 361, 432 - 435.

Teller, J.T. and Lancaster, N., 1986: Lacustrine sediments at Narabeb in the central Namib Desert, Namibia, *Palaeogeography, Palaeoclimatology, Palaeoecology*, Vol. 56, 177 - 195.

Teller, J.T., Rutter, N. and Lancaster, N., 1990: Sedimentology and Paleohydrology of Late Quaternary lake deposits in the northern Namib sand sea, Namibia, *Quaternary Science Reviews*, Vol. 9, 343 - 364.

Thackeray, J.F., 1990: Temperature indices from Late Quaternary sequences in South Africa: Comparisons with the Vostok core, *South African Geographical Journal*, Vol. 72, 47 - 49.

Thackeray, J.F. and Herbert, R.S., 1991: Environmental indices from planktonic foraminifera in Late Holocene sediments off Walvis Bay, *South African Journal of Science*, Vol. 87, 611 - 613.

Thackeray, J.F. and Lee-Thorp, J.A., 1992: Isotopic analysis of equid teeth from Wonderwerk Cave, northern Cape Province, South Africa, *Palaeogeography, Palaeoclimatology, Palaeoecology*, Vol. 99, 141 - 150.

Thurman, H.V., 1991: *Introductory Oceanography*, MacMillan Publishing Company, New York.

Thompson, L.G., Mosley-Thompson, E., Davis, M.E., Lin, P.-N., Henderson, K.A., Cole-Dai, J., Bolzan, J.F. and Liu, K.-B., 1995: Late Glacial Stage and Holocene tropical ice core records from Huascaran, Peru, *Science*, Vol. 269, 46 -50.

Tyson, P.D., 1986: *Climatic Change and Variabilities in Southern Africa*, Oxford, Cape Town.

Tyson, P.D. and Lindesay, J.A., 1992: The climate of the last 2000 years in southern Africa, *The Holocene*, Vol. 2, 271 - 278.

Verbitsky, M. and Saltzman, B., 1994:, Heinrich-type glacial surges in a low-order dynamical climate model, *Climate Dynamics*, Vol. 10, 39 - 47.

Verbitsky, M. and Saltzman, B., 1995: A diagnostic analysis of Heinrich glacial surge events, *Paleoceanography*, Vol. 10, 59 - 65.

Veum, T., Jansen, E., Arnold, M., Beyer, I. and Duplessy, J-C., 1992: Water mass exchange between the North Atlantic and the Norwegian Sea during the past 28 000 years, *Nature*, Vol. 356, 783 - 785.

Vogel, J.C., ed., 1984: *Late Cainozoic Palaeoclimates of the Southern Hemisphere*, A.A. Balkema, Rotterdam.

Scott, L., Cooremans, B., de Wet, J.S. and Vogel, J.C., 1991: Holocene environmental changes in Namibia from pollen analysis of swamp and lake deposits, *The Holocene*, Vol. 1, 8 - 13.

Shaw, P.A., Cooke, H.J. and Thomas, D.S.G., 1988: Recent advances in the study of Quaternary landforms in Botswana, *Palaeoecology of Africa*, Vol. 19, 15 - 26.

Shemesh, A., Burckle, L.H. and Hays, J.D., 1994: Meltwater input to the Southern Ocean during the Last Glacial Maximum, *Science*, Vol. 266, 1542 - 1544.

Short, D. and Mengel, J.G., 1986: Tropical climatic phase lags and the Earth's precession cycle, *Nature*, Vol. 323, 48 - 50.

Souchez, R., Lemmens, M. and Chappellaz, J., 1995: Flow-induced mixing in the GRIP basal ice deduced from the CO_2 and CH_4 records, *Geophysical Research Letters*, Vol. 22, 41 - 44.

Sowers, T. and Bender, M., 1995: Climate records covering the Last Deglaciation, *Science*, Vol. 269, 210 - 214.

Squire, V.A., 1994: Atmosphere-ice-ocean: Do we really understand what is going on?, in: Hempel, (ed), *Antarctic Science*, Springer-Verlag, Berlin.

Steele, J.H., 1989: The message from the oceans, *Oceanus*, Vol. 32, 5 - 9.

Stocker, T.F, Wright, D.G. and B[illegible]cker, W.S., 1992a: The influence of high-latitude surface forcing on the global thermohaline circulation, *Paleoceanography*, Vol. 7, 529 - 541.

Stocker, T.F, Wright, D.G. and Mysak, L.A., 1992b: A zonally averaged, coupled ocean-atmosphere model for paleoclimatic studies, *Journal of Climate*, Vol. 5, 773 - 797.

Street-Perrott, F.A. and Perrott R.A., 1990: Abrupt climate fluctuations in the tropics: the influence of Atlantic Ocean circulation, *Nature*, Vol. 343, 607 - 611.

Takahashi, T., 1989: The carbon dioxide puzzle, *Oceanus*, Vol. 32, 22 - 29.

Talma, A.S. and Vogel, J.C., 1992: Late Quaternary palaeotemperatures derived from a speoleothem from Cango Caves, Cape Province, South Africa, *Quaternary Research*, Vol. 37, 203-213.

Taylor, K.C., Hammer, C.U., Alley, R.B., Clausen, H.B., Dahl-Jensen, D., Gow, A.J., Gundestrup, N.S., Kipfstuhl, J., Moore, J.C. and Waddington, E.D., 1993b, Electrical conductivity measurements from the GISP2 and GRIP Greenland ice cores, *Nature*, Vol. 366, 549 - 552.

Ryabchenko, V.A., 1989: Causes of decrease in concentration of atmospheric CO_2 at the peak of the last glaciation, *Oceanology*, Vol. 19, 49 -54.

Sakai, K. and Peltier, W.R., 1995: A simple model of the Atlantic thermohaline circulation: internal and forced variability with palaeoclimatological implications, *Journal of Geophysical Research*, Vol. 100, 13 455 - 13 479.

Sanyal, A., Hemming, N.G., Hanson, G.N. and Broecker, W.S., 1995: Evidence for a higher pH in the glacial ocean from boron isotopes in foraminifera, *Nature*, Vol. 373, 234 - 236.

Scott, L., 1987a: Late Quaternary forest history in Venda, southern Africa, *Review of Palaeobotany and Palynology*, Vol. 53, 1 - 10.

Scott, L., 1987b: Pollen analysis of hyena coprolites and sediments from Equus Cave, Taung, southern Kalahari (South Africa), *Quaternary Research*, Vol. 28, 144 - 156.

Scott, L. and Thackeray, J.F., 1987: Multivariate analysis of Late Pleistocene and Holocene pollen spectra from Wonderkrater, Transvaal, South Africa, *South African Journal of Science*, Vol., 83, 93 - 98.

Scott, L., 1989a: Climatic conditions in southern Africa since the Last Glacial Maximum, inferred from pollen analysis, *Palaeogeography, Palaeoclimatology, Palaeoecology*, Vol. 70, 345 - 353.

Scott, L., 1989b: Late Quaternary vegetation history and climatic change in the eastern Orange Free State, South Africa, *South African Journal of Botany*, Vol. 35, 107 - 116.

Scott, L., 1991: Past vegetation changes in mountainous areas in South Africa as revealed by pollen analysis of hyrax middens. Paper presented at AETFAT Congress, Malawi.

Scott, L., 1993: Palynological evidence for late Quaternary warming episodes in Southern Africa, *Palaeogeography, Palaeoclimatology, Palaeoecology*, Vol. 101, 229 - 235.

Scott, L., and Brink, J.S., 1991: Quaternary palaeoenvironmnts of pans in central South Africa: palynological and palaeontological evidence, *South African Geographer*, Vol. 19, 22 - 34.

Scott, L., and Thackeray, J.F., 1987: Multivariate analysis of late Pleistocene and Holocene pollen spectra from Wonderkrater, Transvaal, South Africa, *South African Journal of Science*, Vol. 83, 93 - 98.

Scott, L. and Cooremans, B., 1990: Late Quaternary pollen from a hot spring in the upper Orange River basin, South Africa, *South African Journal of Science*, Vol. 86, 154 - 156.